



# **Operation and Assessment of Wind Energy on Power System Reliability Evaluation**

A thesis submitted for the degree of

**Doctor of Philosophy**

At the University of Strathclyde

By

**Shuai Shi**

**Supervisor: Professor K. L. Lo**

**Power Systems Research Group**

**Department of Electronic and Electrical Engineering**

**University of Strathclyde**

**May 2014**

# **Declaration of Author's Right**

This thesis is the result of the author's original research. It has been composed by the author and has not been previously submitted for examination which has led to the award of a degree.

The copyright of this thesis belongs to the author under the terms of the United Kingdom Copyright Acts, as qualified by University of Strathclyde Regulation 3.50. Due acknowledgement must always be made of the use of any material contained in, or derived from, this thesis.

# Acknowledgement

First of all, I would like to express my sincere appreciation to my supervisor, Professor K. L. Lo, Head of the Power System Research Group (PSRG), for his supervision and support throughout my research work. The completion of this thesis would not have been possible without his constant encouragement and patient guidance.

I also wish to extend my gratitude to my colleagues at PSRG for providing a stimulating and fun environment. My colleagues, and the many friends outside work that I would like to thank, are too numerous to be squeezed into one page. Special thanks to Jiangfeng Lu and Jun Xia, for their help and support at various stages of this research work.

Most importantly, I wish to express my sincere gratitude to my parents for their financial support, love and inspiration during my studies.

# Abstract

Power companies around the world are incorporating wind power into their electricity networks. Wind power is an intermittent source of energy and its technical and financial impacts on the transmission and distribution networks are not yet totally investigated. This thesis investigates the impact of wind power on power system reliability evaluation. The investigation includes long-term system planning and short-term operational planning on reliability evaluation taking into accounts different penetration levels of wind power.

This thesis presents a Wind-Hydro Cooperation (WHC) method for reducing the effects of wind power fluctuations on system operation and maintaining similar power system reliability level at different wind penetrations.

The thesis starts by gaining insights into methodologies of power system reliability evaluation. These methodologies are described and discussed in details. Then, relations between the wind speed and the wind turbine power output are explored for modelling the wind farm output. The output fluctuation of wind power affects the power system operation. The system requires additional operating reserve to maintain the original system reliability. To mitigate these effects of wind output fluctuation, the study explores the use of Pump-Hydro technology to cooperate with wind power to meet the increased operating reserve requirements.

In order to verify and analyze the validity of the WHC method on reducing the effect of wind power fluctuation on power output and maintaining the system reliability, an extensive set of case studies are performed.

Following this, the reliability analyses focus on three aspects: *a)* a small system for initial validation of the idea; *b)* a larger system for analysing the effects of the WHC method on long-term system planning and short-term operational planning; *c)* application of a real practical system.

All the above tests involve investigation of wind penetration at different level starting from 10% to 40%. The period of investigation ranges from one day, one week, one month and then extending it to one full year.

# Table of Contents

<b>Declaration of Author’s Right</b> .....	<b>i</b>
<b>Acknowledgement</b> .....	<b>ii</b>
<b>Abstract</b> .....	<b>iii</b>
<b>List of Figures</b> .....	<b>x</b>
<b>List of Tables</b> .....	<b>xiv</b>
<b>Nomenclature</b> .....	<b>xvii</b>
<b>Chapter 1. Introduction</b> .....	<b>1</b>
1.1 Motivation.....	1
1.2 Challenge .....	4
1.3 Objectives and Research Questions .....	6
1.4 Contributions .....	9
1.5 Thesis Structure.....	11
1.6 Publications.....	15
<b>Chapter 2. Wind Energy and the Associated Issues of Wind Power Integration</b> <b>16</b>	
2.1 Introduction.....	16
2.2 Wind Energy Development and Benefits .....	18
2.3 Status of Wind Power Worldwide .....	22
2.3.1 Leader in Wind Power Installed Capacity- China.....	23
2.3.2 Leader in Wind Power Electricity Production- United States .....	25
2.3.3 Leader in Wind Penetration level- Denmark .....	25
2.3.4 Leader in Offshore Wind Energy- United Kingdom.....	26
2.4 Wind Turbine Technology.....	28
2.5 Overview of Wind Power Generation .....	29
2.5.1 Wind Speed Model.....	29

2.5.2	Wind Turbine Output Model.....	34
2.5.3	Classifications of the Wind Farm.....	35
2.6	Policies for Wind Energy .....	37
2.7	Impacts of Wind Power Integration on Power Systems Reliability.....	40
2.7.1	Basic Concepts of Power Systems Reliability Analysis.....	40
2.7.2	Elements in Generating Unit Model.....	44
2.7.3	Generating Unit State Model .....	46
2.7.4	Adequacy Index for Generation Reliability .....	47
2.7.5	Reliability Worth Assessment.....	49
2.7.6	Effect of Wind Energy on System Reliability .....	51
2.8	Overview of Power System Operating Reserve Assessment Method .....	52
2.8.1	Conventional Operating Reserve Assessment Method .....	52
2.8.2	Operating Reserve Assessment of Wind Power Generation.....	57
2.8.3	Review of Hydropower Generation.....	58
2.9	Summary.....	60
<b>Chapter 3.</b>	<b>Power System Reliability Methods for Wind Energy .....</b>	<b>62</b>
3.1	Introduction.....	62
3.2	Analytical Methods for Reliability Assessment .....	63
3.2.1	Capacity Outage Probability Table .....	64
3.2.2	Loss of Load Expectation Method (LOLE Method).....	69
3.2.3	Markov Chain Method.....	74
3.2.4	Frequency and Duration Method (F&D Method) .....	79
3.3	Simulation Method for Reliability Assessment .....	90
3.3.1	Monte Carlo Simulation Methodology .....	90
3.3.2	State Duration Sampling Approach.....	92
3.3.3	Simulation Terminating Criteria .....	94

3.4 Effect of Wind Power Generation on Reliability Assessment.....	95
3.4.1 Effects of Wind Power on Analytical Methods .....	95
3.4.2 Effects of Wind Power on Monte Carlo Simulation .....	96
3.5 Reliability Standard of Power System.....	97
3.6 Summary.....	99
<b>Chapter 4. Reliability Evaluation of Modified Roy Billinton Test System ....</b>	<b>100</b>
4.1 Introduction.....	100
4.2 Description of Modified Roy Billinton Test System (MRBTS).....	101
4.3 Load Model.....	102
4.4 Generating System Model .....	111
4.5 Results and Discussions of MRBTS Reliability Evaluation .....	118
4.5.1 Number of Samples .....	118
4.5.2 Results.....	120
4.6 Summary.....	121
<b>Chapter 5. Weibull Distribution for Power Output of Wind Farms .....</b>	<b>122</b>
5.1 Introduction.....	122
5.2 Overview of Wind Characteristics .....	123
5.2.1 Wind Speed Variation .....	123
5.2.2 Example: Wind Speed Distribution in the Peninsular Malaysia .....	124
5.3 Weibull Distribution.....	126
5.3.1 The Weibull Scale Parameter.....	128
5.3.2 The Weibull Shape Parameter.....	130
5.3.3 Seasonal Variation of Weibull Distribution.....	131
5.4 Artificial Generated Wind Speed .....	132
5.5 Weibull Distribution for Wind Turbine Output Calculation .....	135
5.6 Power Outputs of Multiple Wind Farms .....	139

5.7 Summary.....	143
<b>Chapter 6. Wind-Hydro Cooperation in Power System Reliability Assessment</b>	<b>144</b>
6.1 Introduction.....	144
6.2 Pump-Hydro Combined Energy Storage (PHCES) Technology .....	145
6.2.1 Overview of PHES .....	145
6.2.2 Modelling PHES Unit.....	148
6.2.3 Operation of PHCES System .....	148
6.3 Proposed Method: Wind-Hydro Cooperation.....	150
6.3.1 Methodology and Prerequisite .....	150
6.3.2 Mathematical Model and Calculation Procedure .....	152
6.3.3 Flow Chart .....	162
6.4 Illustrative Example .....	164
6.4.1 Data and Assumptions for the Test System .....	164
6.4.2 Results and Discussions.....	166
6.5 PHCES Operation .....	182
6.5.1 Generating-Pumping Process.....	182
6.5.2 Stored Energy and Available Power.....	185
6.5.3 Verifying Operation Mode.....	186
6.6 Summary.....	191
<b>Chapter 7. Reliability Evaluation of Modified IEEE 118-Bus Test System...193</b>	<b>193</b>
7.1 Introduction.....	193
7.2 Evaluation of Modified IEEE 118-Bus Test System: Long-term System Planning.....	195
7.3 Long-term System Planning: Results and Discussions .....	200
7.3.1 The Impacts of Different Wind Penetrations on the System Reliability .200	200

7.3.2 The Improvement of Wind-Hydro Cooperation in Reliability .....	204
7.3.3 Determine the Optimal Cooperation Scenario .....	225
7.4 Evaluation of Modified IEEE 118-Bus Test System: Short-term Operational Planning.....	233
7.5 Short-term Operational Planning: Effects on Electric Network Losses.....	237
7.5.1 Impacts of Load Variation and Wind Power Fluctuation on Network Losses & Effects of WHC on Reducing Network Losses.....	238
7.5.2 Impacts of Different Wind Power Penetration Levels on Network Losses & Effects of WHC on Reducing Network Losses .....	245
7.5.3 Impacts of Multiple Wind Farm Outputs on Electric Network Losses ...	250
7.6 Summary.....	253
<b>Chapter 8. Reliability Evaluation of Eastern Gansu Power Grid .....</b>	<b>255</b>
8.1 Introduction.....	255
8.2 Description of Eastern Gansu Power Grid (EGPG).....	256
8.3 Eastern Gansu Power Grid (EGPG) Reliability Evaluation: 8% Wind Penetration.....	261
8.4 Eastern Gansu Power Grid (EGPG) Reliability Evaluation: 20% Wind Penetration.....	267
8.5 Effect of Wind-Hydro Cooperation on EGPG Reliability in 20% Wind Penetration.....	273
8.6 Summary.....	281
<b>Chapter 9. Conclusions .....</b>	<b>282</b>
9.1 Introduction.....	282
9.2 Contributions and Findings of this Research.....	284
9.3 Future Work.....	291
<b>Reference.....</b>	<b>293</b>
<b>Appendix .....</b>	<b>308</b>

# List of Figures

Figure 2.1: Top 10 Countries by Installed Wind Power Capacity as End of 2012 [35] .....	19
Figure 2.2: Global Total Installed Wind Capacity 1996-2012.....	20
Figure 2.3: Wind Power Installed Capacity and Growth Rate from 2006 to 2012 ....	24
Figure 2.4: Wind Turbine Power Output Curve [69].....	34
Figure 2.5: UK Annual Mean Wind Speed at 25m above Ground Level [69] .....	36
Figure 2.6: Hierarchical Levels of the Power System .....	41
Figure 2.7: Generating Capacity Reliability Evaluation Model.....	43
Figure 2.8: The Relationship between MTTF, MTTR and MTBF .....	44
Figure 2.9: Two-State Generating Unit Model.....	46
Figure 2.10: Three-State Generating Unit Model.....	47
Figure 2.11: Seven Components used in Canadian Electricity Market [80].....	50
Figure 2.12: UEM to Consumers as a Function of the Installed Reserve Margin.....	56
Figure 3.1: Daily Peak Load Variation Curve.....	72
Figure 3.2: Time Periods during Which Loss of Load Occurs .....	72
Figure 3.3: State Space Diagram for a Two-component System .....	75
Figure 3.4: Two-state model for a base load unit .....	79
Figure 3.5: Three-unit state space diagram[5].....	81
Figure 3.6: Convergence Process in Monte Carlo Simulation [80].....	94
Figure 4.1: Single Line Diagram of MRBTS [103].....	102
Figure 4.2: Annual Load Curve of MRBTS with 8736 Load Points .....	108
Figure 4.3: Weekly Load Curve of MRBTS with 168 Load Points .....	109
Figure 4.4: Daily Load Curve of MRBTS with 24 Load Points .....	110
Figure 4.5: 5-MW Unit Generation Output Model.....	113
Figure 4.6: MRBTS Total Generation Output.....	115
Figure 4.7: Superimposition of System Capacity and Load.....	117
Figure 4.8: MRBTS LOLE Results of Different Number of Samples .....	119
Figure 5.1: Wind Speed Distribution at Kuala Terengganu.....	126

Figure 5.2: Cumulative Weibull Probability Distribution ( $c = 7$ & $k = 2$ ) .....	128
Figure 5.3: Weibull Distribution Density versus Wind Speed under a Constant Value of $k=2$ and Different Values of $c$ .....	129
Figure 5.4: Weibull Distribution Density versus Wind Speed under a Constant Value of $c=7$ and Different Values of $k$ .....	130
Figure 5.5: Seasonal Variation of Probability Density Function versus Wind Speed at Aimangala Station.....	132
Figure 5.6: Snap Shot of Simulated Wind Speed (300 hours) .....	134
Figure 5.7: Flow Chart for Wind Turbine Power Output Model .....	137
Figure 5.8: Snapshot of Simulated Wind Farm Power Output.....	138
Figure 5.9: Power Output Comparison of Single Wind Farm and 2-Wind Farm (100 hours) .....	140
Figure 5.10: Power Output Comparison of Single Wind Farm and 3-Wind Farm (100 hours) .....	141
Figure 5.11: Power Output Comparison of Single Wind Farm and 5-Wind Farm (100 hours) .....	142
Figure 6.1: Pumped Hydro Energy Storage (PHES) Diagram [114].....	146
Figure 6.2: Generating Facility of PHES [114].....	146
Figure 6.3: Flow Chart for the Wind-Hydro Cooperation Method .....	163
Figure 6.4: Comparison of the Impact on the LOLE & LOLF .....	168
Figure 6.5: Comparison of the Impact on the LOEE.....	168
Figure 6.6: Effects of Cooperation Scenarios on LOLE at 10% Wind Penetration Level .....	171
Figure 6.7: Comparison of Different Dispatch Ratios on LOLE ( $CF=0.8$ ) .....	172
Figure 6.8: Total Cost of Suitable Cooperation Scenarios at 10% wind penetration level.....	175
Figure 6.9: Effects of Cooperation Scenarios on LOLE at 15% Wind Penetration Level .....	177
Figure 6.10: Unserved Energy Cost for Suitable Cooperation Scenarios at 15% wind penetration level .....	179
Figure 6.11: Comparison of Reliability Improvements on LOLE at Different Wind Penetration Levels.....	181

Figure 6.12: Cooperation of Pump-Hydro Energy Storage Unit and Wind Farm[126]	183
.....	183
Figure 6.13: Wind Power Output Curve (168 hours)	187
Figure 6.14: Variation of the Water Level in the Upper Reservoir	188
Figure 6.15: Variation of Water Level at Each Time Interval	190
Figure 7.1: The Diagram of Modified IEEE 118-Bus Test System	196
Figure 7.2: The Impact of Wind Penetration on LOLE & LOLF.....	202
Figure 7.3: The Impact of Wind Penetration on LOEE .....	202
Figure 7.4: Effects of Cooperation Scenarios on Reliability Index LOLE (10% Wind Penetration)	205
Figure 7.5: Effects of DR on LOLE in CF=0.6, 0.7 & 0.8 (10%).....	207
Figure 7.6: Effects of DR on LOEE in CF=0.6, 0.7 & 0.8 (10%).....	208
Figure 7.7: Effects of Cooperation Scenarios on Reliability (15% Wind Penetration)	211
.....	211
Figure 7.8: Effects of Cooperation Scenarios on Reliability (20% Wind Penetration)	215
.....	215
Figure 7.9: Effects of Cooperation Scenarios on Reliability (25% Wind Penetration)	219
.....	219
Figure 7.10: Effect of Cooperation Factor (CF) on Reliability Indices (30% Wind Penetration)	222
Figure 7.11: Effect of Cooperation Factor (CF) on Reliability Indices (40% Wind Penetration)	224
Figure 7.12: Unserved Energy Costs of Suitable Cooperation Scenarios (10%) .....	228
Figure 7.13: Unserved Energy Costs of Suitable Cooperation Scenarios (15%) .....	229
Figure 7.14: Unserved Energy Costs of Suitable Cooperation Scenarios (20%) .....	230
Figure 7.15: Unserved Energy Costs of Suitable Cooperation Scenarios (25%) .....	232
Figure 7.16: Diagram of Modified IEEE 118-Bus Test System for Short-term Operating [130].....	234
Figure 7.17: Daily Load Curve (24 hours, 48 load points) .....	235
Figure 7.18: Impacts of Load Variations on Network Losses.....	239
Figure 7.19: Impacts of Wind Power Output Fluctuations on Network Losses.....	240

Figure 7.20: Effects of WHC on Reducing Electric Network Losses in 10% Wind Penetration (No Pumping Process).....	242
Figure 7.21: Effects of WHC on Reducing Electric Network Losses in 10% Wind Penetration (with Pumping Process).....	243
Figure 7.22: Electric Network Losses at 4 Different Wind Penetration Levels .....	246
Figure 7.23: Effects of WHC on Reducing Electric Network Losses at 10, 15%, 20%&25% Wind Penetration Levels .....	247
Figure 7.24: Impacts of Single-Wind Farm Output and 5-Wind Farm Output on Electric Network Losses (10%, 15%, 20%&25% Wind Penetrations) .....	251
Figure 8.1: Location of Gansu Province in China [131].....	257
Figure 8.2: City Distribution in Gansu Province [133].....	257
Figure 8.3: Transmission Network of Western Gansu in 2010 [140].....	260
Figure 8.4: Grid-dispatching Installed Capacity Ratio of Different Energy Sources in May 2009.....	262
Figure 8.5: Superimposition of Conventional Generation & Load in EGPG .....	264
Figure 8.6: Superimposition of Total Generation & Load in EGPG (8% Wind Penetration) .....	265
Figure 8.7: Growth Rates per year of Generating System & Load (May 2009 to May 2013) .....	268
Figure 8.8: Grid-dispatching Installed Capacity Ratio of Different Energy Sources in May 2013.....	269
Figure 8.9: Superimposition of Total Generation & Load in EGPG (20% Wind Penetration) .....	270
Figure 8.10: Comparison of LOLE between 8 % and 20% Wind Penetration .....	272
Figure 8.11: Effect of Wind-Hydro Cooperation on LOLE in EGPG (20% Wind Penetration Level).....	275
Figure 8.12: Seven Components in Eastern Gansu Electricity Market [141] .....	276
Figure 8.13: Unserved Energy Costs of Suitable Cooperation Scenarios.....	277
Figure 8.14: Superimposition of Total Generation & Load in EGPG with WHC (20% Wind Penetration).....	279

# List of Tables

Table 2.1: Top 10 Countries by Installed Wind Power Capacity as end of 2012 [35] .....	19
Table 2.2: Annual Growth Rate (%) of Installed Wind Capacity 1999-2012.....	20
Table 2.3: New Installed Wind Power Capacity Jan- Dec 2012 [35].....	22
Table 2.4: Wind Power Installed Capacity and Growth Rate from 2006 to 2012.....	24
Table 2.5: Global Offshore Wind Installed Capacity .....	27
Table 2.6: Comparison of Different Wind Speed Models .....	33
Table 2.7: Classifications of the Wind Farm.....	35
Table 2.8: Major Policy mechanisms and support schemes used in 9 wind markets[71] .....	39
Table 2.9: Generating Unit's Data for the Example .....	45
Table 2.10: Customer Damage Function for Seven Components [80] .....	50
Table 2.11: Generating Unit Reliability Data .....	52
Table 2.12: Percentage Reserve Margin Calculation for System 1 .....	53
Table 2.13: Percentage Reserve Margin Calculation for System 2 .....	54
Table 2.14: Percentage Reserve Margin Calculation for System 3 .....	54
Table 2.15: Operating Characteristics of Generating Plants .....	60
Table 3.1: COPT Construction Example .....	65
Table 3.2: Generating Units' FOR of Example I.....	66
Table 3.3: COPT for Example I (2 units).....	66
Table 3.4: COPT for Example II (5 units) .....	68
Table 3.5: COPT for the five units system.....	71
Table 3.6: LOLE Calculated by Using Individual Probabilities .....	73
Table 3.7: LOLE for Example System .....	73
Table 3.8: System Data .....	80
Table 3.9: System States .....	80
Table 3.10: Departure Rates of Two- Component System .....	82
Table 3.11: Capacity model with Unit 1 .....	84
Table 3.12: Individual Probability $p(X)$ Calculation (Unit1&Unit2) .....	85
Table 3.13: Upward Departure Rate $\lambda + (X)$ Calculation (Unit1&Unit2) .....	85

Table 3.14: Downward Departure Rate $\lambda - (X)$ Calculation (Unit 1 & Unit 2) .....	86
Table 3.15: Capacity Model with Unit 1 & Unit 2 .....	87
Table 3.16: Individual Probability $p(X)$ Calculation (Unit 1 & Unit 2 & Unit 3) .....	87
Table 3.17: Upward Departure Rate $\lambda + (X)$ Calculation .....	87
Table 3.18: Downward Departure Rate $\lambda - (X)$ Calculation .....	88
Table 3.19: Capacity Model with Unit 1 & Unit 2 & Unit 3 .....	88
Table 3.20: Complete Generation Model .....	89
Table 3.21: Reliability Standard LOLE in 10 countries .....	98
Table 4.1: Weekly Peak Load in Per cent of Annual Peak .....	104
Table 4.2: Daily Peak Load in Per cent of Weekly Peak .....	105
Table 4.3: Hourly Peak Load in Per cent of Daily Peak .....	106
Table 4.4: Generating Unit Reliability Data [81] .....	111
Table 4.5: Failure Rates of Generating Units .....	112
Table 4.6: MRBTS LOLE Results of Different Number of Samples .....	119
Table 4.7: Results of MRBTS Reliability Assessment .....	120
Table 5.1: Wind Speed Data in Frequency Distribution and Cumulative Frequency Distribution Formats at Kuala Terengganu [108] .....	125
Table 5.2: Weibull Distribution Parameters at Aimangala Station .....	131
Table 5.3: Wind Turbine Parameter Data .....	138
Table 6.1: Wind Farm Output Annual Performance ( $c=7$ & $k=2$ ) .....	156
Table 6.2: Test System Data .....	164
Table 6.3: Customer Interruption Cost for Residential Users .....	166
Table 6.4: Reliability Indices of the Test System at 10% & 15% Wind Penetration Level .....	167
Table 6.5: Operation Pattern of PHES .....	184
Table 6.6: Data and Assumptions for Operation Verification .....	186
Table 7.1: Modified IEEE 118-Bus Test System Data .....	195
Table 7.2: Conventional Generator Reliability Data [4] .....	197
Table 7.3: Wind Turbine Parameters .....	198
Table 7.4: CIC for Residential Users .....	198
Table 7.5: Basic System Data for Case 1~ Case 6 .....	199
Table 7.6: Reliability Indices of the Modified IEEE 118-Bus Test System .....	201

Table 7.7: Comparison of LOLE Values on Low, Medium, High & Extreme High Penetration Levels.....	203
Table 7.8: Improvements on LOLE by DR in CF=0.6, 0.7&0.8 (10%).....	207
Table 7.9: Improvements on LOEE by DR in CF=0.6, 0.7&0.8 (10%) .....	208
Table 7.10: Improvements on LOLE & LOEE by DR in CF=0.6, 0.7&0.8 (15%) .	213
Table 7.11: Improvements on LOLE & LOEE by DR in CF=0.6, 0.7&0.8 (20%) .	217
Table 7.12: Improvements on LOLE & LOEE by DR in CF=0.6, 0.7&0.8 (25%) .	221
Table 7.13: Required Acceptable Reliability with WHC .....	226
Table 7.14: 24-Hour Load Data with 30 Minutes Time Interval .....	236
Table 7.15: Optimal Cooperation Scenarios in Different Wind Penetrations.....	237
Table 7.16: Performances of WHC on Network-Loss Reductions.....	249
Table 7.17: Performance of Multiple Wind Farm Output on Electric Network Losses Reductions .....	252
Table 8.1: Basic System Data of EGPG in May 2009 [121].....	262
Table 8.2: Conventional Generating Unit Reliability Data.....	263
Table 8.3: Reliability Indices of EGPG in 8% Wind Penetration (May 2009) .....	266
Table 8.4: Increments on Generation Capacity & Load .....	268
Table 8.5: Reliability Indices of EGPG in 20% Wind Penetration (May 2013) .....	272
Table 8.6: Effect of Wind-Hydro Cooperation on EGPG Reliability Indices .....	274
Table 8.7: CIC for Seven Components in Eastern Gansu Electricity Market.....	276
Table 9.1: Improvements of Wind-Hydro Cooperation Method.....	288
Table 9.2: Advantages of the Proposed Operational Mode .....	290

# Nomenclature

WHC	Wind-Hydro Cooperation
PHCES	Pump-Hydro Combined Energy Storage
PRM	Percentage Reserve Margin
UEM	Unserved Equivalent Minutes
CC	Cooperation Criterion
PHES	Pump-Hydro Energy Storage
F&D	Frequency & Duration
MCS	Monte Carlo Simulation
RPS	Renewable Portfolio Standard
OR	Operating Reserve
WECS	Wind Energy Conversion System
WTG	Wind Turbine Generator
Ob	Observed wind speeds
Mob	Mean observed wind speeds
ARMA	Autoregressive Moving Average
$V_{ci}$	cut-in speed of the wind turbine

$V_r$	rated speed of the wind turbine
$V_{co}$	cut-out speed of the wind turbine
$ws$	Wind speed
$P_{wr}$	rated power output of the wind turbine
NRET	National renewable energy targets
MRET	Mandatory renewable energy targets
AWEA	American Wind Energy Association
R&D	Research and Development
LLU	Loss of Largest Unit
CRM	Capacity Reserve Margin
FOR	forced outage rate
MTTF	Mean Time to Failure
MTTR	Mean Time to Repair
MTBF	Mean Time between Failure
$\lambda$	failure rate
$\mu$	repair rate
RBTS	Roy Billiton Test System

LOLP	Loss of Load Probability
LOLE	Loss of Load Expectation (days/year or hours/year)
LOEE	Loss of Energy Expectation (MWh/year)
LOLF	Loss of Load Frequency (occurrences/year)
LOLD	Loss of Load Duration (hours/occurrence)
S	the total number of evaluated states
T	the duration of state $i$
$C_i$	loss of load for state $i$ in MW
$p_i$	probability of loss of load state $i$
CIC	customer interruption cost
CDF	customer damage function
SIC	Standard Industrial Classification
IP	individual probability
CP	cumulative probability
CCP	complementary cumulative probability
$r_{eq}$	Unserved equivalent minutes (minutes/year)
$\Delta E$	Unserved energy (MWh)

$E$	Annual energy demand (MWh)
SO	System Operator
CBA	Cost-Benefit Analysis
COPT	Capacity outage probability table
$p_k$	Individual probability associated with the capacity outage that will lead to loss of load
$t_k$	The number of days (hours) that an outage would cause a loss of load
$P_{ij}$	The probability of the process moving from State $S_i$ to State $S_j$ is denoted by the transition probability
$P_{ii}$	The probability of the process remains in the same state is denoted by the probability
$\mathbf{P}$	The state probability vector and
$\mathbf{T}$	The transition matrix
$\mathbf{I}$	The identity matrix.
$p(X)$	the individual probability of capacity outage $X$ after the unit is added
$p'(X)$	the individual probability of capacity outage $X$ before the unit is added
$\lambda_+(X)$	the upward capacity departure rate after the unit is added
$\lambda_-(X)$	the downward capacity departure rate after the unit is added
$N_s$	the sampling time

$LLD_i$	the sampled loss of load duration for state $i$
$ENS_i$	the sampled energy not supplied in MWh for state $i$
$LLO_i$	the sampled loss of load occurrence for state $i$
$U$	a uniformly distributed random number between [0, 1]
MRBTS	Modified Roy Billinton Test System
MWS	the mean wind speed
$f(v)$	the probability of occurrence of wind speed $v$ ( $v \geq 0$ )
$c$	Weibull scale parameter
$k$	Weibull shape parameter
$C_w$	the rated wind farm capacity
$P_{wi}$	the power output from the wind farm at the $i$ th hour
CF	Cooperation Factor
$C_{PH}$	installed capacity of PHES for cooperation
$C_{WP}$	total installed capacity of wind power generation
DR	Dispatch Ratio
$H_{CO}$	amount of PHCES for the generating-pumping process
$C_{PH}$	total installed capacity of PHCES in the system

<i>RARL</i>	The required acceptable reliability level for all suitable cooperation scenarios
$C_j$	The total costs at <i>j</i> th cooperation scenario.
<i>CC</i>	capital costs
<i>UEC</i>	unserved energy costs
<i>CS</i>	Cooperation Scenario
<i>EGPG</i>	eastern Gansu power grid
<i>NEA</i>	National Energy Administration

# Chapter 1. Introduction

## 1.1 Motivation

Recently, electric networks are targeting the future sustainable power systems encouraged by the national energy policies to reduce carbon emissions. For instance, according to the UK Government's Renewable Energy Strategy, it is expected that 15% of its total energy consumption coming from renewable energy sources by 2020 [1]. This target represents a huge increase considering that the share of renewable energy is 3.8% in 2011 [1], up from 1.5% in 2005 [2]. In the meantime, the targets proposed by the UK Climate Change Committee are to reduce UK carbon emissions by 26% in 2020 and by 80% in 2050 compared to 1990 levels [3]. To meet these targets will require a radical change. Among current renewable sources, wind power is the most promising, fastest developing and cost-effective renewable energy source for electricity generation. So, wind power generation is expected to experience a rapid increase.

### *Characteristics of Wind Power Generation*

Intermittency is the inherent characteristic of wind power generation. This feature will make wind generation behaviour completely different with conventional generation sources. The output of wind power generation is characterised by high variability, depending on the availability of the energy resource. Also, this makes it difficult to perform short-term and long-term forecast of wind power generation output, which can be characterised by high uncertainty. Therefore, wind power generation is an inconstant and intermittent energy source and wind power output is constantly fluctuating.

The fluctuation of wind power output changes the system overall adequacy and security. The system will require more frequent plant start/stop, part loaded operation and additional operating reserve to ensure the system reliability.

In power systems, the system reliability relates to the existence of sufficient generating capacity within the system to satisfy the consumer load and the associated transmission and distribution networks requirements. The conventional operating reserve assessment methods have been developed and analysed in many studies, such as Percentage Reserve Margin (PRM) method, Unserved Equivalent Minutes (UEM) method and Outage Probabilistic method [4-6]. Most of them are based on deterministic or statistics and average probability values, which indicate that they do not consider stochastic influences (only suitable for particular system conditions) and cannot analyse the true reliability risk consistently. So, it is clear that the conventional operating reserve assessment methods are not able to reflect the impact of frequency and duration of wind speed variation on power output fluctuations.

Furthermore, some complex reliability assessment methodologies to determine operating reserves with increasing wind penetration have been addressed in [7-9]. These methods combined the outage frequency and duration method with the cost-benefit analysis theory to support system operators in defining the operating reserve needs, taking into account conventional generation outages, load variations and wind power output uncertainty. The combined analysis theory has been proved able to reflect the effect of wind power output fluctuation on the system reliability and associated reliability worth. However, it is critical to find a fast response, clean and sustainable energy source to generate the additional operating reserve determined by the reliability analysis theory. Consequently, the cooperation between renewable energy sources attracts the attention of system operators to meet the requirement of operating reserve.

Among the renewable sources (hydro, solar and tidal), hydro power remains the most important and the largest well-developed renewable energy source for electricity production worldwide. In order to compensate the sudden variations of wind power output, the controllable power plants must possess load following capabilities and adjust their power output accordingly. Hydro power plants equipped with pumping system has been recognized as the more capable solution of providing power compensation, as they can change their power output approximately 100% in one minute [10]. It allows the surplus of wind power production to pump water to their upper reservoirs, keeping it available to be used when more power is needed due to low wind power output.

Recently, the research area of the wind-hydro cooperation has been addressed in many published papers. The coordination between wind farms and hydro power plants is considered in generation expansion planning in [11]. In [12-14] the coordinated operation of several geographically spread wind farms and hydro power plants sharing the same transmission capacity is simulated and the effect of wind power on the market price is analysed. Several planning algorithm for hydropower systems coordinated with wind power to minimize wind curtailment and wind farm imbalance costs due to transmission congestions are presented in [15-19]. In addition, the maximization of the daily operational profit of a wind-hydro pumping/generation plant is proposed in [17]. The long-term economic feasibility of the operation of a wind farm cooperating with two water reservoirs, involving a micro-hydroelectric power plant and water pump station is discussed in [20-23]. The impacts of increasing wind penetration on the unit commitment and dispatch of the power system with pumped storage are discussed in [24, 25]. Economic benefits for the joint operation of large-scale wind farms with existing hydropower plants are analysed in [26-28].

The aims of cooperating wind and hydro power in these methods are to maximize the wind energy utilization, minimize the wind power curtailment and maximize

economic operation profits. So, the objective of these studies is mainly focused on evaluating the economic benefits from the wind-hydro hybrid operation. The impacts of wind and hydro power cooperation on the system reliability have not been fully considered.

In [29] a methodology for hydro plant and wind farm coordination is developed using a Monte Carlo Simulation technique considering the chronological variation in the wind, water and the load demand. This work has investigated the cooperation of a wind farm and hydropower plant in the system reliability evaluation. The results were mainly focused on the operation of hydro power plant, such as water in-flow rate and water reservoir volume.

However, there are very few studies about the cooperation between wind farms and hydro power plants equipped with pumping system have been reported. It is expected that the proposed cooperation can reduce the effect of wind power output fluctuation on the system reliability.

## **1.2 Challenge**

Since the cooperation of wind farms and hydro power plants equipped with pumping system have not been fully investigated, this work will develop a methodology of wind-hydro cooperation and investigate the effect of the proposed cooperation on the system reliability with increasing wind penetration. Also, the associated economic benefits of the proposed cooperation will be analysed.

Due to the intermittency and non-controllability of wind power generation, wind power output is highly fluctuating. The wind power output fluctuation may affect the overall system adequacy and security. Potential operational problems could emerge at generation/ transmission levels in power systems:

- **Generation level:** problem of generation-load balance, which can be represented by the customer load demand exceeding the total available generation due to the sudden variations of wind power output.
- **Transmission level:** wind penetration may cause increasing electric energy transmission losses at high wind power output situations.

More specifically, major areas investigated include:

***1. Determine the cooperation criterion for the wind-hydro cooperation***

The hydro power plants equipped with pumping system has been assigned to cooperate with wind power. The power output of wind generation is constantly fluctuating due to its intermittent nature. It is important to determine the cooperation criterion (*CC*) for the joint operation between wind and hydro power generation. In this work, the cooperation criterion can be represented by a percentage of the rated wind farm capacity. If the power output from the wind farm is less than the pre-determined value of *CC*, the assigned hydro power to cooperate with wind power is responsible for providing the required support.

***2. Propose an operational mode of the assigned hydro power plant equipped with pumping system***

The hydro power plant equipped with pumping system can be expressed as Pump-Hydro Energy Storage (PHES) system in electric networks. The details of PHES operation have not been investigated widely in power systems. It is critical for PHES system to propose an operational mode that could guarantee the availability of the upper reservoir, which means that the assign PHES system can cooperate with wind power output fluctuations constantly.

Accordingly, new techniques will be required to provide possible solutions for the existing challenges. Moreover, the proposed wind-hydro cooperation should be viewed from either from a system planning or system operation perspective.

## 1.3 Objectives and Research Questions

Wind power is an intermittent source of energy and its technical and financial impacts on electric networks have not totally known. It is necessary to investigate the impact of wind power on the power systems reliability. The overall aim of the thesis is to analyse the cooperation of renewable energy in electric networks with increasing wind penetration. Within this background of the thesis, the key objective of the research is to develop a new methodology of renewable energy cooperation to reduce the effect of wind power fluctuation on power systems reliability.

The objective of this thesis are realised by addressing four research questions. These research questions are outlined as follows:

***RQ 1: How to evaluate the power systems reliability with increasing wind penetration?***

Answering this question requires an adequate knowledge of power systems reliability assessment methodologies. Also, the relationship between wind speed variation and wind power output is analysed in details.

The specific processes required to respond this question include:

- Reach a deep understanding of the system adequacy & security for future reliability analysis.

- Compare the advantages/disadvantages of many popular analytical reliability assessment methods, including Capacity Outage Probability Table (COPT), Loss of Load Expectation (LOLE), Markov Chain (MC) and Frequency & Duration (F&D), including relevant literature review of the subject.
- Describe the detailed information of Monte Carlo Simulation (MCS) method, including sampling approach and terminating criteria.
- Perform a wind power output model by considering the wind speed profile, Weibull distribution function and wind turbine output model.
- Develop a combined reliability assessment methods by combining F&D method with MCS method to analyse the power systems reliability with increasing wind penetration.

***RQ 2: What is the wind-hydro cooperation and how does it reduce the effect of wind power fluctuation on the reliability?***

Wind-Hydro Cooperation (WHC) is proposed to reduce the effects of wind power fluctuations on system reliability by combining the advantages of MCS method and F&D method and the flexibility of Pump-Hydro Combined Energy Storage (PHCES) generating system. It can provide flexible, quick start generation to stabilize the intermittent power output and is also able to store excess energy.

The specific processes required to respond this question include:

- Understand the system condition that needs the assigned PHCES system to cope with the wind fluctuations.

- Investigate the impact of increasing wind penetration on the reliability in different power systems.
- Quantify the reliability improvement on reducing the effects of wind power fluctuations by using the reliability evaluation methods in *MATLAB* and identify the key cooperation parameters that drive this improvement.

***RQ 3: What influence does the wind-hydro cooperation bring to the electric transmission networks?***

Wind-Hydro Cooperation could provide fast-response, clean and sustainable energy source to generate electricity for cooperating with wind power fluctuations. However, the impacts of the increasing wind penetration and associated cooperation on electric networks are not analysed.

The specific processes of this question include:

- Study how *MATPOWER* analyses the electric network power-flows at different wind penetration levels.
- Model the short-term system operation by using *MATPOWER* software to obtain the electric energy transmission losses of each wind penetration level.
- Assess the impacts of the increasing wind penetration on electric network power-flows and the effects of WHC on reducing the electric energy transmission losses at different wind penetration levels.

***RQ 4: How does the proposed Pump-Hydro Combined Energy Storage (PHCES) system operate?***

This section of the work extends the investigation of the wind-hydro cooperation. The objective of PHCES system is to cooperate with wind power fluctuations by generating electricity when wind power output is low and pumping water back to the upper reservoir when wind power output is high. The generating-pumping process is used to guarantee the availability of the upper reservoir for cooperating with wind power output fluctuations constantly.

Addressing this question involves following objectives:

- Develop a deep understanding of the PHCES system operation and analyse the impacts of generating-pumping process on the availability of the upper reservoir.
- Develop an operation pattern for the generating-pumping process to fulfil the requirements of the wind-hydro cooperation and the availability of PHCES system.

## **1.4 Contributions**

The main original contributions of the thesis are listed as:

**Contribution 1:** The first main contribution of the work is the development of the combined reliability assessment method of Frequency & Duration (F&D) method and Monte Carlo Simulation (MCS) method, which can analyse the power system reliability in different wind penetrations. This involved the following specific contributions:

- The feature of new reliability analysis method is based on the advantages of both F&D method and MCS method. Each component in the system including wind generation can be simulated in continuously operating, repairing and maintaining power systems.
- The operation model of each component in the system is constructed by using *MATLAB* software tool with associated reliability data. It is an effective tool to analyse the intermittent nature of wind power and the impacts of wind penetration on the system reliability.

**Contribution 2:** Another key contribution of this work is proposing a Wind-Hydro Cooperation (WHC) method to reduce the effect of wind power fluctuation on power output and maintain the power system reliability. The intermittent nature of wind energy caused the high fluctuation on the system power output. It may affect the overall system reliability, which can be represented by the increasing occurrences of customer load demand exceeds the available generation output and a large amount of unserved energy due to those occurrences. The studies focus on the cooperation of Pump-Hydro Combined Energy Storage (PHCES) technology and wind power generation. The work can be explained as storing excess energy to reduce surplus wind generation at high output levels; generating electricity to compensate the output shortage due to low wind output situation. The effects of WHC method on three different power systems with increasing wind penetrations are analysed and discussed.

**Contribution 3:** The final contribution of this work is the proposal of a new operational mode of Pump-Hydro Combined Energy Storage (PHCES) system to cooperate with wind power output fluctuations. This can be achieved by modelling a weekly operation cycle with consideration of the short-term operational periods and proposing a generating-pumping process to guarantee the availability of PHCES system for the wind-hydro cooperation. The effect of this operational mode on the

electric energy transmission/distribution losses can be investigated by using *MATPOWER*.

## 1.5 Thesis Structure

Based on the objectives and the proposed methodology, this thesis consists of nine chapters. The contents are summarised as:

**Chapter 2** provides an overview of wind power generation technology. Firstly, the current worldwide wind power generation development is introduced. Then, it also explores wind power generation system, including Weibull Distribution Function, wind speed model, wind turbine output model, classification of wind farms and latest worldwide wind energy policies. Several representative power system reliability indices and mathematical model of probabilistic methods are introduced. Conventional operating reserve methods and associated impacts of wind power integration on these methods are discussed in details.

**Chapter 3** presents an important literature review of power system reliability evaluation methods. Basic theories and concepts of reliability assessment are conducted. There are two main parts of reliability evaluation: analytical methods and simulation method. Each proposed approach in this chapter contains a simple and illustrative example for understanding the methodologies. The reliability standard of power systems is also discussed in this chapter.

**Chapter 4** uses the Monte Carlo Simulation method combined with Outage F&D method to analyse the reliability assessment of a conventional power system. The test system is modified based on the Roy Billinton Test System (RBTS), which is proper for the development of basic concepts. The reliability evaluation includes two main parts: generating system output model and load demand model. The simulation

results show that the proposed approach can effectively evaluate the power systems reliability.

**Chapter 5** proposes a calculation model of wind power generation output for evaluating the impact of wind power penetration on electric networks. Weibull distribution function is described in details. Then, using the inverse transform method and Weibull distribution generates the artificial wind speed profile. Wind farm output can be calculated by using the simulated artificial wind speeds. Furthermore, the power output characteristics of multiple wind farms are also investigated for future studies.

**Chapter 6** proposes a new wind-hydro cooperation (WHC) method to reduce the effects of wind power fluctuations on system outputs and maintain the system reliability. The detailed explanation of the mathematical model and the entire simulation procedure including flow charts are presented. Pump-Hydro Combined Energy Storage (PHCES) system is introduced in details. The modified Roy Billinton test system (MRBTS) is applied to illustrate the proposed WHC method at two different wind penetration levels. The final section of this chapter presents a generating-pumping process in the operational mode of PHCES system.

**Chapter 7** investigates the application of WHC in a large power system (modified IEEE 118-Bus test system) and discusses the simulation results. This chapter is divided into two parts: long-term system planning and short-term operation planning. Four different types of wind penetration (low, medium, high and extreme high level) are discussed in details. The simulation results indicate that WHC method is able to make a great contribution for reducing the effects of wind power fluctuations on system outputs and maintain the reliability in long-term system planning and is also effective for short-term operation planning by reducing the electric energy transmission/distribution network losses.

**Chapter 8** applies the proposed WHC method to a practical power system (eastern Gansu power grid) for solving the actual system-planning reliability problems. First, the situations of conventional generation, hydropower, wind power generation and PHCES system are introduced. Then, the development of wind power integration in eastern Gansu power grid is described. The application results prove that WHC is an effective tool for eastern Gansu power grid to solve the development of the electricity market with increasing wind penetration.

**Chapter 9** summarizes the conclusions of this thesis and discusses possible future works.

The main document is complemented by several Appendices.

**Appendix I:** A comparison of individual, cumulative & complementary cumulative probability.

**Appendix II:** Matlab codes for system load model in Chapter 4.

**Appendix III:** Matlab codes for conventional generator power output model in Chapter 4.

**Appendix IV:** Reliability indices of all cooperation scenarios (CS) in modified Roy Billinton Test System at 10% wind penetration level, which are used in Chapter 6.

**Appendix V:** Reliability indices of all cooperation scenarios (CS) in modified Roy Billinton Test System at 15% wind penetration level, which are used in Chapter 6.

**Appendix VI:** Wind power output data for 1 week (168 hours), which are used in Chapter 6.

**Appendix VII:** Generators' output data in the modified IEEE 118-bus test system, which are used in Chapter 7.

**Appendix VIII:** Reliability indices for all cooperation scenarios in 10%, 15%, 20%, 25%, 30% and 40% wind penetrations, which are used in Chapter 7.

**Appendix IX:** Wind power output data (in percentages (%) of the rated output) in 10% wind penetration, which are used in Chapter 7.

**Appendix X:** Electric network losses in 10%, 15%, 20% and 25% wind penetrations, which are used in Chapter 7.

**Appendix XI:** Electric network losses with WHC method in 10%, 15%, 20% and 25% wind penetrations, which are used in Chapter 7.

**Appendix XII:** Electric network losses in 10%, 15%, 20% and 25% wind penetrations in the Five-wind farm case, which are used in Chapter 7.

## 1.6 Publications

Based on the results of the research work reported in this thesis, the following papers have been published:

- Shuai Shi and K. L. Lo, “*Reliability assessment of power system considering the impact of wind energy*”, in *Universities Power Engineering Conference (UPEC2012)*, London, 47<sup>th</sup> International 2012
- Shuai Shi and K. L. Lo, “*An overview of wind energy development and associated power system reliability evaluation methods*”, in *Universities Power Engineering Conference (UPEC2013)*, Dublin, 48<sup>th</sup> International 2013
- Shuai Shi and K. L. Lo, “*Application of Monte Carlo Simulation in Power System Reliability Evaluation with Increasing Wind Penetration*”, under preparation for journal submission (expected submission date: October 2014)
- Shuai Shi and K. L. Lo, “*Optimization of Pump-Hydro Energy Storage Operation in a Wind-Hydro Hybrid System*”, under preparation for journal submission

# **Chapter 2. Wind Energy and the Associated Issues of Wind Power Integration**

## **2.1 Introduction**

Global environmental concerns associated with conventional energy generation have led to the rapid growth of renewable energy in power systems. Nowadays renewable resource integration plays an important role to reduce dependence on fossil fuels and greenhouse gas emissions. Many countries have implemented policies to encourage renewable energy, such as the Renewable Portfolio Standard (RPS) [30]. Acceptance of the RPS is a commitment to produce a specified percentage of the total power generation from renewable sources within a certain date. In order to meet the RPS, a significant amount of renewable generation, including wind, solar and geothermal generation resources need to be developed. Among these many renewable resources, wind power is the most promising renewable energy source for the sustainable development due to its advanced and mature technologies, as well as the promising commercial prospects.

The development of wind power has fluctuated with oil prices. The technology of wind power was first boosted during the 1970s oil crisis; later, the market began to stagnate. During the last decade, due to the encouraging policies adopted by many countries in the world, wind energy has experienced an important evolution over time. The traditional wind energy markets are mostly located at Europe and North America. However, there are some new wind energy markets developing very fast, such as China, India and Brazil. Over the last decade, the world's wind power

generation capacity has been growing at an incredible speed, with an average annual growth of about 30%.

It is known that wind power generation is an inconstant and intermittent energy source. Therefore, wind behaviour is quite different from that associated with conventional generation sources. Due to the variable and intermittent nature of wind, there are many considerations when incorporating wind power in power systems reliability assessment. There is a wide range of studies focusing on the impact of wind energy on system reliability evaluations. The studies show that the contribution of wind energy to the reliability performance of a generation system can be quantified and is highly dependent on the wind region conditions. Wind energy can make a significant reliability contribution given a highly stable wind speed. Also, high wind penetration can lead to high risk levels in power systems reliability.

The basic factor of power system expansion is the comparison between the wind power generation and the traditional power generation in aspect of capacity. The capacity credit is a straightforward way to compare these two types of power generation [31]. Capacity credit of wind power generation can be defined as the amount of conventional power generation capacity that can be replaced with wind power generation capacity, while maintaining the existing levels of security of supply [32-34]. For instance, 1000 MW of installed wind power with a capacity credit of 20% can avoid a 200 MW investment in conventional power.

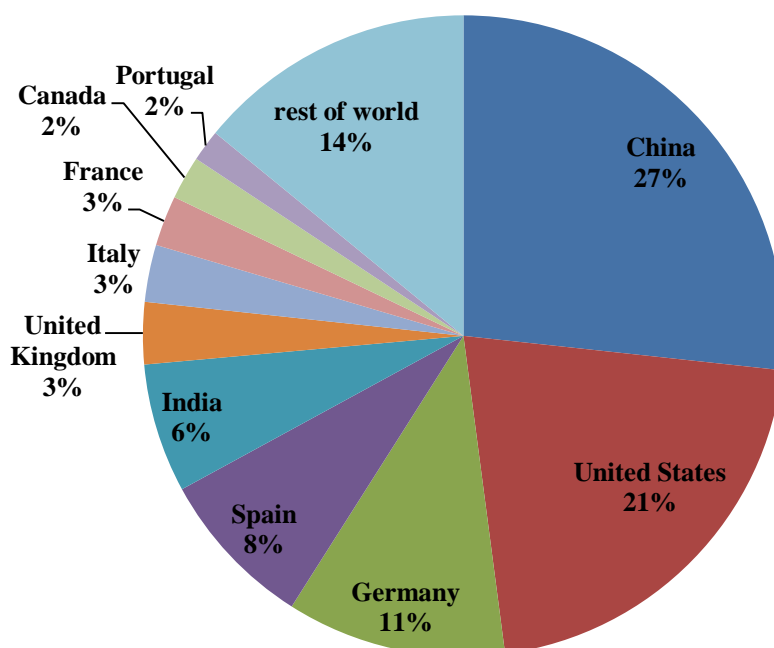
Power systems must have enough generation to meet the load demand at each moment and also have enough reserve to deal with unexpected contingencies. Recently the increase in the penetration level of wind power generation has led to a lot of challenges in the calculations of power systems reliability assessment. The most important calculation in this field is the capacity credit of wind power generation [32]. Unfortunately, the capacity credit of wind power generation is not a fixed value due to the wind power output fluctuation. So, it is necessary to

investigate the operating reserve (OR) to accommodate the wind power output fluctuation.

This chapter presents an overview of wind energy development and the associated integration impacts on power systems reliability. The development and benefits of wind energy are briefly described in *section 2.2*. In *section 2.3*, it introduces the current status of wind power worldwide, including several of the most representative countries in world wind markets. *Section 2.4* and *2.5* present the wind turbine technology and wind power generation models. Some popular wind power policies are discussed in *section 2.6*. The basic concepts and reliability indices of power system reliability evaluation are explained in details in *section 2.7*. *Section 2.8* presents several power system operating reserve assessment methods. The associated operating reserve (OR) assessment for wind power generation and a review of hydropower generation are also explained in this section.

## **2.2 Wind Energy Development and Benefits**

There are almost two hundred thousand wind turbines operating, with a total installed capacity of 282,482 MW as of the end of 2012 [35]. According to the World Wind Energy Association, wind power generated about 2.5% of worldwide electricity usage [36], up from 1.5% in 2008 and 0.1% in 1997 [37]; the number can be expected to increase by 8- 12% in 2020. World wind generation capacity is more than quadrupled between 2000 and 2006, doubling approximately every three years [38]. The annual growth of Chinese wind market is 39.4% in 2011. Wind energy has now become an important player in the world's energy markets. In terms of economic value, the global wind market is estimated to be worth about \$36 billion per year in new generating equipment [39]. The ten most leading countries around the world in wind power industry are represented by percentages of the total installed capacity, which shown in *Figure 2.1* and *Table 2.1*.

**Top 10 Countries by Installed Wind Power Capacity**

*Figure 2.1: Top 10 Countries by Installed Wind Power Capacity as End of 2012 [35]*

*Table 2.1: Top 10 Countries by Installed Wind Power Capacity as end of 2012 [35]*

Country	Installed Wind Power Capacity (MW)	% Share
China	75,564	26.8
United States	60,007	21.2
Germany	31,332	11.1
Spain	22,796	8.1
India	18,421	6.5
United Kingdom	8,845	3.0
Italy	8,144	2.9
France	7,196	2.5
Canada	6,200	2.2
Portugal	4,525	1.6
Rest of world	39,853	14.1
<b>World total</b>	<b>282,482 MW</b>	<b>100%</b>

Wind energy is the most promising renewable energy source than other sources. It can be seen from the results of *Figure 2.2* and *Table 2.2*. The growth trend shows how dramatically wind energy grew over the last decade. The annual growth rate of wind power is higher than any other generation sources. It has remained at approximately 20% per year even when the total installed capacity has reached a significant level in power systems.

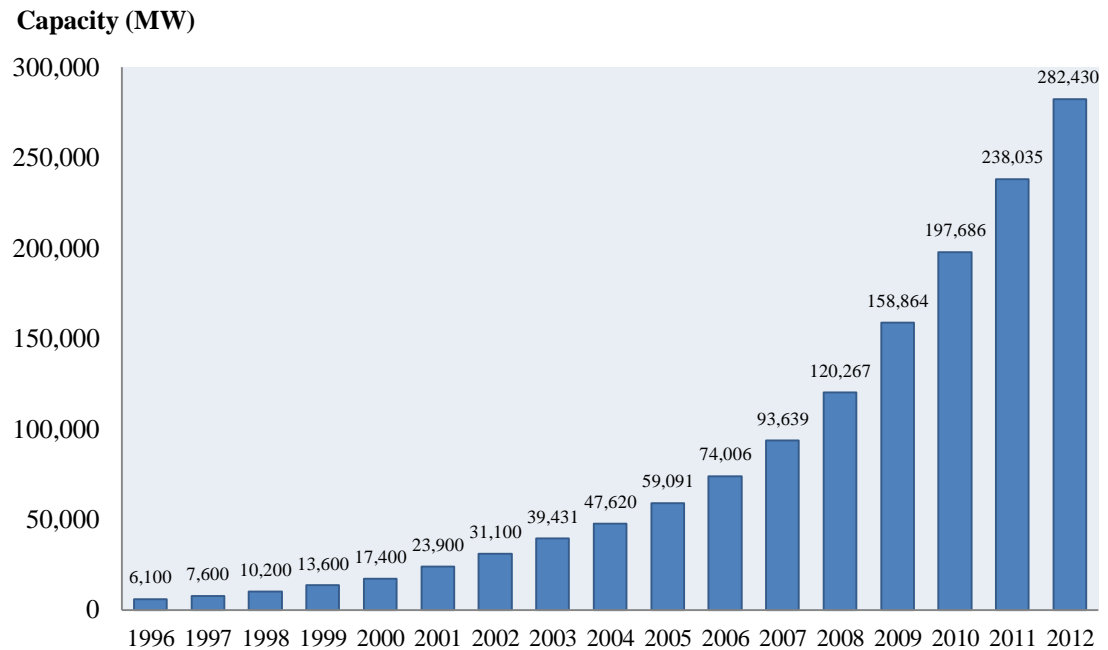


**Figure 2.2: Global Total Installed Wind Capacity 1996-2012**

**Table 2.2: Annual Growth Rate (%) of Installed Wind Capacity 1999-2012**

Year	<b>1999</b>	<b>2000</b>	<b>2001</b>	<b>2002</b>	<b>2003</b>	<b>2004</b>	<b>2005</b>
Growth Rate (%)	33%	28%	37%	30%	27%	21%	24%
Year	<b>2006</b>	<b>2007</b>	<b>2008</b>	<b>2009</b>	<b>2010</b>	<b>2011</b>	<b>2012</b>
Growth Rate (%)	25%	27%	28%	32%	24%	20%	19%

Wind power generation is a fast-growing industry. It is one of the cleanest and most abundant forms of renewable energy. In fact, new researches show that the global wind resources are significantly greater than previously estimated due to better wind

turbine technology and more refined wind measurements [40]. The development of wind power generation is driven by following benefits [41-44]:

- **Clean & Renewable:** wind power is a clean and renewable energy source. Electricity generated from wind turbines does not have environmental pollution. A single 1 MW wind turbine can displace 1,800 tons of carbon dioxide (CO<sub>2</sub>) in 1 year (equivalent to planting 1 square mile of forest). Unlike conventional fossil fuels, wind energy is inexhaustible, abundant energy that will be available for future generations.
- **Economic competitiveness:** with today's rising coal and fuel prices, wind power becomes more competitive compared with conventional generation. It is expected that cost reductions will continue as the technology improves and new market develops. Moreover, wind turbines require minimal maintenance and have lower operating costs.
- **Secure:** wind energy is an indigenous energy source that contributes to national security. Wind power generation can reduce vulnerability to price spikes and fossil fuel supply disruptions.
- **Efficiency:** wind power farms generate between 17 and 39 times as much power as they consume, compared to 16 times for nuclear plants and 11 times for coal plants.
- **Water conservation:** unlike most other electricity generation sources, wind turbines do not need to consume water for generating electricity. Irrigation and thermal electrical generation account for nearly 77% of United States fresh water use. Conventional plants generate power from fossil fuels and nuclear materials, which use large amount of water for cooling; the operations of wind turbines do not need water.

- **Create jobs:** wind energy development creates thousands of long-term, high-paying jobs in fields such as wind turbine component manufacturing, construction and installation, maintenance and operations, legal and marketing services, transportation and logistical services, and more. There are over 670,000 workers employed worldwide by the wind industry in 2011.

## 2.3 Status of Wind Power Worldwide

Although the cumulative installed wind power capacity is still increasing, wind energy changes to a steady development from the rapid expansion. From *Table 2.2*, the annual growth rate of installed wind power capacity began to decrease since 2010. According to Global Wind Energy Council report in 2012, the new installed capacity from January to December 2012 is 44.7 GW; China, European Union and USA still dominate world wind energy development. They have up to 73.5% share of world wind energy market, which shown in *Table 2.3*.

*Table 2.3: New Installed Wind Power Capacity Jan- Dec 2012 [35]*

Country	Capacity (MW)	%Share
China	13,200	30
USA	13,124	29
EU	6,731	14.5
India	2,336	5
Brazil	1,077	2.4
Canada	935	2.1
Romania	923	2.1
Rest of the World	6,385	14.3
<b>Total Top 3</b>	<b>33,055</b>	<b>73.5</b>
World Total	44,711	100

Unlike the traditional markets in Europe and United States, new wind energy markets play an important role in promoting the development, such as India, Canada and Brazil. The local governments in these countries encourage the development by enacting renewable energy laws. Now, wind energy development becomes a part of the most dynamically growing markets in the world.

The following parts introduce the wind development situation of most representative countries on the world.

### **2.3.1 Leader in Wind Power Installed Capacity- China**

China overtook the place of the United States as the leading total installed capacity of wind power generation in 2010; the installed wind capacity added 16.5 GW over that year, a 64% increase over 2009 [45]. At the end of 2012, the total wind capacity is 75,564 MW in China [35]. *Figure 2.3* and *Table 2.4* show the data of China's installed capacity during the last 7 years [35, 46]. Compared with 2,537 MW in 2006, the installed capacity has increased with an average annual growth rate of 83.9% during the last 7 years. However, the development of installed capacity seems to slow down in the recent 3 years. For instance, the annual growth rate in 2012 is only 21%. It is because the Chinese government started to consider the economic return aspects of the wind energy development.

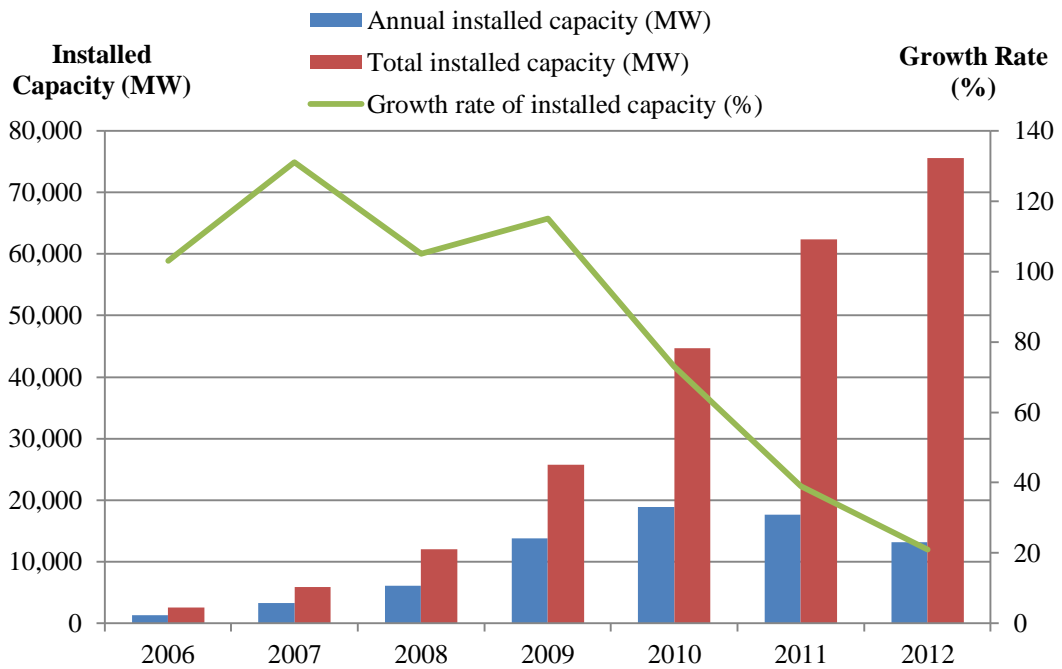


**Figure 2.3: Wind Power Installed Capacity and Growth Rate from 2006 to 2012**

**Table 2.4: Wind Power Installed Capacity and Growth Rate from 2006 to 2012**

Year	Annual installed capacity (MW)	Total installed capacity (MW)	Growth rate of installed capacity (%)
2006	1,288	2,537	103
2007	3,311	5,848	131
2008	6,153	12,002	105
2009	13,803	25,805	115
2010	18,928	44,733	73
2011	17,631	62,364	39
2012	13,200	75,564	21

Chinese government's wind power development strategy is to construct large-scale power base in wind-rich areas and transmit power to the load centres. Besides, the source of wind energy is abundant in China, second to the capacity of the US. The total potential wind capacity of China for both onshore and offshore is around 700-1,200 GW, according to the third National Wind Energy Resources Census [47]. It is

hoped that wind power will play a major part in China's energy structure in the middle of this century with government support and enterprises' enthusiasm [46, 48].

### **2.3.2 Leader in Wind Power Electricity Production- United States**

Although the United States' wind power installed capacity was surpassed by that of China in 2010, up to 5.1 GW were installed in the USA in 2011, making the total installed capacity 60 GW at the end of 2012 [35, 47]. In 2011, wind power electricity production is over 120 TWh, which is 26.2% of world total wind power electricity production. Currently, USA is world No.1 in total wind power electricity production and No.2 in total wind installed capacity [49].

2009 was a record year for the US wind energy industry; its new annual installed capacity was more than 10 GW with the support of the federal tax policies. Despite the growth rate slowed down in 2010, the 1.2 GW of new installed wind capacity in the first half of the year can still generate enough electricity for 9.7 million homes [36, 47]. It is estimated that by 2030, wind energy will generate 20% of the US electricity, while now it only provides 2% of the country's electricity.

### **2.3.3 Leader in Wind Penetration level- Denmark**

Wind power penetration can be specified for different scales of duration. On an annual basis, a number of countries are beginning to achieve relatively high levels of wind power penetration in their electricity grids; end-of-2011 wind penetration levels: Denmark -26%, Portugal-19%, Spain-19%, Ireland-18% and Germany-11% [50]. The wind penetration level in this thesis is defined as the ratio of the installed wind generation capacity to the total-installed system generation capacity (includes installed wind capacity and other conventional generation capacities). Moreover,

Danish government is the first government to announce a target of weaning off fossil fuels by 2050. At that time, the Danish energy system will consist purely of renewable energy, with wind power being the main contributor [51]. The data mean that Denmark took the No.1 place in world wind penetration and also for its wind turbine industry.

Accordingly, the wind penetration may divide into four ranges for future studies:

- Low level ( $\leq 15\%$ ): several countries have been accomplished this target.
- Medium level (15%~25%): few countries can reach this target.
- High level (25%~30%): only Denmark has been accomplished this penetration level.
- Extreme high level ( $>30\%$ ): there is no country that can reach this penetration level.

### **2.3.4 Leader in Offshore Wind Energy- United Kingdom**

While onshore wind energy is developing by leaps and bounds, in the meantime, offshore wind has also attracted people's attention in recent years. Offshore wind has many advantages compared with its onshore counterpart. It can provide greater electricity production due to stronger and more continuous wind. Huge potential offshore wind resources make it possible to build larger wind farms. The offshore wind turbines are far away from the shore and human life that the issues of visual impact and noise can be ignored.

Europe has always been the leader in offshore wind technology and has developed much faster than other regions. The largest offshore wind farms are all distributed in

Europe. The UK has some of the best wind resources in Europe and is the world leader in offshore development [52]. From *Table 2.5*, it is obvious that United Kingdom is the leader in offshore wind energy development, with the largest installed capacity. The newly installed capacity in 2012 is 854.2 MW, which is 66% of the world's total annual installed capacity [35]. It is predicted that the total installed capacity of offshore wind in the UK will reach 20 GW in 2020 [47].

**Table 2.5: Global Offshore Wind Installed Capacity**

Country	Total installed capacity 2011 (MW)	New installed capacity 2012 (MW)	Total installed capacity 2012 (MW)
<b>UK</b>	<b>2,093.6</b>	<b>854.2</b>	<b>2,947.9</b>
Denmark	874.3	46.8	921.1
China	262.6	127	389.6
Netherlands	246.8	0	246.8
Germany	200.3	80	280.3
Belgium	195	184.5	379.5
Sweden	163.7	0	163.7
Finland	26.3	0	26.3
Ireland	25.2	0	25.2
Japan	25.2	0.1	25.3
<b>Total</b>	<b>4,113</b>	<b>1,292.6</b>	<b>5,405.6</b>

## 2.4 Wind Turbine Technology

A wind turbine is a device that converts kinetic energy from the wind, into mechanical energy for electricity production. Modern wind turbines are predominantly based on aerodynamic lift. Lift force use aerofoils (blades) that interact with the incoming wind. Wind turbines using aerodynamic lift can be further divided according to the orientation of the spin axis into horizontal-axis and vertical-axis type turbines [53, 54]. Most of the currently installed wind turbines have a horizontal axis. Horizontal-axis wind turbines typically use a different number of blades, depending on the purpose of the wind turbine. Two- or three-bladed turbines are usually used for electricity power generation [53]. Currently, three-bladed wind turbines dominate the market for grid-connected, horizontal-axis wind turbines. The turbines are better to handle and have lower noise level than two-bladed wind turbines. Two-bladed wind turbines have the advantages of lighter weight and lower related costs. As noise levels are less important offshore, the lower costs might be attractive and lead to the development of two-bladed turbines for the offshore market [55].

Main components of a wind turbine include blades, rotor, gearbox, brake, regulation system and generator. The generator can operate either with a fixed speed or a variable speed. The fix-speed wind turbine has the advantages of being simple, reliable and well proven. Its disadvantages are uncontrollable reactive power consumption, mechanical stress and limited power quality control [56]. During the past few years, the variable-speed wind turbine has become the dominant type among the installed wind turbines. It is designed to achieve maximum aerodynamic efficiency over a range of wind speeds and has improved power quality. The disadvantages are losses in power electronics, the use of more components and the increased cost of equipment due to the power electronics [56].

The wind turbine technologies have developed for over a hundred years since 1900. Nowadays, there are more than 200,000 wind turbines operating around the world [57]. Typical modern wind turbines have diameters 40 to 100 metres and are rated between 500 kW and 3 MW. The most powerful wind turbine model is *E-126* manufactured by the German wind turbine producer *Enercon*. It has a rated capacity of 7.5 MW and a diameter of 127 m [58]. Wind turbines' rated capacities may develop larger, and the related operating costs may continue to drop in the future due to mature and advanced technologies. Now, at least five popular wind industry companies are working on the development of a 10 MW turbine.

## 2.5 Overview of Wind Power Generation

A wind energy conversion system (WECS) model consists two main parts, the wind speed model and the wind turbine generator (WTG) model [59]. Different models have been used to represent wind speeds and simulate wind power [60, 61]. There is a nonlinear relationship between the power output of the WTG and the wind speed, which can be described by the operating parameters of the WTG. Three commonly used parameters are the cut-in, rated and cut-out wind speeds [62].

### 2.5.1 Wind Speed Model

The power output from a wind turbine generator (WTG) at a specific site is highly dependent on the wind regime at that location. There are a number of wind speed models in power system reliability evaluation [38, 63, 64]. Six of the most popular models can be briefly described as follows.

#### *I. Observed Wind Speeds*

This model uses an observed hourly wind speed data set repetitively in the reliability evaluation process.

## ***II. Mean Observed Wind Speeds***

It uses the hourly mean observed wind speed data set repetitively in the reliability evaluation process. The mean observed wind speed for each hour is calculated based on different annual wind speed data sets.

## ***III. ARMA Model***

In statistics and econometrics, an autoregressive integrated moving average (ARIMA) model is a generalization of an autoregressive moving average (ARMA) model [65]. These models are fitted to time series data either to use a mathematical model to simulate the sequence or to predict the future values of the time series [66]. There are three parameters in an ARIMA ( $p, d, q$ ) model where  $p$ ,  $d$  and  $q$  are non-negative integers that refer to the order of the autoregressive, integrated and moving average parts of the model. When one of the three parameters is zero, it is usual to drop “AR”, “I” or “MA”. For instance, ARIMA(0, 0, 1) is MA and ARIMA (1, 0, 1) is ARMA [65].

This model uses the autoregressive moving average (ARMA) time series to predict wind speeds in the reliability evaluation process [59]. The general expression is as follows:

$$y_t = \phi_1 * y_{t-1} + \phi_2 * y_{t-2} + \dots + \phi_n * y_{t-n} + \alpha_t - \theta_1 * \alpha_{t-1} - \theta_2 * \alpha_{t-2} - \dots - \theta_m * \alpha_{t-m} \quad (2.1)$$

Where  $y_t$  is the time-series value at hour  $t$ ,  $\phi_i$  ( $i=1, 2, 3 \dots n$ ) and  $\theta_j$  ( $j=1, 2, 3 \dots m$ ) are the autoregressive and moving average parameters of the model respectively, which can be estimated by computer program using the algorithm provided in [67];  $\{\alpha_t\}$  is a normal white noise process with zero mean and a variance of  $\sigma_a^2$  (i.e.,  $\alpha_t \in NID(0, \sigma_a^2)$ ), where normal independent distribution is denoted NID.

The hourly wind speed  $SW_t$  at hour  $t$  is obtained from the mean wind speed  $\mu_t$ , its standard deviation  $\sigma_t$  and the time-series  $y_t$ , as shown in

$$SW_t = \mu_t + \sigma_t y_t \quad (2.2)$$

From *Equation 2.1* and *Equation 2.2*, it can be seen that the ARMA model is formed based on the observed wind speed data and incorporates the yearly wind speed variations.

#### ***IV. 6-step Common Wind Speed Model***

The determination of a proper wind speed model for a wind farm location is a complicated process as described in *ARMA Model*. It requires historical wind speed data collected over a significant period. It would be very helpful for practical power systems if a common wind speed model can be used to obtain power output from wind turbines at different sites with reasonable accuracy [67]. This model is based on the *ARMA* model and details are presented in [67, 68]. The only data required are the annual mean wind speed  $\mu$  and the standard deviation  $\sigma$  for that site. The results from those research works proved the model can be used in the reliability evaluation process with reasonable accuracy.

#### ***V. Markov Chain Model***

The wind speed is represented by a Markov chain with a finite number of states. This method in reference [60] introduces a wind speed model which considers not only the probability but also the frequency and duration characteristics of wind speed. Parameters can be calculated using the observed wind speeds. The transition rates between wind speed states are needed in order to simulate wind speeds in the reliability evaluation process.

## ***VI. Weibull Distribution***

Weibull distribution can be used to represent many different distribution characteristics by appropriate adjustment to its parameter  $c$  and  $k$ . The wind speed is simulated using Weibull distribution and used in a sequential Monte Carlo simulation process. The only data required are the mean wind speed and shaping parameter  $k$ , which is normally set to 2 [38].

As shown in *Table 2.6*, it shows that Observed wind speeds model is the basic part for wind speed modelling. ARMA model is formed based on the Ob model, which provides a more comprehensive representation of wind speeds. Then, the 6-step common wind speed model is an extension of ARMA model, which is useful for prospective wind farm locations lacking adequate historical data. Markov chain model considers not only the probability but also the frequency and duration characteristics of wind speed. But it only can represent wind speeds with a finite number of states.

Weibull distribution combined with Monte Carlo simulation method shows an excellent performance on wind speeds modelling. It can accommodate the wind speed fluctuation by modifying the parameters. Therefore, it is accepted that this model can be used to simulate the wind speed variation characteristics. Further details will be described in Chapter 5.

**Table 2.6: Comparison of Different Wind Speed Models**

<b>Wind Speed Model</b>	<b>Advantages</b>	<b>Disadvantages</b>
<b>Observed wind speeds (Ob)</b>	Easy and straightforward	Highly dependent on the wind regimes in the years utilized, particularly when only a small number of years of data are used
<b>Mean observed wind speeds (Mob)</b>	Better performance than Ob method, if the mean wind speed is close to the actual wind speed	The differences are more considerable when a site has a better wind regime
<b>ARMA model</b>	Provide a more comprehensive representation of wind speeds than Ob method; the most suitable model for use in a sequential simulation process	Complex computation process and difficult to change time intervals of wind speeds if lack of historical wind speed data
<b>6-step common wind speed model</b>	Can be applied to obtain a wind speed model for any geographic location if the mean wind speed and standard deviation are known	The accuracy of the wind speed model can only maintain at a reasonable level
<b>Markov Chain model</b>	Consider not only the probability but also the frequency and duration of wind speeds	It only has a finite number of states, which makes it inefficient for actual wind speeds fluctuation
<b>Weibull Distribution</b>	Can be shaped to represent wind speed variation; the simulated results are close to actual wind speed profiles by using Monte Carlo simulation for massive calculation	The accuracy of wind speed model is limited by the Weibull parameters

## 2.5.2 Wind Turbine Output Model

It is important to accurately assess the electric power generated by a wind turbine generator at a specific location in power systems reliability analysis. Wind energy is completely different from other conventional energy sources. The power output of a WTG can be determined from its power curve, which has a nonlinear relationship between the wind turbine output and the wind speed [38]. *Fig 2.4* shows a typical power curve of a WTG. There are three primary parameters for the output model: cut-in speed, rated speed and cut-out speed. Cut-in speed is the minimum wind speed that can drive wind turbine blades to generate electricity. Rated speed makes the WTG works at rated power output. Maximum wind speed limit for the WTG is cut-out speed. Wind speed beyond the designed maximum speed can lead load turbulence and cause blades damage. For example, the cut-in, rated and cut-out speed in *Fig 2.4* shown as 3.5 m/s, 14 m/s and 25 m/s.

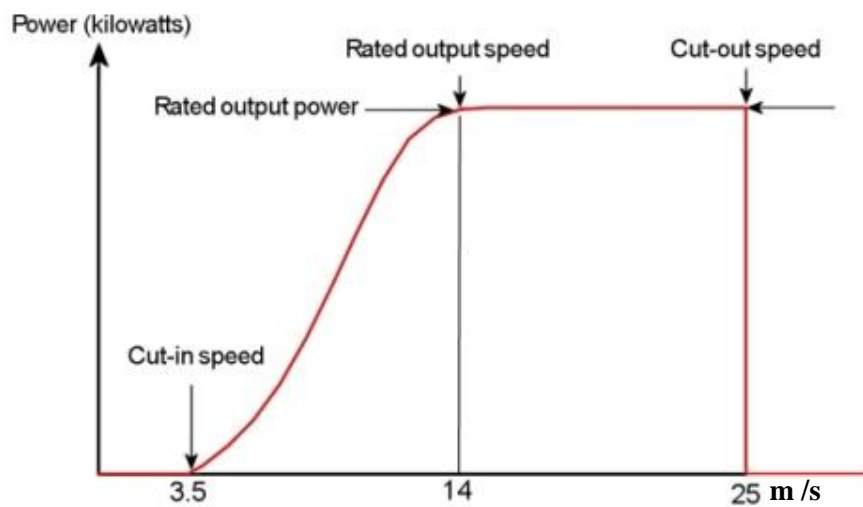


**Figure 2.4: Wind Turbine Power Output Curve [69]**

The wind power output characteristics have two distinct regions: one is the interval between cut-in and rated wind speeds in which the power output increases with wind speed (known as maximum power output region); another is the interval between rated and cut-out wind speeds when the power output is maintained constant at the rated value (known as power regulation region) [70].

The wind power output characteristics can be described in a general expression as *Equation 2.3*.

$$P_w = \begin{cases} 0, & ws < V_{ci} \\ (A + B * ws + C * ws^2) * P_{wr}, & V_{ci} \leq ws < V_r \\ P_{wr}, & V_r \leq ws < V_{co} \\ 0, & ws \geq V_{co} \end{cases} \quad (2.3)$$

Where:

$ws$  = the wind speed (m/s)

$V_{ci}$  = cut-in speed of the WTG (m/s)

$V_r$  = rated speed of the WTG (m/s)

$V_{co}$  = cut-out speed of the WTG (m/s)

$P_{wr}$  = rated power output of the WTG (MW)

The constants A, B and C are presented in [62], which can be calculated by using the cut-in, rated and cut-out wind speeds. Further details about the power output of wind farms will be illustrated in Chapter 5.

### 2.5.3 Classifications of the Wind Farm

According to the textbook of Environmental Impact Evaluation of Construction Project in 2011, which is approved by China Appraisal Centre for Environment & Engineering Ministry of Environmental Protection, wind farms can be classified into three groups in *Table 2.7*.

**Table 2.7: Classifications of the Wind Farm**

Classification	Annual mean wind speed
1 <sup>st</sup> Class	10 m/s
2 <sup>nd</sup> Class	8.5 m/s
3 <sup>rd</sup> Class	7 m/s

*Figure 2.5* shows a map of the annual mean wind speed in the United Kingdom. Some sites are windier than others. A lowland site in the middle of southern England might have an average wind speed of 6 m/s, whereas an exposed site in Scotland might have an average wind speed of 9m/s.

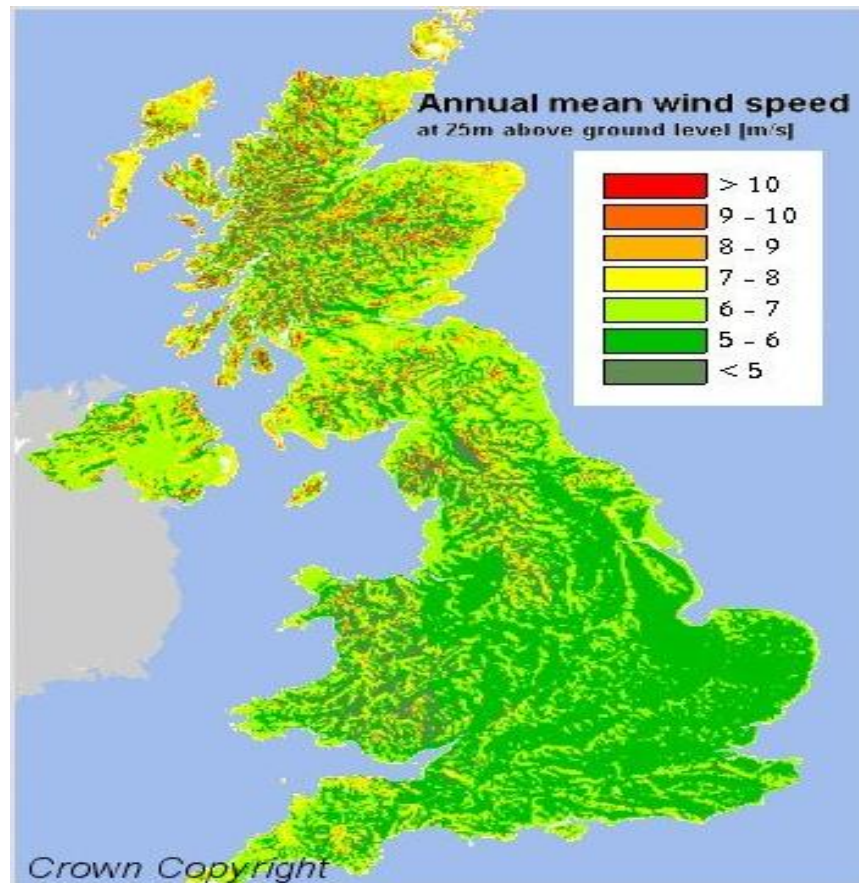


*Figure 2.5: UK Annual Mean Wind Speed at 25m above Ground Level [69]*

## 2.6 Policies for Wind Energy

The development of renewable energy technologies is strongly driven by the energy policies. The role of the governments is critical in the development and is able to attract large investments to the sector. Support schemes differ noticeably between different markets, and most of the countries have several different support schemes. Also, it should be noted that support for renewable energy sources through an incentive or subsidy is often a necessity, but never a sufficient condition.

The cost of wind energy has declined significantly over the past few years. In some locations, wind is now competitive with conventional generating sources including gas. The reasons for this include a technically advanced and mature supply chain at a global scale. The most representative renewable energy support mechanisms are described in details in [30, 62, 71, 72].

- *National Renewable Energy Targets*

National renewable energy targets (NRET) (also called mandatory renewable energy targets (MRET), renewables portfolio standards (RPS), or purchase obligations) are a new policy mechanism, which is being used in several countries. This policy requires that a fixed percentage of electricity in each retail supplier should be generated by renewable resources. It has been implemented as RPS in 21 US States, as the national MRET in Australia, and as a Renewables Obligation in the UK.

The American Wind Energy Association (AWEA) seeks a target for 20% of the nation's electricity to come from wind energy by 2030 [73]. Germany has pushed strongly for the development of renewable energies and their integration into the existing network. Germany's federal goal is to achieve 30% of its electrical power generation from renewable sources by 2020 with a long term goal of 50% by 2050 [30].

- ***Local Content Requirements***

This policy mandates a certain percentage of local content for wind turbine systems installed in some or all projects within the country. Spanish government agencies have mandated the incorporation of local content in wind turbines installed on Spanish soil. Local content requirements are currently being used in Canada, Brazil, China and Spain. The potential genitive impact of this policy on market competitiveness has been raised in Canada and China. Therefore, this policy can work but should apply in markets with sufficient market potential.

- ***Financial and Tax Incentives***

Financial incentives may include awarding developers with low-interest loans for project financing or providing financial subsidies to developers. Tax incentives can be used to encourage local companies to get involved in the wind industry.

Canada has implemented a tax credit on wages paid out to the local labour to encourage large wind turbine manufacturers to shift jobs to Canada. Australia, China, and many US states have also employed plenty of different tax incentives to encourage the wind development. In September 2001, the Chinese government reduced the value-added tax (VAT) for wind power from 17% to 8.5% [74].

- ***Research and Development (R&D)***

Sustained public research support for wind turbines can be crucial to the success of domestic wind industry. R&D has been found to be most effective when private wind companies cooperate with public institutions like national laboratories and universities. The Japanese government has investigated the feasibility of offshore projects, and an R&D project was expected to start in 2008 [75]. The barriers to the development of offshore wind farms in Japan are social issues, such as public acceptance and compensation for the fishery industry. Also, it has planned to start R&D for deep offshore wind technology to capture the potential wind resources in deep offshore areas around Japan.

- ***Feed-in Tariffs***

Feed-in Tariffs for wind power set to encourage the development of wind energy through government legislation. It requires electricity utilities to purchase electricity generated from renewable sources at above market rates (set by the government). It has been shown to be one of the most effective ways to develop wind projects as this policy can directly provide a stable and profitable market for the development.

The level of tariff and its characteristics depend on the specific country with consideration. If it is designed to have a long term reach and sufficient profit, feed-in tariffs will be extremely valuable for encouraging wind energy industries to invest in wind technology innovation. Germany, Denmark and Spain have been the most successful countries at creating stable markets for wind power; all three of these countries also have a history of stable and profitable feed-in tariff policies to promote wind energy development. Moreover, Japan, Brazil and some regions in China have also experimented with feed-in tariffs, with varying levels of success [30, 46].

***Table 2.8: Major Policy mechanisms and support schemes used in 9 wind markets[71]***

	National targets	Local content requirements	Incentives	R & D	Feed-in Tariffs	Priority access to the grid
China	✓	✓		✓	✓	✓
Denmark	✓		✓	✓	✓	✓
Germany	✓	✓		✓	✓	✓
India	✓	✓	✓	✓	✓	
Italy	✓			✓		✓
Portugal	✓			✓		✓
Spain	✓	✓		✓	✓	✓
UK	✓			✓	✓	✓
USA	✓	✓	✓	✓		

## **2.7 Impacts of Wind Power Integration on Power Systems Reliability**

Wind power generation is an inconsistent and intermittent energy source. The fluctuation of wind speed is constant and also depends on the wind farm location. It means that the power output from the wind turbine also fluctuates. The generation fluctuation of intermittent sources can harm the reliability level of power systems. Due to this situation, it is necessary to study the impacts of wind energy on power systems reliability.

### **2.7.1 Basic Concepts of Power Systems Reliability Analysis**

Power system reliability analysis can be divided into two aspects: system adequacy analysis and system security analysis.

The concept of adequacy is considered to be the existence of sufficient facilities within the system to satisfy the consumer demand. The facilities include those necessary to generate sufficient electricity to the actual consumer load points and the associated transmission and distribution networks requirements. Therefore, it is related to static conditions that do not include system dynamic disturbances [76]. Security is considered to relate to the ability of the system to respond to disturbances arising within the system. Therefore, it is associated with the response of the system to disturbances [76].

The reliability analysis in this thesis focuses on the generation adequacy issues considering wind power integration. So, the term ‘reliability’ used in this thesis means the system adequacy.

A modern power system is complex, highly integrated and is very large. However, the system can be divided by its intended functions. The functional zones of a power system (generation, transmission and distribution) have three hierarchical levels shown in *Figure 2.6*. The first level (HLI) relates to generation facilities, the second level (HLII) refers to the integration of generation and transmission, and the third level (HLIII) refers to the complete system including distribution [77]. This thesis only focused on the first level (HLI) of power systems.

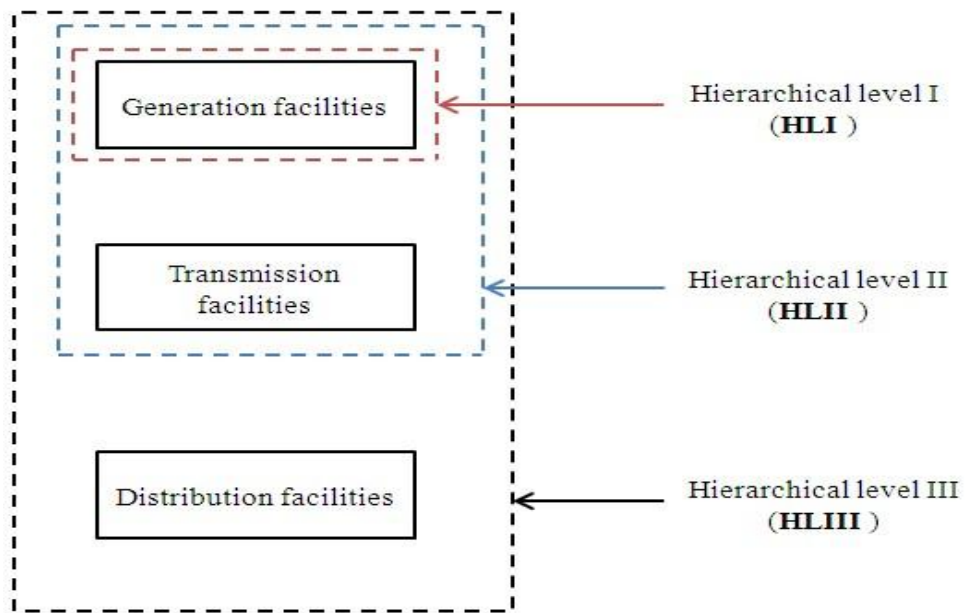


*Figure 2.6: Hierarchical Levels of the Power System*

Reliability assessment methods can be divided into two subjects: **a)** deterministic and **b)** probabilistic methods. Recently most large electric power companies use the probabilistic methods instead of deterministic methods, especially when there are increasing wind power integrated into networks [78]. The probabilistic method can have a better performance on the integration analysis due to the intermittent nature of wind power generation output.

***a) Deterministic methods***

Historically, power system reliability has been assessed using deterministic methods for generating capacity planning and operation. Many published methods have developed over the period, such as Loss of Largest Unit (LLU), Loss of Largest Unit plus a Percentage margin and Capacity Reserve Margin (CRM).

- ***Loss of Largest Unit (LLU)***

This method sets the capacity reserve (RC) equal to or greater than the size of the largest generator unit (LGU) in the system shown in *Equation 2.4*. It is simple to use, but does not consider the system risk when there is an outage of multiple generating units.

$$RC \geq LGU \quad (2.4)$$

- ***Capacity Reserve Margin (CRM)***

The capacity reserve in this method is the difference between the total installed generating capacity (TIGC) and the system peak load (SPL), which is expressed as a fixed percentage of the total installed generating capacity as shown in *Equation 2.5*. The drawback of this method is that it does not consider individual generating units reliability data and different load characteristics.

$$RC = \frac{TIGC - SPL}{TIGC} * 100\% \quad (2.5)$$

Therefore, the power system adequacy evaluation cannot be analysed by deterministic methods due to the insufficient system considerations.

### ***b) Probabilistic Methods***

Probabilistic methods can reflect the nature of system components and the load demand changes in the adequacy computations. The basic approach to evaluating the adequacy of a particular generation configuration is fundamentally the same for any technique. It consists of three parts as shown in *Figure 2.7* [79]. The calculated indices of this method do not reflect generation deficiencies at any individual customer load point but measure the overall adequacy of the generation system.

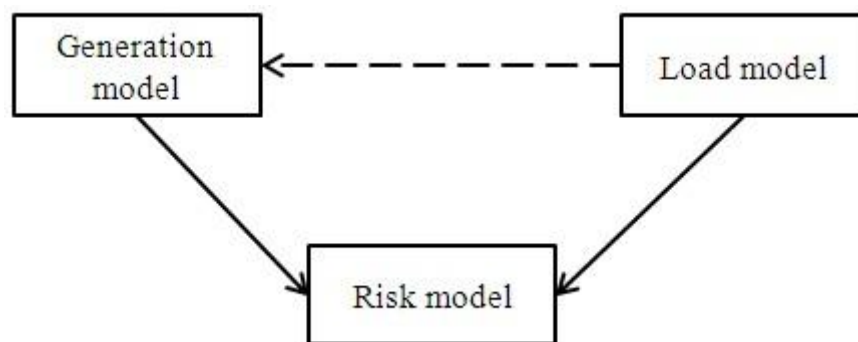


***Figure 2.7: Generating Capacity Reliability Evaluation Model***

The probability of finding a generating unit on forced outage at some distant time in the future called the forced outage rate (FOR) or generating unit unavailability [79], which is the basic parameter used in building a probabilistic generation model. The FOR can be illustrated generally in the following equation and details are described in *section 2.7.2*.

$$FOR = \frac{\Sigma[\text{down time}]}{\Sigma[\text{up time}] + \Sigma[\text{down time}]} \quad (2.6)$$

## 2.7.2 Elements in Generating Unit Model

There are some important elements for modelling generating units. In this section, four of the most representative factors will be discussed [80].

### I. Mean Time to Failure (MTTF)

MTTF means the system components' average 'up time' of a failure-repair cycle in an operating duration, when applied in a power system reliability analysis. The multiplicative inverse of MTTF is the component's failure rate  $\lambda$ .

### II. Mean Time to Repair (MTTR)

MTTR is the average repair time for a system component. In addition, the multiplicative inverse of MTTR is the component's repair rate  $\mu$ .

### III. Mean Time between Failure (MTBF)

MTBF is the average time between each occurrence during an operating duration. It has significant conceptual difference with MTTF. The difference is shown clearly in *Figure 2.8*. It can be seen that  $MTBF = MTTF + MTTR$ , which depends on MTTR (normally very small).

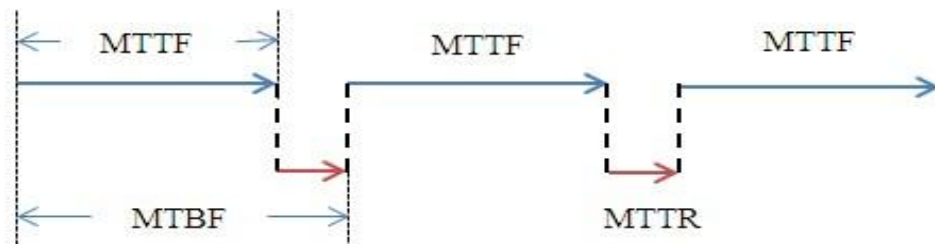


*Figure 2.8: The Relationship between MTTF, MTTR and MTBF*

### IV. Forced Outage Rate (FOR)

As discussed in the previous section, FOR is defined as a ratio of two time values that represents the expected unavailability of a system in some distant time in the future.

Unavailability (FOR):

$$U = \frac{\lambda}{\lambda + \mu} = \frac{r}{m + r} = \frac{r}{T} = \frac{\Sigma[\text{down time}]}{\Sigma[\text{up time}] + \Sigma[\text{down time}]} \quad (2.7)$$

Availability:

$$A = \frac{\mu}{\lambda + \mu} = \frac{m}{m + r} = \frac{m}{T} = \frac{\Sigma[\text{up time}]}{\Sigma[\text{up time}] + \Sigma[\text{down time}]} \quad (2.8)$$

Where

$\lambda$  = expected failure rate

$\mu$  = expected repair rate

$m$  = mean time to failure = MTTF =  $1/\lambda$  (hours)

$r$  = mean time to repair = MTTR =  $1/\mu$  (hours)

$m + r$  = mean time between failure = MTBF =  $T$  (hours)

$T$  = cycle time (hours)

Using Roy Billiton Test System (RBTS) as an illustrated example for the evaluation calculation, the system data are shown in *Table 2.9* [81].

**Table 2.9: Generating Unit's Data for the Example**

Unit	Capacity (MW)	Failure rate per year ( $\lambda$ )	Repair rate per year ( $\mu$ )
1	5	2.0	198.0
2	10	4.0	196.0
3	20	2.4	157.6
4	20	5.0	195.0
5	40	3.0	147.0
6	40	6.0	194.0

Forced outage rates (FOR) for generating units in *Table 2.9* can be calculated with *Equation 2.7*. The calculation results are shown as follows:

$$\text{FOR (Unit 1)} = 2.0 / (2.0 + 198.0) = 0.010$$

$$\text{FOR (Unit 2)} = 4.0 / (4.0 + 196.0) = 0.020$$

$$\text{FOR (Unit 3)} = 2.4 / (2.4 + 157.6) = 0.015$$

$$\text{FOR (Unit 4)} = 5.0 / (5.0 + 195.0) = 0.025$$

$$\text{FOR (Unit 5)} = 3.0 / (3.0 + 147.0) = 0.020$$

$$\text{FOR (Unit 6)} = 6.0 / (6.0 + 194.0) = 0.030$$

### 2.7.3 Generating Unit State Model

In power systems reliability assessment, generating units can be divided into two groups: two-state and multiple-state.

- **Two-State Model**

Two-state model means the unit has only two operating states, considered either fully available (up state) or fully out of service (down state). The state model is shown in *Figure 2.9*, where  $\lambda$  and  $\mu$  are unit failure rates and repair rates respectively.

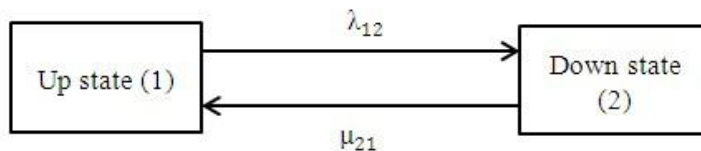


**Figure 2.9: Two-State Generating Unit Model**

- **Multiple-State Model**

Sometimes generating units can be in the up-state, but only able to generate part of their rated output. Therefore, it is necessary to consider the generating units have multiple states. This situation is called derated state. A three-state model is shown in *Figure 2.10*.

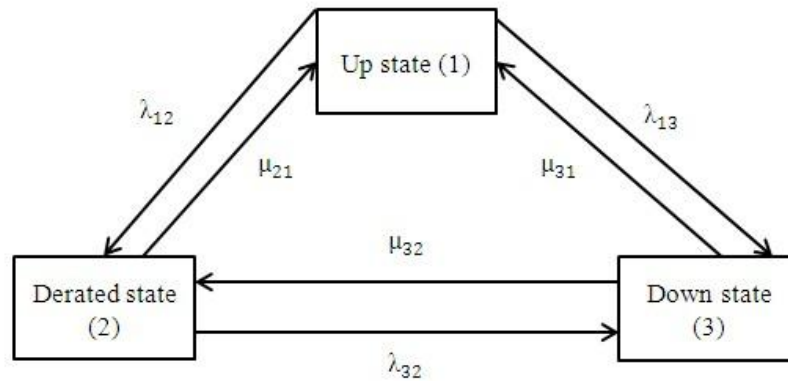


**Figure 2.10: Three-State Generating Unit Model**

It is clearly that increasing derated states number will increase the complexity of the reliability assessment. The topic in this thesis is focused on the impacts of wind power integration, so the conventional generating units used for computations are considered as two-state model, either fully generate rating output or fully out of service. Moreover, a wind turbine generator can be considered as a multiple-state model with an infinite number of states.

## 2.7.4 Adequacy Index for Generation Reliability

As introduced in *section 2.7.1*, the functional zones of a power system (generation, transmission and distribution) have three hierarchical levels. Generation reliability evaluation focuses on generation facilities in HLI. This section presents some of the most widely used adequacy indices in reliability analysis [38, 62, 77, 80, 82].

### 1) Loss of Load Probability, LOLP

It is the oldest and most basic probabilistic index. It is the probability that the load will exceed the available generation. But it does not consider the level of capacity or energy shortage.

### 2) *Loss of Load Expectation, LOLE (days/year or hours/year)*

LOLE is now the most widely used probabilistic index in determining future generation capacity. It is the average number of days or hours on which the load is expected to exceed the available generating capacity, represented by Equation 2.9.

$$LOLE = \sum_{i \in S} p_i T_i \quad (2.9)$$

Where:

$p_i$  = probability of loss of load state  $i$

$S$  = the total number of evaluated states

$T$  = the duration of state  $i$

### 3) *Loss of Energy Expectation, LOEE (MWh/year)*

It is defined as the expected energy that will not be supplied due to those occasions when the load exceeds the available generation.

$$LOEE = \sum_{i \in S} 8760 C_i p_i \quad (2.10)$$

Where:

$p_i$  = probability of loss of load state  $i$

$S$  = the total number of evaluated states

$C_i$  = loss of load for state  $i$  in MW

### 4) *Frequency and Duration, LOLF (occurrences/year) & LOLD (hours/occurrence)*

It identifies expected frequency of encountering deficiencies and the expected duration of the deficiencies. This criterion has not been used very widely in generating system reliability analysis.

It can be seen that all the above indices are expectations (average values of probability distributions). They provide valuable indicators of the adequacy of a

system taking into account the stochastic and deterministic characteristics of the generating system and load demands.

### **2.7.5 Reliability Worth Assessment**

In the current worldwide electricity market environment, it is becoming significantly important to justify capital, operating and maintenance expenditures based on the benefits of utilities and customers. There are two issues of crucial importance: relate the economics with reliability and evaluate the worth of investment on increasing the system reliability. The reliability worth can be calculated directly or indirectly. However, it is difficult to assess the reliability worth directly.

In reliability cost and worth analyses of power systems, customer interruption cost (CIC) is used as a substitute in the reliability worth assessment. Therefore, the generally preferred indirect method is that using the CIC of losses of expected power supply to represent the value of power systems reliability [83]. It is known as a customer damage function (CDF). According to the Standard Industrial Classification (SIC), there are seven main types of customers: industrial, residential, agriculture, government, commercial, large user and office. *Figure 2.11* shows the proportion of the components based on the data in [80]. The CDF is built on survey of actually loss reported by customers as shown in *Table 2.10*.

The results show that Office has the highest value in all time intervals. When the duration is less than 1 hour, Residential has the minimum value; however, when the duration continues to go up, Agriculture has the lowest value between all seven categories.

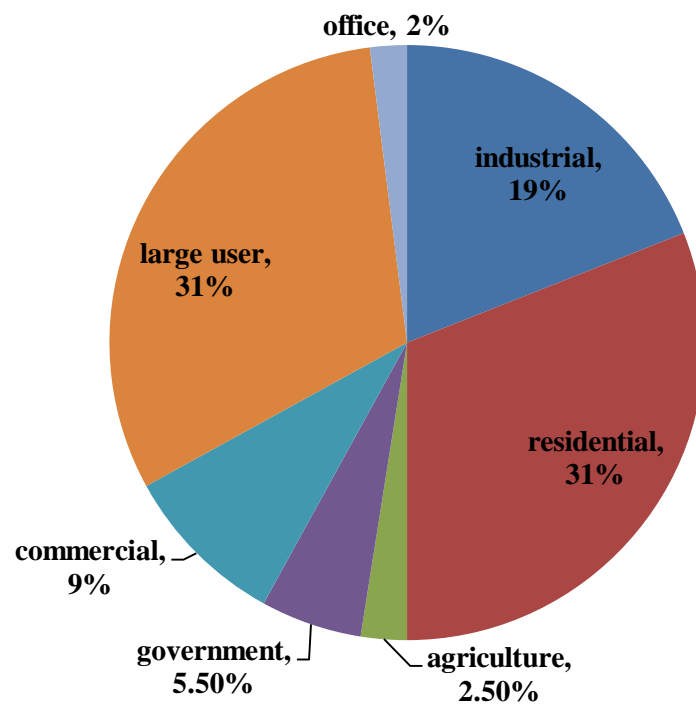


*Figure 2.11: Seven Components used in Canadian Electricity Market [80]*

*Table 2.10: Customer Damage Function for Seven Components [80]*

Customer Damage Function (£/kWh)							
Duration	Large user	Res.	Agri.	Govern.	Indus.	Com.	Office
1 min	1.005	<b>0.001</b>	0.060	0.044	1.625	0.381	<b>4.778</b>
20 mins	1.508	<b>0.093</b>	0.343	0.369	3.868	2.969	<b>9.878</b>
1 hour	2.225	<b>0.482</b>	0.649	1.492	9.083	8.552	<b>21.038</b>
4 hours	3.968	4.914	<b>2.064</b>	6.558	25.163	31.317	<b>68.83</b>
8 hours	8.240	15.69	<b>4.120</b>	26.040	55.808	83.008	<b>119.16</b>

## **2.7.6 Effect of Wind Energy on System Reliability**

It is well understood that wind power generation is an inconsistent and intermittent energy source. Therefore, the power outputs from wind turbines have fluctuations. These fluctuations can cause negative influences on the overall system health. As discussed in *section 2.7.3*, the wind turbine unit is a multiple-state model with an infinite number of states, which is very different from the conventional generating unit. It makes the output models of wind power generating units difficult to build in reliability evaluation.

The values of reliability indices (LOLE, LOEE and LOLF) will become bigger than before due to wind power integration. Accommodating wind power generation will cause impact on generating system reliability and such impact will increase as the wind penetration level is increased. Therefore, it is necessary to provide additional operating reserve to overcome the fluctuation from wind and maintain the reliability level.

## 2.8 Overview of Power System Operating Reserve Assessment Method

### 2.8.1 Conventional Operating Reserve Assessment Method

#### 1) *Percentage Reserve Margin*

This method is one of the most popular used operating reserve (OR) assessment methods. A fixed percentage of generation output is used as operating reserve.

An example will be used to illustrate this method. 3 test systems and their parameter data are shown in *Table 2.11 [81]*. The expected load demands are 400 MW for these three systems. **The fixed percentage** =  $\{(480-400) \div 400\} \times 100\% = 20\%$ . Therefore, the percentage of the OR for all the three systems is 20%.

*Table 2.11: Generating Unit Reliability Data*

System No.	Unit size (MW)	No. of units	Generation capacity (MW)	Forced Outage Rate
System 1	20	24	480	0.015
System 2	40	12	480	0.02
System 3	40	12	480	0.03

Apply the forced outage rate combined with Sampling Distributions Theory in [84] to obtain the calculation results. In addition, there are two important terms in the calculation: the individual probability (IP) and the complementary cumulative probability (CCP). The value of individual probability is the probability of each outage equals to outage level exactly. The CCP is the probabilities for those equals to and bigger than the given outage.

The calculation procedure for System 1 is shown below; apply the same procedure to System 2 and System 3.

Individual probabilities (IP):

$$p(0) = (1-0.015)^{24} * C_{24}^0 = 0.695776;$$

$$p(20) = (1-0.015)^{23} * 0.015 * C_{24}^1 = 0.254294;$$

$$p(40) = (1-0.015)^{22} * (0.015)^2 * C_{24}^2 = 0.044534;$$

$$p(60) = (1-0.015)^{21} * (0.015)^3 * C_{24}^3 = 0.004973;$$

$$p(80) = (1-0.015)^{20} * (0.015)^4 * C_{24}^4 = 0.000398;$$

$$p(100) = (1-0.015)^{19} * (0.015)^5 * C_{24}^5 = 0.000024;$$

Complementary cumulative probabilities (CCP):

$$P(100) = p(100) = 0.000024;$$

$$P(80) = P(100) + p(80) = 0.000422;$$

$$P(60) = P(80) + p(60) = 0.005395;$$

$$P(40) = P(60) + p(40) = 0.049929;$$

$$P(20) = P(40) + p(20) = 0.304223;$$

$$P(0) = P(20) + p(0) = 1;$$

System 1:

**Table 2.12: Percentage Reserve Margin Calculation for System 1**

In Service (MW)	Out of Service (MW)	IP	CCP
480	0	0.695776	1
460	20	0.254294	0.304223
440	40	0.044534	0.049929
420	60	0.004973	0.005395
400	80	0.000398	0.000422
380	100	0.000024	<b>0.000024</b>

System 2:

**Table 2.13: Percentage Reserve Margin Calculation for System 2**

In Service (MW)	Out of Service (MW)	IP	CCP
480	0	0.784718	1
440	40	0.192176	0.215214
400	80	0.021571	0.023038
360	120	0.001467	<b>0.001467</b>

System 3:

**Table 2.14: Percentage Reserve Margin Calculation for System 3**

In Service (MW)	Out of Service (MW)	IP	CCP
480	0	0.693842	1
440	40	0.257509	0.305828
400	80	0.043803	0.048319
360	120	0.004516	<b>0.004516</b>

From *Table 2.12- 2.14*, the complementary cumulative probabilities in System 1, 2 and 3 are 0.000024, 0.001467 and 0.004516, respectively. These results represent the probabilities in which capacity outages exceed the Percentage Reserve Margin. Although the reserve margins are at the same level, the risk indices (CCP) of above three systems are significantly different with each other. The system risk depends on the FORs of the units, number of units in the system and the load demand.

Therefore, Percentage Reserve Margin method does not consider enough factors, only suitable for one particular system, which means this method cannot reflect the true reliability risk consistently.

## 2) *Unserved Equivalent Minutes*

It was developed to determine the actual reliability of supply to consumers as a function of the installed generation reserve margin that results from the reliability criterion for the planning period [6]. An appropriate reliability criterion is necessary

for generation system planning in order to ensure regular and reliable supply of electricity to consumers. The reliability of the generation system can be affected by many disturbances. The effects of the disturbances can be quantified by unserved energy equivalent to minutes to the consumers. A high reliability criterion of the generation system is reflected in a high installed generation reserve margin. So, the reliability of supply to consumers is expected to be high.

The relationship between the unserved equivalent minutes (UEM) and the installed generation capacity reserve can be modelled by using historical data. UEM is used to determine the amount of reserve, which is required in a particular system to maintain a certain reliability criteria, which is defined in *Equation 2.11*.

$$r_{eq} = \frac{\Delta E}{E} * 8760 * 60 \quad (2.11)$$

Where:

$r_{eq}$  : Unserved equivalent minutes (minutes/year)

$\Delta E$  : Unserved energy (MWh)

$E$  : Annual energy demand (MWh)

In *Figure 2.12*, the UEM values and the generation reserve values are shown. It can be seen that an increase in generation reserve decreases the UEM almost exponentially. This method can be used by the System Operator (SO) for long term generation planning to achieve a predetermined UEM.

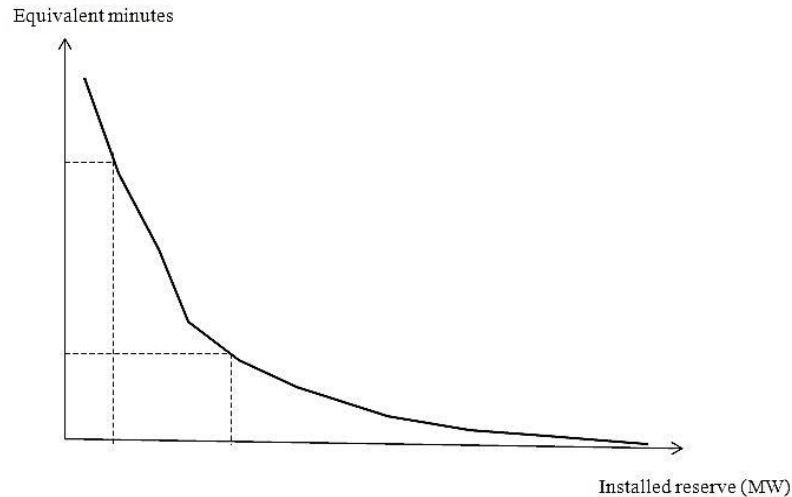


**Figure 2.12: UEM to Consumers as a Function of the Installed Reserve Margin**

### **3) Outage Probabilistic Method**

As discussed in the previous sections, it shows that those deterministic methods can lead to a very different assessment result even when the systems are similar. The operating reserve margin can be consistent and reliable when applying outage probabilistic based method.

The basic concept of these methods is to evaluate the probability of the available generation capable or fail to satisfy the load demand during a certain period that the outage cannot be covered with other generations, and demand is assumed to remain constant for that period [5]. The period is called the time interval. The change of load profile is 1 hour based or 30 minutes based in power systems and the value of this interval can be changed to accommodate the system reliability evaluation required. If the time interval is set to 1 hour, then each single outage period means 1 hour. So, the outage duration and frequency can be assessed. This method has been modified and improved since it was first introduced in 1958 in [5]. For reliability assessment in this thesis, outage probabilistic method will be represented by Outage Frequency & Duration method.

#### **4) Cost Benefit Analysis Method**

This method determines the system operating reserve based on cost benefit analysis. It is completely different from the previous methods, and it is more superior because it aims to optimise the OR to limited cost. It will justify the financial aspect and impact on energy cost to consumers. Quantitative reliability assessments permit a cost benefit analysis for every system reinforcement plan by including customer outage cost into the planning model before the reinforcement plan is implemented [4].

The Cost-Benefit Analysis (CBA) method uses probabilistic approaches to determine the generation capacity outage, including the outage duration and frequency. Then, quantify the cost of generation inadequacy to the system. The results can be compared with the costs of different OR scenarios, and determine the optimal OR value for the power system.

### **2.8.2 Operating Reserve Assessment of Wind Power Generation**

The operating reserve that is estimated by traditional approaches in power systems is clearly insufficient to accommodate the possible fluctuation of wind energy due to its intermittent nature. In modern power systems, the quantified amount of reserve does not usually consider the intermittent nature of wind power generation, so it is necessary to estimate the operating reserve amount with a new theory that is applicable for different wind penetration levels.

Many published methods in [38, 59, 63, 64, 67, 68] are based on deterministic or statistics and average probability values. These methods discussed in the previous section are not capable of reflecting the impact of frequency and duration of wind speed variation and the reliability worth of operating reserve.

As discussed in *section 2.8.1*, the outage frequency and duration method based on the cost-benefit analysis is able to reflect the impact from wind energy and the associated reliability worth. In addition, it is possible for this method to analyse the impact of wind energy on power system reliability and operating reserve assessment. However, it is important to find a fast response, clean and sustainable energy source to generate the required operating reserve. Correspond to the requirements; hydropower seems like a feasible solution for the power system.

### **2.8.3 Review of Hydropower Generation**

Hydropower remains by far the most important of renewable energy for electrical power production worldwide. The World Hydropower Atlas 2000, published by the International Journal of Hydropower and Dams, reported that the world's technically feasible hydro potential is estimated at 14,730 TWh/year, which is equal to 100% of today's global electricity demand. The economically feasible proportion of this is currently considered to be 8,080 TWh/year [85].

Now, there are three main types of hydroelectric schemes around the global hydropower market.

- ***Storage Schemes (Impoundment)***

In storage schemes, a dam impounds water in a reservoir that feeds the turbines and generators. It is the most common type of hydropower and is suitable for water with high head. The biggest dam ever built is the Three Gorges dam in China, which is a storage scheme, with a capacity of 18 GW. So, there are many factors can influence the amount of electricity from this scheme, such as the water head, reservoir capacity, and generator capacity.

- ***Run-of-river schemes***

This scheme uses the natural flow of the river, where the continuity of flow can be achieved by a weir. It is similar with the storage scheme; the only difference is that it does not need to build a high dam for water impoundment.

- ***Pump-Hydro Storage Schemes***

This scheme is also called as Pump-Hydro Energy Storage (PHES). It is currently the only commercially proven large scale (>100 MW) energy storage technology with over 300 plants installed worldwide and with a total installed capacity of over 95 GW [86]. These PHES are originally built to regulate the non-load following nuclear power stations. PHES is playing a very important role in power systems in many countries with the increasing penetration of renewable energy and customers' growing demand on the system operation. It is predicted that the installed capacity by 2015 will be up to 188 GW [87]. In the United States, there are 40 PHES stations with a total capacity of 20 GW. Meanwhile, PHES has become one of the most important generation sources in meeting the fast growing wind power generation [88].

The fundamental principle of PHES is to store electric energy in the form of hydraulic potential energy. The plant pumps water in a reservoir in low price periods, working as a load, and then discharging the stored water during high price periods, operating as hydraulic generator. PHES power plants are originally built to regulate the non-load falling of nuclear power station. PHES can provide flexible generation to stabilize the intermittent power output, which is very attractive for wind power integration. Further details will be described in Chapter 6. The advantages of PHES to power system can be summarized briefly as follows [87].

- Supply energy in periods of high demand
- The flexible generation of PHES can provide both up and down regulation, which could stabilize the intermittent output of renewable energy resources in the power system
- Suitable for black starts

A comparison of the operational characteristics of PHES and other power plants is shown in *Table 2.15*.

***Table 2.15: Operating Characteristics of Generating Plants***

<b>Characteristics</b>	<b>Nuclear</b>	<b>Coal</b>	<b>Oil</b>	<b>PHES</b>
Load following	NO	YES	YES	YES
Quick start (<10 minutes)	NO	NO	NO	YES
Black start	NO	NO	NO	YES

## 2.9 Summary

This chapter has presented the development of wind energy and the benefits of wind power generation. Four of the most representative countries in wind energy development have also been introduced by their leading positions.

Then, wind power generation is explained in three main parts: wind speed model, wind turbine output model and classification of the wind farm. Wind turbine technology is also briefly introduced in this section. The global encouraging policies for wind energy development are summarized, and five popular policies are discussed.

The latter sections in this chapter discuss the basic concepts of power system reliability assessment analysis. Then, several reliability elements in generating unit model are reviewed, including forced outage rate (FOR), MTTF, MTTR and MTBF. Adequacy indices in reliability evaluation are also presented in details by explaining their definitions and the calculation equations. Reliability worth assessment is briefly illustrated by using customer damage function (CDF) method.

The intermittent nature of wind power generation will cause power output fluctuations in power systems. It is necessary to investigate the influences of wind

energy on electric networks. It is a challenge that estimates precise additional operating reserve for wind power output fluctuations. Several famous operating reserve assessment methods are reviewed, and the impacts of wind energy are also considered. As a result, it is found in this chapter, the outage frequency and duration method based on the cost benefit analysis is capable of reflecting the impact from wind power output fluctuation and the associated reliability worth. Then, hydropower seems like a perfect renewable energy source to generate the required electricity to accommodate the fluctuation.

At last, a brief overview of hydropower generation is presented. It focuses on the pumped hydro energy storage schemes (PHES), and the advantages of PHES are introduced. Further details about the new reliability assessment method will be discussed in Chapter 6.

# Chapter 3. Power System Reliability Methods for Wind Energy

## 3.1 Introduction

The primary function of the power system is to provide electrical power to its customers as economically as possible with an acceptable degree of quality. Reliability of power supply is one of the most important features of power quality [89]. There are two main categories of reliability evaluation techniques: analytical and simulation. Analytical methods represent the system by mathematical models and evaluate the reliability indices using mathematical solutions. Simulation methods evaluate the reliability indices by simulating actual process and random behaviour of the system.

Popular analytical and simulation methods will be presented in this chapter. Capacity Outage Probability Table (COPT) is one of the most widely used approaches for the conventional generation system reliability assessment. In addition, Loss of Load Expectation (LOLE) method, Markov Chain method and Frequency and Duration (F & D) method are also described in details. Each of these methods will be illustrated by a simple example. Simulation techniques, on the other hand, treat the reliability indices as a series of real experiments conducted in simulated time. Monte Carlo Simulation (MCS) is presented in this chapter. It samples the random variables of generating units' states without consideration of the units' output intermittent nature.

Consequently, it is necessary to investigate the advantages and disadvantages of both methods and study the effects of wind power generation on both analytical and simulation methods. Furthermore, the reliability standards of power systems will be presented in the last part of this chapter.

This chapter is focus on the power system reliability methods and the effects on these methods caused by wind energy. Four of the most representative analytical methods are presented in *section 3.2*. Monte Carlo Simulation method is described in *section 3.3*. The effects of wind power generation on analytical methods and Monte Carlo Simulation method are briefly introduced in *section 3.4*. At last, *section 3.5* will discuss different reliability standards of power systems.

## **3.2 Analytical Methods for Reliability Assessment**

In power system reliability studies, a single all-purpose reliability formula or approach does not exist. The approaches and formulae, if they exist, depend on the problem and the assumptions utilised. Most of the assumptions must be made in practical applications of probability and statistical theory, which was introduced in Chapter 2. Analytical approaches represent the power system by mathematical models and evaluate the reliability indices from these models by using mathematical solutions. There are five main steps to choose the most appropriate assessment technique [90]:

- Understand the way the system operates.
- Identify the ways in which it can fail.
- Deduce the consequences of the failures.
- Derive models to represent these characteristics.
- Select the reliability assessment method.

Now, there are four most popular analytical methods are shown as follows:

### 3.2.1 Capacity Outage Probability Table

The purpose of the capacity model is to analyse the probabilistic nature of available generation capacity. The analytical generation model is usually in the form of discrete levels of available capacity (or unavailable capacity) and their respective probabilities. The basic generating unit parameter used in reliability evaluation is the probability of finding the unit on forced outage at some distant time in the future. It is known as the unit forced outage rate (FOR), which is mentioned in *Section 2.7.2*. Capacity outage probability table (COPT) is one of the most widely used approaches for the conventional generation system reliability evaluation. As the name suggests, the COPT is a simple array of capacity levels with their probabilities. It consists of every capacity outage level and associated probability of the outage in the generating system. The basic assumptions for the COPT are as follows:

- a) Each generating unit exists in one of two states, operating (“up” state) or non-operating (“down” state). All conventional generating units in this thesis are considered as two-state units, which are discussed in *section 2.7.3*.
- b) The failure situation of a unit is independent of other units, the operating status of the system, and the system load.

In addition, there are two important probability functions need to be considered, which is known as the cumulative distribution function (CDF) and the complementary cumulative probability function (CCDF). The CDF describes the probability that a real-valued random variable  $X$  with a given probability distribution will be found at a value equal to or less than  $x$ . On the opposite side, the CCDF is used to study how often the random variable is above a particular level.

The CCDF will be used in this section. It is the probability of finding a quantity of capacity on outage equal to or greater than the indicated amount. The COPT can also be developed by using the complementary cumulative probability (CCP). For instance, the complementary cumulative probability of capacity outage  $\geq 0$  MW is unity.

The COPT can be easily obtained by using the sampling distribution of statistics theory in mathematical statistics methodology [84]. For a generating system whose total capacity is  $N$  MW and  $p$  is the probability of the generating unit being out of service, the COPT is constructed as *Table 3.1*.

**Table 3.1: COPT Construction Example**

Capacity out of service (MW)	Capacity in service (MW)	State Probability	CCP
$0$	$N$	$p(0)$	$1$
.....	.....	.....	.....
$X$	$N-X$	$p(X)$	$P(X)$
.....	.....	.....	.....
$N$	$0$	$p(N)$	$P(N)$

The  $p(X)$  in *Table 3.1* represents the state (individual) probability of capacity outage level  $X$ , the relationship between the state and complementary cumulative probability is shown in *Equation 3.1*.

$$\begin{cases} \sum_{i=1}^S p(X_i) = 1 \\ p(X_i) = P(X_i) - P(X_{i+1}), & i < S \\ p(X_i) = P(X_i), & i = S \end{cases} \quad (3.1)$$

Where:

$S$  is the total number of capacity out of service levels

This method can be further illustrated by using two examples. All the conventional generating units in this thesis are considered have two states, either in service or out of service. Example I is a system with one 5 MW unit and one 10 MW with forced outage rates of 0.01 and 0.02 [81], which are shown in *Table 3.2*. Example II is a mathematical example with 5 different generating units with the different forced outage rates.

**Table 3.2: Generating Units' FOR of Example I**

Unit No.	Capacity (MW)	Forced Outage Rate (FOR)
1	5	0.01
2	10	0.02

- **Example I:**

Forced outage rate also means the generating unit unavailability, which is 0.01 and 0.02 in this example. Therefore, the probabilities of these two units in service are 0.99 and 0.98. Then, COPT for Example I can be constructed as *Table 3.3*.

**Table 3.3: COPT for Example I (2 units)**

State $i$	Capacity out of service (MW)	Capacity in service (MW)	State Probability $p_i$	Complementary Cumulative Prob. $P_i$
1	0	15	$0.99*0.98=0.9702$	$0.9702+0.0298=1.0000$
2	5	10	$0.01*0.98=0.0098$	$0.0098+0.02=0.0298$
3	10	5	$0.99*0.02=0.0198$	$0.0198+0.0002=0.02$
4	15	0	$0.01*0.02=0.0002$	0.0002

From *Table 3.3*, it can be seen that the complementary cumulative probability values decrease as the capacity on outage increases. And the complementary cumulative probability of capacity outage  $\geq 0$  MW is 1.0000.

- ***Example II***

The capacities of the generating units are  $C_1$ ,  $C_2$ ,  $C_3$ ,  $C_4$  and  $C_5$  with forced outage rates of  $p_1$ ,  $p_2$ ,  $p_3$ ,  $p_4$  and  $p_5$ . Example II uses the sampling distribution of statistics theory to obtain the COPT. The results of capacity outage levels and associated state probabilities are shown in *Table 3.4*.

**Table 3.4: COPT for Example II (5 units)**

Capacity outage (MW)	State Probability $p$
0	$(1-p_1)(1-p_2)(1-p_3)(1-p_4)(1-p_5)$
C5	$(1-p_1)(1-p_2)(1-p_3)(1-p_4)p_5$
C4	$(1-p_1)(1-p_2)(1-p_3)p_4(1-p_5)$
C3	$(1-p_1)(1-p_2)p_3(1-p_4)(1-p_5)$
C2	$(1-p_1)p_2(1-p_3)(1-p_4)(1-p_5)$
C1	$p_1(1-p_2)(1-p_3)(1-p_4)(1-p_5)$
C4+C5	$(1-p_1)(1-p_2)(1-p_3)p_4p_5$
C3+C5	$(1-p_1)(1-p_2)p_3(1-p_4)p_5$
C3+C4	$(1-p_1)(1-p_2)p_3p_4(1-p_5)$
C2+C5	$(1-p_1)p_2(1-p_3)(1-p_4)p_5$
C2+C4	$(1-p_1)p_2(1-p_3)p_4(1-p_5)$
C2+C3	$(1-p_1)p_2p_3(1-p_4)(1-p_5)$
C1+C5	$p_1(1-p_2)(1-p_3)(1-p_4)p_5$
C1+C4	$p_1(1-p_2)(1-p_3)p_4(1-p_5)$
C1+C3	$p_1(1-p_2)p_3(1-p_4)(1-p_5)$
C1+C2	$p_1p_2(1-p_3)(1-p_4)(1-p_5)$
C3+C4+C5	$(1-p_1)(1-p_2)p_3p_4p_5$
C2+C4+C5	$(1-p_1)p_2(1-p_3)p_4p_5$
C2+C3+C5	$(1-p_1)p_2p_3(1-p_4)p_5$
C1+C4+C5	$p_1(1-p_2)(1-p_3)p_4p_5$
C1+C3+C5	$p_1(1-p_2)p_3(1-p_4)p_5$
C1+C2+C5	$p_1p_2(1-p_3)(1-p_4)p_5$
C2+C3+C4	$(1-p_1)p_2p_3p_4(1-p_5)$
C1+C3+C4	$p_1(1-p_2)p_3p_4(1-p_5)$
C1+C2+C4	$p_1p_2(1-p_3)p_4(1-p_5)$
C1+C2+C3	$p_1p_2p_3(1-p_4)(1-p_5)$
C2+C3+C4+C5	$(1-p_1)p_2p_3p_4p_5$
C1+C3+C4+C5	$p_1(1-p_2)p_3p_4p_5$
C1+C2+C4+C5	$p_1p_2(1-p_3)p_4p_5$
C1+C2+C3+C5	$p_1p_2p_3(1-p_4)p_5$
C1+C2+C3+C4	$p_1p_2p_3p_4(1-p_5)$
C1+C2+C3+C4+C5	$p_1p_2p_3p_4p_5$

From *Table 3.4*, it is clear that COPT is easy and simple to apply and contains all outage levels in the generating system. But when there are many generating units in the system, the size of the outage table becomes very large and complex. Because for a system of  $n$  generating units, each with an operating or failed state, the number of outage levels that exist is equal to  $2^n$ . For Example I, 2 generating units have  $2^2 = 4$  outage levels; there are  $2^5 = 32$  outage levels in Example II.

### **3.2.2 Loss of Load Expectation Method (LOLE Method)**

Loss of Load Probability (LOLP) is the probability that the load will exceed the available generation, and it does not consider the capacity shortage level. This index has been superseded by the LOLE in most planning applications in power system. The LOLE is defined as the average number of days (or hours) on which the daily peak load is expected to exceed the available generation. Therefore, it indicates the expected number of days (or hours) for which a loss of load or deficiency may occur.

The LOLE method is using the system load characteristics combined with the generation system, which is represented by the applicable capacity outage probability table (COPT) to give an expected risk of loss of load.

Prior to combining the outage probability table it should be realized that there is a difference between the terms ‘capacity outage’ and ‘loss of load’. The term ‘capacity outage’ indicates a loss of generation that may or may not result in a loss of load. It depends on the generating capacity reserve margin and the system load level. The term ‘loss of load’ occurs when the capability of the generating capacity remaining in service is exceeded by the system load level.

The expected risk in this method is designated as the loss of load expectation (LOLE), which was discussed in *section 2.7.4*. The expression is shown as *Equation 3.2*.

$$LOLE = \sum_{k=1}^n p_k t_k \quad (3.2)$$

Where:

$p_k$  : Individual probability associated with the capacity outage that will lead to loss of load

$t_k$  : The number of days (hours) that an outage would cause a loss of load

This method can be illustrated by a simple numerical example in [5]. Considering a system containing five 40 MW units each with a FOR of 0.01. Because all the units in the example are identical, the COPT can be easily obtained by using the Binomial distribution, which the expression is as follows:

$$P_i = C_n^i U^i A^{n-i} \quad (3.3)$$

Where:

$i$ : number of units in the “down” state

$P_i$ : the probability of  $i$  units in the “down” state

$C$ : the Binomial coefficient [90]

$U$ : unit unavailability (FOR)

$A$ : unit availability

Calculation procedure:

Probability of zero units is in the failed state:

$$p_0 = C_5^0 (0.01)^0 (0.99)^{5-0} = 0.950990$$

Similarly, the probabilities of other capacity outage levels can be calculated:

$$p_1 = C_5^1 (0.01)^1 (0.99)^{5-1} = 0.048030$$

$$p_2 = C_5^2 (0.01)^2 (0.99)^{5-2} = 0.000970$$

$$p_3 = C_5^3 (0.01)^3 (0.99)^{5-3} = 0.000010$$

$$p_4 = C_5^4 (0.01)^4 (0.99)^{5-4} = 4.95 * 10^{-8}$$

$$p_5 = C_5^5 (0.01)^5 (0.99)^{5-5} = 1 * 10^{-10}$$

The capacity outage probability table for this system is shown in *Table 3.5*.

**Table 3.5: COPT for the five units system**

No. of units in Down-state	Capacity out of service (MW)	State Probability	CCP
0	0	0.950990	1.000000
1	40	0.048030	0.049010
2	80	0.000970	0.000980
3	120	0.000010	0.000010
4	160	$4.95 * 10^{-8}$	
5	200	$1 * 10^{-10}$	

Theoretically, the COPT incorporates all the generation system capacity. The table can, however, be truncated by omitting all capacity outages for which the complementary cumulative probability is less than a specified value. This results in a considerable saving in calculation time as the table is truncated. In this example, probability values less than  $10^{-6}$  have been neglected.

The system load model is represented by the daily peak load variation curve shown in *Figure 3.1*. The test period in this case is assumed to be a year, so 0 to 1 p.u on the abscissa corresponds to 0 to 365 days. The peak load for this system is 160 MW. From *Figure 3.1*, it can be seen that the system load is always above 64 MW but never exceeded 160 MW.

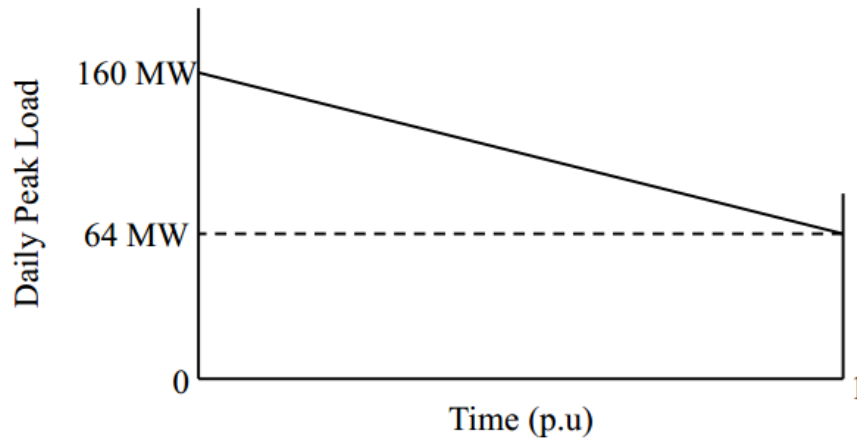


**Figure 3.1: Daily Peak Load Variation Curve**

The daily peak load variation curve is assumed to be linear in order to simplify the calculations, although such a linear relationship is not likely to occur in practice. Through the linear relationship between the load curve and the test period in *Figure 3.2*, it can be seen that the system load is above 80 MW for 0.834 (p.u) of the test period; above 120 MW for 0.417 (p.u) of the test period.

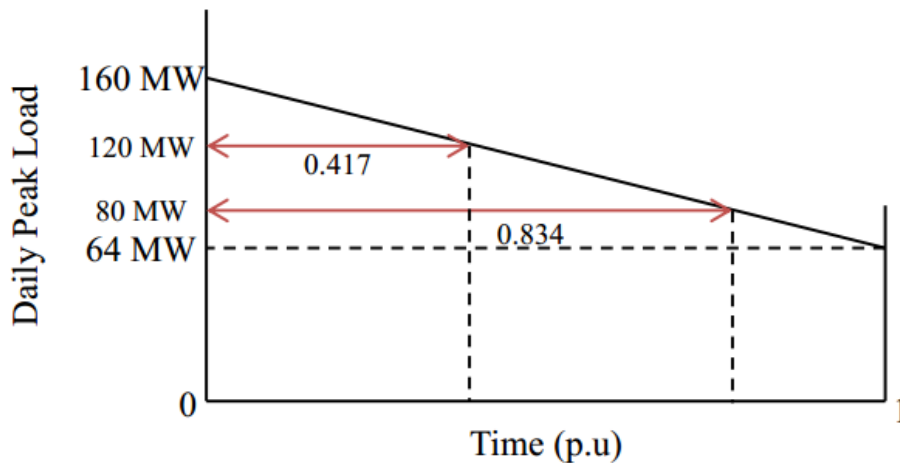


**Figure 3.2: Time Periods during Which Loss of Load Occurs**

In this example, the system capacity is 200 MW and the peak load is 160 MW, so the reserve capacity is 40 MW. The LOLE can be calculated by multiplying the capacity outage probabilities by the related durations of the test period as shown in *Table 3.6*.

**Table 3.6: LOLE Calculated by Using Individual Probabilities**

Capacity out of service (MW)	Capacity in service (MW)	State Probability	Time (p.u)	LOLE
0	200	0.950990	0	0
40	160	0.048030	0	0
80	120	0.000970	0.417	0.00040449
120	80	0.000010	0.834	0.00000834
Total LOLE				0.00041283

For capacity outages of 0 and 40 MW, the LOLE values are zero, because the outage capacities are less than or equal to the system reserve capacity. But when the outage capacities reach 80 and 120 MW, the load does exceed the available generating for 0.417 (p.u) and 0.834 (p.u) of the test period respectively. The individual outage state LOLE can be calculated by using these values multiplied by the individual probabilities. The result of this example is summarized in *Table 3.7*:

**Table 3.7: LOLE for Example System**

Risk index	Period (p.u)	Period (days)
LOLE	0.00041283	$0.00041283 * 365 = 0.15 \text{ days} = 3.6 \text{ hours}$

The result of this example system shows that there is a 3.6 hours period that the daily peak load is expected to exceed the available capacity. Therefore, the LOLE method can only indicate the expected number of days (or hours) for which a loss of load or deficiency may occur. It cannot recognize the degree of capacity shortage.

### 3.2.3 Markov Chain Method

Each of the above two methods can be applied to both non-repairable and repairable systems; however, in repairable systems the repair process assumes to be instantaneous or negligible compared with the operating time. This is a restriction if this assumption is not valid. There is an important technique that overcomes this issue, which is known as the Markov approach. This approach can be applied to the random behaviour of systems that vary discretely or continuously with respect to time and space [90]. And this discrete or continuous random variation is known as a stochastic process.

A Markov process is a continuous stochastic process in which the future states are conditional only on the present state and are independent of previous states, such as a random time-varying process in which future states may be predicted only using the current state as an input [89]. A Markov chain is a type of Markov process in which there are a number of finite states ( $N_1, N_2, N_3 \dots N_n$ ) that the process may exist at any given time. The probability of the process moving from State  $S_i$  to State  $S_j$  is denoted by the transition probability  $P_{ij}$  and the probability of the process remains in the same state is denoted by the probability  $P_{ii}$ . Given that the conditions described above are applicable, the Markov Chain method can calculate the probability of each system state by using the system components' failure rates and repair rates whether the systems are either non-repairable or repairable, and many applications have been used in [91-93].

The system of two repairable components is used as an example to explain the Markov Chain method.

If the system consists of two repairable components, there are four possible states in which the system can exist. If  $\lambda_1, \mu_1$  and  $\lambda_2, \mu_2$  are the failure and repair rates of components 1 and 2, respectively, the state space diagram including the relevant transition rates is shown in *Figure 3.3*.

For example, State 1 is both of components are in “up” state, State 2 is that Component 1 is in “down” state and Component 2 remains in “up” state, so the transition rate from State 1 to State 2 is  $\lambda_1$  as shown in *Figure 3.3*. Similarly, the transition rate from State 2 to State 4 is  $\lambda_2$ . It is clear that there are no transitions in two situations: from State 1 to State 4 and from State 2 to State 3 due to the nature of the Markov process, which are also shown in the figure.

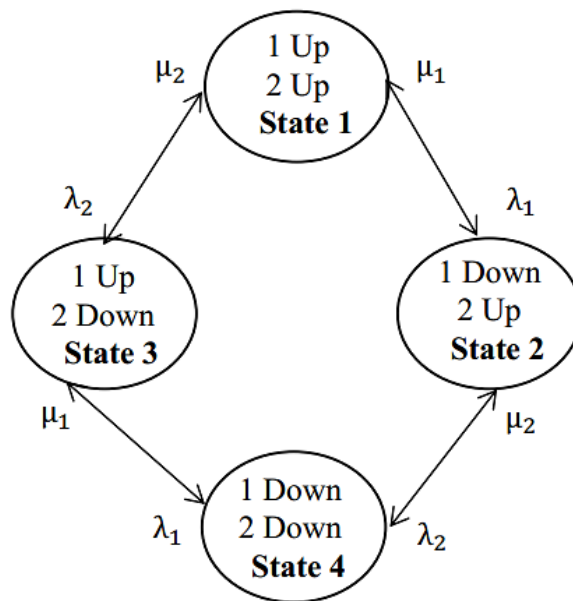


*Figure 3.3: State Space Diagram for a Two-component System*

The procedure of the Markov Chain method includes the following steps:

**Step 1:** Construct a state diagram according to the transitions of component states. *Figure 3.3* shows a diagram for the two components system. The failure rate ( $\lambda$ ) and repair rate ( $\mu$ ) for each component are also represented in the diagram.

**Step 2:** Build the transition matrix based on the state diagram. For a system of  $m$  states, the transition matrix will have a dimension  $m * m$ . The matrix is created by observing the changes between states and entering either the failure or repair rate causing the transition into the transition matrix. For a transition between state  $i$  to

state  $j$  ( $i \neq j$ ), the transition rate is entered into the  $i$ th row and  $j$ th column of the matrix. The main diagonal elements of the matrix should be equal to 1 minus the sum of the other elements on the row. Other elements are filled by zero. It should be noted that the transition matrix is not a probability matrix since the failure and repair rate are not probabilities. It is a way to develop the Markov equation to solve the state probabilities. For the given example, the matrix is shown as *Equation 3.4*.

$$\mathbf{T} = \begin{bmatrix} 1 - (\lambda_1 + \lambda_2) & \lambda_1 & \lambda_2 & 0 \\ \mu_1 & 1 - (\mu_1 + \lambda_2) & 0 & \lambda_2 \\ \mu_2 & 0 & 1 - (\mu_2 + \lambda_1) & \lambda_1 \\ 0 & \mu_2 & \mu_1 & 1 - (\mu_1 + \mu_2) \end{bmatrix} \quad (3.4)$$

**Step 3:** Apply the Markov method, which states that the probabilities would not change in the further transition process. Therefore, it can be expressed as *Equation 3.5*:

$$\mathbf{PT} = \mathbf{P} \quad (3.5)$$

Where:  $\mathbf{P}$  is the state probability vector and  $\mathbf{T}$  is the transition matrix. In addition,  $\mathbf{P}$  represents the mathematical information in this equation so it may equal to zero in some cases for solving the equation. Actually,  $\mathbf{P} \neq \mathbf{0}$  is not possible in practical system applications, because the state probabilities cannot be 0.

Therefore, *Equation 3.5* can be rewritten as:

$$\mathbf{P}(\mathbf{T} - \mathbf{I}) = \mathbf{0} \quad (3.6)$$

Where:  $\mathbf{I}$  is the identity matrix.

Substituting the transition matrix T into the above equations obtains *Equation 3.7*.

$$\begin{aligned}
 [P_1 \ P_2 \ P_3 \ P_4] * \begin{bmatrix} -(\lambda_1 + \lambda_2) & \lambda_1 & \lambda_2 & 0 \\ \mu_1 & -(\mu_1 + \lambda_2) & 0 & \lambda_2 \\ \mu_2 & 0 & -(\mu_2 + \lambda_1) & \lambda_1 \\ 0 & \mu_2 & \mu_1 & -(\mu_1 + \mu_2) \end{bmatrix} \\
 = [0 \ 0 \ 0 \ 0] \quad (3.7)
 \end{aligned}$$

Applying the transpose of *Equation 3.7*, the general expression is obtained as *Equation 3.8*.

$$\begin{bmatrix} -(\lambda_1 + \lambda_2) & \lambda_1 & \lambda_2 & 0 \\ \mu_1 & -(\mu_1 + \lambda_2) & 0 & \lambda_2 \\ \mu_2 & 0 & -(\mu_2 + \lambda_1) & \lambda_1 \\ 0 & \mu_2 & \mu_1 & -(\mu_1 + \mu_2) \end{bmatrix} \begin{bmatrix} P_1 \\ P_2 \\ P_3 \\ P_4 \end{bmatrix} = \begin{bmatrix} 0 \\ 0 \\ 0 \\ 0 \end{bmatrix} \quad (3.8)$$

**Step 4:** It is important to know that the sum of these probabilities must be unity. For instance, the system must either remain in the state being considered or make a transition out of the state. This principle applies to all systems no matter what degree of complexity exists or how many transition statuses there are of moving out a given state, the sum of the probabilities of remaining in or moving out of the state must be unity [90].

Therefore, the full probability condition- the sum of the probabilities of all system states in this example should be equal to 1. For the given example, it is

$$[P_1 + P_2 + P_3 + P_4] = 1 \quad (3.9)$$

This full probability condition is required to be able to solve the above equations as it contains only  $n-1$  independent equations, and there are four state probabilities involved. Therefore, any row within the above equation can be replaced with this condition. For instance, the first row is replaced by this condition as *Equation 3.10*.

$$\begin{bmatrix} 1 & 1 & 1 & 1 \\ \mu_1 & -(\mu_1 + \lambda_2) & 0 & \lambda_2 \\ \mu_2 & 0 & -(\mu_2 + \lambda_1) & \lambda_1 \\ 0 & \mu_2 & \mu_1 & -(\mu_1 + \mu_2) \end{bmatrix} \begin{bmatrix} P_1 \\ P_2 \\ P_3 \\ P_4 \end{bmatrix} = \begin{bmatrix} 1 \\ 0 \\ 0 \\ 0 \end{bmatrix} \quad (3.10)$$

**Step 5:** Solving the Markov matrix equation using linear algebra. For the given example, the solution is as follows:

$$P_1 = \frac{\mu_1 \mu_2}{(\mu_1 + \lambda_1)(\mu_2 + \lambda_2)} \quad (3.11)$$

$$P_2 = \frac{\lambda_1 \mu_2}{(\mu_1 + \lambda_1)(\mu_2 + \lambda_2)} \quad (3.12)$$

$$P_3 = \frac{\mu_1 \lambda_2}{(\mu_1 + \lambda_1)(\mu_2 + \lambda_2)} \quad (3.13)$$

$$P_4 = \frac{\lambda_1 \lambda_2}{(\mu_1 + \lambda_1)(\mu_2 + \lambda_2)} \quad (3.14)$$

It can be seen that the number of states in the state space diagram increases as the number of system components increases. For a system containing  $n$  components with each having two states (up and down), the number of system states is  $2^n$ . When  $n$  becomes large, the method can become unmanageable for large systems [94].

The main advantage of this method is the clear picture of all states and transitions between them. It is extremely useful in modelling the outages of individual components in the system. One drawback is the difficulty in the applications of large systems. Furthermore, this method can be enhanced significantly by introducing recursive techniques and frequency and duration concepts, which will be described in the next section.

### 3.2.4 Frequency and Duration Method (F&D Method)

It is beneficially for evaluating a power system that is continuously operated, repaired and maintained, which requires the additional reliability indices. Suggested reliability indices are the frequency of encountering a system state and the average duration of remaining in the state. The method of deriving these additional indices can be designated as the Frequency and Duration (F&D) method.

Frequency and duration method is a more complex extension of the LOLE method; it uses the Markov model to represent the generating units and the system load [5, 95]. The LOLE method gives neither any indication of the frequency of occurrence of insufficient capacity condition nor the duration of the condition. Frequency and duration are the most useful indices for customer or load point evaluation [89].

Frequency and duration method requires additional data on the generating unit and state transition rates. The LOLE method requires only the steady state availability  $A$  and unavailability  $U$  parameters. But the frequency and duration method uses the transition rate parameters  $\lambda$  and  $\mu$  in addition to the  $A$  and  $U$  parameters. Parameter  $\lambda$  represents the failure rate. Parameter  $\mu$  represents the repair rate. *Figure 3.4* shows a two- state model for a base load unit.

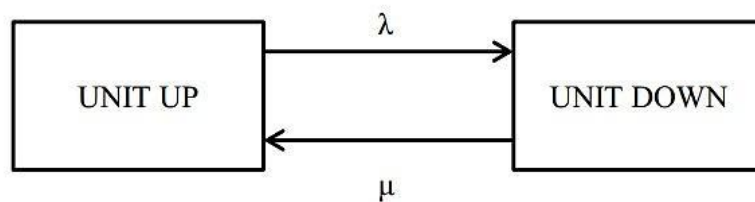


*Figure 3.4: Two-state model for a base load unit*

In generating capacity reliability evaluation, the generating units are described by two-state or multi-state capacity models. As discussed in the *section 2.7.3*, the conventional generating units used for computations are considered as two-state models.

The concepts can be easily evaluated by using a simple numerical example. The test system described in *Table 3.8* contains the basic data required for the F & D methods.

**Table 3.8: System Data**

Unit No.	Capacity (MW)	FOR	Failure rate $\lambda$ (occ./day)	Repair rate $\mu$ (occ./day)
1	40	0.04	0.01	0.49
2	40	0.04	0.01	0.49
3	50	0.02	0.01	0.49

If each unit can exist in two states, then there are  $2^n$  state in the test system where  $n$ = number of units (i.e.  $2^3$  in this case). The total number of states in the test system of *Table 3.8* is summarized in *Table 3.9*.

**Table 3.9: System States**

State No.	1	2	3	4	5	6	7	8
Unit 1	U	D	U	U	D	D	U	D
Unit 2	U	U	D	U	D	U	D	D
Unit 3	U	U	U	D	U	D	D	D
Capacity Out (MW)	0	40	40	50	80	90	90	130

U= Up, D=Down, Capacity Out= Capacity out of service

These states can also be represented as a state transition diagram by using the Markov model as shown in *Figure 3.5*. This diagram enumerates all the possible system states and also shows the transition modes from one state to another.

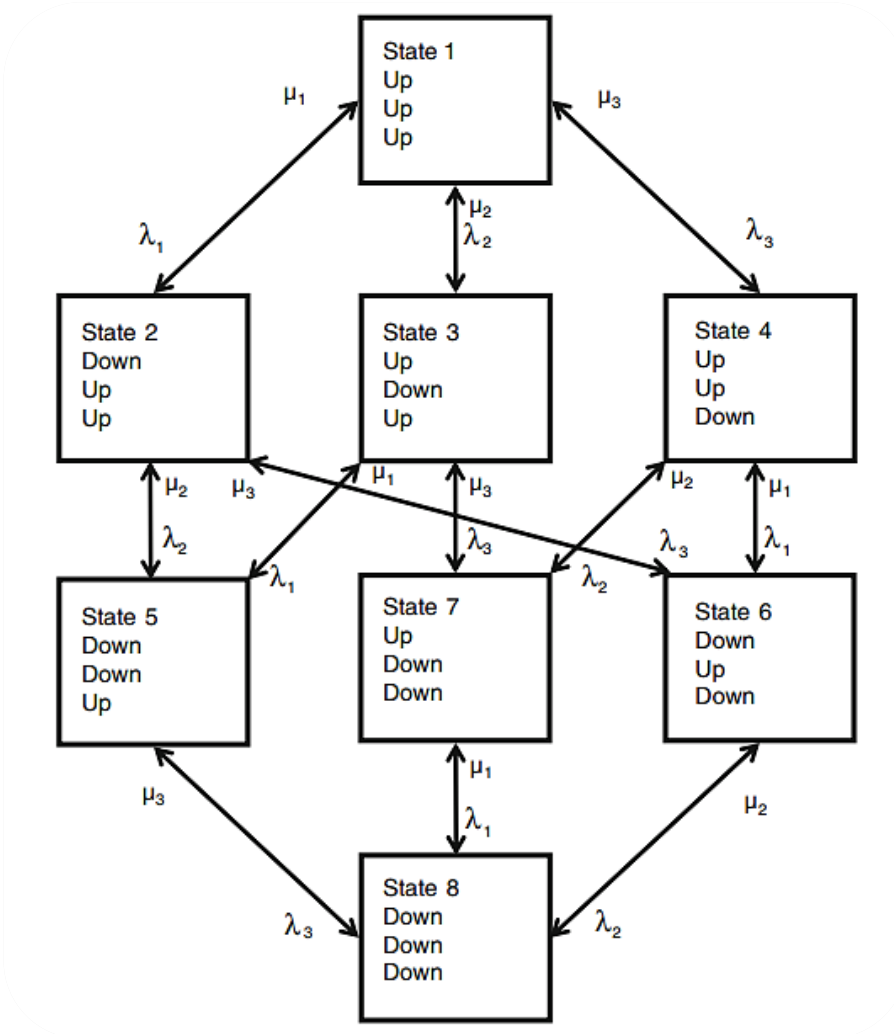


**Figure 3.5: Three-unit state space diagram[5]**

Given that the test system is in State 3 in which unit 2 is down and the others are up, the test system can transit to States 1, 5 or 7 in the following ways:

From State 3 to 1: if unit 2 is repaired

From State 3 to 5: if unit 1 fails

From State 3 to 7: if unit 3 fails

The total rate of departure of State 3 is the sum of the individual rates of departure ( $\mu_2 + \lambda_1 + \lambda_3$ ).

The fundamental approach of generation capacity model building uses the state space diagram. It is not useful for larger systems. Calculation becomes too complex due to a large number of system states. Many practical approaches for large-system analysis are using the recursive technique [5, 96], which will be discussed in the following section. The algorithm can be easily computer processed. The technique provides a fast approach for building capacity models. The definition of the algorithm and its calculation procedure are summarized from [5, 62, 89, 95]. A detailed example is also given in the following section.

### ***Recursive Algorithm:***

Recursive algorithm is preferred due to its advantage in fast calculating for the computer process procedure and higher accuracy. The loss of load probability of each outage level is defined in terms of cumulative probability, which is discussed in the previous *section 2.8.1*. The recursive approach is an algorithm to create the capacity model which contains generation outage and relevant outage probability.

Moreover, there is one important parameter in the F&D method, which is known as the departure rate. It includes all the transition rates from one specific state move to other possible states. The example used in *section 3.2.3*, which is the system of two repairable components.  $\lambda_1$ ,  $\mu_1$  and  $\lambda_2$ ,  $\mu_2$  are the failure and repair rates of components 1 and 2, respectively. The related departure rates of *Figure 3.3* are tabulated in *Table 3.10*.

***Table 3.10: Departure Rates of Two- Component System***

State No.	Component 1	Component 2	Departure Rate
1	Up	Up	$\lambda_1 + \lambda_2$
2	Down	Up	$\lambda_2 + \mu_1$
3	Up	Down	$\lambda_1 + \mu_2$
4	Down	Down	$\mu_1 + \mu_2$

For the generating unit added to the power system whose rating capacity is  $C$  MW, the individual probability of  $X$  MW outage can be divided into two parts:

- (1) The added unit is in “up” state, and the generation outage is already  $X$  MW before the new unit is added.
- (2) The added unit is in “down” state, and the generation outage is  $(X - C)$  MW.

The individual probability of an outage capacity  $X$  MW can be calculated by using *Equation 3.15* in this algorithm.

$$p(X) = p'(X)(1 - U) + p'(X - C)(U) \quad (3.15)$$

Where  $p(X)$  is the individual probability of capacity outage  $X$  after the unit is added;  $p'(X)$  is the individual probability of capacity outage  $X$  before the unit is added;  $U$  is the forced outage rate (FOR) of the new added unit.

$$\lambda_+(X) = \frac{p'(X)(1-U)\lambda'_+(X) + p'(X-C)(U)(\lambda'_+(X-C) + \mu)}{p(X)} \quad (3.16)$$

$$\lambda_-(X) = \frac{p'(X)(1-U)(\lambda'_-(X) + \lambda) + p'(X-C)(U)(\lambda'_-(X-C))}{p(X)} \quad (3.17)$$

Where:

$\lambda_+(X)$  = the upward capacity departure rate after the unit is added

$\lambda_-(X)$  = the downward capacity departure rate after the unit is added

If  $X$  is less than  $C$ :

$$p'(X - C) = 0$$

$$\lambda'_+(X - C) = 0$$

$$\lambda'_-(X - C) = 0$$

The recursive procedure is initiated with the addition of the first unit ( $C_1$ ). In this scenario:

$$\begin{aligned}\lambda_+(0) &= 0 \\ \lambda_-(0) &= \lambda_1 \\ \lambda_+(C_1) &= \mu_1 \\ \lambda_-(C_1) &= 0 \\ \lambda_+(X) &= \lambda_-(X) = 0, \text{ for } X \neq 0, C_1\end{aligned}$$

It is evident from the above equations that the recursive algorithm is straightforward and relatively simple. The calculation procedure can be easily simulated by computer process. There is a numerical example in the next section to illustrate this algorithm.

### ***Example: Recursive Algorithm for Capacity Model Building***

The concept of the recursive algorithm can be most easily seen by using a simple numerical example. The system described in *Table 3.8* contains the basic system data required for the F&D method. This section illustrates the development of the capacity model by using the recursive technique shown by *Equations 3.15- 3.17*.

The F&D method is illustrated by the following steps:

#### **Step 1: add the first unit**

***Table 3.11: Capacity model with Unit 1***

Capacity Out (MW)	Probability $p(X)$	$\lambda_+(X)$ (occ./day)	$\lambda_-(X)$ (occ./day)
0	0.96	0	0.01
40	0.04	0.49	0

**Step 2: add the second unit**

The columns in *Table 3.12* have been given numbers and are referred to as Col (2), Col (3) and Col (4). This will be applied to each table in this example for reducing the amount of calculation. In addition, the tables are used to calculate the results of *Equations 3.15- 3.17*.

**Table 3.12: Individual Probability  $p(X)$  Calculation (Unit1&Unit2)**

Col (1) Capacity Out (MW)	Col (2) $p'(X)(1-U)$	Col (3) $p'(X- C)U$	Col (4) $p(X)$ (4)=(2)+(3)
0	0.96* 0.96	0* 0.04	0.9216
40	0.04* 0.96	0.96* 0.04	0.0768
80	0* 0.96	0.04* 0.04	0.0016

Partial explanations for *Table 3.12*:

In Col (2), Row 4:  $p'(80)$  has not been defined, so  $p'(80) = 0$ .

In Col (3), Row 2:  $X= 0, C= 40 \rightarrow X < C \rightarrow p'(X- C) = 0$ .

In Col (3), Row 3:  $X= 40, C= 40 \rightarrow p'(X- C) = p'(0) = 0.96$  (see *Table 3.11*).

In Col (3), Row 4:  $X= 80, C= 40 \rightarrow p'(X- C) = p'(40) = 0.04$  (see *Table 3.11*).

**Table 3.13: Upward Departure Rate  $\lambda_+(X)$  Calculation (Unit1&Unit2)**

Col (1) Capacity Out (MW)	Col (5) (2)* $\lambda'_+(X)$	Col (6) (3)*( $\lambda'_+(X-C)+\mu$ )	Col (7) $\lambda_+(X)$ (7)=[(5)+(6)] / (4)
0	0.9216* 0	0* (0+0.49)	0
40	0.0384* 0.49	0.0384* (0+0.49)	0.49
80	0* 0	0.0016* (0.49+ 0.49)	0.98

Explanations for *Table 3.13*:

In Col (5), Row 2:  $\lambda'_+(0) = 0$  (see *Table 3.11*).

In Col (5), Row 3:  $\lambda'_+(40) = 0.49$  (see *Table 3.11*).

In Col (5), Row 4:  $\lambda'_+(80)$  has not been defined, so  $\lambda'_+(80) = 0$ .

In Col (6), Row 2:  $X=0, C=40 \rightarrow X < C \rightarrow \lambda'_+(X-C) = 0$ .

In Col (6), Row 3:  $X=40, C=40 \rightarrow \lambda'_+(X-C) = \lambda'_+(0) = 0$  (see *Table 3.11*).

In Col (6), Row 4:  $X=80, C=40 \rightarrow \lambda'_+(X-C) = \lambda'_+(40) = 0.49$  (see *Table 3.11*).

**Table 3.14: Downward Departure Rate  $\lambda_-(X)$  Calculation (Unit1&Unit2)**

Col (1)	Col (8)	Col (9)	Col (10)
Capacity Out (MW)	(2)*( $\lambda'_-(X)+\lambda$ )	(3)* $\lambda'_-(X-C)$	$\lambda_-(X)$ (10)=[(8)+(9)] / (4)
0	0.9216* (0.01+0.01)	0* 0	0.02
40	0.0384* (0+0.01)	0.0384* 0.01	0.01
80	0* (0+0.01)	0.0016* 0	0

Explanations for *Table 3.14*:

In Col (8), Row 2:  $\lambda'_-(0) = 0.01$  (see *Table 3.11*).

In Col (8), Row 3:  $\lambda'_-(40) = 0$  (see *Table 3.11*).

In Col (8), Row 4:  $\lambda'_-(80)$  has not been defined, so  $\lambda'_-(80) = 0$ .

In Col (9), Row 2:  $X=0, C=40 \rightarrow X < C \rightarrow \lambda'_-(X-C) = 0$ .

In Col (9), Row 3:  $X=40, C=40 \rightarrow \lambda'_-(X-C) = \lambda'_-(0) = 0.01$  (see *Table 3.11*).

In Col (9), Row 3:  $X=80, C=40 \rightarrow \lambda'_-(X-C) = \lambda'_-(40) = 0$  (see *Table 3.11*).

Therefore, the capacity model of Unit 1 & Unit 2 is the combination of the results in *Table 3.12- 3.14*. It can be summarized as *Table 3.15*.

**Table 3.15: Capacity Model with Unit 1&Unit 2**

Capacity Out (MW)	Probability $p(X)$	$\lambda_+(X)$ (occ./day)	$\lambda_-(X)$ (occ./day)
0	0.9216	0	0.02
40	0.0768	0.49	0.01
80	0.0016	0.98	0

**Step 3: add the third unit****Table 3.16: Individual Probability  $p(X)$  Calculation (Unit 1&Unit 2&Unit 3)**

Col (1) Capacity Out (MW)	Col (2) $p'(X)(1-U)$	Col (3) $p'(X-C)U$	Col (4) $p(X)$ (4)=(2)+(3)
0	0.9216* 0.98	0* 0.02	0.903168
40	0.0768* 0.98	0* 0.02	0.075264
50	0* 0.98	0.9216* 0.02	0.018432
80	0.0016* 0.98	0* 0.02	0.001568
90	0* 0.98	0.0768* 0.02	0.001536
130	0 * 0.98	0.0016* 0.02	0.000032

**Table 3.17: Upward Departure Rate  $\lambda_+(X)$  Calculation  
(Unit 1&Unit 2&Unit 3)**

Col (1) Capacity Out (MW)	Col (5) (2)* $\lambda'_+(X)$	Col (6) (3)*( $\lambda'_+(X-C)+\mu$ )	Col (7) $\lambda_+(X)$ (7)=[(5)+(6)] / (4)
0	0.903168* 0	0* (0+0.49)	0
40	0.075264* 0.49	0* (0+0.49)	0.49
50	0* 0	0.018432* (0+0.49)	0.49
80	0.001568* 0.98	0* (0+0.49)	0.98
90	0* 0	0.001536* (0.49+0.49)	0.98
130	0* 0	0.000032* (0.98+0.49)	1.47

**Table 3.18: Downward Departure Rate  $\lambda_-(X)$  Calculation****(Unit 1&Unit 2&Unit 3)**

<b>Col (1)</b>	<b>Col (8)</b>	<b>Col (9)</b>	<b>Col (10)</b>
Capacity Out (MW)	(2)*( $\lambda'_-(X)+\lambda$ )	(3)* $\lambda'_-(X-C)$	$\lambda_-(X)$ (10)=[(8)+(9)] / (4)
0	0.903168* (0.02+0.01)	0* 0	0.03
40	0.075264* (0.01+0.01)	0* 0	0.02
50	0* (0+0.01)	0.018432* 0.02	0.02
80	0.001568* (0+0.01)	0* 0	0.01
90	0* (0+0.01)	0.001536* 0.01	0.01
130	0* (0+0.01)	0.000032* 0	0

Therefore, the capacity model of Unit 1 & Unit 2 & Unit 3 is the combination of the results in Table 3.16- 3.18. It can be summarized as Table 3.19.

**Table 3.19: Capacity Model with Unit 1&Unit 2&Unit 3**

Capacity Out (MW)	Probability $p(X)$	$\lambda_+(X)$ (occ./day)	$\lambda_-(X)$ (occ./day)
0	0.903168	0	0.03
40	0.075264	0.49	0.02
50	0.018432	0.49	0.02
80	0.001568	0.98	0.01
90	0.001536	0.98	0.01
130	0.000032	1.47	0

The individual capacity state probabilities can be combined with  $\lambda_+(X)$  and  $\lambda_-(X)$  to calculate the individual and the complementary cumulative frequencies (CCF) by using Equation 3.18 and Equation 3.19. Also, it is convenient to obtain the complementary cumulative probabilities (CCP) by using Equation 3.20.

$$f(X) = p(X)\{\lambda_+(X) + \lambda_-(X)\} \quad (3.18)$$

$$F(X) = F(Y) + p(X)\{\lambda_+(X) - \lambda_-(X)\} \quad (3.19)$$

$$P(X) = P(Y) + p(X) \quad (3.20)$$

$Y$ : the capacity outage state equals to or greater than  $X$  MW [89].

The complete capacity model is shown in *Table 3.20*.

**Table 3.20: Complete Generation Model**

Capacity Out (MW)	Probability $p(X)$	$\lambda_+(X)$ (occ./day)	$\lambda_-(X)$ (occ./day)	Frequency (occ./day) $f(X)$	CCP $P(X)$	CCF $F(X)$
0	0.903168	0	0.03	0.027095	1.000000	0.020000
40	0.075264	0.49	0.02	0.038385	0.096832	0.047095
50	0.018432	0.49	0.02	0.009400	0.021568	0.011721
80	0.001568	0.98	0.01	0.001552	0.003136	0.003058
90	0.001536	0.98	0.01	0.001521	0.001568	0.001537
130	0.000032	1.47	0	0.000047	0.000032	0.000047

The average duration of a particular capacity condition can be obtained as [5]:

$$\text{Average duration} = \text{probability of the condition} / \text{frequency of the condition}$$

Therefore, the average duration could be obtained for either an individual or cumulative capacity condition. The complete generation capacity model is achieved by combining the results in *Tables 3.11*, *3.15* and *3.19* to solve the components of *Equations 3.15 – 3.20*. The recursive algorithm shown with this simple example is ideally suited for digital computer application and provides a fast technique for building capacity models.

## **3.3 Simulation Method for Reliability Assessment**

The analytical methods described in the previous section, work well for conventional generating systems throughout the industry world. But they cannot provide satisfactory reliability assessment due to the random, time-correlated chronological variation of the energy source like wind energy.

The power system reliability also can be evaluated by simulation method. One of the most popular simulation techniques is Monte Carlo Simulation (MCS). The purpose of MCS is to estimate the operation of generating units and other components of the power system by simulating random process.

### **3.3.1 Monte Carlo Simulation Methodology**

Monte Carlo methods are a broad class of computational algorithms that rely on repeated random sampling simulations many times to obtain numerical results. They are mainly used in two aspects: optimization and generation of samples from a probability distribution. In power system research studies, MCS can apply random number and different kinds of distribution function to simulate the operation of each component in the system. The applications of MCS in power system reliability assessment can be categorized as being sequential or non-sequential procedures [97]. In the sequential MCS method, the simulation process is advanced sequentially or chronologically and the system state at a given time point is correlated with that at previous time points. In the non- sequential MCS method, the process is not chronological, each time point is considered independently without considering transitions between previous system states. The sequential MCS process is used in this thesis as it can simulate chronological issues and provide additional time-related indices such as frequency and duration of load losses.

MCS do not always require truly random numbers to be useful. Many of the most useful techniques use deterministic, pseudorandom numbers, making it easier to test and repeat the simulations [98, 99]. The random numbers applied in the simulation of this thesis are generated with a digital computer process by using the software Matlab R2012a. These random numbers are pseudorandom numbers, so they must be tested in the following aspects in order to guarantee their performances [80]:

- (1) The random numbers should have minimal correlation between each other.
- (2) The random numbers should be uniformly distributed between [0, 1].
- (3) The random numbers should be tested in a sufficiently long period.
- (4) The random numbers should not repeat itself in a sufficiently long period.

The basic system reliability indices in *section 2.7.4* for a sampling period of  $N$  can be estimated using the following equations [80]:

- (1) Loss of Load Expectation, LOLE (days/year or hours/year)

$$LOLE = \frac{\sum_{i=1}^{i_S} LLD_i}{N_S} \quad (3.21)$$

In *Equation 3.21*,  $N_S$  is the sampling time,  $S$  is the total number of evaluated states and  $LLD_i$  is the sampled loss of load duration for state  $i$ .

- (2) Loss of Energy Expectation, LOEE (MWh/year)

$$LOEE = \frac{\sum_{i=1}^{i_S} ENS_i}{N_S} \quad (3.22)$$

In *Equation 3.22*,  $N_S$  is the sampling time,  $S$  is the total number of evaluated states and  $ENS_i$  is the sampled energy not supplied in MWh for state  $i$ .

- (3) Loss of Load Frequency, LOLF (occ./year)

$$LOLF = \frac{\sum_{i=1}^{i_S} LLO_i}{N_S} \quad (3.23)$$

In *Equation 3.23*,  $N_S$  is the sampling time,  $S$  is the total number of evaluated states and  $LLO_i$  is the sampled loss of load occurrence for state  $i$ .

### 3.3.2 State Duration Sampling Approach

The generation capacity model in a sequential MCS is the available generating capacity at points in time established chronologically by random sampling. Then, the generation capacity model is superimposed on the chronological load model to build a risk model [100]. Mean Time to Failure (MTTF) and Mean Time to Repair (MTTR) are usually used to build an operational history.

These parameters can be related with random numbers between 0 and 1 to produce a state history for each generating unit, which is a series “up” and “down” periods called state residence time (state duration). The state residence time is sampled from its probability distribution.

If the state residence time is represented by an exponentially distributed random variable  $t$ , it has the probability density function as [80]:

$$f(t) = xe^{-xt} \quad (3.24)$$

$t$ : the mean value of the exponential distribution

The complementary cumulative probability function (CCDF), which has been introduced in *section 3.2.1*, describes the probability is given as:

$$F(t) = 1 - e^{-xt} \quad (3.25)$$

Using the inverse transform method, the random variable  $T$  can be calculated as:

$$T = -\frac{1}{x} \ln(1 - U) \quad (3.26)$$

$U$ : a uniformly distributed random number between [0, 1]

Because  $(1 - U)$  is uniformly distributed,  $U$  is in the same way as  $(1 - U)$  in [0, 1]. Therefore, the random variable  $T$  can be represented by *Equation 3.27*:

$$T = -\frac{1}{x} \ln U \quad (3.27)$$

As mentioned in the previous sections, all generating units in this thesis are considered as two-state units. If the generating unit is in “up” state, then  $x$  in *Equation 3.27* is the failure rate  $\lambda$  of the unit, which is the reciprocal of the MTTF. If the generating unit is in “down” state, then  $x$  in *Equation 3.27* is the repair rate  $\mu$  of the unit, which is the reciprocal of the MTTR.

Therefore, the state duration sampling approach can be represented by *Equation 3.27*. The programme codes for simulation are written in Matlab R2012a. The general simulation procedure can be concluded in the following 4 main steps:

**Step 1:**

Sample the operating characteristics of each generating unit in the system. The duration of each generating unit will be in the form of chronological up-down-up operating cycle.

**Step 2:**

After all the generating units are sampled, combine the operating cycles to obtain the total system available generating capacity.

**Step 3:**

The load model can be used to represent only the daily peaks, giving 365 values for any given year, or to represent the hourly (or half-hourly) values, giving 8760 (or 17,520) values for any given year. With provided load profile, the system available margin model is obtained by superimposing the total system availability curve on the chronological load curve.

A positive margin denotes that the total system generation is sufficient to meet the system load; while a negative margin means that the total available generation is insufficient or the system load has to be curtailed.

**Step 4:**

Compute the system reliability indices. It is simple and convenient to obtain the loss of load duration ( $LLD_i$ ), the energy not supplied ( $ENS_i$ ), and the loss of load occurrence ( $LLO_i$ ) by observing the system available margin model.

### 3.3.3 Simulation Terminating Criteria

Monte Carlo Simulation is a continuous varying convergence process; thus it requires a large number of computing time to simulate the actual operation of the power system. *Figure 3.6* shows a fluctuating convergence process created by Monte Carlo Simulation.

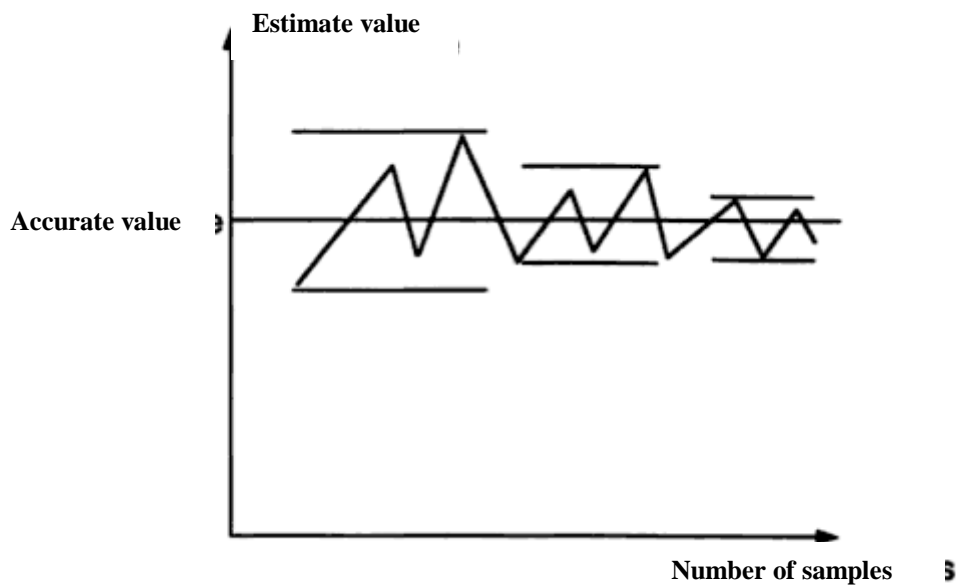


*Figure 3.6: Convergence Process in Monte Carlo Simulation [80]*

It can be seen that there is no guarantee that a few more samples will lead to a smaller error. It is true, however, that the error bound decreases as the number of samples increases [80]. It is important to achieve a certain accuracy level before the simulation is terminated. However, it is not appropriate to keep the simulation

running for a large number of samples in order to achieve an extremely high level of accuracy. There are two main terminating criteria to stop the simulation.

- a. Setting a fixed number of samples before the simulation. For instance, if the fixed number sets to 1,500 means the simulation will sample 1,500 times then stop. It is straightforward to apply in computer programming. However, the number is critical, if it is too big, the computation time and cost will be significantly more than necessary. If the fixed number is too small, the simulation results may not achieve the required accuracy level.
- b. The simulation will pause after a set number of samples, and check to see if the required accuracy level has been reached if not, the simulation will continue running for the set number of samples and check again until the simulation results reach the required accuracy level.

In this thesis, the first terminating criteria will be used for simulation and further details will be described in Chapter 4.

## **3.4 Effect of Wind Power Generation on Reliability Assessment**

### **3.4.1 Effects of Wind Power on Analytical Methods**

The analytical methods as introduced in the previous section are popular approaches for conventional generation reliability assessment. However, the calculations of these methods will become inconvenient, and the scales of the result tables will become unmanageable, while the power system has high wind power penetration level.

The negative effects on reliability analytical methods:

- (1) The size of the outage table in each analytical method depends on the number of total generating units and the number of each unit's states. In this thesis, all the conventional generating units only have two states, so the total outage levels in the system will be limited. But the wind turbines' outputs have high fluctuation due to the intermittent nature of wind energy. For instance, if a wind farm output is 20 MW, because of the wind speed is high variable, even the evaluated outage levels are 1 MW for each level, then the outage table will become significantly large. The calculation time and the result storage become unacceptable for power system reliability assessment when wind power is integrated into practical systems.
  
- (2) The wind turbine power output is not constant and nonlinearly distributed due to the wind speed fluctuation. It will make the computation of the recursive algorithm more complex, so it is difficult to construct a capacity outage table for the analytical method. For instance, when the wind speed is between the cut-in speed and the rated speed, different wind speeds will lead to different wind turbine outputs. When the wind speed is between the rated wind speed and the cut-out speed, different wind speeds will lead to the same wind turbine output.

### **3.4.2 Effects of Wind Power on Monte Carlo Simulation**

Compared with analytical methods, Monte Carlo Simulation samples the random variables of system components states without consideration of the generating units' output nature, which makes it an effective tool to accommodate wind turbine output fluctuations [38]. It is easy to modify the operating history by modifying the unit's state or insert a new unit, such as a wind turbine. The system components' states can

be replaced by real industrial data; therefore MCS is flexible and practical for power system reliability assessment with wind power integration.

## 3.5 Reliability Standard of Power System

One of the key objectives of power systems is to ensure that the total available generation meet the load demand. The standard on the power system reliability assessment is needed to ensure the reliability analysis will be investigated under the same circumstance.

There are a number of indices that could be used to set a reliability standard. The most common of these indices include:

- (1) Loss of load expectation (*LOLE*), this index can be divided into two parts:  
*LOLE* (days/year) and *LOLE* (hours/year)
- (2) Expected energy not supplied (*EENS*)
- (3) Failure frequency and duration (*F & D*)

Nowadays, *LOLE* represents the reliability standard used in many countries. Most of them set the standard level to  $LOLE = 0.1 \sim 1$  day/year. *Table 3.21* shows some countries' reliability standards [101, 102].

**Table 3.21: Reliability Standard LOLE in 10 countries**

Country	LOLE (days/year)	LOLE (hours/year)
Australia		5~7
Belgium		16
Brazil	2.5	
Canada	0.1	
France		3
Japan	0.3	
Republic of Ireland		8
Spain	0.1	
China	1~2	
UK		3

In this thesis, the reliability standard level sets to 1~2 days with the consideration of wind power integration. In addition, a case study of Eastern Gansu Power Grid in China will be described in Chapter 8, and this standard will be tested in a Chinese power system.

## 3.6 Summary

This chapter has presented two main categories of evaluation approaches: analytical methods and Monte Carlo Simulation method. In order to evaluate the power system reliability, many assessment methods have been developed and widely used. Four most representative analytical methods were introduced in details as COPT, LOLE, Markov Chain, and F&D method. The first two methods are simple, straightforward process. The outage tables of these methods can be constructed by using the sampling distribution of statistics theory.

Markov Chain and F&D method are theoretically more complex than COPT and LOLE. The frequency and duration method (F&D) was introduced to improve the weak points of COPT and LOLE. It is a more complex extension of the LOLE method and applies the Markov model to represent the generating units and the system load. The F & D method requires additional data on the generating units' state transition rates. A detailed example of the recursive algorithm for F&D method to construct the outage table is explained in this chapter.

The power system reliability also can be evaluated by the simulation method. Monte Carlo Simulation method was discussed in the latter part. Then, the state duration sampling approach for MCS was presented.

The behaviour of wind power is significantly different from other conventional generation sources due to its inconsistent and intermittent nature. Therefore, the effects of wind power generation on both analytical methods and simulation method were investigated in this chapter. Finally, a brief overview of the reliability standard of the power system was presented.

# Chapter 4. Reliability Evaluation of Modified Roy Billinton Test System

## 4.1 Introduction

Chapter 2 presented an overview of power system reliability analysis. Basic concepts and system components' models were also introduced. Chapter 3 introduced several popular analytical methods and simulation method for the power systems reliability assessment. Frequency and Duration (F&D) method can provide the frequency of occurrence of insufficient capacity condition and the duration of the condition. On the other hand, Monte Carlo Simulation (MCS) method can apply random number and different kinds of distribution functions to simulate the operation of each component in the system. Consequently, this chapter uses the Monte Carlo Simulation method combined with F&D method to analyse the reliability assessment of a conventional power system for future evaluations in this thesis.

The power systems reliability assessment presented in this thesis adopts the combined method of F&D method and MCS method. The basic concepts and theories of the combined method have been introduced in *section 3.2.4* and *section 3.3*. This chapter will explain the mathematic model to apply the combined method in evaluating system components, present and discuss the calculation results of the test system.

Therefore, it is important to select an applicable test system. The test system used in this chapter is modified based on the Roy Billinton Test System (RBTS) [81]. It is suitable for the development of basic concepts and an appreciation of the assumptions associated with practical system reliability studies. There are three main

steps for testing: load model building, generating system model building, and simulating the system reliability by combining these two models.

In this chapter, an application of the combined method in reliability evaluation of a conventional power system is reported. Frequency & Duration method and Monte Carlo Simulation method are applied in Matlab to gain the reliability assessment results. The Matlab program codes of load and generation model can be found in Appendix II and III. *Section 4.2* provides a detailed description of the modified RBTS test system for reliability assessment and simulation. In *section 4.3*, different load profiles are presented and illustrated by figures. The generating system output model is described in *section 4.4*. At last, *section 4.5* presents the results and discussions of the Modified RBTS reliability evaluation.

## **4.2 Description of Modified Roy Billinton Test System (MRBTS)**

The MRBTS is a six-bus system with two generator buses and four load buses. The system peak load is 185 MW, and total installed generating capacity is 240 MW, comprising 110 MW at bus 1 (four units) and 130 MW at bus 2 (seven units). There are nine transmission lines connecting the six buses and five load points as shown in *Figure 4.1* [103]. The voltage level of the transmission system is 230 kV and the voltage limits for the system buses are assumed to be 1.05p.u and 0.97p.u, respectively.

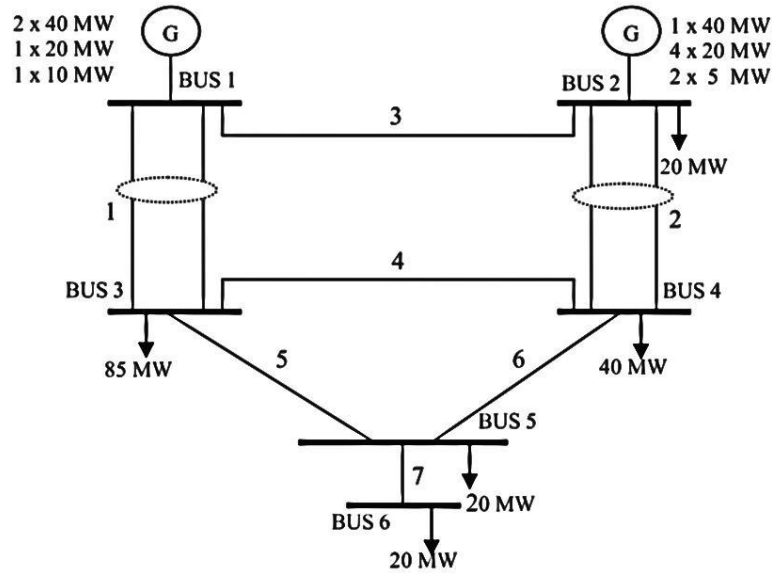


*Figure 4.1: Single Line Diagram of MRBTS [103]*

## 4.3 Load Model

In a power system, the load curve or the load profile is a graph of the variation in the electrical load over a specific time. A load profile will vary according to customer types (including residential, commercial and industrial), temperature and seasons. So, it is difficult to predict and forecast accurately. In this thesis, a load model with certain load variation pattern and adjustable annual peak load demand is used in the reliability evaluations.

The IEEE Subcommittee on the Application of Probability Methods has developed a Reliability Test System (RTS) [104] which includes both generation and load facilities. The load model data which is used in this thesis are modified based on the IEEE-RTS [105, 106].

Meanwhile, there are four important elements that need to be defined in a load profile and summarized below:

- ***Annual peak load***: the highest amount of electricity being consumed at any one point in time during a year.
  
- ***Weekly peak load***: the highest amount of electricity being consumed at any one point in time during a week.
  
- ***Daily peak load***: the highest amount of electricity being consumed at any one point in time during a day.
  
- ***Hourly peak load***: the highest amount of electricity being consumed at any one point in time during an hour.

The calculation process of the annual load curve is simple. Setting the value of the annual peak load and using the value as a reference value for load modelling. The details of the load model are presented below in *Tables 4.1, 4.2 and 4.3*. Then, the load models in the MRBTS with an annual peak of 185 MW will be illustrated through *Figures 4.2- 4.4*.

*Table 4.1* gives data on weekly peak load in per cent of the annual peak load. The annual peak load occurs in Week 51. The data in *Table 4.1* show a typical pattern, with two seasonal peaks. The second peak is in Week 23 (90%). If Week 1 is taken as January, *Table 4.1* describes a winter peaking system. If Week 1 is taken as a summer month, a summer peaking system can be described.

***Table 4.1: Weekly Peak Load in Per cent of Annual Peak***

<b>Week</b>	<b>Peak load (%)</b>						
<b>1</b>	86.2	<b>14</b>	75.0	<b>27</b>	75.5	<b>40</b>	72.4
<b>2</b>	90.0	<b>15</b>	72.1	<b>28</b>	81.6	<b>41</b>	74.3
<b>3</b>	87.8	<b>16</b>	80.0	<b>29</b>	80.1	<b>42</b>	74.4
<b>4</b>	83.4	<b>17</b>	75.4	<b>30</b>	88.0	<b>43</b>	80.0
<b>5</b>	88.0	<b>18</b>	83.7	<b>31</b>	72.2	<b>44</b>	88.1
<b>6</b>	84.1	<b>19</b>	87.0	<b>32</b>	77.6	<b>45</b>	88.5
<b>7</b>	83.2	<b>20</b>	88.0	<b>33</b>	80.0	<b>46</b>	90.9
<b>8</b>	80.6	<b>21</b>	85.6	<b>34</b>	72.9	<b>47</b>	94.0
<b>9</b>	74.0	<b>22</b>	81.1	<b>35</b>	72.6	<b>48</b>	89.0
<b>10</b>	73.7	<b>23</b>	90.0	<b>36</b>	70.5	<b>49</b>	94.2
<b>11</b>	71.5	<b>24</b>	88.7	<b>37</b>	78.0	<b>50</b>	97.0
<b>12</b>	72.7	<b>25</b>	89.6	<b>38</b>	69.5	<b>51</b>	100.0
<b>13</b>	70.4	<b>26</b>	86.1	<b>39</b>	72.4	<b>52</b>	95.2

*Table 4.2* gives a daily peak load cycle, in per cent of the weekly peak. The same weekly peak load cycle is assumed to apply for all seasons. The data in *Tables 4.1* and *4.2*, together with the annual peak load define a daily peak load model of  $52 * 7 = 364$  days, with Monday as the first day of the year.

***Table 4.2: Daily Peak Load in Per cent of Weekly Peak***

Day	Peak load (%)
Monday	93
Tuesday	100
Wednesday	98
Thursday	96
Friday	94
Saturday	77
Sunday	75

*Table 4.3* gives weekday and weekend hourly load models for each of four seasons. A suggested interval of weeks is given for each season. The first two columns reflect a winter season (evening peak), while the next two columns reflect a summer season (afternoon peak). *Table 4.3* represents a winter peaking system. If *Table 4.1* is started with a summer month, then the intervals for application of each column of the hourly load model in *Table 4.3* should be modified accordingly.

**Table 4.3: Hourly Peak Load in Per cent of Daily Peak**

Hour	Winter Weeks 1-8 & 44-52		Summer Weeks 18-30		Spring/ Fall Weeks 9-17 & 31-43	
	Wkdy	Wknd	Wkdy	Wknd	Wkdy	Wknd
12- 1am	67	78	64	74	63	75
1-2	63	72	60	70	62	73
2-3	60	68	58	66	60	69
3-4	59	66	56	65	58	66
4-5	59	64	56	64	59	65
5-6	60	65	58	62	65	65
6-7	74	66	64	62	72	68
7-8	86	70	76	66	85	74
8-9	95	80	87	81	95	83
9-10	96	88	95	86	99	89
10-11	96	90	99	91	100	92
11-12	95	91	100	93	99	94
12-1pm	95	90	99	93	93	91
1-2	95	88	100	92	92	90
2-3	93	87	100	91	90	90
3-4	94	87	97	91	88	86
4-5	99	91	96	92	90	85
5-6	100	100	96	94	92	88
6-7	100	99	93	95	96	92
7-8	96	97	92	95	98	100
8-9	91	94	92	100	96	97
9-10	83	92	93	93	90	95
10-11	73	87	87	88	80	90
11-12	63	81	72	80	70	85

Therefore, the combination of *Tables 4.1, 4.2 and 4.3* with the annual peak load defines an hourly load model of  $364 * 24 = 8736$  hours. The annual load model will be simulated in Matlab. The matlab program codes of load model can be found in Appendix II.

The simulation results are represented by figures to illustrate the load performance. *Figure 4.2* shows an annual load curve of MRBTS and the peak load is 185 MW. *Figures 4.3 and Figure 4.4* show the load curves of the first week and the first day (Monday) of the year. These figures will make for a better understanding of the system load profile. In addition, the simulation results of annual load model can be combined with the simulation results of available system generation capacity to analyse the system reliability evaluation.

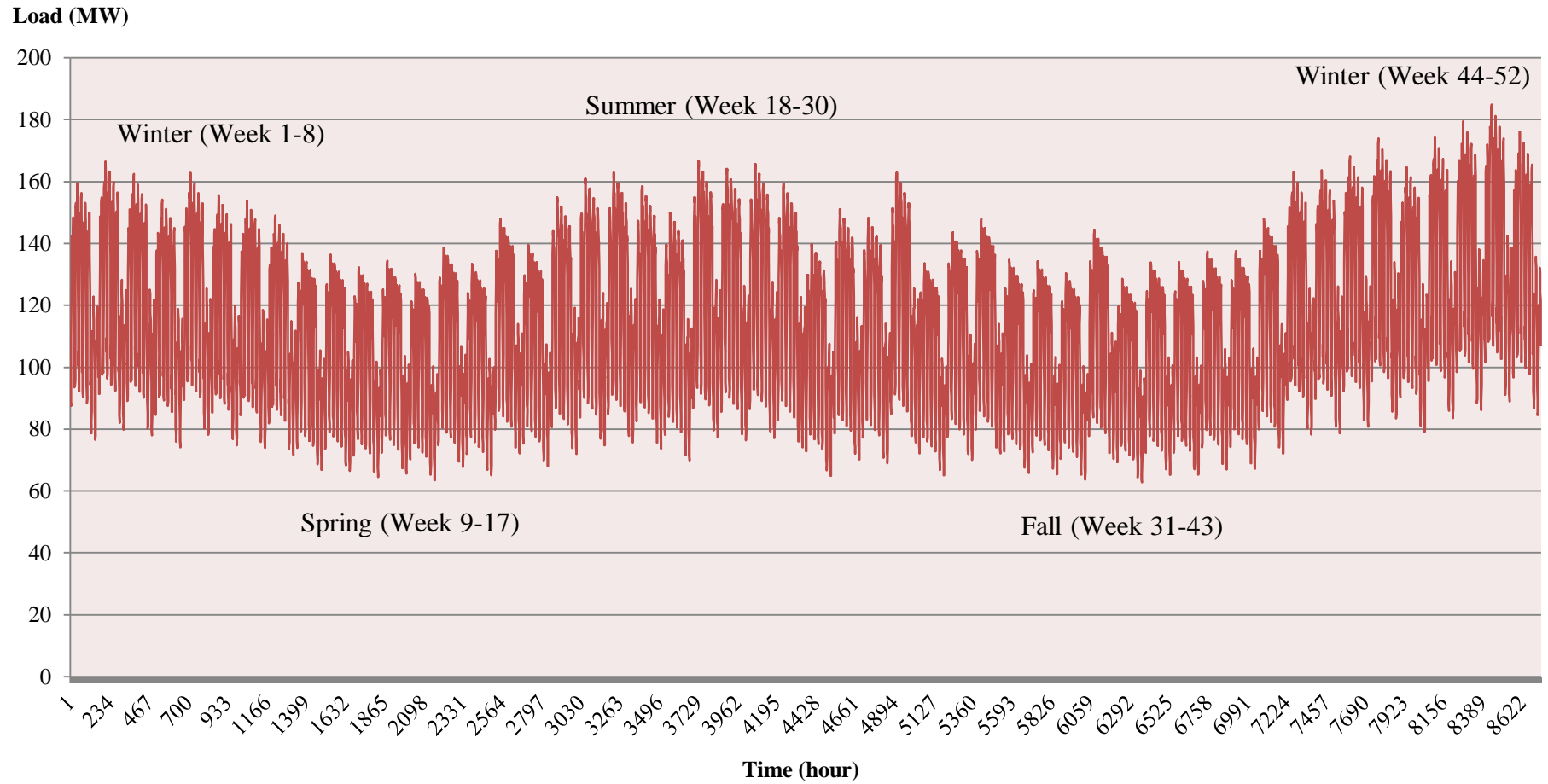


**Figure 4.2: Annual Load Curve of MRBTS with 8736 Load Points**

*Figure 4.2* describes a winter peaking system with Week 1 is taken as the beginning of January. It is clearly that the load demand in the winter and summer is higher than spring and autumn. In the winter, the temperature is low so that the residential electricity consumption for heating is increasing. In the summer, the opposite situation happens. Most of the residential consumption is used for air-conditioning.

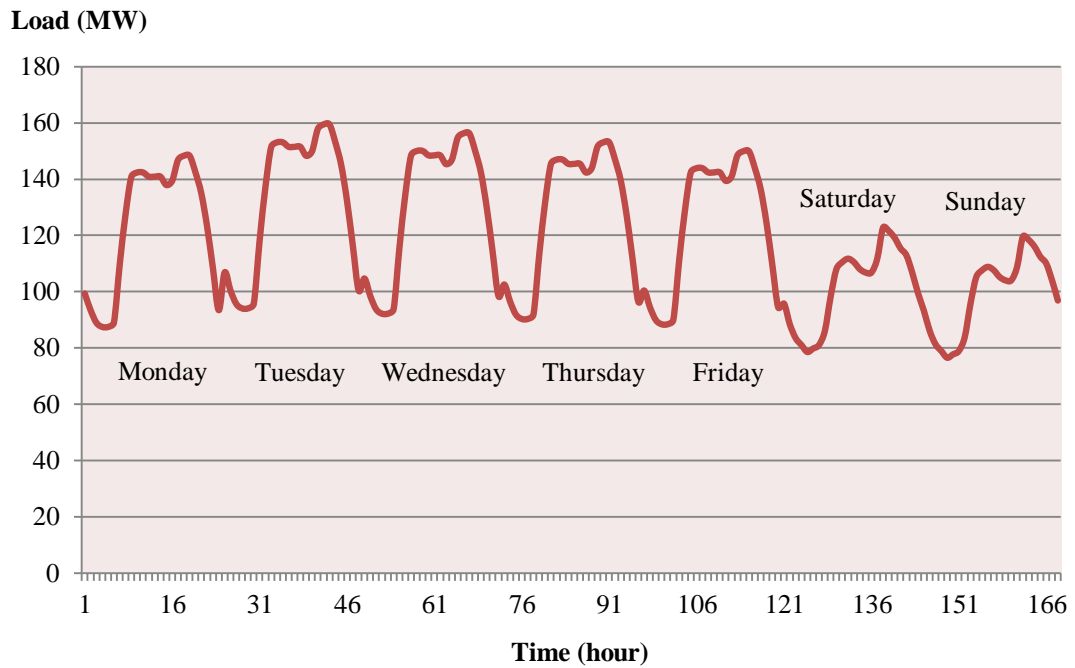


**Figure 4.3: Weekly Load Curve of MRBTS with 168 Load Points**

The weekly load curve is shown in *Figure 4.3*. The patterns of load demand between weekdays are similar, but it can be seen that the load demand in weekend decreases due to the reductions of electricity consumption in industrial, government and office users.

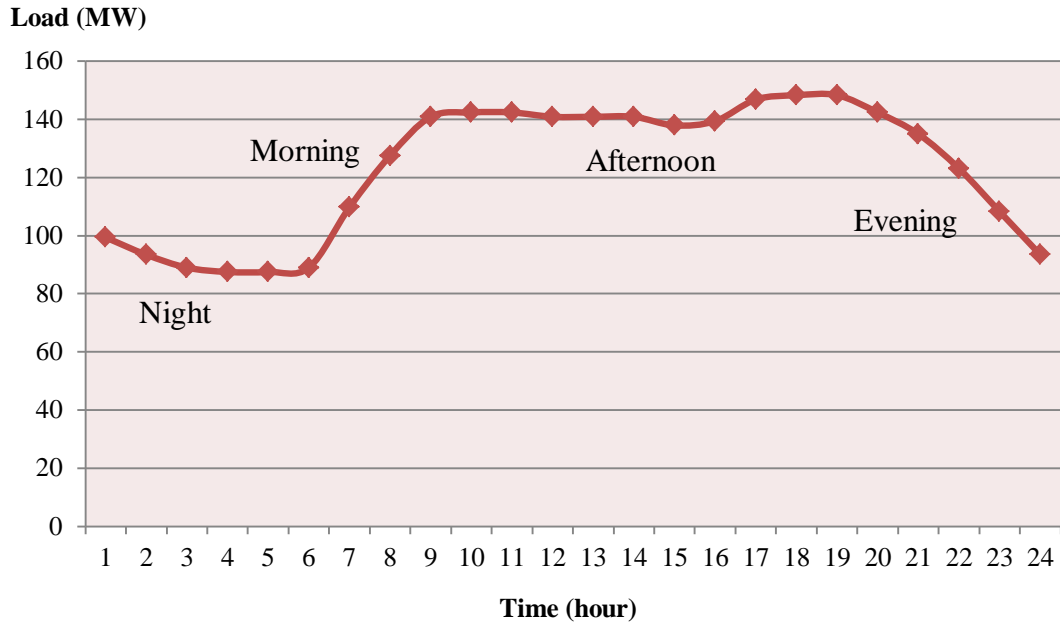


**Figure 4.4: Daily Load Curve of MRBTS with 24 Load Points  
First Day (Monday) of the Year**

Figure 4.4 shows a typical daily load curve. The load demand is increasing during the morning and decreasing during the evening. The peak periods of load demand occur at the afternoon and the off-peak periods occur during the night. In this thesis, it is assumed that the peak time is 7:00~22:00 and the off-peak time is 22:00~ 7:00, which will be used in Chapter 7 for calculating the electric energy transmission/distribution losses.

Furthermore, the annual load model will be combined with the available system generation capacity to analyse the system reliability evaluation. And the generating system model presents in the latter section.

## 4.4 Generating System Model

The power output of a generating unit can be simulated by its failure rate per year and Mean Time to Repair in the Simulation. The approach theory is that the time of the generating unit in “down” state is represented by its failure rate per year; the period of the generating unit in “down” state is represented by its MTTR. As introduced in *section 2.7.2* and *section 3.2.4*,  $\lambda$  represents the number of failure per year. In this simulation procedure,  $\lambda$  means that how many times the unit is out of service, and MTTR means that the period of each “out of service” state. The output of a generating unit can be obtained by combining these two elements together. Then, the total available system generation capacity can be calculated by combining the outputs of all the generating units in the system.

*Table 4.4* gives a list of generating units’ capacities and reliability data of the modified RBTS test system. In addition to Forced Outage Rate, the parameters which will be needed for Frequency & Duration method are given (MTTF and MTTR).

***Table 4.4: Generating Unit Reliability Data [81]***

Unit size (MW)	No. of units	Forced Outage Rate	MTTF (hours)	MTTR (hours)
5	2	0.010	4380	45
10	1	0.020	2190	45
20	4	0.015	3650	55
20	1	0.025	1752	45
40	1	0.020	2920	60
40	2	0.030	1460	45

The failure rate of each generating unit can be calculated from *Table 4.4*. As discussed in *section 2.7.2*,  $MTTF = 1/\lambda$ . So, the failure rates can be calculated and the results are shown in *Table 4.5*.

**Table 4.5: Failure Rates of Generating Units**

Unit size (MW)	Failure rate per year
5	2.0
10	4.0
20	2.4
20	5.0
40	3.0
40	6.0

Therefore, the generating unit output model can be built using its failure rate per year and Mean Time to Repair (MTTR) in *Tables 4.5* and *4.4*.

The generation output model building approach in Matlab is to use  $\lambda$  as the number of failure per year. For example, the 5-MW unit has 2 failures per year and each failure will last for 45 hours, according to the unit's MTTR. *Figure 4.5* shows the generation output curve of the 5-MW unit for a whole year.

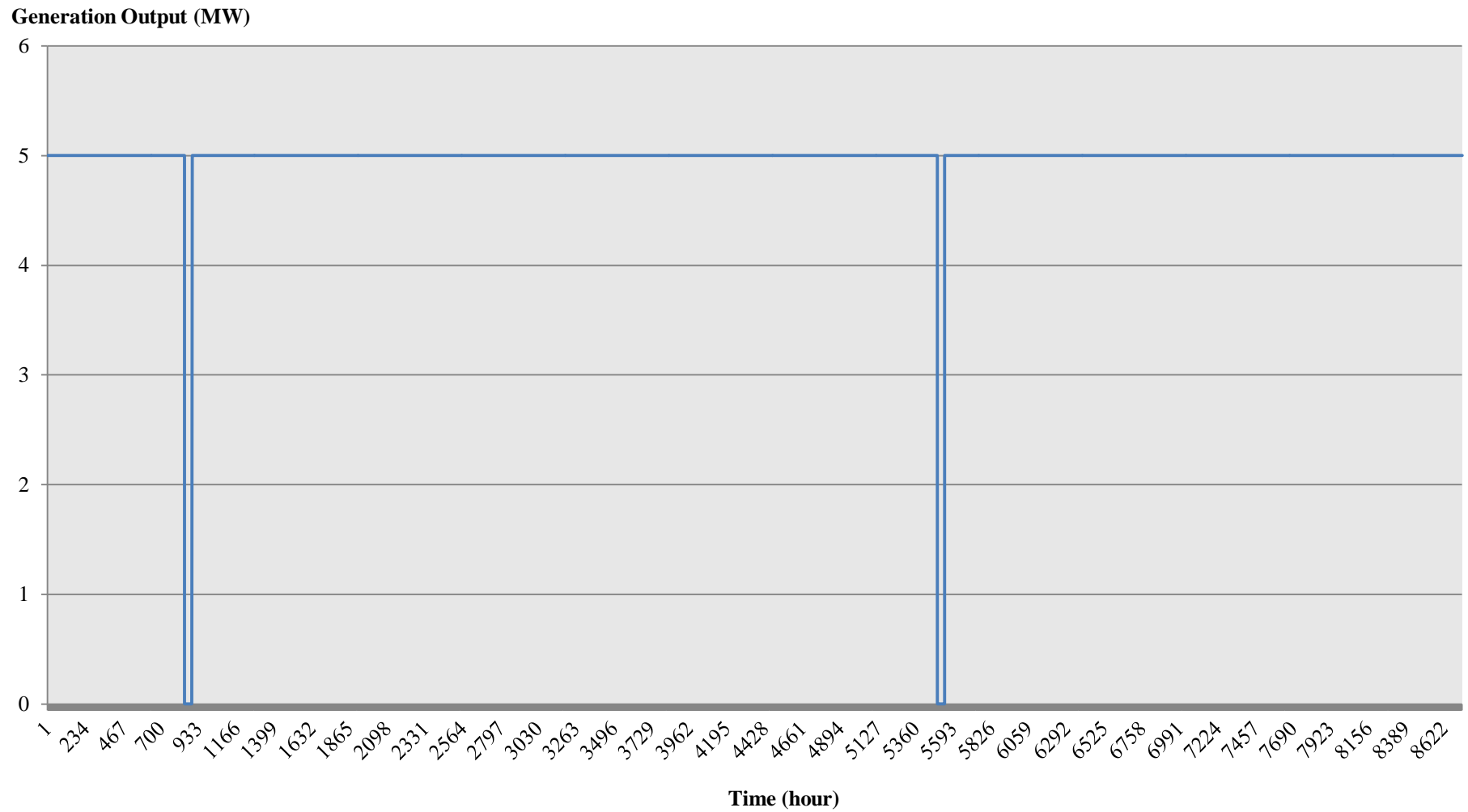


Figure 4.5: 5-MW Unit Generation Output Model

It is clear that there are two “down” states in its operation cycle. The durations of these “down” states can be found from the simulation results in Matlab as:

**Duration 1:** from the time interval 848 to 893. And in the simulation procedure, each time interval represents 1 hour. So, the duration is 45 hours, which is the MTTR of the 5-MW unit.

**Duration 2:** from the time interval 5496 to 5541, the duration is also 45 hours.

Therefore, the failure rate per year and Mean Time to Repair of the 5-MW generating unit are perfectly presented in *Figure 4.5*. The matlab program codes of the generating unit model can be found in Appendix III. Applying the generation output model building approach to each generating unit in MRBTS, the total generation output model can be obtained, which is shown in *Figure 4.6*.

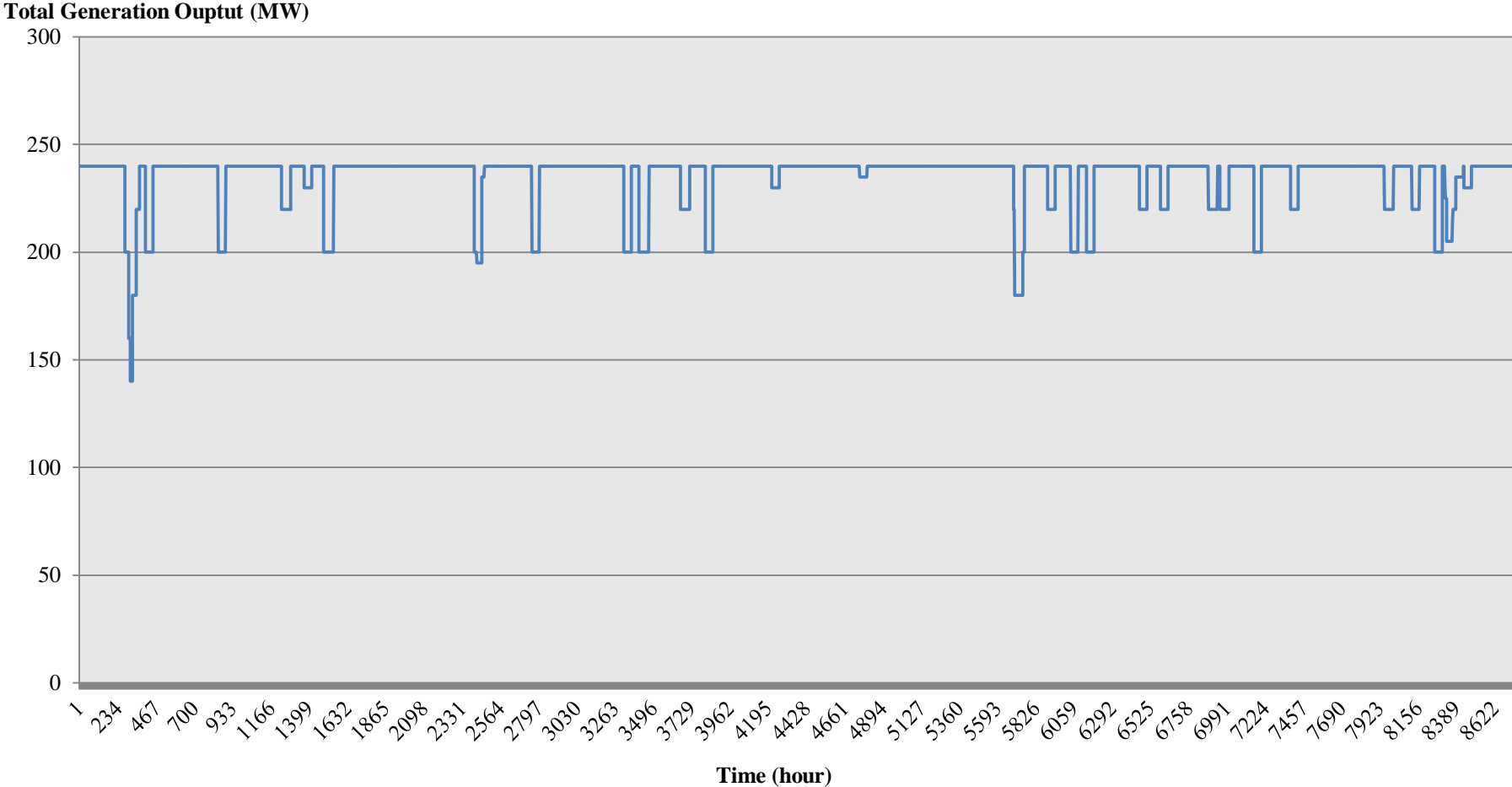


Figure 4.6: MRBTS Total Generation Output (1 Sample)

The total available generation capacity of MRBTS is shown in *Figure 4.6*, and the annual load demand is shown in *Figure 4.2*. The reliability assessment can be evaluated by combining the available generation capacity with the load demand to compute required reliability index. *Figure 4.7* shows the superimposition of chronological available system capacity and system load, an outage is counted when the load exceeds the available system capacity.

From the figure and the simulation results in this example, the system capacity is always higher than the load. It means that there is no outage during the whole year in this simulation. Therefore, the simulation must be tested and repeated many times to obtain the results close to the practical applications, which will be discussed in the latter section.

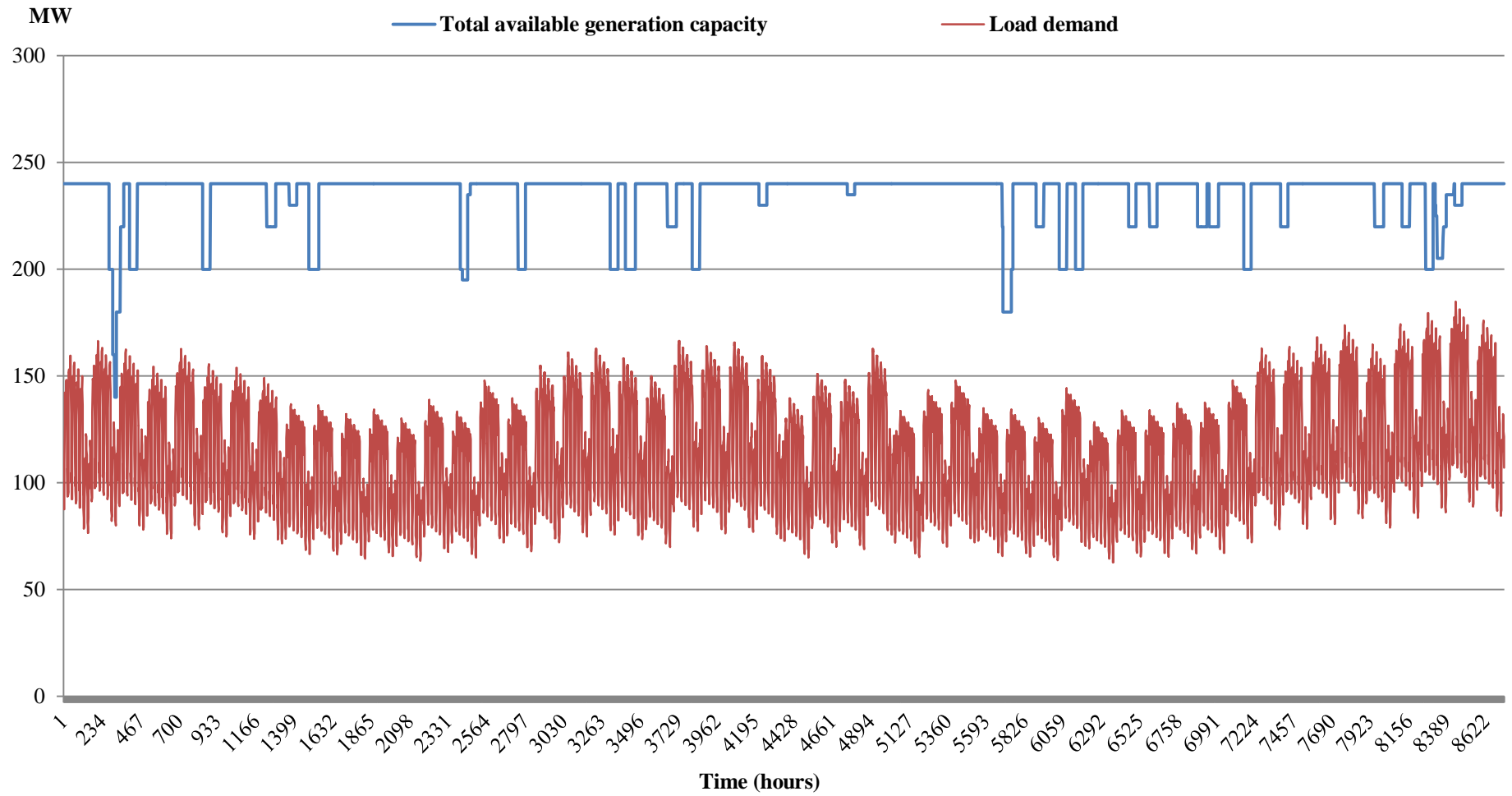


Figure 4.7: Superimposition of System Capacity and Load

## 4.5 Results and Discussions of MRBTS Reliability Evaluation

The reliability evaluation results can be obtained by superimposing the load model (*Figure 4.2*) on the total generation output model (*Figure 4.6*), an outage is counted when the load is higher than system capacity. The results shown in *sections 4.3* and *4.4* are calculated by Matlab and the simulation only takes 1 sample. In order to make the simulation results get close to the practical values of the modified test system, Monte Carlo Simulation method is used in this section. The method can apply random number and different kinds of distribution function to simulate the operation of each unit in the system.

As discussed in *section 3.3.3*, MCS is a continuous varying convergence process and it cannot provide real value for the expected reliability index but can approach it. It is important to keep MCS sampling repeatedly for many times within a long test period to achieve a certain accuracy level of the simulation results.

### 4.5.1 Number of Samples

The random numbers are pseudorandom numbers, so they must be tested in a sufficiently long period in order to guarantee their performances. The basic system reliability indices (LOLE, LOEE and LOLF) in *section 3.3.1* are used in this part. In this section, LOLE results are used to demonstrate which number of samples is applicable for the simulation. The parameter settings of generating units (rated power output, failure per year and forced outage rate) are the same in all samples; it is the prerequisite of the simulation. *Table 4.6* and *Figure 4.8* show the LOLE results of different number of samples.

**Table 4.6: MRBTS LOLE Results of Different Number of Samples**

N	LOLE (hours/year)	N	LOLE (hours/year)
1	3.00	1,000	1.25
2	6.00	3,000	1.12
3	4.30	5,000	1.21
5	0.40	6,000	1.15
10	1.40	7,000	1.18
50	1.06	10,000	1.14
100	1.29	20,000	1.12
200	0.77	50,000	1.15
500	1.53	70,000	1.14



**Figure 4.8: MRBTS LOLE Results of Different Number of Samples**

*Figure 4.8* proves the convergence of MCS in reliability results, which was discussed in *section 3.3.3*. However, large number of samples will cause the calculation time of the computer program increased significantly. It can be seen from the figure and table, the value of LOLE at  $N=6000$  is very close to the values of LOLE at  $N=50000$  or  $70000$ . Therefore, the setting of the number of samples is 6,000 in this thesis, according to the balance between the reliability evaluation cost and accuracy.

## 4.5.2 Results

From the previous section, the number of samples has been confirmed to 6,000. So, the results of MRBTS reliability assessment can be obtained by using Monte Carlo Simulation based on Frequency & Duration method in Matlab, which are shown in *Table 4.7*.

***Table 4.7: Results of MRBTS Reliability Assessment***

LOLE (hours/year)	1.15
LOEE (MWh/year)	10.5
LOLF (occ./year)	0.24

From *Table 4.7*, the average number of hours on which the load is expected to exceed the available generating capacity is 1.15 hours/year. The expected energy that will not be supplied due to those periods when the load exceeds the available generation is 10.5 MWh/year. And the expected frequency of encountering deficiencies is 0.24 occ. /year.

Therefore, the proposed approach (combine Monte Carlo Simulation with F&D method) proved to be effective to analyse the reliability assessment of a conventional power system. And the calculated reliability indices of the Modified RBTS will also be used in Chapter 6 for further investigation on the reliability evaluation.

## 4.6 Summary

This chapter has presented a reliability assessment example of the Modified Roy Billinton Test System (MRBTS). The load model data was modified based on the IEEE-Reliability Test System (RTS). Three types of load curves have explained and simulated in this part as daily load curve, weekly load curve and annual load curve. Each of these curves represents a different pattern. For the annual load curve, it can be seen that the winter load demand is larger than the summer. Then, the weekly load curve shows that the weekend load demand is smaller than weekdays load demand. During a 24-hour period, it is clear that 7:00~22:00 is the peak period, and 22:00~7:00 is the off-peak period.

According to the generating units' reliability data, the total system generation output model can be obtained by using Monte Carlo Simulation based on F&D method. Then, the modified test system reliability assessment can be simulated by MCS method combined with the outage frequency and duration. In addition, the setting of the number of samples has also been discussed in this chapter and it is set to 6000, which will be used in future simulations in this thesis.

The reliability assessment results of MRBTS are represented by three important reliability indices, LOLE, LOEE and LOLF. The results in *Table 4.7* will be used in future chapters for analysing the impact of wind power integration on power systems reliability.

# Chapter 5. Weibull Distribution for Power Output of Wind Farms

## 5.1 Introduction

Chapter 2 introduced wind energy in 3 aspects: wind speed model, wind turbine output model, and classifications of the wind farm. Chapter 4 presented an approach for the power system reliability assessment, which is the combined approach of Frequency & Duration (F&D) method and Monte Carlo Simulation (MCS) method. Then, the total available system generation and load model were also discussed in the test system. It was found that the proposed approach is an effective tool to analyse the conventional power system reliability assessment. Consequently, this chapter proposes a calculation model of wind farm power outputs for evaluating the impact of wind power penetration on power systems.

Therefore, it is important to build a wind farm power output model for the reliability evaluation. This chapter uses the Weibull distribution function to represent the wind speed variations by modifying Weibull scale and shape parameters. Weibull distribution has an important characteristic: no specific shape. It can be shaped to represent many distributions by changing its parameters, as long as they are positive. Then, the wind farm power output can be calculated based on the wind speed profile.

This chapter is structured as follows. *Section 5.2* presents an overview of wind characteristics. An illustrated example of the wind speed distribution will also be explained in this section. The details of Weibull distribution are discussed in *section 5.3*. The complementary cumulative Weibull probability distribution combined with inverse transform method are used in *section 5.4* to obtain the artificial wind speed model. The power output model of the wind turbine is described in *section 5.5*,

including the calculation procedure and the flow chart. *Section 5.6* presents the comparisons between multiple wind farm outputs.

## 5.2 Overview of Wind Characteristics

### 5.2.1 Wind Speed Variation

The energy available in the wind varies as the fluctuation of the wind speed. So, an understanding of wind characteristics is critical to all aspects of wind energy development. For instance, the cost/ benefit viability of wind farm projects, site selections for wind farms and the effect of wind speed fluctuations on wind turbine technology and electric networks.

The most outstanding characteristic of the wind is its variability. The wind speed is highly variable, both geographically and temporally [38]. On a large scale, the variability represents the fact that there are many different climatic regions in the world, some much windier than others, like Scotland. More locally, the terrain has a significant effect on the wind speed. For example, more wind is experienced on the tops of hills and mountains than in the lee of high ground or in sheltered valleys.

At a given location, temporal variability on a large scale means that the amount of wind may vary from one year to the next. These long-term variations are difficult to predict for the wind farm site selection. On a shorter timescale, seasonal variations are much more predictable, although there are still large variations within the period. On a specific wind farm site, diurnal variations are usually fairly predictable. Wind speed variations on these timescales have effects on integrating wind power generation into the electricity network. On shorter timescales of minutes down to seconds, wind speed variations can have a significant impact on the design and performance of the wind turbine and the quality of power delivered to the electric network [107].

## 5.2.2 Example: Wind Speed Distribution in the Peninsular Malaysia

The wind speed data are available in time series format, in which each data represents an instantaneous sample wind speed or an average of wind speed taken at short time intervals of time [108]. The data used in this example is the hourly wind speed data measured from January 1995 to December 2000. The wind speed is measured by Kuala Terengganu wind speed station at the east coast of Peninsular Malaysia. The wind speed data can be converted to the frequency distribution format whereby the frequency with which the wind speed falls within various ranges. *Table 5.1* shows the wind speed data of Kuala Terengganu in the frequency distribution format. The table will consist of 5 columns including 21 states divided by wind speeds variable ranges. The initial recorded wind speed is 0.25 m/s, and the variable range is 0.50 m/s per state. For instance, State 1: the range of the wind speed is 0~0.25 m/s; State 2: the range of the wind speed is 0.25~0.75 m/s.

And wind speeds were recorded for a total number of 41,339 times. So, wind speeds can be expressed by their individual frequencies and cumulative frequencies. Both of these terms were discussed in details in *section 3.2.1*. In this case, the term of frequency (number) means how many times each state has been recorded, and the frequency (%) represents the number of recorded times at each individual state in percent of the total recorded time. Moreover, the term of cumulative frequency (%) presents the frequencies of wind speeds are equal to or less than the indicated wind speed.

**Table 5.1: Wind Speed Data in Frequency Distribution and Cumulative Frequency Distribution Formats at Kuala Terengganu [108]**

(1)	(2)	(3)	(4)	(5)
State No.	Wind speed (m/s)	Frequency (number)	Frequency (%)	Cumulative frequency (%)
1	0.25	3626	8.771	8.771
2	0.75	4696	11.359	20.13
3	1.25	5741	13.887	34.017
4	1.75	5179	12.528	46.545
5	2.25	4665	11.284	57.829
6	2.75	4554	11.016	68.845
7	3.25	3650	8.829	77.674
8	3.75	3483	8.425	86.099
9	4.25	1876	4.538	90.637
10	4.75	1832	4.432	95.069
11	5.25	752	1.819	96.888
12	5.75	506	1.224	98.112
13	6.25	353	0.854	98.966
14	6.75	198	0.479	99.445
15	7.25	92	0.223	99.668
16	7.75	76	0.184	99.852
17	8.25	35	0.085	99.937
18	8.75	16	0.039	99.976
19	9.25	5	0.012	99.988
20	9.75	3	0.008	99.996
21	10.25	1	0.003	100.000

The wind speed distribution can be obtained by using the wind speed profile as the horizontal axis and the individual wind speed frequency as the vertical axis, which is shown in *Figure 5.1*. Wind speeds were recorded over 6 years; it is clear that in most areas strong winds are rare, while moderate winds are quite common. It is very

important for the power system to be able to describe and analyse the variation of wind speeds. The wind variation for a specific wind farm site is usually described using the so-called Weibull distribution. The details of Weibull distribution will be presented in the following section.

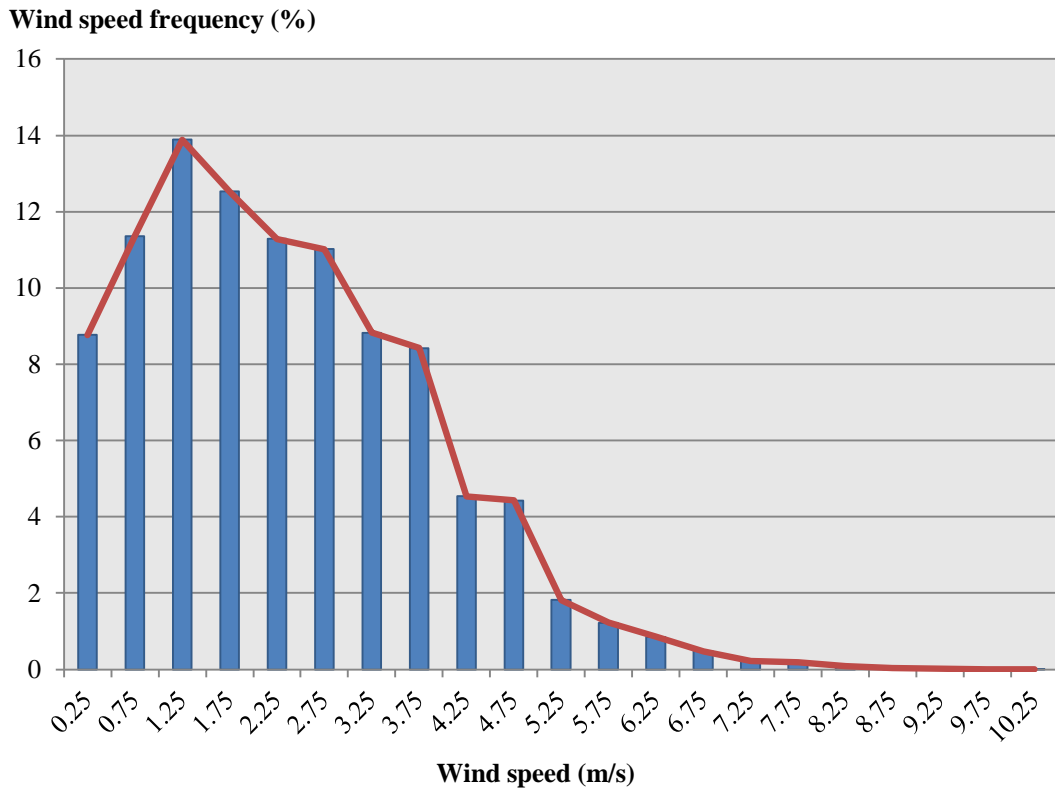


*Figure 5.1: Wind Speed Distribution at Kuala Terengganu*

## 5.3 Weibull Distribution

Although wind is an intermittent source of energy, it represents a reliable and renewable energy resource from a long-term energy policy viewpoint. At a specific wind farm, the available electricity generated by a wind turbine depends on the mean wind speed (MWS) and the standard deviation of wind speed. Since yearly variation on annual MWS is difficult to predict, wind speed variations can be well characterized in terms of a probability distribution function (pdf) [109]. Recently,

Weibull distribution has been employed to represent the variation of hourly MWS over a year in many studies [38, 62, 110, 111].

In probability theory and statistics, Weibull distribution is a continuous probability distribution. As introduced in *section 2.5.1*, Weibull distribution can be shaped to represented wind speed variations by modifying the scale parameter  $c$  and the shape parameter  $k$ . The expression of individual Weibull probability distribution function is as *Equation 5.1*.

$$f(v) = \frac{kv^{k-1}}{c^k} \exp\left[-\left(\frac{v}{c}\right)^k\right] \quad (5.1)$$

Where:  $f(v)$ : the probability of occurrence of wind speed  $v$  ( $v \geq 0$ )

$c$  ( $c > 0$ ): the Weibull scale parameter

$k$  ( $k > 0$ ): the Weibull shape parameter

And the complementary cumulative Weibull distribution function  $F(v)$  gives the probability of the wind speed exceeding the value  $v$ . The expression is given as *Equation 5.2*.

$$F(v) = \exp\left[-\left(\frac{v}{c}\right)^k\right] \quad (5.2)$$

So, the cumulative Weibull probability distribution function is expressed as *Equation 5.3*:

$$F(v) = 1 - \exp\left[-\left(\frac{v}{c}\right)^k\right] \quad (5.3)$$

Therefore, the distribution characteristic of the cumulative Weibull distribution function is apparently monotonically increasing as shown in *Figure 5.2*.

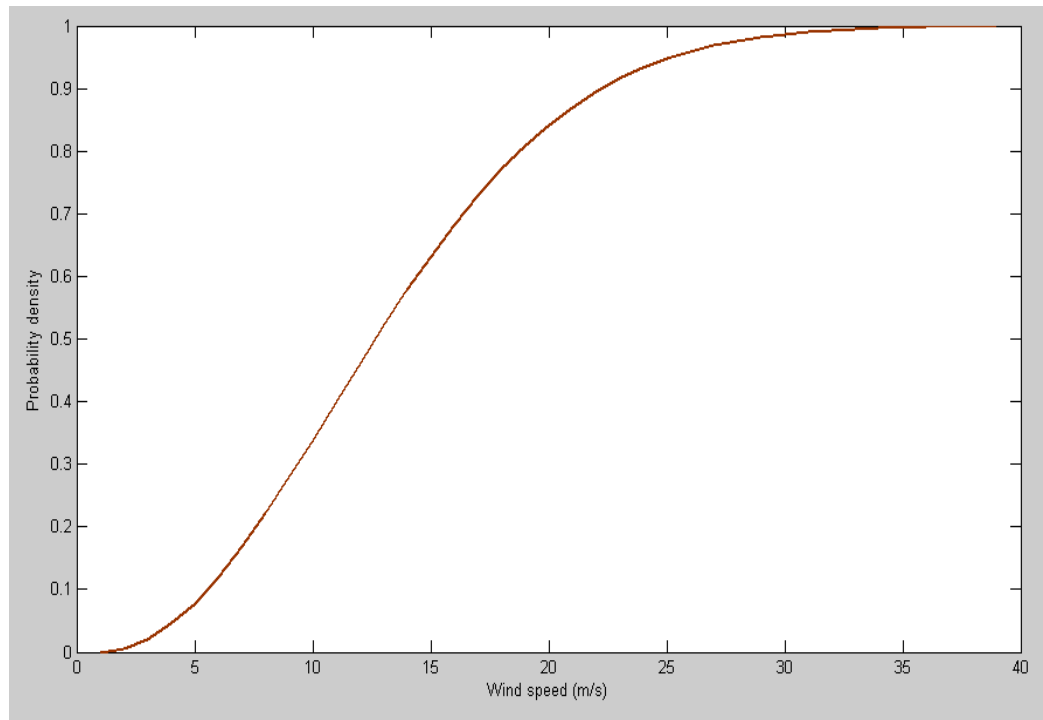


**Figure 5.2: Cumulative Weibull Probability Distribution ( $c = 7$  &  $k = 2$ )**

### 5.3.1 The Weibull Scale Parameter

The scale of the Weibull distribution is determined by  $c$ . In the simulation of the wind speed,  $c$  is the mean wind speed in m/s. A change in  $c$  has the same effect on the distribution as a change of the abscissa scale. Increasing  $c$  will have the effect of stretching out the pdf, when holding  $k$  constant. The higher value of  $c$  indicates that the wind speed is higher. Since the area under a pdf curve is a constant value of 1, the “peak value” of the pdf curve will also decrease with the increasing  $c$  as shown in *Figure 5.3*.

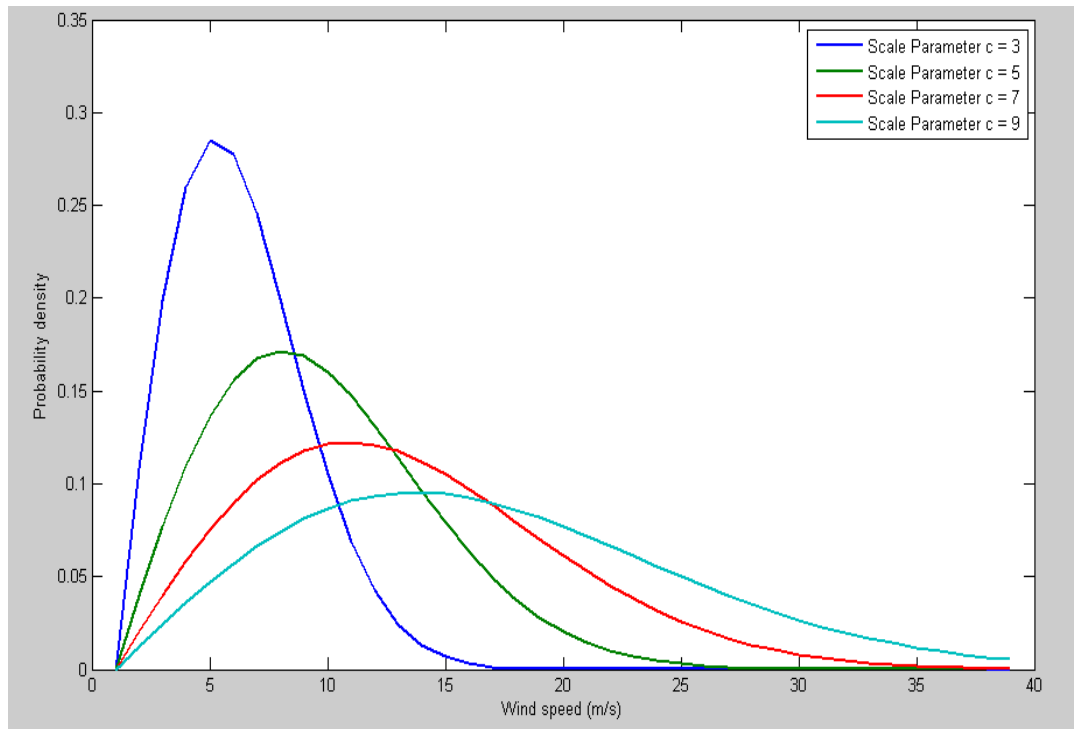


**Figure 5.3: Weibull Distribution Density versus Wind Speed under a Constant Value of  $k=2$  and Different Values of  $c$**

- If  $c$  increases, while  $k$  remains the same, the probability distribution gets stretched out to the right and its height decreases while maintaining its shape and location. It means that high wind speed situations will increase, and the scale of wind speed variations is extending.
- If  $c$  decreases, while  $k$  remains the same, the probability distribution gets pushed in towards the left and its height increases. The wind speed variation is represented by low wind speed situations of the majority.

### 5.3.2 The Weibull Shape Parameter

The shape of Weibull distribution is controlled by shape parameter  $k$ . It is also called the Weibull slope due to the value of  $k$  is equal to the slope of the line in a probability plot. In fact, the Weibull distribution is related to a number of other probability distributions. Some values of the shape parameter will cause the distribution change to other distributions. For example, when  $k = 1$ , the Weibull distribution changes to the exponential distribution; when  $k = 2$ , the Weibull distribution changes to the Rayleigh distribution. In wind power systems, the normal setting of  $k$  for wind speed distribution is 2 [38].

Figure 5.4 shows the effect of different values of the shape parameter  $k$  on the shape of the pdf, while keeping  $c$  constant. It can be seen that the shape of the Weibull distribution can have a variety of forms based on the value of  $k$ . When  $k = 2$ , the shape is similar to the wind speed variations as most of wind speed situations are moderate, and extreme low and high wind speeds are rare.

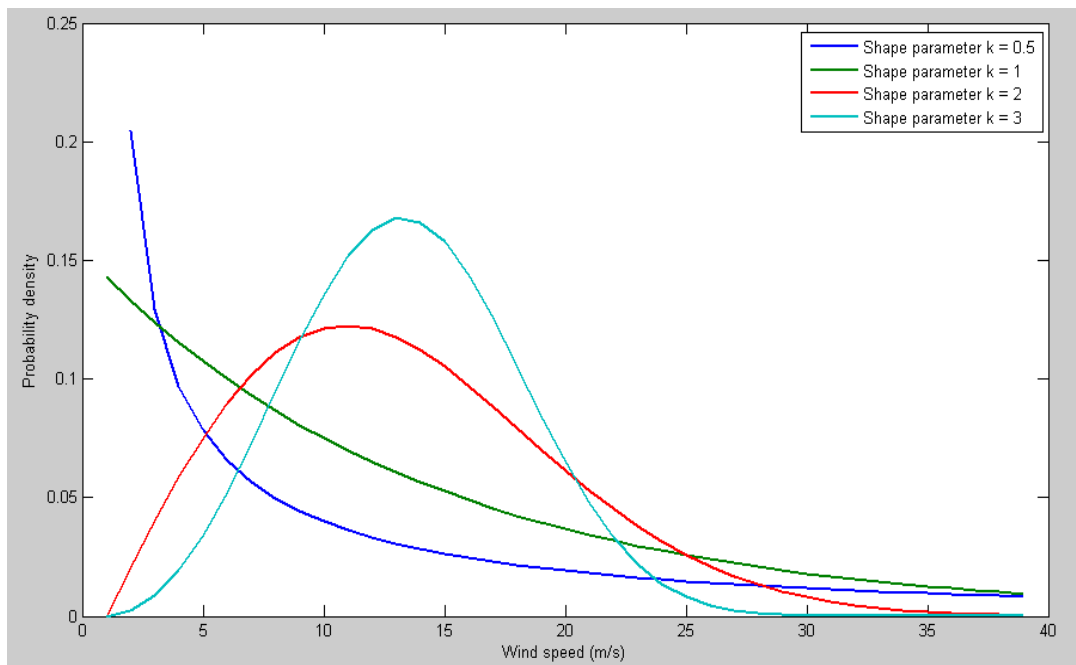


**Figure 5.4: Weibull Distribution Density versus Wind Speed under a Constant Value of  $c=7$  and Different Values of  $k$**

### 5.3.3 Seasonal Variation of Weibull Distribution

The model of wind speed variation is critical for estimating wind energy potential at a typical site. In this section, an example will be analysed to determine wind energy potential for electricity production by grouping the seasonal observations. The Weibull distribution has been used to represent the variation of hourly mean wind speed over a year at Aimangala station in Karnataka, India [110]. The wind speed data and distribution are used in this example are from April 2007 to March 2008, as shown in *Table 5.2*.

**Table 5.2: Weibull Distribution Parameters at Aimangala Station**

No.	Season	Scale parameter $c$ (m/s)	Shape parameter $k$
1	Summer	6.619	2.088
2	Monsoon	10.878	2.679
3	Winter	6.594	2.645

The Weibull distributions can be generated by using the data in *Table 5.2*. And *Figure 5.5* shows that the differences between these three seasons. Apparently, the monsoon has a huge potential of wind energy resources. The wind speeds are mainly distributed between 15 m/s~30 m/s, which are significantly larger than the other two seasons.

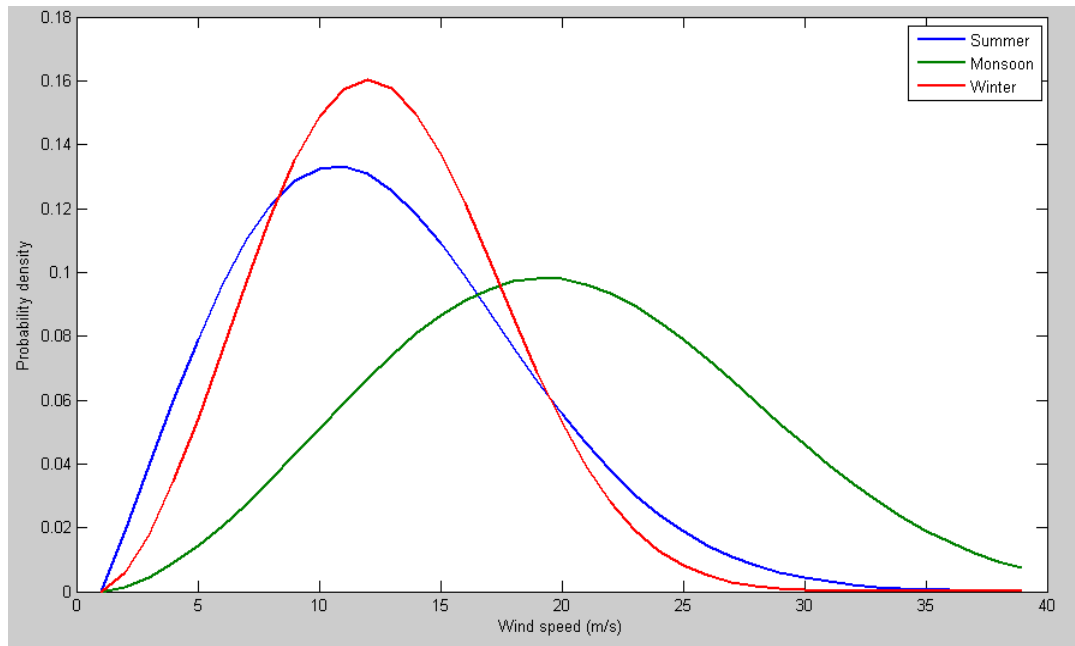


**Figure 5.5: Seasonal Variation of Probability Density Function versus Wind Speed at Aimangala Station**

## 5.4 Artificial Generated Wind Speed

Power system reliability assessment requires the data of wind power generation output. In order to modelling the wind turbine output, it is necessary to build a wind speed model. The wind speed is simulated by combining the Weibull distribution and random variables. The most popular used method in power system simulation for random variable generation is the inverse transform of probability distribution function (pdf) [112, 113].

The cumulative Weibull probability distribution function as shown in *Equation 5.3* is used in this section, and the definition of the cumulative probability distribution function was introduced in Chapter 3. In this section, the cumulative Weibull distribution function  $F(v)$  represents the probability of the wind speed, which is not exceeding the indicated wind speed  $v$ .

Assume:

$$U = F(v) = 1 - \exp\left[-\left(\frac{v}{c}\right)^k\right] \quad (5.4)$$

$U$  is a uniformly distributed random variable between  $[0, 1]$ .

Using the inverse transform method

$$v = c[-\ln(1 - U)]^{\frac{1}{k}} \quad (5.5)$$

Because any  $(1 - U)$  also represents a random variable uniformly distributed between  $[0, 1]$ , then *Equation 5.5* can be simplified:

$$v = c[-\ln(U)]^{\frac{1}{k}} \quad (5.6)$$

Therefore, the wind speed  $v$  can be generated artificially by using *Equation 5.6*. Then, the power output of the wind turbine can be obtained by applying the wind speed into wind turbine output model, which was presented in *section 2.5.2*.

Applying the Weibull distribution function with *Equation 5.6*, where the Weibull parameters set to  $c = 7$  &  $k = 2$ . The simulated wind speed profile for 300 hours is shown in *Figure 5.6*. It can be seen that the wind speed is constantly changing; strong winds and weak winds are rare, most of the situations are moderate winds. From *Figure 5.6*, it is clear that most wind speeds are mainly distributed between 4 m/s and 10 m/s. Therefore, Weibull distribution can have an excellent performance on simulating the wind speed profile by modifying its scale and shape parameters.

**Wind speed (m/s)**

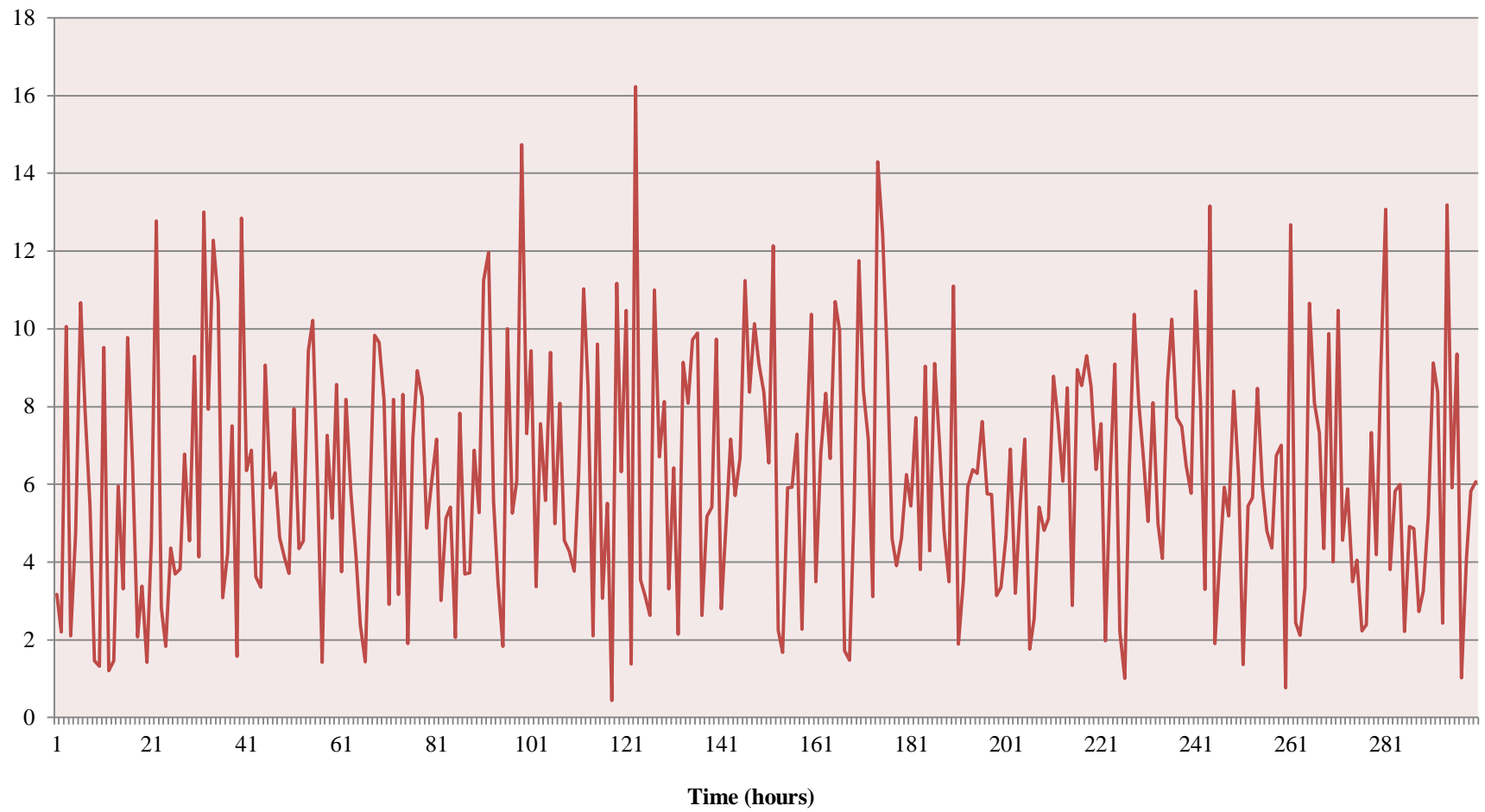


*Figure 5.6: Snap Shot of Simulated Wind Speed (300 hours)*

## 5.5 Weibull Distribution for Wind Turbine Output Calculation

The wind turbine output model has been described in *section 2.5.2*. The model details can be summarized as the following parts.

### Power output:

$$P_w = \begin{cases} 0, & ws < V_{ci} \\ (A + B * ws + C * ws^2) * P_{wr}, & V_{ci} \leq ws < V_r \\ P_{wr}, & V_r \leq ws < V_{co} \\ 0, & ws \geq V_{co} \end{cases} \quad (5.7)$$

Where:

$ws$  = the wind speed (m/s)

$V_{ci}$  = cut-in speed of the WTG (m/s)

$V_r$  = rated speed of the WTG (m/s)

$V_{co}$  = cut-out speed of the WTG (m/s)

$P_{wr}$  = rated power output of the WTG (MW)

### Constants A, B and C:

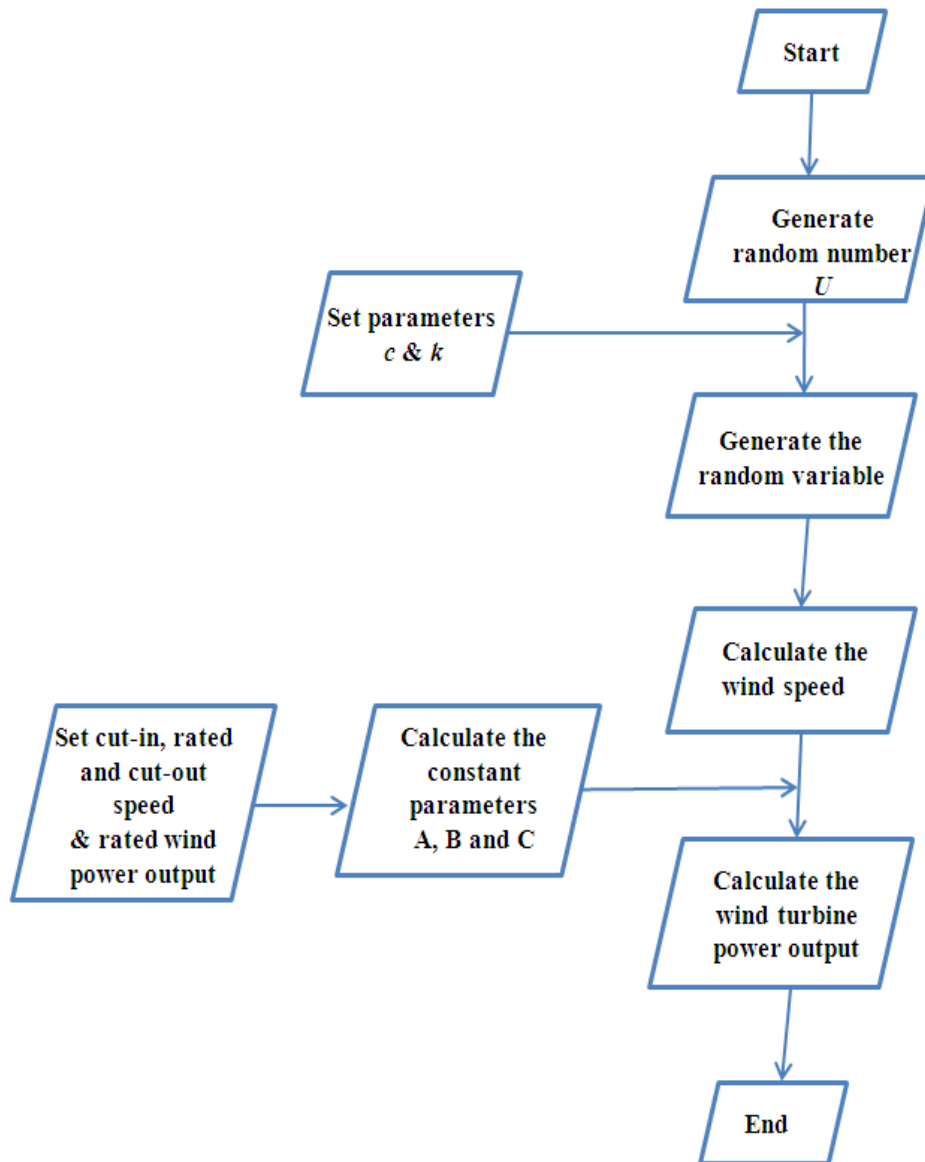
$$A = \frac{1}{(V_{ci} - V_r)^2} [V_{ci}(V_{ci} + V_r) - 4V_{ci}V_r \left(\frac{V_{ci} + V_r}{2V_r}\right)^3] \quad (5.8)$$

$$B = \frac{1}{(V_{ci} - V_r)^2} [4(V_{ci} + V_r) \left(\frac{V_{ci} + V_r}{2V_r}\right)^3 - (3V_{ci} + V_r)] \quad (5.9)$$

$$C = \frac{1}{(V_{ci} - V_r)^2} [2 - 4 \left(\frac{V_{ci} + V_r}{2V_r}\right)^3] \quad (5.10)$$

**Calculation procedure:**

- 1) Set the scale parameter  $c$  and the shape parameter  $k$  for the Weibull distribution, normally the value of  $k$  is 2 respectively.
- 2) A uniformly distributed random number  $U$  between  $[0, 1]$  is generated.
- 3) Generate the random variable with inverse transform of the modified cumulative Weibull distribution function as shown by *Equation 5.3*.
- 4) Calculate the artificial wind speed  $v$  with *Equation 5.6*.
- 5) Set the cut-in, rated and cut-out wind speed, and rated power output for the wind turbine.
- 6) Calculate the constants  $A$ ,  $B$  and  $C$  with *Equations 5.8- 5.10*.
- 7) Calculate the wind turbine power output with *Equation 5.7*.

**Flow chart:**

*Figure 5.7: Flow Chart for Wind Turbine Power Output Model*

**Example:**

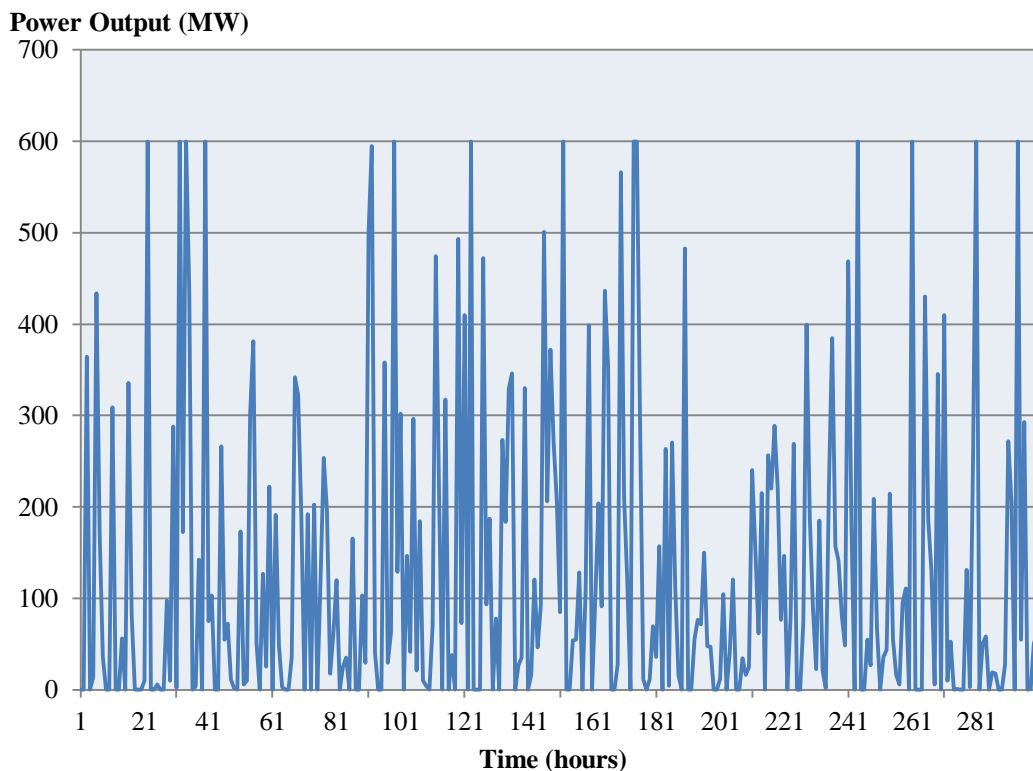
The wind turbine's data are shown in *Table 5.3*. The scale and shape parameters  $c$  &  $k$  will be set to 7 and 2, which is the typical configuration for the wind turbine output calculation.

**Table 5.3: Wind Turbine Parameter Data**

<b>Rated Power Output</b>	5 MW
<b>Cut-in speed</b>	4 m/s
<b>Rated speed</b>	12 m/s
<b>Cut-out speed</b>	25 m/s

There are 120 wind turbines in a single wind farm with a total installed capacity of 600 MW. *Figure 5.8* is the 300 hours snapshot of simulated wind farm power output.

As explained previously, the wind speed can be simulated by Weibull distribution. In this example, the wind farm power output is calculated based on the wind speed profile in *section 5.4*. Therefore, the power system reliability assessment with wind power penetration can be evaluated by combining the conventional evaluation results in Chapter 4 with the wind farm output results in this chapter.

**Figure 5.8: Snapshot of Simulated Wind Farm Power Output**

## 5.6 Power Outputs of Multiple Wind Farms

In the practical applications, it is unrealistic that the wind farm output is concentrated in one wind farm. It is necessary to investigate the power outputs of multiple wind farms. There are 3 scenarios in this section: 2 wind farms, 3 wind farms and 5 wind farms. All of the wind farms will be allocated at different locations and followed by the same Weibull distribution ( $c = 7$  &  $k = 2$ ). Furthermore, each wind farm location is fully independent, and the energy losses when one wind farm is situated downstream from another one can be neglected. Then, the wind turbines which are used in this section have same parameters as introduced in *section 5.5*.

There are 120 wind turbines in each scenario:

2-wind farm (Farm 1 and 2): 60 wind turbines per wind farm

3-wind farm (Farm 1, 2 and 3): 40 wind turbines per wind farm

5-wind farm (Farm 1, 2, 3, 4 and 5): 24 wind turbines per wind farm

The simulation results of these three scenarios will be compared with the simulation results of the single wind farm case in *section 5.5*, which are shown in *Figures 5.9-5.11*.

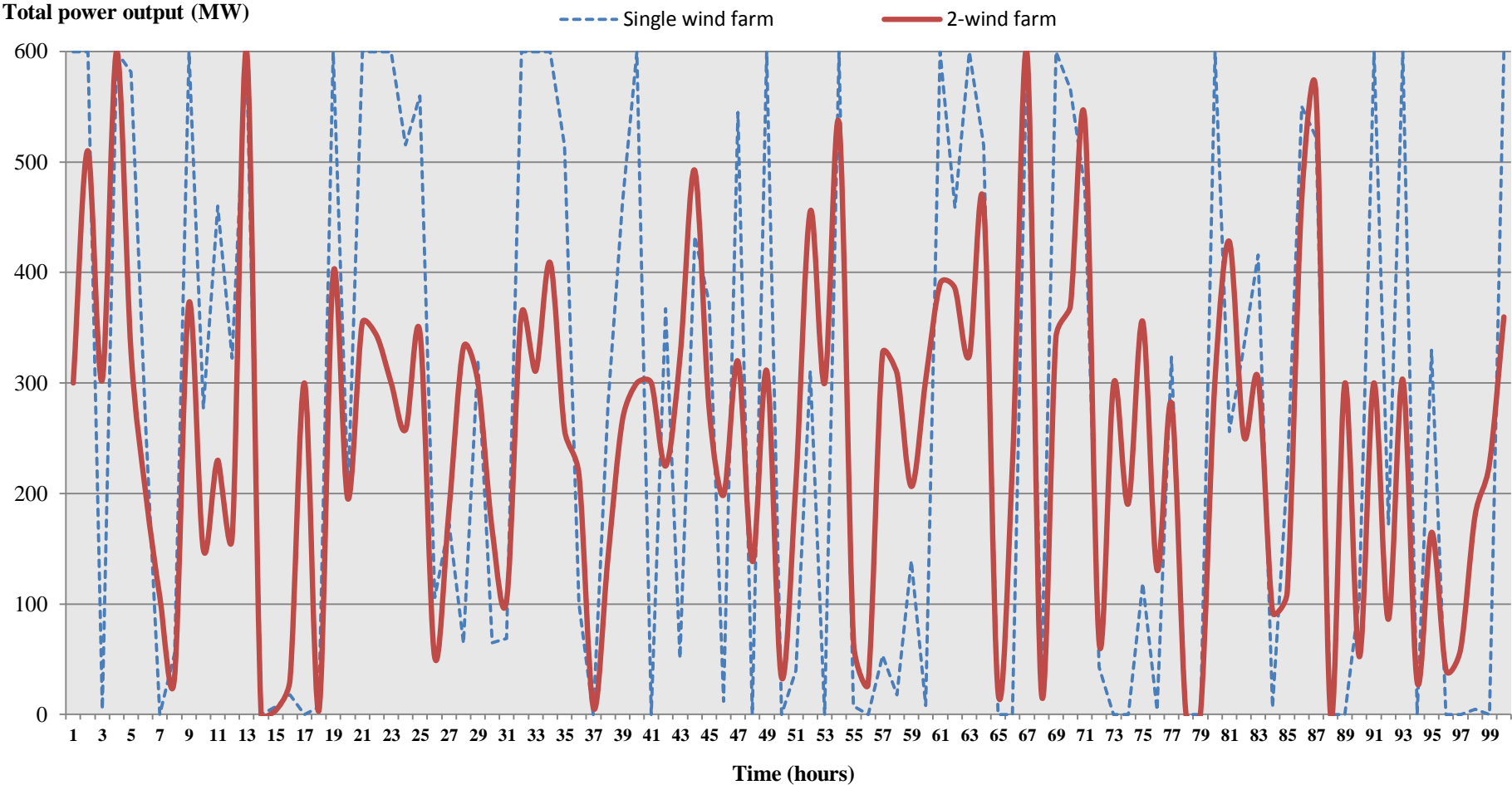


Figure 5.9: Power Output Comparison of Single Wind Farm and 2-Wind Farm (100 hours)

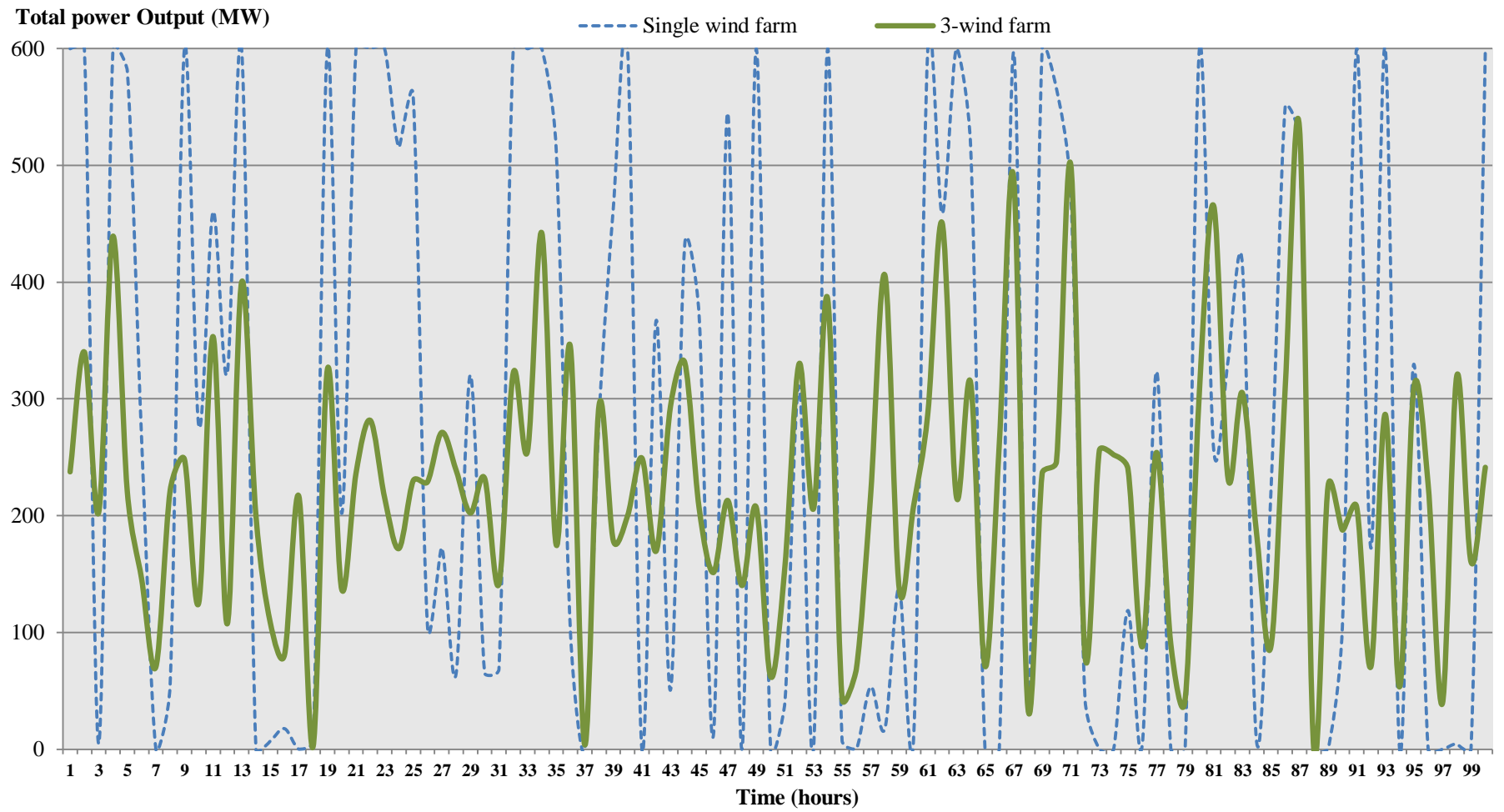


Figure 5.10: Power Output Comparison of Single Wind Farm and 3-Wind Farm (100 hours)

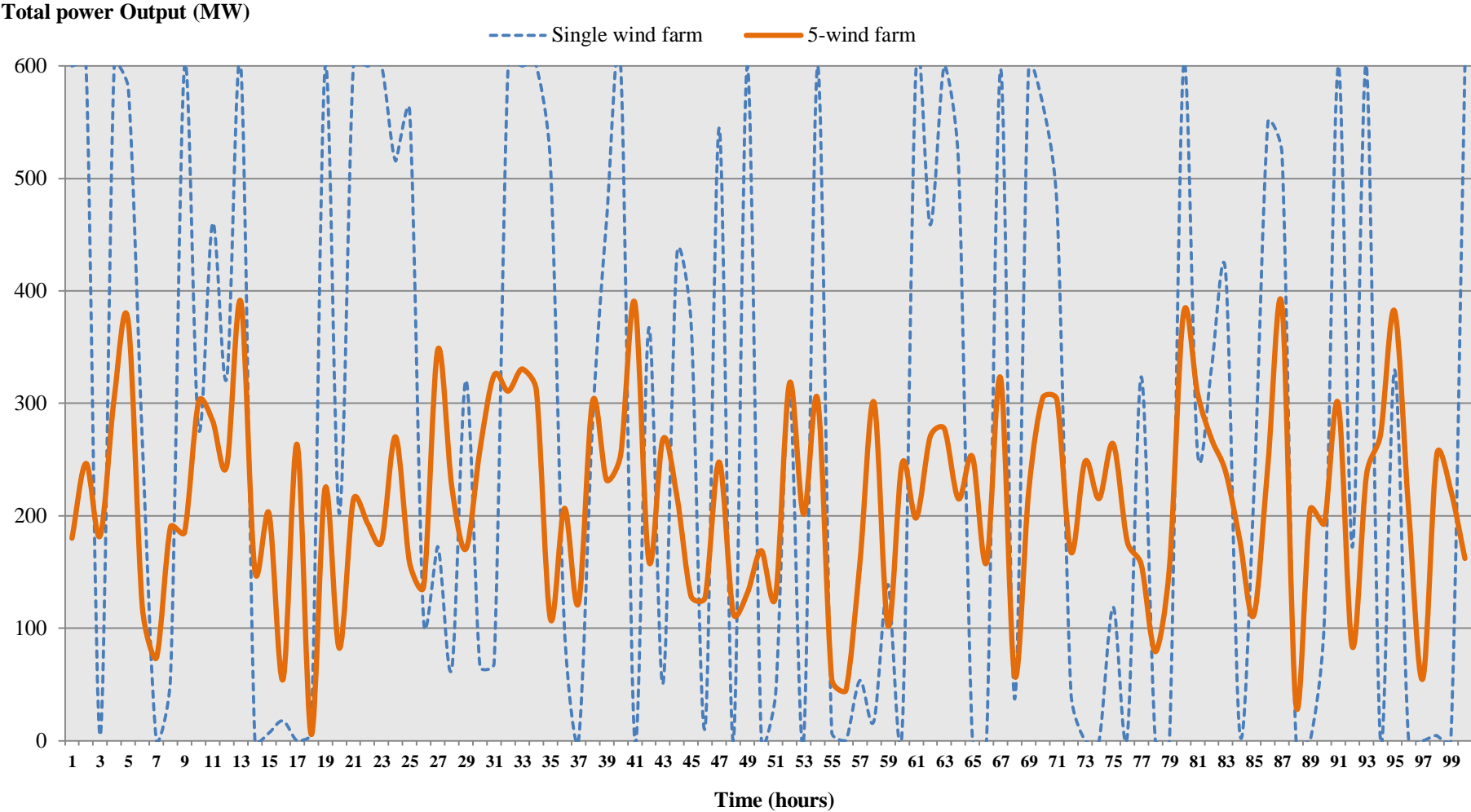


Figure 5.11: Power Output Comparison of Single Wind Farm and 5-Wind Farm (100 hours)

There is a trend that the power output curves will become smoother when the number of wind farms is increasing, which can be seen from *Figures 5.9- 5.11*. It means that the outputs from multiple wind farms can effectively reduce the fluctuation of wind power generation output. However, it is clear that it is difficult to reach higher power output for multiple wind farms situation. Therefore, multiple wind farms situation has a better performance on reducing power output fluctuations for the power system reliability. The simulation results will also be used in further discussions in Chapter 7.

## 5.7 Summary

This chapter emphasizes the related areas about wind energy, including wind speed variation, Weibull distribution, and wind farm power output calculation. It is important to build a wind farm output model for evaluating the impact of integrating wind energy into power system. The power system reliability assessment with wind power penetration can be evaluated by combining the conventional generation-load model in chapter 4 with the wind power output model in this chapter.

Firstly, wind speed variations have been presented in two aspects, geographically and temporally. An illustrated example shows that the wind speed distribution is following a certain pattern, which can be simulated by Weibull distribution function. Then, Weibull distribution was introduced in details. In addition, the settings of Weibull scale and shape parameters were also discussed. The typical setting of Weibull shape parameter  $k$  is 2 for calculating wind turbine outputs.

Therefore, the wind speed can be simulated by combining Weibull distribution with random variables. Finally, the wind turbine power output can be calculated through simulated wind speeds. Power outputs of multiple wind farms also have been analysed in this chapter. By comparing with the single wind farm situation, multiple wind farms situation has less power output fluctuations.

# **Chapter 6. Wind-Hydro Cooperation in Power System Reliability Assessment**

## **6.1 Introduction**

Chapter 2 introduced wind power is the most promising renewable energy source for the sustainable development due to its advanced and mature technologies. The wind power generation is inconsistent and intermittent energy source. The wind speed variation causes the fluctuation of wind power output. High wind penetration can lead to high risk levels of the power system reliability. Also, several operating reserve (OR) assessment methods including Pump-Hydro Energy Storage (PHES) were discussed in Chapter 2. Chapter 3 presented some popular analytical methods and simulation method for power system reliability assessment. It explained the structure and the principle of each method applied in this thesis. The results showed that Frequency and Duration (F&D) method and Monte Carlo Simulation (MCS) method can be combined to a powerful method for power system reliability analysis. Consequently, a new method for reducing the effects of wind power fluctuation on power outputs, Wind-Hydro Cooperation (WHC), is presented in this thesis. It combines the advantages of MCS method and F&D method and the flexibility of PHES to evaluate the impacts of wind power generation on power system reliability for both planning phase and operating phase.

Chapter 4 provided the system load model and the generating system model for the power system reliability evaluation. The modified Roy Billinton Test System was also evaluated by using Monte Carlo Simulation method in Matlab. Chapter 5 presented the power output model of the wind farm. The utilization of the proposed

method for evaluating the effect of wind-hydro cooperation on the modified RBTS reliability at different wind penetration levels will be illustrated in this chapter.

The hydropower generation model and the methodology and the flowchart of the proposed method are explained and discussed. In addition, the Cost-Benefit Analysis (CBA) theory is also presented for determining the optimal reliability performance.

This chapter is arranged as follows: *section 6.2* introduces the model of PHCES system in details. The proposed Wind-Hydro Cooperation (WHC) method is described in details in *section 6.3*. An illustrative example will also be illustrated for proving the proposed method. The benefits of Wind-Hydro Cooperation will be described in *section 6.4*. The operation of the proposed PHCES system will be explained in *section 6.5*.

## **6.2 Pump-Hydro Combined Energy Storage (PHCES) Technology**

### **6.2.1 Overview of PHES**

Chapter 2 briefly introduced the Pumped Hydro Energy Storage (PHES) technology. There have been revived interests in PHES recently with the increasing variable renewable energy sources. In a power system, most conventional generation sources cannot flexibly adjust their outputs. As introduced in *section 2.8.3*, PHES is currently the only commercially proven large scale energy storage technology. It can provide flexible, quick start generation to stabilize the intermittent power output and is also able to store excess energy.

A PHES facility is usually equipped with pumps/generators connecting an upper and a lower reservoir/lake, as shown in *Figure 6.1*. The plant pumps water to the upper reservoir in low-price periods, working as a load, and then discharging the stored

water during high-price periods, operating as a generator [87]. The generating facility is shown in *Figure 6.2* [114].

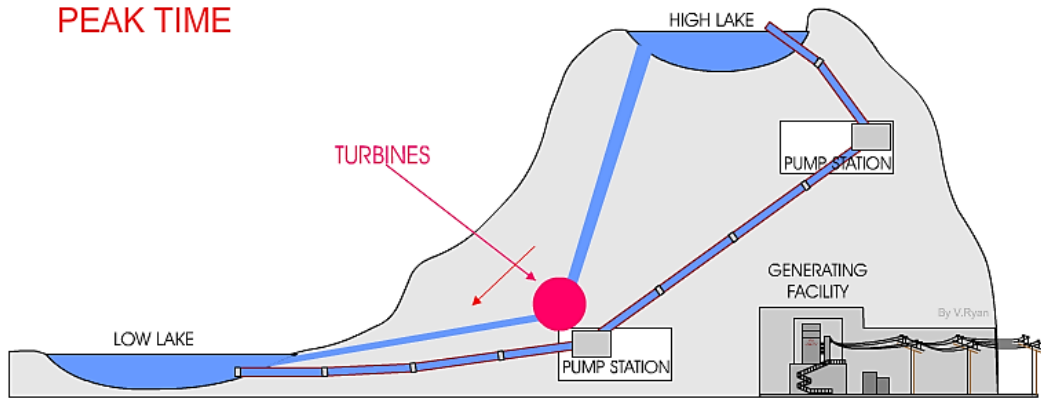


**Figure 6.1: Pumped Hydro Energy Storage (PHES) Diagram [114]**

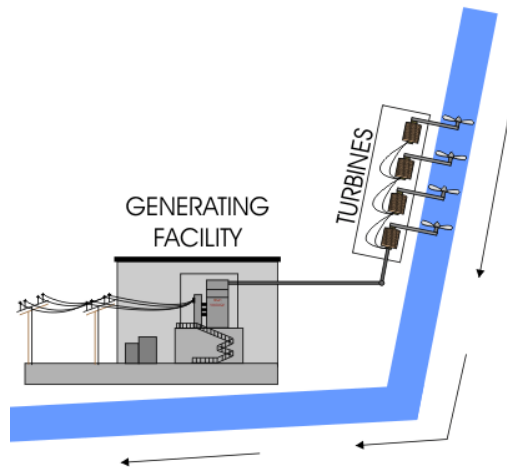


**Figure 6.2: Generating Facility of PHES [114]**

There are two main types of PHES facilities: (1) pure PHES, which depends entirely on the water that were previously pumped into the upper reservoir as a source of energy; (2) combined PHES, which uses both pumped water and natural stream flow water to generate electricity [115]. In this thesis, the large-combined PHES is presented in details for evaluating the Wind-Hydro Cooperation, which will be expressed as Pump-Hydro Combined Energy Storage (PHCES) technology.

However, there are several drawbacks in PHES technology [116]: (a) the deployment of PHES requires suitable terrains with a significant elevation difference between the two reservoirs and a significant amount of water resource; (b) the construction of a PHES station usually takes many years. Although the operation and maintenance cost is low, there is a high upfront capital investment.

Due to the worldwide revived interests in developing PHES projects, many new approaches are also proposed in several countries. For instance, Japan researchers are utilizing seawater to build a PHES system. The Okinawa seawater PHES station, which has commenced operation in 1999, is the world's first seawater PHES system [117]. On the other hand, there is a significant potential in increasing PHES capacity simply by upgrading and renovating many existing conventional hydropower stations equipped with more leading and efficient technologies.

Nowadays PHES is considered the most effective method to overcome the output fluctuation problem due to wind power integration. Storing electrical energy when the wind power output is high and the demand is low. The surplus wind power output will be reduced, and the conventional generating units in the system will operate more efficiently [118]. Generating electricity when the wind power output is low and the demand is high. The shortage of the wind power output will be compensated by the fast-response electricity supply generated by PHES units.

The theory that the intermittency of wind power can be mitigated with hydropower is not very new; many published papers were introduced in Chapter 1. But past works on wind and hydro coordination mainly focus on the economic benefits. In this chapter, a methodology for wind power and PHCES cooperation is developed to evaluate the impacts of wind-hydro cooperation on the system reliability and the associated economic benefits.

## 6.2.2 Modelling PHES Unit

The concepts of availability and unavailability as illustrated in *Equations 2.7* and *2.8* are associated with the simple two-state model shown in *Figure 2.9* in Chapter 2. That model is directly applicable to a thermal generating unit which is either operating or forced out of service. In addition, the two-state model is also applicable to a hydro generating unit. But scheduled outages must be considered separately for the PHES units in the latter section.

PHES units are required to operate intermittently based on the demand for reducing the effects of wind power fluctuation on power outputs. The most critical period in the operation of the PHES unit is the start-up period; in addition, a PHES unit will have fewer operating hours and many more start-ups and shut-downs compared with the thermal generating unit.

## 6.2.3 Operation of PHCES System

A PHCES system uses both pumped water and natural stream flow water to generate electricity, so it consists of hydro generation and PHES generation. Many research works have investigated the operation of PHES and large PHES in power systems with significant amounts of wind energy where PHES is modelled deterministically [24, 25, 119]. For operational modes, PHES can either operate on a fixed cycle which is common (i.e. refill the reservoir during the night of each day) or on a free cycle (pump water at low price periods and generate electricity at high price periods) [24]. These techniques may not be appropriate for large PHES in systems with high wind penetration level for the following reasons: a fixed cycle does not pay attention to wind power fluctuations and may not exploit the storage to its full potential. Secondly, the free cycle operational mode takes no account of a short operational period, and the reservoir may be empty when needed [120].

In this chapter, the operation mode of PHCES system is based on free cycle, which also considers the short-term operational period. Hydro units use natural stream flow water to generate electricity. PHES units generate electricity to reduce the effects of wind power fluctuation on power outputs when the integrated wind power output is low, and pump water back to the reservoir when the power output from wind generation is at a high level. Although PHES units can be generating units or pumping units (load demands), large PHES unit becomes large load may change the system load demand profile. Without reliable information and up-to-date load profile data, load demand is assumed to be changed with certain variations in this thesis (as simulated in Chapter 4) as the focus is on the effect of wind-hydro cooperation on the power system reliability assessment with a significant amount of wind power.

The pumping process uses the surplus of electricity generation (due to high-wind and low-demand) to pump water to the upper reservoir, keeping it available to be used when more generation is needed. In the proposed WHC method, it is assumed that Pump-Hydro Combined Energy Storage (PHCES) systems can coordinate to refill their reservoirs without changing the overall system load demand characteristics. This is a limitation of this analysis and should be borne in mind. The feasibility of this assumption will be verified briefly in *section 6.5*.

In this thesis, there are three important background assumptions for PHCES: **1)** the reliability assessment is addressed from a system operator (SO) point of view and not from a market perspective. The SO coordinates, controls and monitors the operation of the transmission network and the generation system within a single regional power grid, but sometimes encompassing several areas. **2)** large PHCES is considered; this means that the storage energy has high flexibility and large capacity. **3)** the power output from a standard hydro unit is based on the hydro reservoir size, water in-flow and the generating unit ratings. It is assumed that there is no energy limitation for hydro units due to water availability and reservoir capacity. So, the proposed method is mainly focused on the cooperation of wind power generation and PHCES.

## **6.3 Proposed Method: Wind-Hydro Cooperation**

### **6.3.1 Methodology and Prerequisite**

In this thesis, a new method is proposed to reduce the effects of wind power fluctuation from the joint operation of wind farms and Pump-Hydro Combined Energy Storage (PHCES) systems, which is used to maintain reasonable system reliability levels at different wind penetration levels. It is based on the capacity outage frequency and duration method, and combined with the PHES' characteristic of flexibility. The method is called Wind-Hydro Cooperation (WHC). It can mitigate the impacts of wind generation on the power system reliability and leads to different reliability levels associated with different cooperation situations.

WHC has following features:

- The results of the generating unit output model and the wind turbine output model are simulated by MCS in a sufficient long period. Therefore, the results are close to the practical applications in power systems.
- WHC can build a form of reliability levels; each level is obtained by a wind-hydro cooperation scenario. According to the required reliability standard, the optimal scenario can be determined by applying CBA method. This form is similar to Capacity Outage Probability Table (COPT), which is convenient and straightforward for the system operator (SO) to plan the developments of wind power and PHCES in the selected areas.
- In WHC method, wind power is interconnected to the grid. The PHES is applied as an intermittent generation, which is cooperating with wind power, not just as a backup generation.

- WHC can easily be applied in different power systems for reliability evaluations. It only requires the system data to modify generation and load demand. The proposed method will obtain many improved reliability performances for SO to determine for future planning of different levels of wind power penetration in the power system.

Besides there is one critical prerequisite of the proposed method need to be considered, which is presented below.

➤ ***Prerequisite of WHC:***

Essentially, the use of wind energy is expected to provide a solution to solve the fossil fuel consumption and global warming. So, the reliability level of power system with wind power integration may not be able to achieve the original reliability level due to the intermittency of wind energy. In this thesis, the aim of the proposed method is to reduce the effects of wind power output fluctuation on power outputs and retrieve the system reliability to an acceptable or reasonable level.

The standard of an “acceptable” or “reasonable” level depends on the decision made by SO and it may be very different between different wind penetration levels. As discussed in *section 3.5*, LOLE has been used as the standard for the power system reliability. From the point of view of SO, the “acceptable” value of LOLE increases while the wind penetration goes up. So, the reliability level with WHC is not as good as the case in conventional power systems. However, this drawback can be compensated by providing flexible power supply periods and economical electricity prices to the potential consumers and the generated electricity is totally clear and sustainable for the environment. Therefore, it is not necessary for SO to operate a significant amount of generation as operating reserves to “pull back” the reliability to the original level (without wind power integration).

### 6.3.2 Mathematical Model and Calculation Procedure

The calculation process of the proposed WHC method involves 3 main steps, which is briefly summarized as:

- (1) *Combining* the power outputs from conventional generation and wind power generation with the system load to calculate the values of LOLE at different wind penetration levels.
- (2) *Using* the WHC method to reduce the values of LOLE at different wind penetration levels and to obtain several cooperation scenarios for the reliability evaluation.
- (3) *Applying* the Cost-Benefit Analysis (CBA) method to determine the optimal cooperation scenario by satisfying the required values of LOLE from a financial standpoint.

The details of the mathematical model and calculation procedure in this thesis for reducing the impacts of wind power fluctuation on power outputs are presented as the following:

***(1). Calculating the capacity outage (including conventional generation, wind power generation and system load) with Monte Carlo Simulation***

A capacity outage occurs when the load demand exceeds the available system capacity. The capacity outage is modelled by comparing the chronological available system capacity and the corresponding load demand as discussed in Chapter 4. The load model applied in this thesis is a chronological hourly load profile for one year, 364 days (8736 hours), and it is simulated repeatedly by MCS method. It is modified based on the IEEE-Reliability Test System (IEEE-RTS), which can be found in [105,

106] and is the same load model used in Chapter 4. The simulation time interval for power system reliability evaluation is 1hour.

The available system capacity is computed by adding the conventional generating units' capacities and wind power generation output as discussed in Chapter 4 and 5, which can be briefly summarized as follows:

The outputs of conventional generating units are simulated by the state duration sampling approach in MCS, which was introduced in Chapter 3. Each generating unit has only two states, "up" and "down". As presented in Chapter 4, the generating unit output model can be built using its failure rate and Mean Time to Repair (MTTR).

Then, the wind turbine output can be calculated by modelling the wind speed using Weibull probability distribution (*Equation 5.1*), which is shown as:

$$f(v) = \frac{kv^{k-1}}{c^k} \exp\left[-\left(\frac{v}{c}\right)^k\right]$$

And the wind speed can be modelled by *Equation 6.1*, which was presented as *Equation 5.6* in Chapter 5.

$$v_n = c[-\ln(U_n)^{\frac{1}{k}}] \quad (6.1)$$

Where:  $v_n$  represents the wind speed at the  $n$ th hour.  $U_n$  is a uniform distributed random number generated at the  $n$ th hour. The standard setting for  $c$  and  $k$  is 7 and 2 respectively as mentioned in Chapter 5.

Therefore, the power output of the  $m$ th wind turbine at the  $n$ th hour can be calculated by *Equation 6.2*. Forced outage rates (FOR) of wind turbines are not considered as they have insignificant impacts on the overall system reliability [59].

$$P_{mn} = \begin{cases} 0, & v_{mn} < V_{cm} \\ (A + B * v_{mn} + C * v_{mn}^2) * P_{rm}, & V_{cm} \leq v_{mn} < V_{rm} \\ P_{rm}, & V_{rm} \leq v_{mn} < V_{om} \\ 0, & v_{mn} \geq V_{om} \end{cases} \quad (6.2)$$

Where:

$v_{mn}$  = the wind speed (m/s)

$V_{cm}$  = cut-in speed of  $m$ th wind turbine (m/s)

$V_{rm}$  = rated speed of  $m$ th wind turbine (m/s)

$V_{om}$  = cut-out speed of  $m$ th wind turbine (m/s)

$P_{rm}$  = rated power output of  $m$ th wind turbine (MW)

The constant parameters of the wind turbine output model can be calculated by using Equations 6.3-6.5:

$$A = \frac{1}{(V_{cm} - V_{rm})^2} [V_{cm}(V_{cm} + V_{rm}) - 4V_{cm}V_{rm} \left(\frac{V_{cm} + V_{rm}}{2V_{rm}}\right)^3] \quad (6.3)$$

$$B = \frac{1}{(V_{cm} - V_{rm})^2} [4(V_{cm} + V_{rm}) \left(\frac{V_{cm} + V_{rm}}{2V_{rm}}\right)^3 - (3V_{cm} + V_{rm})] \quad (6.4)$$

$$C = \frac{1}{(V_{cm} - V_{rm})^2} [2 - 4 \left(\frac{V_{cm} + V_{rm}}{2V_{rm}}\right)^3] \quad (6.5)$$

Finally, the chronological available system generation capacity can be calculated by summing the conventional generation outputs and wind power generation outputs. Then, if the load demand at the  $n$ th time interval of the simulation period is greater than the available system capacity, a capacity outage is occurred. The system reliability level (LOLE) with wind power generation can be obtained by analysing the simulated capacity outages.

***(2). Applying the WHC method to mitigate the impacts of wind power generation on power system reliability***

As introduced in *section 6.2*, large PHCES is used in this thesis. It consists of both pumped water and natural flow water to generate electricity. In the proposed method, a number of PHES units are assigned to cooperate with wind power to offset the power imbalance caused by wind fluctuation, and the rest are assigned as hydro units to generate electricity. If the power output from the wind farm is less than a specified value termed as the cooperation criterion, the PHES units assigned to cooperate with wind power are responsible for providing the required support.

The cooperation criterion ( $x$ ), which is a percentage of the rated wind farm capacity ( $C_w$ ), is applied to decide the need for PHES units to support wind generation. Assuming that  $P_{wi}$  represents the power output from the wind farm at the  $i$ th hour, then:

- a. If  $P_{wi} < x * C_w$ , PHES units that are assigned to cooperate with wind power are required to provide support.
- b. If  $P_{wi} \geq x * C_w$ , no support from PHES units is required. PHES units operate as load demands to pump water back to the upper reservoir.

The power output from a wind farm is determined by the wind regime and the wind farm location. The proposed method is developed mainly based on Chinese power systems and wind industries, as discussed in *section 3.5*. Therefore, the setting of the cooperation criterion is better close to the actual wind speed profile. In China, the basic standard of effective wind area is the annual available time of wind power is 1800~2000 hours [121]. For the proposed method, the annual available time of wind power can be calculated by using MCS method and Weibull distribution function.

The Weibull distribution parameter settings are 7 and 2 respectively as introduced in Chapter 5. Applying MCS method to model the wind speed profile, and the number of simulations sets to 100,000 times for a better performance of the actual wind speed variations. Long term reliability simulation studies use the hourly time interval, which was mentioned in Chapters 4 and 5. During each time interval, the state of the system is assumed to be constant, and all system changes occur at the beginning of the time intervals. The simulation results of a single wind farm are shown in *Table 6.1*.

**Table 6.1: Wind Farm Output Annual Performance ( $c=7$  &  $k=2$ )**

Case No.	Output performance	Duration (hours)
Case 1	$\geq 100\%$ rated power output	1108
Case 2	$\geq 80\%$ rated power output	1520
Case 3	$\geq 70\%$ rated power output	1850
Case 4	$\geq 60\%$ rated power output	2181
Case 5	$\geq 50\%$ rated power output	2509

As mentioned in *section 5.6*, each wind farm location was presented as fully independent with same Weibull parameters in this thesis. It is clear that Case 3 (1850 hours) is closer to the basic standard of effective wind area (2000 hours). Case 3 can be used as the cooperation criterion for the Wind-Hydro Cooperation.

Therefore, PHES units will generate electricity to cooperate with wind power when the integrated wind generation output is less than 70% of its rated power output; contrarily, PHES units will not provide generation support. In addition, this thesis is focused on the cooperation between PHCES and wind power. The operation mode of PHES units have relatively minor impact on the proposed method, so PHES units can be represented by base loaded generating units (two-state models), which were described in *section 2.7.3* and shown in *Figure 2.9*.

The operation of PHES units coordinate with wind generation can be expressed more straightforward by using simple calculation process and equations. There are two important indices proposed for determining the required amount of PHES units and analysing the operation of the wind-hydro cooperation. The proposed indices are referred to as the Cooperation Factor (CF) and the Dispatch Ratio (DR), respectively.

The CF is defined as the ratio of the installed capacity of PHCES for the cooperation to the total-installed capacity of integrated wind power in the electric network. So, it is used to determine the amount of PHCES for the cooperation. The expression of this index can be represented by *Equation 6.6*:

$$CF = \frac{C_{PH}}{C_{WP}} \quad (6.6)$$

Where:

$C_{PH}$ : installed capacity of PHCES for cooperation

$C_{WP}$ : total installed capacity of wind power generation

It is important to study the utilization of PHCES for the cooperation. In the proposed method, the PHCES can be divided into two parts. The first part will operate as PHES units for the generating-pumping process. Another part will operate as normal hydro generating units for generating-only.

The Dispatch Ratio (DR) is defined as the ratio of the amount of PHCES assigned for the generating-pumping process to the total-installed capacity of PHCES. It is used to analyse the dispatch level of PHCES, and it is also a time-independent index in the proposed method. The expression of this index can be represented by *Equation 6.7*:

$$DR = \frac{H_{CO}}{C_{PH}} \quad (6.7)$$

Where:

$H_{CO}$ : amount of PHCES for the generating-pumping process

$C_{PH}$ : total installed capacity of PHCES in the system

Therefore, the simulation process and the calculation of the system reliability indices can be summarized in the following steps.

- (1) Calculate the power output time series  $\{P_{ci}; i=1, 2, \dots, 8736\}$  for the conventional generating units represented by two-state models.
- (2) Determine the power output time series  $\{P_{wi}; i=1, 2, \dots, 8736\}$  from the wind farm using Weibull distribution.
- (3) Determine the amount of PHCES ( $P_{hi}$ ) at the  $i$ th hour required to cooperate with wind power and it can be expressed as *Equation 6.8*:

$$P_{hi} = \begin{cases} DR_i \times CF_i \times C_w, & P_{wi} < x \times C_w \\ 0, & P_{wi} \geq x \times C_w \end{cases} \quad (6.8)$$

- (4) Calculate the total system power output ( $P_{gi}$ ) at the  $i$ th hour and the expression is shown as *Equation 6.9*:

$$P_{gi} = \begin{cases} P_{ci} + P_{wi} + CF_i \times C_w, & P_{wi} < x \times C_w \\ P_{ci} + P_{wi} + (1 - DR_i) \times CF_i \times C_w, & P_{wi} \geq x \times C_w \end{cases} \quad (6.9)$$

- (5)  $P_{gi}$  is compared with the system load ( $L_i$ ) for each time interval to determine if the loss of load situation exists. The loss of load expectation ( $LOLE_i$ ) and the loss of energy expectation ( $LOEE_i$ ) is computed using *Equations 6.10* and *6.11*, respectively:

$$LOLE_i = \begin{cases} 0, & P_{gi} \geq L_i \\ 1, & P_{gi} < L_i \end{cases} \quad (6.10)$$

$$LOEE_i = \begin{cases} 0, & P_{gi} \geq L_i \\ L_i - P_{gi}, & P_{gi} < L_i \end{cases} \quad (6.11)$$

In Monte Carlo Simulation, the reliability indices LOLE and LOEE for a number of sample simulations (N) are obtained using Equations 6.12 and 6.13, respectively:

$$LOLE = \frac{1}{N} \sum_{i=1}^{8736 \times N} LOLE_i \quad (6.12)$$

$$LOEE = \frac{1}{N} \sum_{i=1}^{8736 \times N} LOEE_i \quad (6.13)$$

In this chapter, the reliability assessment will be illustrated from the simulation results of LOLE (hours/year). The value of LOLE will become significantly large with high wind penetration level. The cooperation is expected to reduce the value of LOLE and can make a positive contribution for the power system reliability. For the WHC method, each cooperation scenario (CF; DR) represents a new reliability level (a reduced value of LOLE). The required reliability level can be obtained by modifying the scenario elements.

***(3). Applying the Cost-Benefit Analysis (CBA) method to determine the optimal cooperation scenario for power system reliability requirement.***

The reliability level of the power system will decrease as wind penetration levels increase. It is not necessary for the proposed method to retrieve the system reliability to the original level, especially when a significant amount of wind power generation is in the system. In this thesis, the proposed method is required to maintain the power system reliability at an acceptable level.

Therefore, there may have several cooperation scenarios satisfy the required reliability level. A basic Cost-Benefit Analysis theory is used to determine the optimal cooperation scenario for the power system reliability. Cost-Benefit analysis (CBA) is a systematic process for calculating and comparing benefits and costs of a project, decision or government policy [122]. In recent years, many cost-benefit approaches have been developed in power systems [123, 124].

Without access to reliable information on the relative costs and benefits of power systems, it is difficult to arrive at an accurate assessment of system reliability. In this thesis, the CBA approach examines the fixed and variable cost components of the power system reliability assessment. The costs that can be examined include total-installed cost, equipment costs, fixed and variable operating and maintenance costs and fuel costs. The analysis of costs can be very detailed, but for comparison purposes and data limitations, the approach used here is a simplified one.

The cost-benefit approach uses the total costs as a basis for ranking cooperation scenarios. Therefore, at a required reliability level, the optimal cooperation scenario can be determined by *Equation 6.14* to minimize the value of  $C$  (total costs).

$$\frac{\text{Cost}}{\text{Benefit}} = \frac{C_j}{RARL} \quad (6.14)$$

$RARL$  is the required acceptable reliability level for all suitable cooperation scenarios.  $C_j$  is the total costs at  $j$ th cooperation scenario.

Total costs  $C$  is defined as:

$$C = CC + UEC \quad (6.15)$$

Where:

$CC$  and  $UEC$  denote the capital costs and unserved energy costs, respectively.

For the CBA approach, the capital costs ( $CC$ ) include facility installation costs and equipment costs (e.g. wind turbines and pump-water turbines). Comparing with the capital costs, the evaluation of  $UEC$  is more complicated.

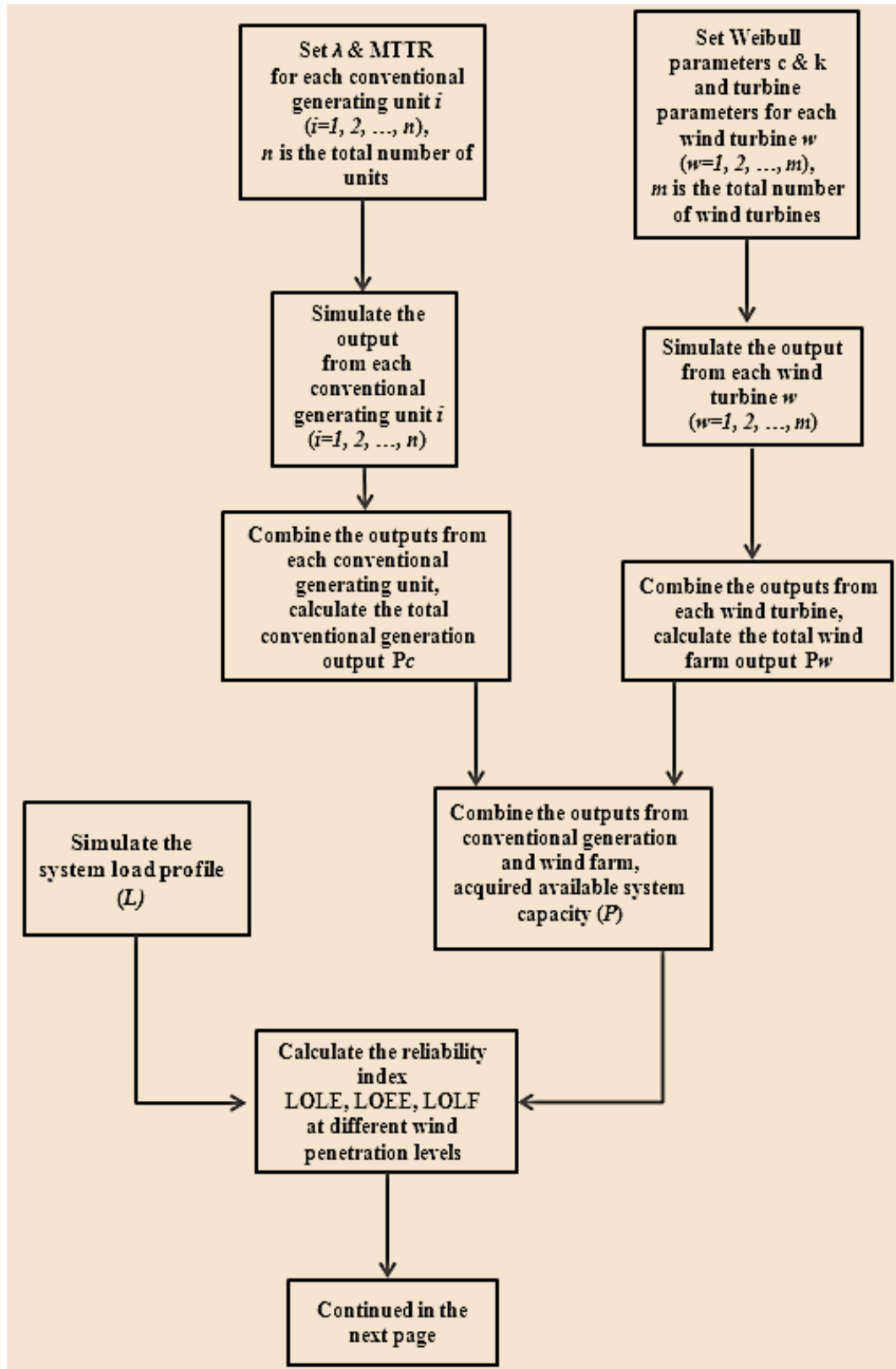
Unserved energy costs represent the cost incurred by the customers as a direct result of electricity supply interruption. For any given interruption, unserved energy costs as a function of many factors, including duration, location and customer types interrupted. As discussed in Chapter 2, there is a customer damage function that

represents the costs of a specific outage as a function of the values of these seven factors for that outage. Therefore, given as the customer interruption cost (*CIC*) in £/kWh, the UEC can be computed as follows:

$$UEC = LOEE \times CIC \quad (6.16)$$

*LOEE* is the loss of energy expectation, which can be simulated by the power system reliability evaluation in MWh. In addition, the customer interruption cost (*CIC*) in this chapter only focuses on the residential users and details of the associated customer damage function (CDF) can be found in *section 2.7.5*.

### 6.3.3 Flow Chart



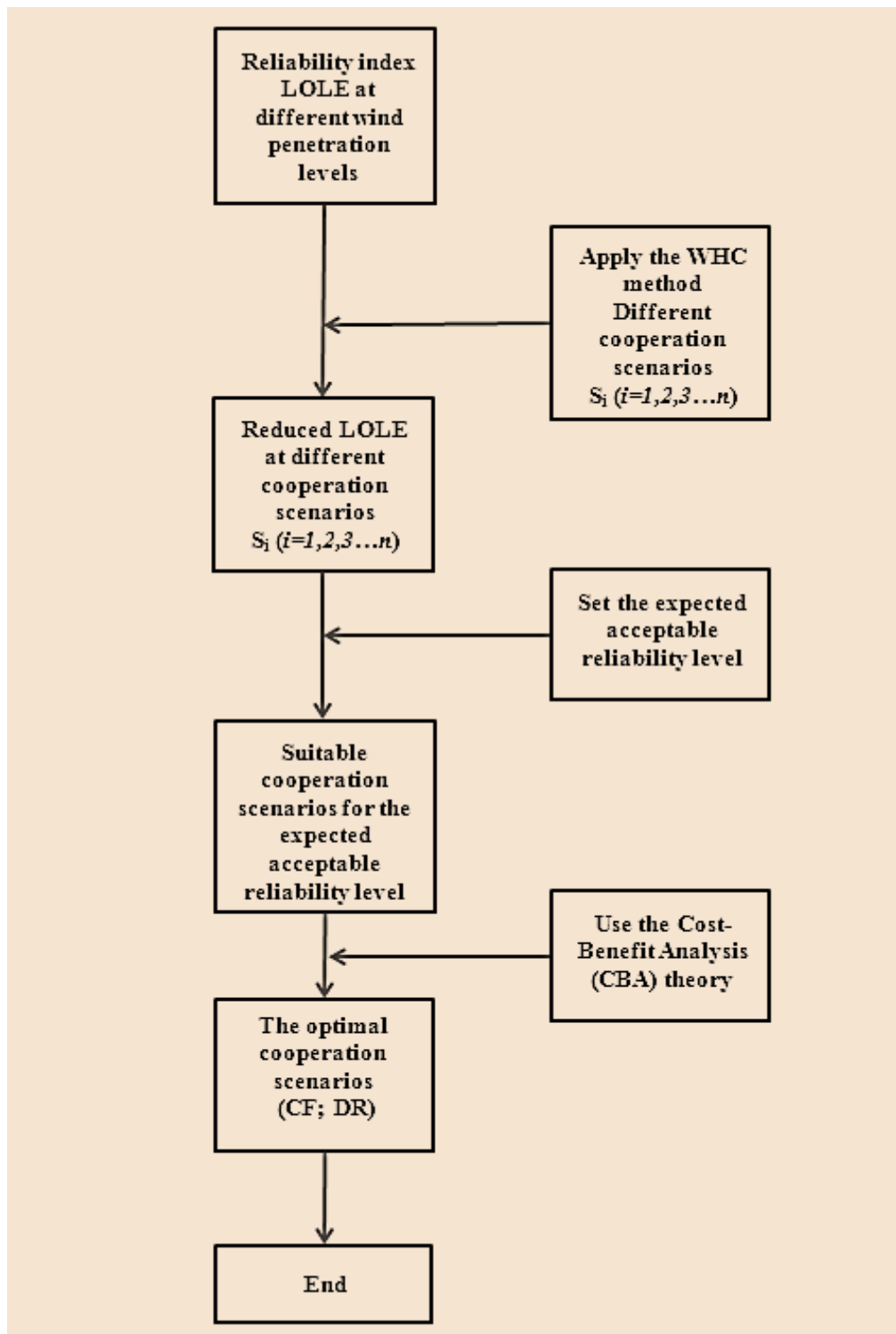


*Figure 6.3: Flow Chart for the Wind-Hydro Cooperation Method*

## 6.4 Illustrative Example

The illustrative example based on the Modified Roy Billiton Test System is used to demonstrate consistency and validity of the proposed method with numerical details. As introduced previously in this chapter, applying the wind-hydro cooperation can reduce the effects of wind power output fluctuation on power outputs. The following example will focus on the cooperation of wind power generation and Pump-Hydro Combined Energy Storage (PHCES) system to mitigate wind energy intermittency and make a positive contribution for the power system reliability. Two wind penetration levels are employed in this section, more comprehensive and realistic case studies can be found in Chapter 7 and Chapter 8.

### 6.4.1 Data and Assumptions for the Test System

- Test system data, load profile and wind penetration levels

The test system is the Modified RBTS, which was used in Chapter 4. The basic system data are shown in *Table 6.2*.

*Table 6.2: Test System Data*

Generators	11
Buses	6
Load points	5
Total generation capacity	240 MW
Peak load	185 MW

As presented in Chapter 4, the load profile applied in the example is an hourly load profile for one year, 364 days (8736 hours), and is modified based on the load model in the IEEE-Reliability Test System (IEEE-RTS).

The wind penetration level in this thesis is defined as the ratio of the installed wind generation capacity to the total-installed system generation capacity (includes installed wind capacity and other conventional generation capacities). The wind power output is considered as must take units; as a consequence, a certain amount of conventional generating units will have to be displaced. In this example, the wind penetration levels are 10% and 15%, and accordingly, the installed wind generation capacity is 24 MW and 36 MW, respectively. This means the displacement of conventional generation is 24 MW and 36 MW, respectively.

The average mean wind speed is set to 7 m/s, and the Weibull shape parameter is defined as 2. The wind speed variations are represented by the Weibull probability distribution. Then, the power output of the wind turbine can be obtained by using wind speed profile and Monte Carlo simulation, which were presented in Chapter 5.

- System available generation capacity

Chapter 4 introduced that the available generation capacity of conventional generating units were simulated with the state duration sampling approach. Combined with the wind turbine output, the system available generation capacity can be obtained. The results of reliability assessment for the modified test system in Chapter 4 will also be used in this section.

- Apply the WHC method

When the wind power generation output from the wind farm is less than a specific value, PHES units will generate electricity to reduce the impacts of wind power fluctuation and retrieve the reliability to an acceptable level.

- Determine the optimal cooperation scenario

In *Equation 6.14*, the required reliability level is the same for all suitable cooperation scenarios. So, the objective of Cost-Benefit analysis is to find the minimum total costs for the cooperation scenario. Use *Equation 6.15* to calculate the total cost of each suitable cooperation scenario for the required reliability level. *Table 6.3* shows

the customer interruption cost of the residential users, which is based on *Table 2.10* in Chapter 2. Moreover, the capital cost for PHES is £400/kW and this assumption is modified based on [125].

**Table 6.3: Customer Interruption Cost for Residential Users**

Duration	CIC (£/kWh)
1 min	0.0006
20 mins	0.058
1 hour	0.299
4 hours	3.047
8 hours	9.728

## 6.4.2 Results and Discussions

Applying WHC method to cooperate with wind power generation and maintain the power systems reliability, the simulation results can be divided into 4 aspects:

- I. Using the combined method of Frequency & Duration method and Monte Carlo Simulation method to evaluate the impacts of wind power generation on the test system reliability in two cases: 10% wind penetration level and 15% wind penetration level.
- II. Applying the Wind-Hydro Cooperation method to the test system at 10% wind penetration level and investigating the effects of Cooperation Factor (CF) and Dispatch Ratio (DR) on reducing the impacts of wind power fluctuations.
- III. Applying the Wind-Hydro Cooperation method to the test system at 15% wind penetration level and investigating the effects of Cooperation Factor

(CF) and Dispatch Ratio (DR) on reducing the impacts of wind power fluctuations.

- IV. Evaluating the performances of the Wind-Hydro Cooperation method on improving the test system reliability at different wind penetration cases (10% and 15%)

***(1) The impacts of wind power generation on power system reliability at 10% and 15% wind penetration level***

In this case, the combined method of F&D method and MCS method will be used to simulate the test system reliability. The simulation results of the modified RBTS reliability assessment without wind power integration will also be used in this section, which was shown in *section 4.5.2*. The simulated values of LOLE, LOEE and LOLF at different wind penetration levels are summarized in *Table 6.4* and *Figures 6.4* and *6.5*. In addition, the reliability analysis in this thesis is mainly focused on the LOLE (hours/year), which was defined as the loss of load expectation and the details were shown in *section 2.7.4*.

***Table 6.4: Reliability Indices of the Test System at 10% & 15% Wind Penetration Level***

Wind Penetration	Reliability Indices		
	LOLE (hours/year)	LOEE (MWh/year)	LOLF (occ./year)
Original Level	1.15	10.5	0.24
10%	6.48	70.39	2.52
15%	14.26	152.5	6.79

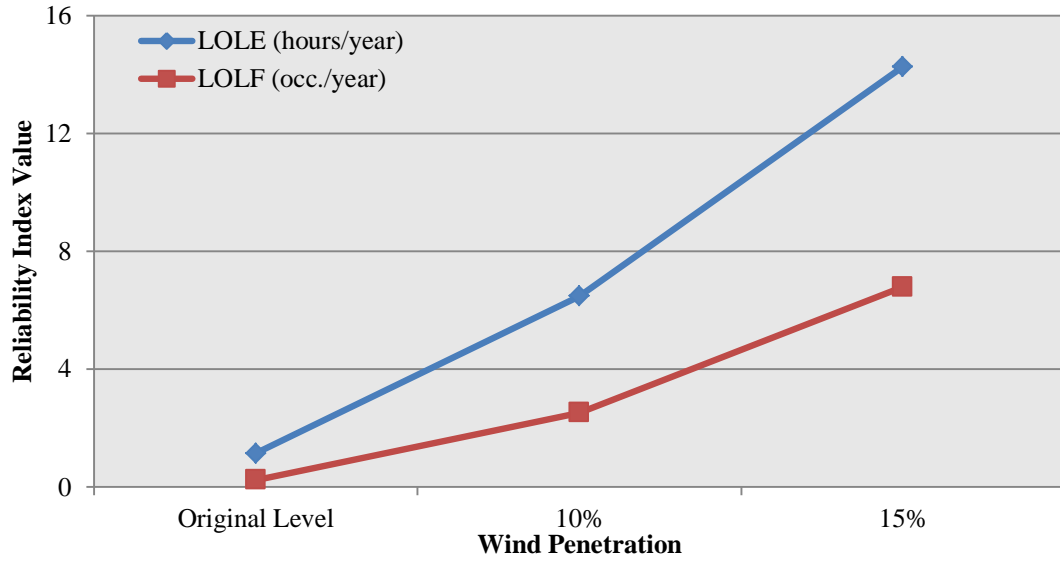


*Figure 6.4: Comparison of the Impact on the LOLE & LOLF*

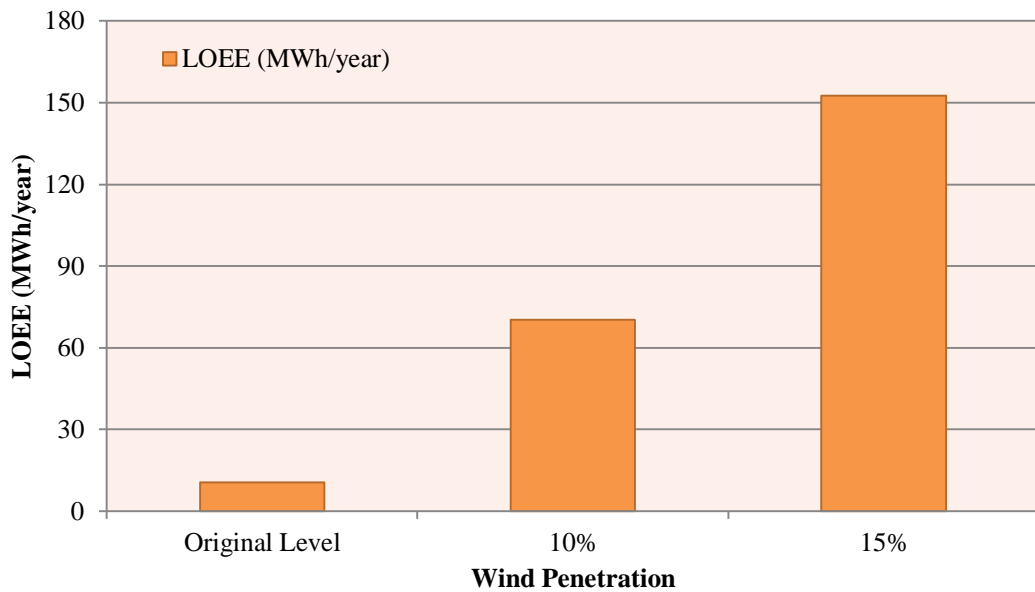


*Figure 6.5: Comparison of the Impact on the LOEE*

Figures 6.4 and 6.5 are the graphical forms of Table 6.5. It is clear that wind power integration could have significant negative impacts on the system reliability. The value of LOLE increases more than 5 times (from 1.15 hours/year to 6.48 hours/year) compared with the original reliability index at 10% wind penetration level. When the wind penetration reaches 15%, the value of LOLE goes up from 1.15 hours/year to

14.26 hours/year, which is more than 12 times over the original case. Furthermore, the values of LOEE and LOLF are increasing rapidly while the wind penetration level goes up.

These negative impacts are caused by the intermittent nature of wind power as it cannot provide stable generation to the power systems compared with the conventional generation. Low wind power outputs will lead to insufficient total available generation and make the system may not able to maintain the generation-demand balance. Then, the number of capacity outages will increase rapidly. Therefore, it is necessary to reduce the impacts of output fluctuations due to wind power generation for the security of power systems.

### ***(2) Wind-Hydro Cooperation (WHC) in 10% wind penetration case***

There are two important indices represented by the Cooperation Factor (CF) and the Dispatch Ratio (DR) in the proposed method. The roles of these indices are summarized as:

- ***Cooperation Factor (CF)***: determine the required amount of PHCES for the cooperation.
- ***Dispatch Ratio (DR)***: determine the dispatch situation of the required PHCES for the Generating-Pumping (PHES units) and Generating-Only (hydro units) processes.

Applying the Wind-Hydro Cooperation (WHC) method to the test system at 10% wind penetration level, the simulation results can be represented by the term of Cooperation Scenario (CS), which can be expressed as (CF; DR). Each cooperation scenario consists of the amount and the operation mode of PHCES.

For the purpose of reducing the simulation time and simplifying the calculation process, five CFs and associated DRs, are considered to illustrate the cooperation on reducing the impacts of wind power fluctuations on power outputs. In this case, the values of CFs are 0.3, 0.5, 0.6, 0.7 and 0.8, respectively. However, the value of CF can be very detailed according to the requirement of System Operator (SO). In a large power system, even a small value of CF may represent a considerable number of installed PHCES capacities.

The Wind-Hydro Cooperation combines the advantages of the combined reliability assessment method and the flexibility of PHES units to reduce the impacts of wind power fluctuation on power outputs and maintain the reliability level. The simulation results of reliability indices in this case are summarized in Appendix IV. *Figure 6.6* shows the effect of cooperation scenarios on the value of LOLE at 10% wind penetration level.

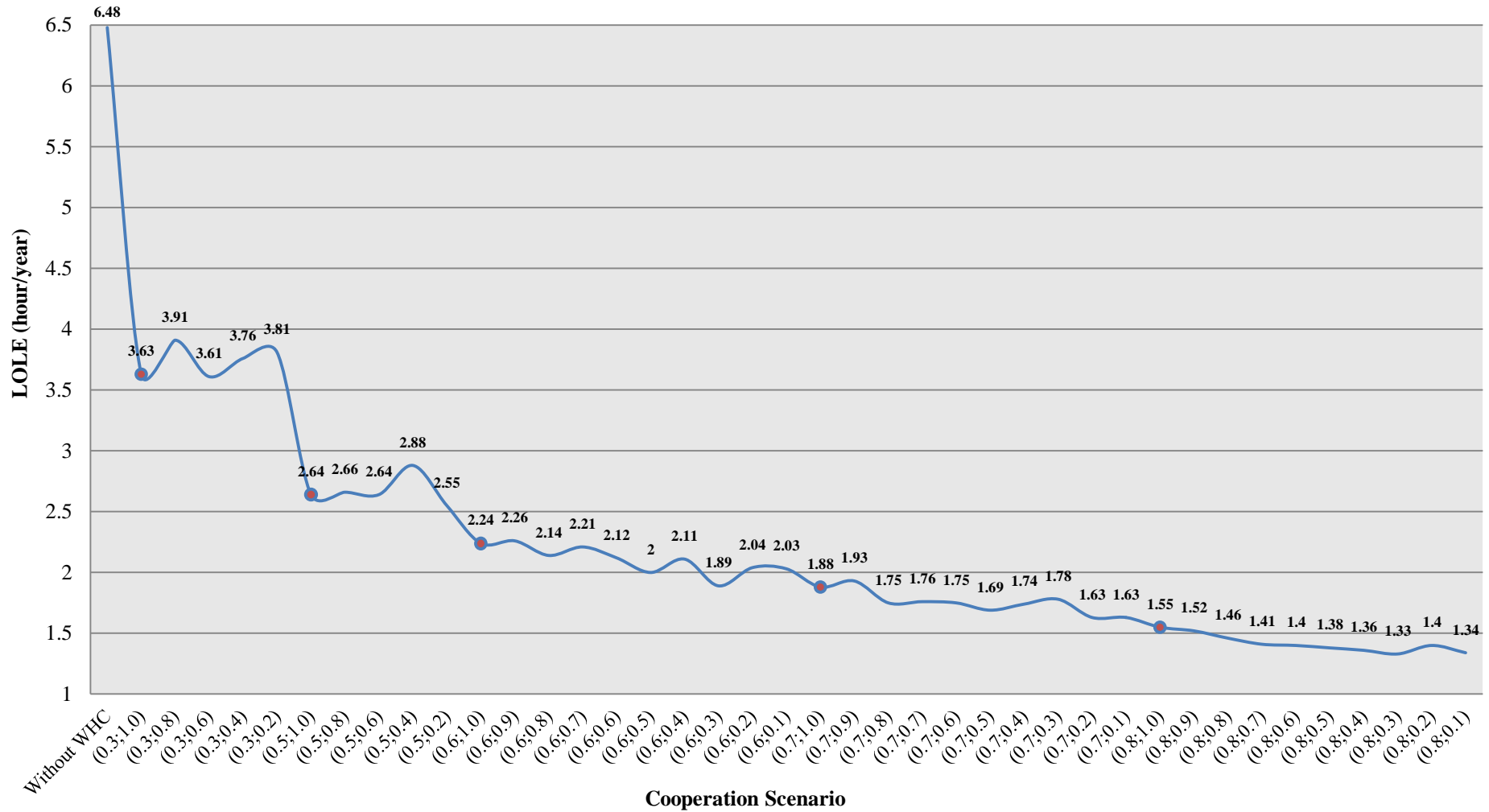
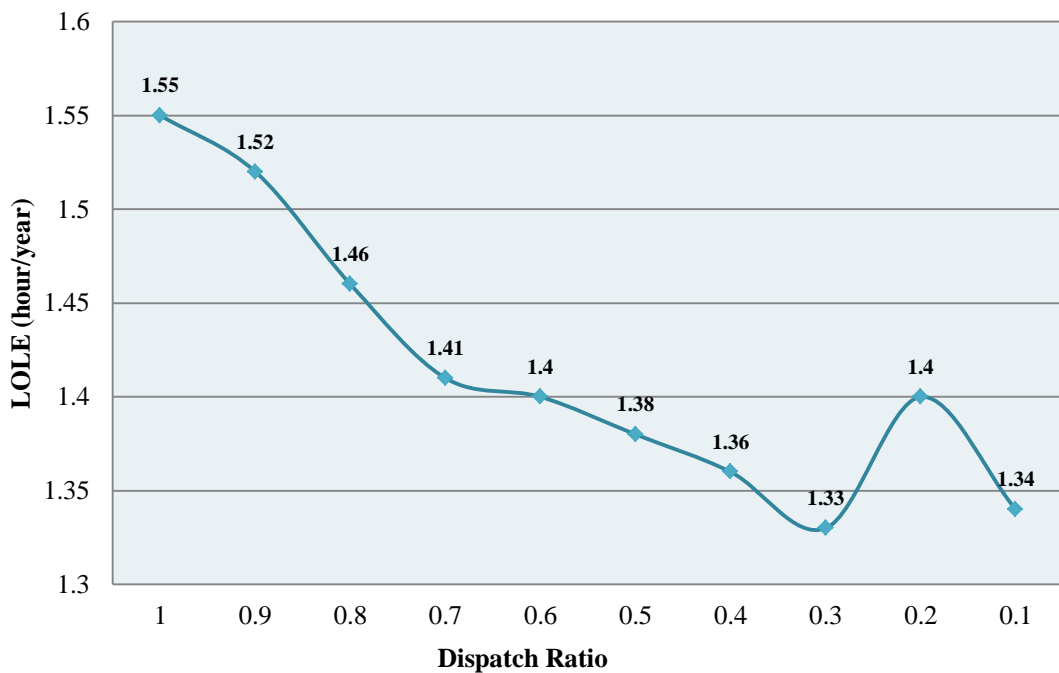


Figure 6.6: Effects of Cooperation Scenarios on LOLE at 10% Wind Penetration Level

*Figure 6.6* shows that the value of LOLE decreases significantly when the amount of PHCES increases. From the figure, it can be seen that the decreasing trend is more obviously at the beginning of the cooperation. Even a small amount of PHCES can make a great contribution to the system reliability. For instance, the value of LOLE drops from 6.48 hours/year to 3.63 hours/year at the cooperation scenario CS (0.3; 1.0), compared with the case without the wind-hydro cooperation.

It is clear that the values of LOLE are fluctuating with the same amount of PHCES but different DRs, which mean different dispatch levels of PHCES, can lead to different reliability levels. Using the cooperation scenarios CS (0.8; 1.0, 0.9... 0.1) as illustrated examples, the simulation results are summarized in *Figure 6.7*.



**Figure 6.7: Comparison of Different Dispatch Ratios on LOLE (CF=0.8)**

From *Figure 6.7*, CS (0.8; 0.3) has the minimum value of LOLE, which is 1.33 hours/year. The cooperation scenario represents the following information:

Installed PHCES Capacity:  $0.8 \times 24 \text{ MW} = 19.2 \text{ MW}$ , including two parts:

Part 1: PHES Capacity:  $0.3 \times 19.2 \text{ MW} = 5.76 \text{ MW}$

Part 2: Hydro Capacity:  $(1-0.3) \times 19.2 \text{ MW} = 13.44 \text{ MW}$

The value of LOLE drops by 14.2% compared with CS (0.8; 1.0). So, DR could make the cooperation operate more efficient and contribute effectively to the system reliability.

Furthermore, the decreasing trend is becoming saturated when large amount of PHCES has been installed in the system and continuing to go up. At CS (0.8; 0.3), the value of LOLE is already dropped to 1.33 hours/year, which is very close to the original reliability level (1.15 hours/year). Therefore, it is possible for WHC to “pull back” the reliability to the original level by installing more PHCES units. However, it could cost more investment and obtain limited improvement on the reliability. As discussed in *section 6.3.1*, the prerequisite of the WHC method defined that it is not necessary to operate large amount of PHCES to “pull back” the reliability to the original level when wind power has been integrated into the electric networks.

For the purpose of illustrating the proposed method, it is assumed that the required acceptable reliability level is approximately 1.9~2.0 hours at 10% wind penetration level. From *Figure 6.6*, it is clearly that there are 6 cooperation scenarios that can satisfy the required acceptable reliability level, which are CS (0.6; 0.5), CS (0.6; 0.3), CS (0.6; 0.2), CS (0.6; 0.1), CS (0.7; 1.0) and CS (0.7; 0.9), respectively. The optimal cooperation scenario can be determined by using *Equations 6.14- 6.16*, which were introduced in *section 6.3.1*.

The required acceptable reliability level (*RARL*) is the acceptable level for all cooperation scenarios. So, the objective of the Cost-Benefit Analysis method is to find the minimum value of the total costs (*C*). As introduced previously, the total costs were defined as  $C = CC + UEC$ .

The calculation process for each part of the total costs is shown as:

**Capital cost (CC):**

In this case, CC is defined as Installed capacity (MW)  $\times$  Price (£/kW). At the same wind penetration level, all suitable cooperation scenarios have the same conventional generation capacity and wind power capacity. So, the capital cost in this example specially designated as the capital cost of PHCES, which was mentioned in *section 6.4.1* as £400/kW.

**Unserved energy costs (UEC):**

As shown in *Equation 6.16*,  $UEC = LOEE \times CIC$ . The simulation results of LOEE in these cooperation scenarios were summarized in Appendix IV. The data of CIC were shown in *Table 6.3*, in *section 6.4.1*.

**Total costs (C):**

Therefore, the total costs of the suitable cooperation scenarios are calculated as follows and illustrated in *Figure 6.8*:

$$C = \text{Installed capacity (MW)} \times \text{Price (£/kW)} + \text{LOEE (MWh/year)} \times \text{CIC (£/kWh)}$$

$$(1) \text{ CS (0.6; 0.5): } C_1 = 0.6 \times 24 \times 10^3 \times 400 + 19.7 \times 10^3 \times 0.299 = 5.766 \text{ £million}$$

$$(2) \text{ CS (0.6; 0.3): } C_2 = 0.6 \times 24 \times 10^3 \times 400 + 19.3 \times 10^3 \times 0.299 = 5.765 \text{ £million}$$

$$(3) \text{ CS (0.6; 0.2): } C_3 = 0.6 \times 24 \times 10^3 \times 400 + 19.2 \times 10^3 \times 0.299 = 5.765 \text{ £million}$$

$$(4) \text{ CS (0.6; 0.1): } C_4 = 0.6 \times 24 \times 10^3 \times 400 + 19.0 \times 10^3 \times 0.299 = 5.764 \text{ £million}$$

$$(5) \text{ CS (0.7; 1.0): } C_5 = 0.7 \times 24 \times 10^3 \times 400 + 17 \times 10^3 \times 0.299 = 6.725 \text{ £million}$$

$$(6) \text{ CS (0.7; 0.9): } C_6 = 0.7 \times 24 \times 10^3 \times 400 + 18.1 \times 10^3 \times 0.299 = 6.73 \text{ £million}$$

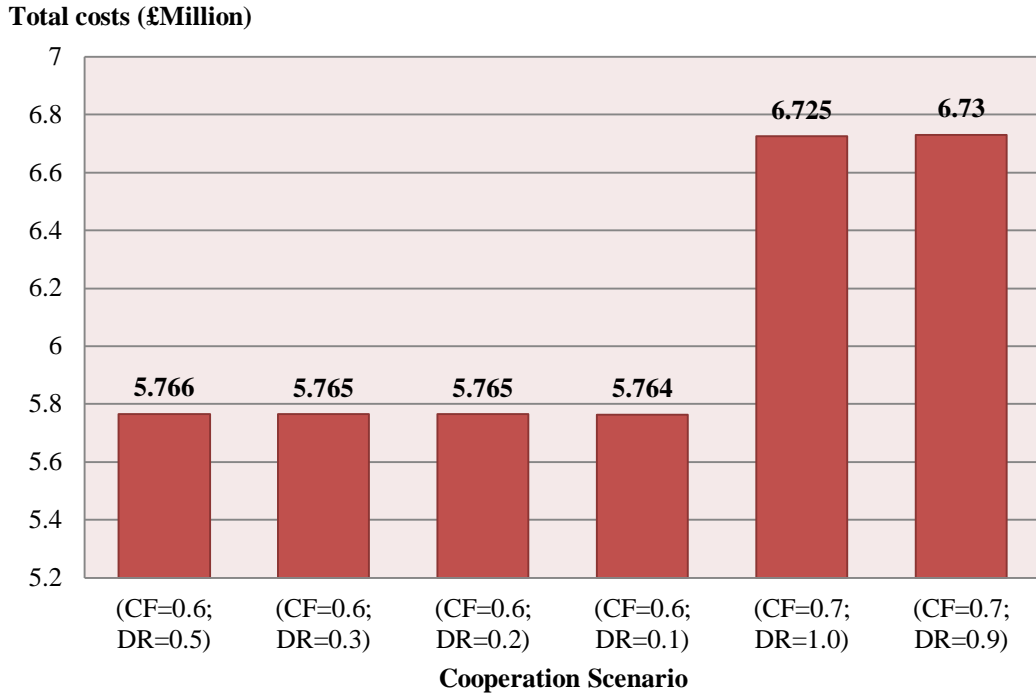


**Figure 6.8: Total Cost of Suitable Cooperation Scenarios at 10% wind penetration level**

It can be seen that CS (0.6; 0.1) has the minimum value of total costs from *Figure 6.8*. The cost differences between different cooperation scenarios are very slight due to the small size of the test system. Therefore, the optimal cooperation scenario for the acceptable reliability level in 10% wind penetration case is CS (0.6; 0.1). From a System Operator (SO) point of view, the optimal cooperation scenario represents:

At 10% wind penetration level, the required reliability level is approximately 1.9~2.0 hours/year. The test system requires PHCES with a total capacity of  $0.6 \times 24 \text{ MW} = 14.4 \text{ MW}$  (PHES Capacity: 1.44 MW; Hydro Capacity: 12.96 MW) to reduce the impacts of wind power fluctuation on power outputs and retrieve the reliability to the required level with the minimum cost.

***(3) Wind-Hydro Cooperation (WHC) in 15% wind penetration case***

Applying the Wind-Hydro Cooperation (WHC) method to the test system at 15% wind penetration level, the simulation results can be represented by the term of Cooperation Scenario (CS), which can be expressed as (CF; DR).

The simulation procedure and selected cooperation scenarios are the same as those situations in 10% wind penetration case. However, the same value of CS represents different installed PHCES capacity compared with the 10% wind penetration case due to increased wind power.

The simulation results of reliability indices in this case are summarized in Appendix V. *Figure 6.9* shows the effect of cooperation scenarios on LOLE at 15% wind penetration level.

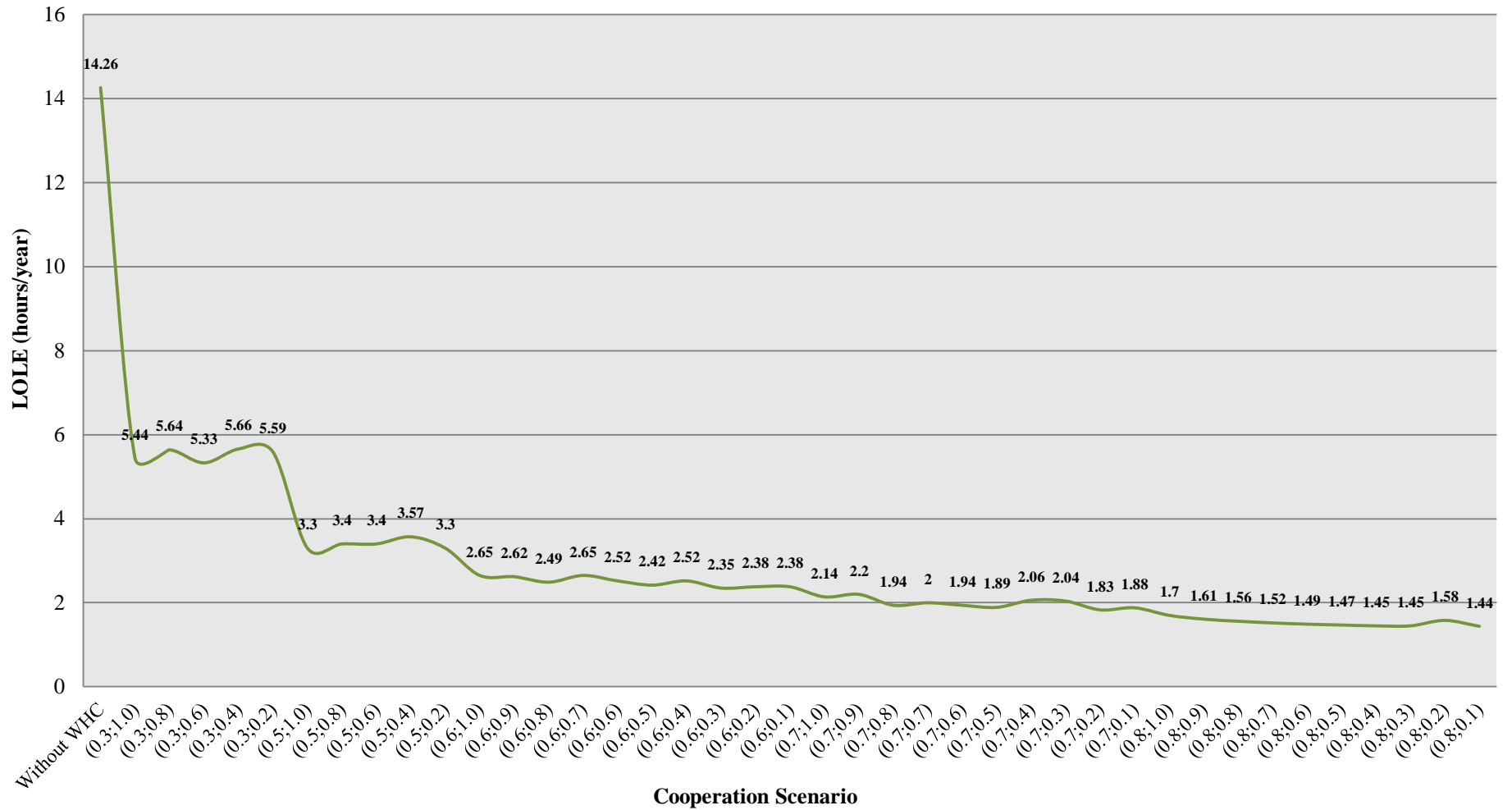


Figure 6.9: Effects of Cooperation Scenarios on LOLE at 15% Wind Penetration Level

It is clear that the value of LOLE decreases significantly when the amount of PHCES increases. From *Figure 6.9*, it can be seen that the cooperation scenario CS (0.8; 0.1) has the minimum value of LOLE among all cooperation scenarios in this case; compared with the scenario without WHC, the value of LOLE drops by 90% from 14.26 hours/year to 1.44 hours/year. The results show a great improvement on reliability by using the proposed method at 15% wind penetration level.

For the purpose of illustrating the proposed method at 15% wind penetration level, it is assumed that the required acceptable reliability level is approximately 2.0~2.1 hours, which is slightly higher than the value in 10% wind penetration case. From *Figure 6.9*, it is clearly that there are 4 cooperation scenarios that can satisfy the required acceptable reliability level, which are CS (0.7; 1.0), CS (0.7; 0.7), CS (0.7; 0.4) and CS (0.7; 0.3), respectively. The optimal cooperation scenario can be determined by using *Equations 6.14- 6.16*, which were presented in *section 6.3.1*. The calculation procedure remains the same as the procedure in 10% wind penetration case.

The required acceptable reliability level (*RARL*) is the acceptable level for all cooperation scenarios. So, the objective of the Cost-Benefit Analysis method is to find the minimum value of the total costs (*C*). In addition, the suitable cooperation scenarios have the same value of CF in this case, which mean that the installed amount of PHCES is the same for all scenarios. Therefore, the optimal CS can be determined by the minimum value of the unserved energy costs (*UEC*).

***Unserved energy costs (UEC):***

As shown in *Equation 6.16*,  $UEC = LOEE \times CIC$ . The simulation results of LOEE in these cooperation scenarios were summarized in Appendix V. The data of CIC were shown in *Table 6.3*, in *section 6.4.1*. Therefore, the unserved energy costs of the suitable cooperation scenarios are calculated as follows and illustrated in *Figure 6.10*.

$$(1) \text{ CS } (0.7; 1.0): UEC_1 = 19.9 \times 10^3 \times 0.299 = \text{£}5950$$

$$(2) \text{ CS } (0.7; 0.7): UEC_2 = 19.0 \times 10^3 \times 0.299 = \text{£}5681$$

$$(3) \text{ CS } (0.7; 0.4): UEC_3 = 18.5 \times 10^3 \times 0.299 = \text{£}5532$$

$$(4) \text{ CS } (0.7; 0.3): UEC_4 = 20.0 \times 10^3 \times 0.299 = \text{£}5980$$

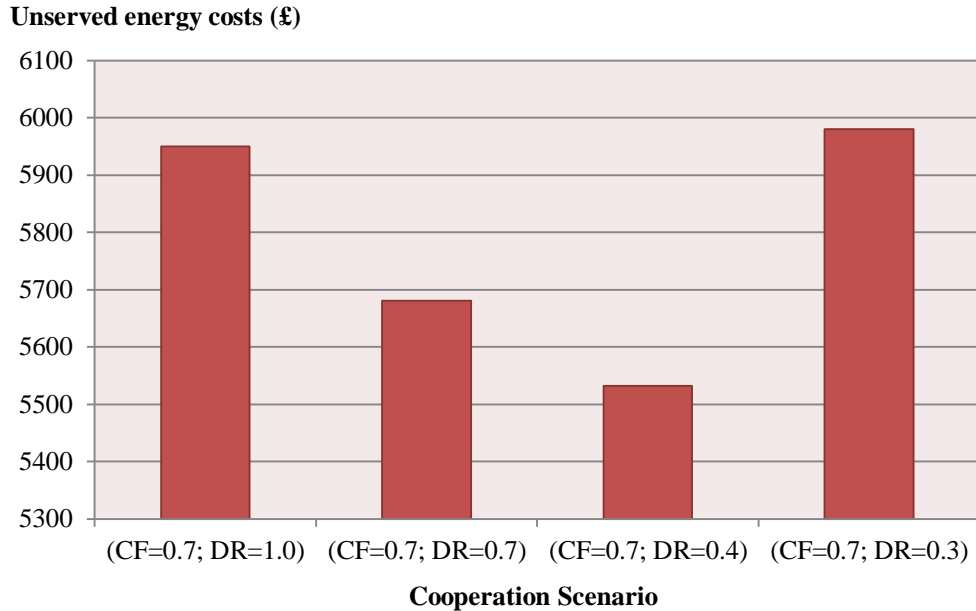


**Figure 6.10: Unserviced Energy Cost for Suitable Cooperation Scenarios at 15% wind penetration level**

It can be seen that CS (0.7; 0.4) has the minimum value of unserved energy costs from *Figure 6.10*. Therefore, the optimal cooperation scenario for the acceptable reliability level in 15% wind penetration case is CS (0.7; 0.4). From a System Operator (SO) point of view, the optimal cooperation scenario represents:

At 15% wind penetration level, the required reliability level is approximately 2.0~2.1 hours/year. The test system requires PHCES with a total capacity of  $0.7 \times 36 \text{ MW} = 25.2 \text{ MW}$  (PHES Capacity: 10.08 MW; Hydro Capacity: 15.12 MW) to reduce the impacts of wind power fluctuation on power outputs and retrieve the reliability to the required level with the minimum cost.

***(4) Evaluate the performance of WHC on reliability improvements at different wind penetration cases (10% & 15%)***

*Figure 6.11* combines *Figure 6.6* with *Figure 6.9* to illustrate the performances of the proposed method on reducing the impacts of wind power fluctuation and retrieving the system reliability at different wind penetration cases. From *Figure 6.11*, it is clearly that the Wind-Hydro Cooperation can make a significant contribution to the system reliability by cooperating with wind power generation at both wind penetration levels. For both of these cases, a small amount of PHCES can reduce the value of LOLE effectively at the beginning of the cooperation and the decreasing trend on the LOLE is more obviously than the rest of cooperation scenarios. When the amount of PHCES is continuing to go up, the decrease trends are also becoming saturated.

For the same cooperation scenario CS (0.8; 1.0), the values of LOLE at 10% and 15% wind penetration levels are 1.55 hours/year (from *Figure 6.6*) and 1.7 hours/year (from *Figure 6.9*), respectively. The results show that the capability of the cooperation decreases when the wind penetration increases.

However, the reduced values of LOLE at 15% wind penetration level by WHC are very close to those reduced values at 10% wind penetration level. It indicates that WHC can effectively mitigate the impacts of wind power generation on power outputs and efficiently retrieve the power system reliability even when the wind penetration level increased.

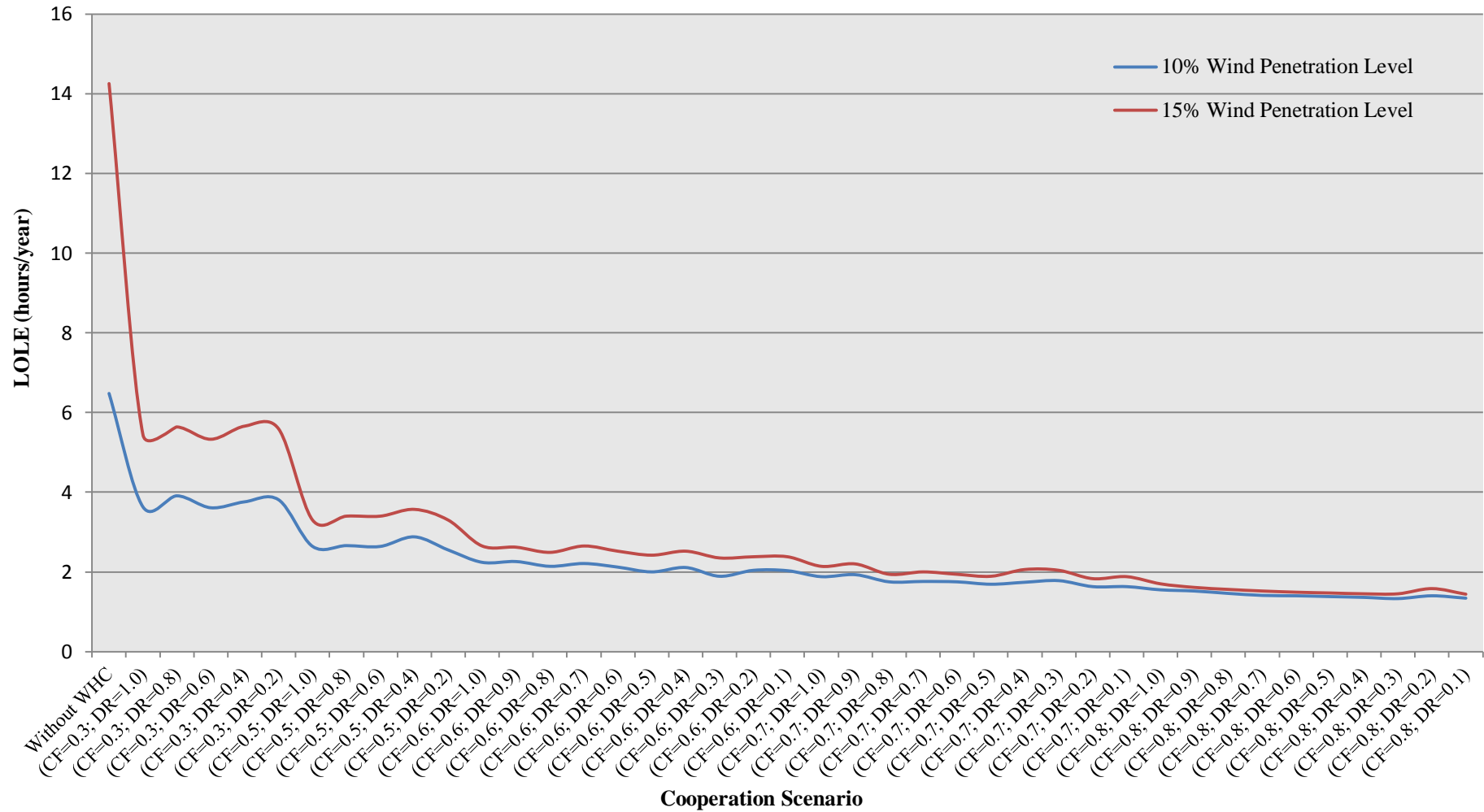


Figure 6.11: Comparison of Reliability Improvements on LOLE at Different Wind Penetration Levels

## 6.5 PHCES Operation

The proposed method mainly focused on the cooperation of PHCES and wind power. In the previous section, load demand was assumed to change with certain variations in this thesis. Due to this limitation, the proposed method assumed that PHCES can coordinate to refill their reservoirs without changing the overall system load demand characteristics. However, it is necessary to study the operation mode of the proposed PHCES system to verify its feasibility.

In this section, the operation mode of generate-electricity-pump-water process will be presented to verify the feasibility of the proposed WHC method. This operation mode is not optimum for the Wind-Hydro Cooperation. The aim of this operation mode is to set an operation cycle to guarantee the **availability** of the upper reservoir. The availability represents the water volume in the upper reservoir is equal to or greater than the initial value of the water volume after an operation cycle.

### 6.5.1 Generating-Pumping Process

As presented in *section 6.2.3*, the operation mode of PHCES was based on a free cycle (pump water at low price periods and generate electricity at high price periods), which also considered the short-term operational period. Therefore, a weekly operation cycle is proposed in this section for verifying the PHCES operation. The details of the weekly operation cycle are summarized as:

- **Generating Process:** PHES units will generate electricity when the integrated wind generation output is less than 70% of its rated power output.
- **Pumping Process:** the proposed operation cycle contains two pumping processes. **(1)** PHES units will pump water back to the upper reservoir when the integrated wind generation output is more than 70% of its rated power output. **(2)** PHES units will pump water to the upper reservoir during daily

off-peak periods (the daily off-peak period is 22:00~7:00, which was mentioned in Chapter 4).

For a better understanding of the generating-pumping process, *Figure 6.12* is used for demonstrating the cooperation of PHES units and the wind farm. The turbines power the generators to create electricity. Water is pumped back to the upper reservoir by linking a pump shaft to the turbine shaft, using a motor to drive the pump.

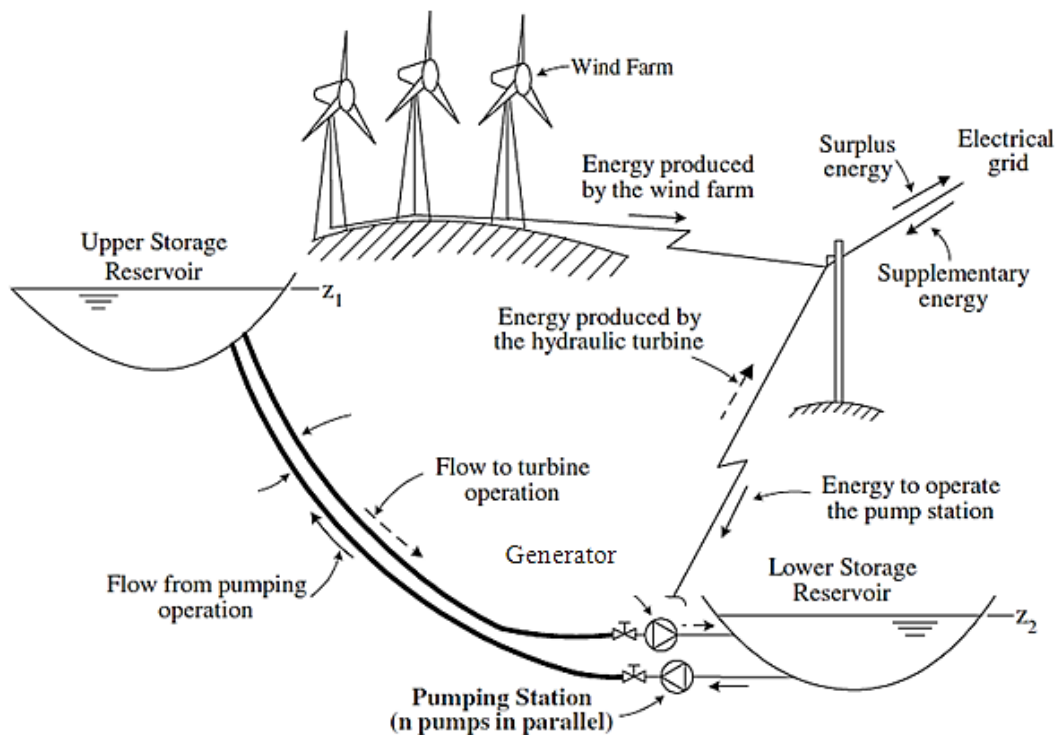


**Figure 6.12: Cooperation of Pump-Hydro Energy Storage Unit and Wind Farm[126]**

In the power plant, it contains several generator and pump turbine units connected in parallel. Also, there are two important assumptions for the proposed operation cycle: **a)** it is assumed in the simulation that the number of units available for pumping and generation is greater than that purely used for generating. **b)** Larger number of turbine units for the pumping process can work during the weekend off-peak periods, because the load demands during weekends are less than the demands during

weekdays. According to the stated assumptions, the operation pattern of the PHEs is proposed in *Table 6.5*, which is modified based on [127]. It is apparent that there are four different operation scenarios for the generating process due to the wind power output fluctuations, and the pumping process has three independent operation scenarios.

**Table 6.5: Operation Pattern of PHEs**

Status	Process No.	No. of Turbine Unit	Operating condition
Generating Process	I	4	Wind output is (0~10%) of rated wind power output
	II	3	Wind output is (10%~30%) of rated wind power output
	III	2	Wind output is (30%~50%) of rated wind power output
	IV	1	Wind output is (50%~70%) of rated wind power output
Pumping Process	I	6	Wind output is (70%~100%) of rated wind power output
	II	6	Weekday off-peak periods (22:00~7:00)
	III	8	Weekend off-peak periods (22:00~7:00)

Furthermore, there is another popular generating-pumping process for the pump storage system operation. It uses the same units for both generating and pumping process. When a generator need to reverse to pumping process the turbine has to stop and then reverse the direction of rotation. This reversible involves a time delay. For instance, the Bath County pumped-storage power station in Virginia has used this type of process for the operation. The generation period from stop to full power output is 180s, and the period from pumping status changing to generating status is 10 minutes [128, 129]. This delay may have impacts on the cooperation between wind farms and pump storage stations.

In this thesis the generating and pumping processes are considered as independent of each other. This type of operation scheme can have both generating and pumping acting simultaneously and has been used in some pump storage stations, especially for those old stations which have been upgraded in the developed countries [130].

## 6.5.2 Stored Energy and Available Power

Water held at a height represents stored potential energy. In this thesis, large reservoirs are concerned, whose capacities are given in cubic metres, rather than kilograms. Normally, one cubic metre of fresh water has a mass of 1000 kg. Therefore, within this degree of precision, the energy stored by a volume of  $V$  cubic metres raised through a height  $H$  is given by *Equation 6.17* [131]:

$$\text{Stored energy} = 1000 \times V \times g \times H \quad (6.17)$$

Where:  $g$  is the acceleration due to gravity (about  $10 \text{ m/s}^2$  for rough calculations).

So, the energy will be released when this volume of water falls through a vertical distance  $H$ . The power supplied by a hydroelectric unit, the number of watts, is the rate at which it delivers energy: the number of joules per second. It will obviously depend on the **volume flow rate** of the moving water. This is not just the speed of the water; it is the number of cubic metres per second passing through the unit, usually represented by the symbol  $Q$  [131]. Therefore, the power  $P$  (in watts), which is the energy per second, will be calculated by *Equation 6.18*:

$$P = 1000 \times Q \times g \times H \quad (6.18)$$

If  $P$  and  $Q$  are given, the vertical distance  $H$  that the volume of water falls during a specific period can be calculated by using *Equation 6.18*. Therefore, the proposed operation mode can be verified by using *Table 6.5* and *Equation 6.18*. In addition,

the generating and pumping efficiencies of turbine units are not considered in this case due to the lack of reliable industry information.

### 6.5.3 Verifying Operation Mode

In *section 6.4.2*, the cooperation scenario CS (0.7; 0.4) has been proved as the optimal cooperation scenario for the acceptable reliability level in 15% wind penetration case. This case will be used to verify the proposed operation mode in this section. According to the simulation results, the PHES capacity is approximately 10 MW in this case. The data and assumptions are summarized in *Table 6.6*.

**Table 6.6: Data and Assumptions for Operation Verification**

Installed PHES capacity		10 MW
Volume flow rate (Q)		1 m <sup>3</sup> /s
Upper reservoir	Initial head	100 m
	Minimum head	85 m
	Maximum head	115 m
Operation cycle		168 hours (7days)

According to the information in *Table 6.5* and *Table 6.6*, the water level of the upper reservoir can be calculated by using *Equation 6.18*. For the purpose of simplifying the calculation procedure, it is assumed that all turbine units are identical, and four units have a total capacity of 10.08 MW. Therefore, the calculation process of each operation mode can be calculated and shown as:

**Generating process:**

Generating process I (4 units):  $H = \frac{10 \times 10^6}{1000 \times 1 \times 3600 \times 10} = 0.28 \text{ m } (\downarrow)$ , this means that the water level of the upper reservoir drops 0.28 m after an hour operation.

Generating process II (3 units):  $H = \frac{0.75 \times 10 \times 10^6}{1000 \times 1 \times 3600 \times 10} = 0.21 \text{ m } (\downarrow)$

$$\text{Generating process III (2 units): } H = \frac{0.5 \times 10 \times 10^6}{1000 \times 1 \times 3600 \times 10} = 0.14 \text{ m } (\downarrow)$$

$$\text{Generator process IV (1 unit): } H = \frac{0.25 \times 10 \times 10^6}{1000 \times 1 \times 3600 \times 10} = 0.07 \text{ m } (\downarrow)$$

***Pumping process:***

Pumping process I (6 units):  $H = \frac{1.5 \times 10 \times 10^6}{1000 \times 1 \times 3600 \times 10} = 0.42 \text{ m } (\uparrow)$ , this means that the water level of the upper reservoir rises 0.42 m after an hour operation.

$$\text{Pumping process II (6 units): } H = \frac{1.5 \times 10 \times 10^6}{1000 \times 1 \times 3600 \times 10} = 0.42 \text{ m } (\uparrow)$$

$$\text{Pumping process III (8 units): } H = \frac{2 \times 10 \times 10^6}{1000 \times 1 \times 3600 \times 10} = 0.56 \text{ m } (\uparrow)$$

A weekly wind power output curve is randomly chosen from the annual simulation results in *section 6.4*, and the data of wind power output are shown in Appendix VI. The graphical form of the weekly wind power output is shown as *Figure 6.13*. The starting point of this weekly operation is 7:00 on Monday. Therefore, the water level of the upper reservoir can be calculated during the selected weekly operation, and the results are shown in *Figure 6.14*.

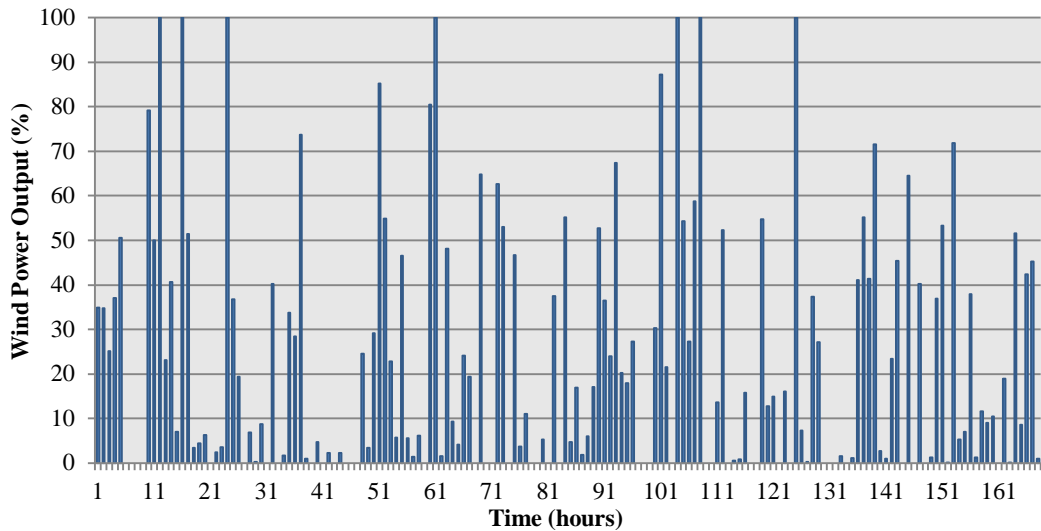


***Figure 6.13: Wind Power Output Curve (168 hours)***

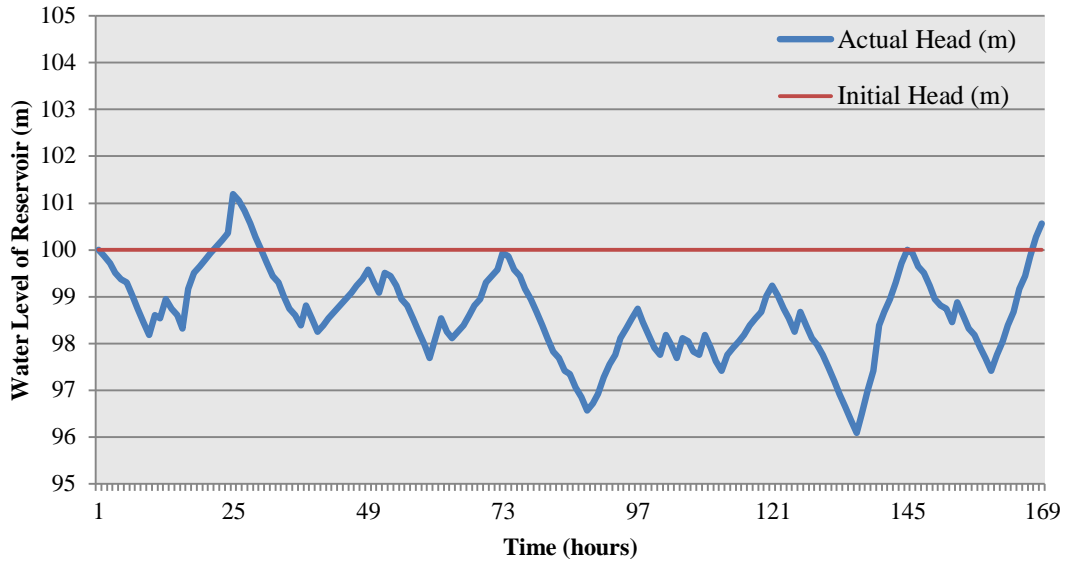


**Figure 6.14: Variation of the Water Level in the Upper Reservoir**

For most of the time, the wind power output is less than 50% of its rated power output, which is shown clearly in *Figure 6.13*. It means that the periods of generating processes are much longer than the periods of pumping processes. So, the power output of pumping mode needs to be more powerful than the output from the generating process. This was considered in the assumptions of PHES operation pattern in the previous section. It can be seen that there is another situation of wind power output curve in *Figure 6.13*. There are some periods of zero or “nearly zero” wind output situations, so the water level of the upper reservoir is only maintained by an independent pump, which will be a very powerful pumping device during the weekend off-peak periods.

The results in *Figure 6.14* proved that the proposed operation mode and pattern can guarantee the availability of the upper reservoir. At the end of the operation cycle, the water level is slightly higher than the initial value, because it is not an optimum case. In the worst circumstance (no wind during the whole operation cycle), the water level will drop by  $0.28 \text{ (m/hour)} \times 168 \text{ (hours)} = 47.04 \text{ m}$ ; and the water level will increase by  $0.42 \text{ (m/hour)} \times 45 \text{ (hours)} + 0.56 \text{ (m/hour)} \times 18 \text{ (hours)} = 28.98 \text{ m}$ . As presented in *Table 6.6*, the minimum water level is 85 m, so the available head is  $100 - 85 = 15 \text{ m}$ . Therefore, in the worst situation, the proposed operation mode still

can cover more than 90% of the period for generating electricity to reduce the impacts of wind power fluctuation on power outputs.

*Figure 6.15* shows the variation of water level at each time interval. The amount of pumped water mainly depended on the Pumping Process (2), which was introduced in *section 6.5.1*. The pumping process will be extremely efficient when the wind power outputs are high during the off-peak periods. For instance, at the Interval Point 140 (2:00 AM on Sunday), the amount of pumped water can be used to generate 100% of rated power output for 3.5 hours. This proposed operation mode is used to verify the feasibility of WHC method, and it is not the optimum operation of the generating-pumping process.

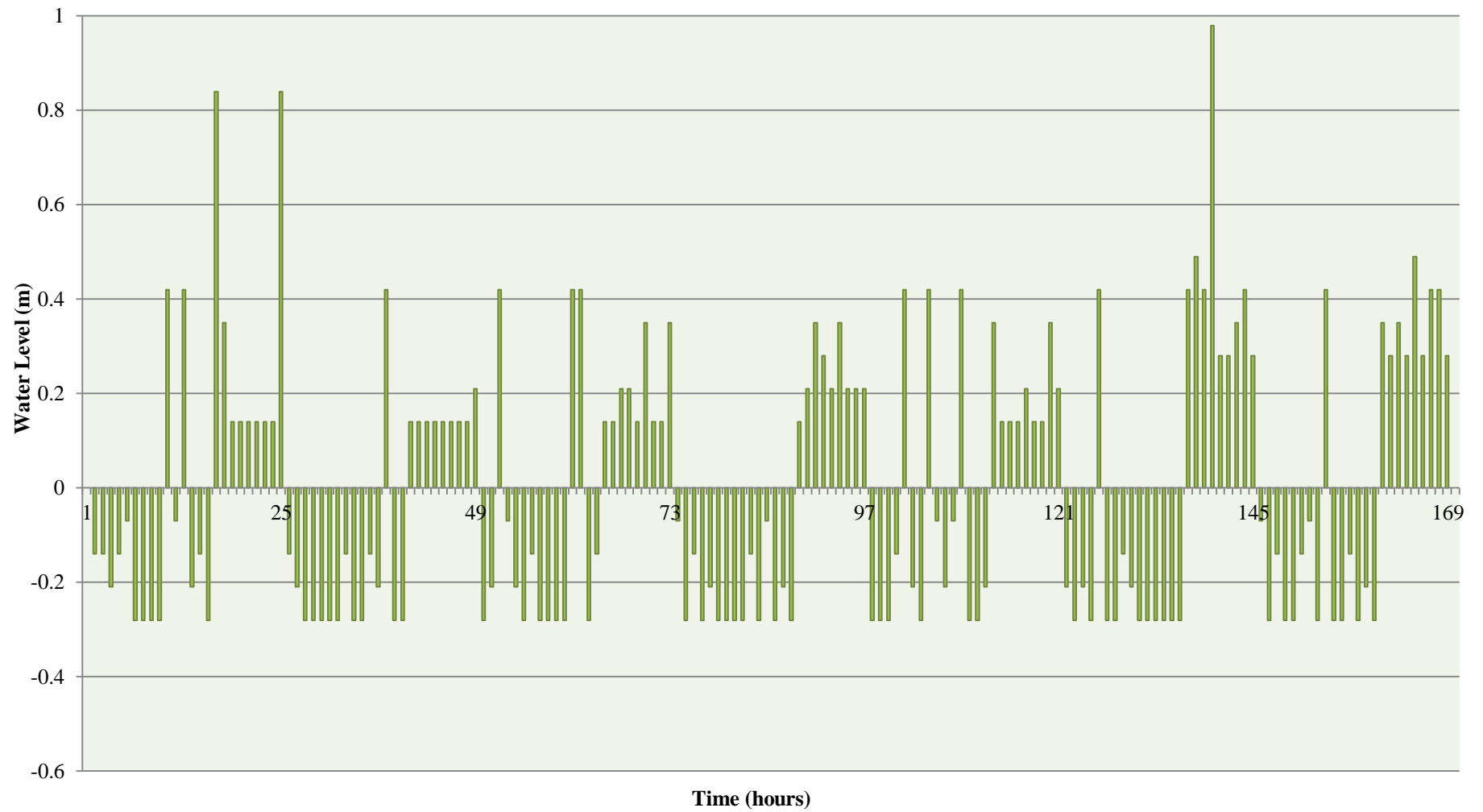


*Figure 6.15: Water Level at Each Time Interval*

## 6.6 Summary

This chapter proposed a new method, Wind-Hydro Cooperation (WHC), to reduce the impacts of wind power fluctuation on power outputs. The methodology is based on the combined method of MCS and F&D, which is used to analysis the power system reliability. Pump-Hydro Combined Energy Storage (PHCES) also has been described in details. The operational mode of PHCES was still a new research area, so there have been few published papers about the operation of a PHCES station. In this chapter, there were many important assumptions in the proposed method for PHCES to cooperate with wind power.

The simulation results presented in this chapter evidently support following conclusions:

- The combined method of Frequency & Duration method (F&D) and Monte Carlo Simulation (MCS) method can effectively simulate the power system reliability with wind power integration. The results indicate that wind power generation can harm the power system reliability by its output fluctuations, especially when the wind penetration is significant.
- WHC is effective to overcome the wind power fluctuation problem by combining the advantages of the combined reliability analysis method and the flexibility of PHCES technology. The cooperation indices in WHC are represented by many cooperation scenarios (CS), each CS is associated with improved reliability level. According to the required reliability level determined by the System Operator (SO), the optimal cooperation scenario can be determined by using the Cost-Benefit Analysis (CBA) method.
- WHC is convenient and straightforward for SO to analyse the impacts of wind power generation on the power system reliability and the effects of

WHC on reducing the impacts of wind power fluctuation for different practical power systems. With reliable system information on conventional generation, wind power penetration levels, and assumptions of PHCES have been determined, WHC can mitigate the impacts of wind power integration on electric networks caused by the intermittency of wind power.

The studies also presented a further section to verify the feasibility of the proposed operation mode. A weekly operation cycle was used to illustrate the generate electricity- pump water process. The assumptions of the proposed operation mode were close to the settings of practical hydropower plant, and the weekly load curve also has been considered in the weekly operation cycle. It is an attempt to analysis and study the operation of a Pump-Hydro Combined Energy Storage system. In this thesis, the operation of the generating-pumping process is not optimum for the proposed WHC method.

WHC can effectively mitigate the impacts of wind power generation on power outputs and efficiently maintain the power system reliability in the Modified Roy Billinton Test System. Furthermore, WHC will apply to more realistic power systems to verify the feasibility and validity at many different wind penetration levels.

# Chapter 7. Reliability Evaluation of Modified IEEE 118-Bus Test System

## 7.1 Introduction

Chapter 6 presented the proposed method of Wind-Hydro Cooperation (WHC), which was used to reduce the effect of wind power output fluctuations and improve the power systems reliability with a significant amount of wind power generation. The modified Roy Billinton Test System (MRBTS) with two different wind penetration levels was used to illustrate the proposed WHC method. The results from the illustrative example proved that the proposed WHC method could effectively reduce the impacts of wind power generation on power systems reliability at different wind penetration levels. However, MRBTS is a basic test system for the reliability analyses, and the size of the test system is small.

This chapter is concerned with the validity of the WHC method in large power systems. Consequently, WHC method will be tested in a large electric network for both long-term system planning and short-term operational planning. In this chapter, the periods for long-term and short-term planning are one year and 24 hours, respectively. Without access to up-to-date information on the generators' data, transmission line parameters and actual load variations, it is critical to select a test system which has been proved extremely valuable in reliability analysis studies.

The IEEE 118-Bus Test Case has been extensively used over the power systems industry. It represents a portion of the American Electric Power System (in the Midwestern US) [132]. The data of generators, branches and load demands are in [62, 133]. In addition, the generator cost data and power flow data are described in a Matlab power system simulation package, called MATPOWER.

Therefore, the modified IEEE 118-Bus Test System has sufficient system data to test the validity of the proposed WHC method for both long-term and short-term power system operations. In the long-term planning, the same simulation procedure of reliability evaluation as applied in Chapter 6 will be used to determine optimal cooperation scenarios at different wind penetration levels. In the short-term operation, WHC method will be applied to an actual daily load curve to evaluate the effects of Wind-Hydro Cooperation on electric energy transmission/distribution losses due to wind power integration.

This chapter is structured as follows: *section 7.2* briefly expresses the data and the assumptions of the modified IEEE 118-Bus Test System and 6 different wind penetration levels (10%, 15%, 20%, 25%, 30% and 40%) for the system reliability evaluation. *Section 7.3* presents the results and discussions of the long-term planning on several aspects including the impacts of wind power integration and the improvements on reliability by applying the Wind-Hydro Cooperation method. *Section 7.4* presents a 24-hour daily load curve for the system short-term operating and the characteristics of power outputs from multiple wind farms are also described. *Section 7.5* mainly discusses the improvements of WHC method on reducing transmission/distribution energy losses.

## 7.2 Evaluation of Modified IEEE 118-Bus Test System: Long-term System Planning

In this section, the proposed WHC method will be applied to the reliability evaluation of the modified IEEE 118-Bus Test System for the long-term planning. Six wind penetration levels are employed to analysis the impacts of wind power integration on power systems reliability and cooperate with Pump-Hydro Combined Energy Storage (PHCES) system to reduce the effects of wind power fluctuations on power outputs.

The diagram of modified IEEE 118-Bus Test System is shown in *Figure 7.1* for illustration [132]. Most of the bus names were in a small font. After many generations of copying, the legibility was poor so errors of transcription may have occurred. It is still applicable to analyse the long-term system planning of power systems reliability. In the latter section, a clear one-line diagram of IEEE 118-Bus system will be applied to the power systems reliability assessment for analysing the short-term operation. The basic system data are shown in *Table 7.1*. The information and assumptions of the test system are organized as follows.

***Table 7.1: Modified IEEE 118-Bus Test System Data***

Generators	54
Buses	118
Load points	99
Total generation capacity	9000 MW
Peak load	7780 MW



**(1). Conventional Generating System:**

The data of the generators' rated power outputs are summarized in *Appendix VII*. It is assumed that the generators with the same rate output have the same failure rates and Mean Time to Repair (MTTR), which will be presented in *Table 7.2* for Monte Carlo simulation and the data are modified based on IEEE Reliability Test System (RTS) [104].

**Table 7.2: Conventional Generator Reliability Data [4]**

Rated Output (MW)	No. of generator	MTTF (hours)	Failure rate per year	MTTR (hours)
400	6	1100	7.9	150
350	8	1150	7.6	100
200	8	950	9.2	50
100	12	1200	7.3	50
50	20	1980	4.4	20

**(2). Wind Power Generation:**

As presented in Chapter 5, the wind speed variations were represented by the Weibull probability distribution. Then, the power output of the wind turbine can be obtained by using wind speed profile and Monte Carlo simulation. Finally, the power output of the wind farm can be calculated by summing the outputs from all the wind turbines.

The average mean wind speed is set to 7 m/s, and the Weibull shape parameter is defined as 2. So, the scale parameter ( $c$ ) and shape parameter ( $k$ ) of Weibull Distribution will be set to 7 and 2, accordingly. The wind turbine data presented in Chapter 5 are shown in *Table 7.3*. In this chapter, the settings of Weibull distribution parameters and the mean wind speed remain the same in Chapter 5.

**Table 7.3: Wind Turbine Parameters**

<b>Rated Power Output</b>	<b>Cut-in speed</b>	<b>Rated speed</b>	<b>Cut-out speed</b>
5 MW	4 m/s	12 m/s	25 m/s

**(3). Load Demand:**

The annual peak load of the system is presented in *Table 7.1*, which is 7780 MW. And the annual load variation can be represented by the same load model in Chapter 4 and Chapter 6.

**(4). Assumptions:**

The results presented in Chapter 6 of this thesis focused on the wind-hydro cooperation. Then, the optimal cooperation scenarios can be determined by using Cost-Benefit Analysis (CBA) approach. It is assumed that load demand is only consumed by residential users. The customer interruption cost (CIC) of the residential users is shown in *Table 7.4*, which is modified based on *Table 6.3*. Furthermore, the capital cost for Pumped Hydro Energy Storage (PHES) is £400/kW as introduced in Chapter 6.

**Table 7.4: CIC for Residential Users**

Duration	CIC (£/kWh)
1 hour	0.299
4hours	3.047
8 hours	9.728

**(5). Wind Penetration Level:**

Past studies in Chapter 6 were only focused on low wind penetration levels in a relatively small size of the test system (Modified RBTS). In this chapter, six different wind penetration cases will be employed to analyse the effect of Wind-Hydro Cooperation (WHC) on reducing the impacts of wind power output fluctuations to maintain an acceptable reliability level of the modified IEEE 118-Bus Test System and calculating the optimal cooperation scenarios to minimize the total costs. As discussed in Chapter 6, the wind penetration level is defined as the ratio of the installed wind generation capacity to the total installed generation capacity. And the conventional generation is displaced by the wind power generation in each case. The details of wind penetration levels are summarized in *Table 7.5*, which includes four situations of the wind penetration: low, medium, high and extreme high levels (introduced in *section 2.3.3*).

**Table 7.5: Basic System Data for Case 1~ Case 6**

	<b>Case 1</b>	<b>Case 2</b>	<b>Case 3</b>	<b>Case 4</b>	<b>Case 5</b>	<b>Case 6</b>
<b>Wind Penetration</b>	<b>10%</b>	<b>15%</b>	<b>20%</b>	<b>25%</b>	<b>30%</b>	<b>40%</b>
<b>Level</b>	<b>Low</b>	<b>Low</b>	<b>Medium</b>	<b>Medium</b>	<b>High</b>	<b>Extreme high</b>
Wind Turbines Number	180	270	360	450	540	720
Wind Generation Capacity (MW)	900	1350	1800	2250	2700	3600
Total Generation Capacity (MW)	9000	9000	9000	9000	9000	9000
Peak Load (MW)	7780	7780	7780	7780	7780	7780

## **7.3 Long-term System Planning: Results and Discussions**

Applying the proposed Wind-Hydro Cooperation (WHC) method to reduce the impacts of wind power fluctuations on power outputs and retrieve the power systems reliability, the analyses of the simulation results can be divided into 3 aspects:

- I. Use the combined method of Frequency & Duration method and Monte Carlo Simulation method to evaluate the impacts of wind power generation on the test system reliability in six cases: 10%, 15%, 20%, 25%, 30% and 40% wind penetration levels.
- II. Apply the WHC method to the test system in each wind penetration level and investigate the effects of Cooperation Factors (CF) and Dispatch Ratios (DR) on reducing the impacts of wind power fluctuations on system reliability.
- III. Determine the optimal cooperation scenarios for each wind penetration case by using CBA approach to calculate the minimum total costs.

### **7.3.1 The Impacts of Different Wind Penetrations on the System Reliability**

The output of a conventional generator can be obtained by combining its failure rate ( $\lambda$ ) and Mean Time to Repair (MTTR) into Monte Carlo Simulation (MCS). Then, the total conventional generation can be calculated by combining the outputs of all the generators in the system. The output of the wind farm is calculated by using Weibull distribution and MCS. And the annual load variation follows the pattern,

which was introduced in Chapter 4 and used in Chapter 6. A capacity outage will occur when the load demand exceeds the total available system generation capacity.

The **original reliability level** (without wind power) of the modified IEEE 118-Bus Test System has been calculated by using the combined reliability analysis method. In the reliability evaluation, an outage is counted when the load is higher than the conventional generation capacity.

And the reliability evaluations of six different wind penetrations have also been simulated in the same procedure. In these reliability evaluations, an outage occurs when the load is higher than the summation of wind power generation and displaced conventional generation. The results of reliability evaluations are represented by the values of LOLE (Loss of Load Expectation), LOEE (Loss of Energy Expectation) and LOLF (Loss of Load Frequency), which are summarized in *Table 7.6*, *Figure 7.2* and *Figure 7.3*.

**Table 7.6: Reliability Indices of the Modified IEEE 118-Bus Test System**

Wind penetration level	Original (without wind)	10%	15%	20%	25%	30%	40%
<b>LOLE</b> (hours/year)	3	29.8	96	238.6	537.8	941	2002.5
<b>LOEE</b> (MWh/year)	661	7900	29631	84860	237195	514195	1649806
<b>LOLF</b> (occ./year)	0.8	14.4	49	123	271	459	911

**Reliability Index Value**

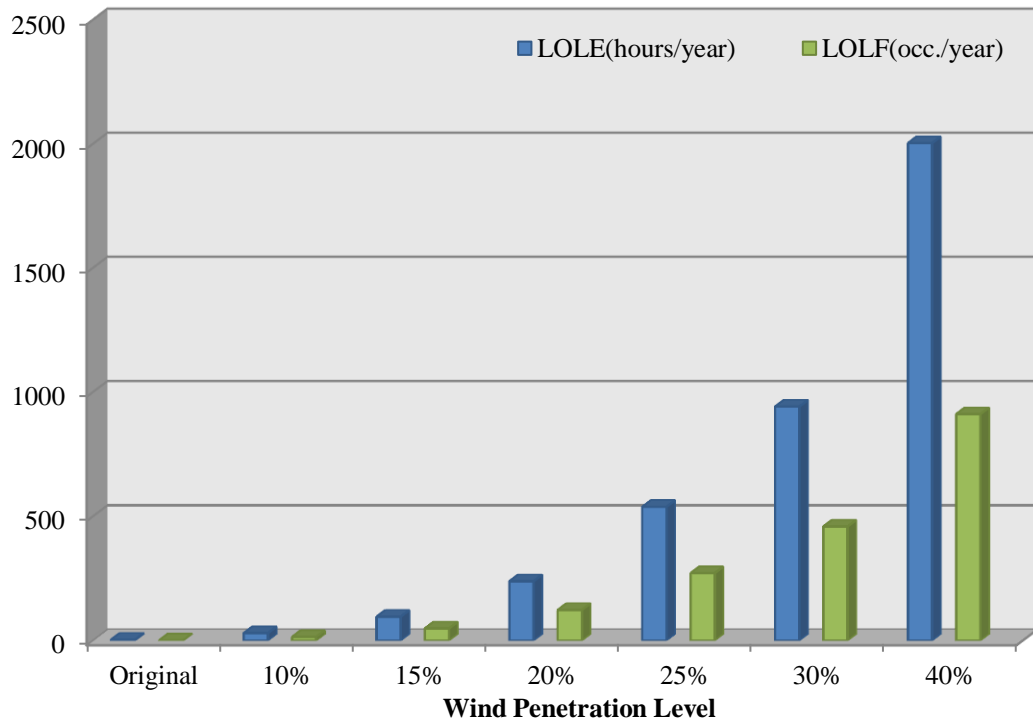


*Figure 7.2: The Impact of Wind Penetration on LOLE & LOLF*

**LOEE (MWh/year)**

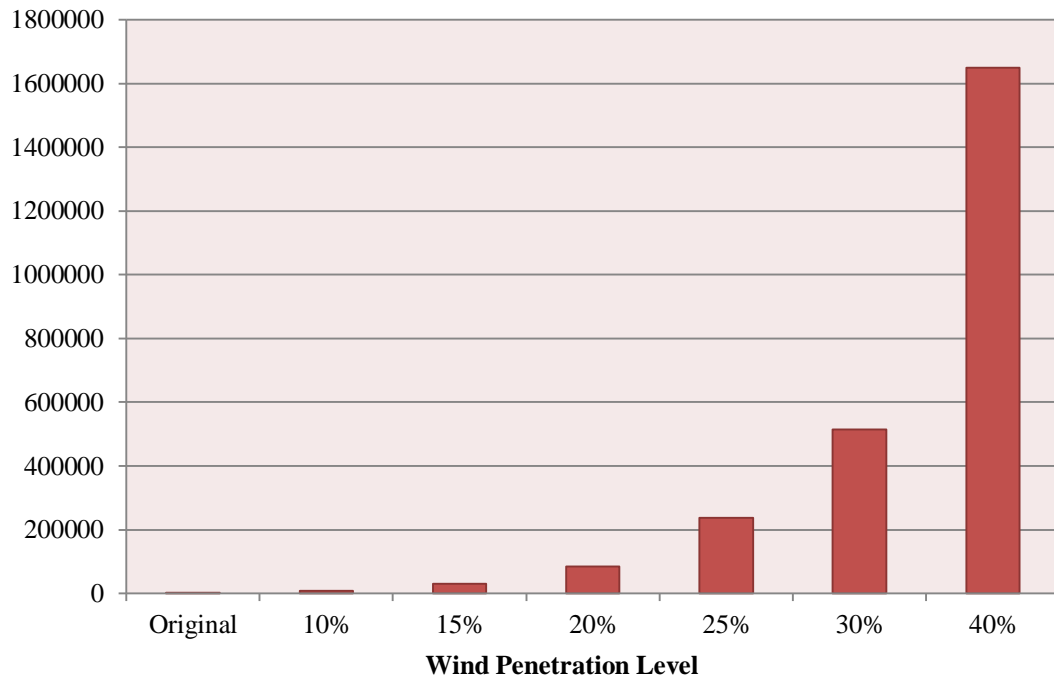


*Figure 7.3: The Impact of Wind Penetration on LOEE*

From *Figures 7.2 and 7.3*, it is apparent that the displacement on conventional generation by wind power generation will harm the generating system reliability and the significance of this impact is amplified with the increasing penetration level. Because the wind power generation does not have stable power output compared with the conventional generation, and the intermittency of the power output becomes more obviously while the wind penetration increases.

For instance, the comparison of LOLE values between low, medium, high and extreme high wind penetration levels is shown in *Table 7.7*.

**Table 7.7: Comparison of LOLE Values on Low, Medium, High & Extreme High Penetration Levels**

Scenario	LOLE (hours/year)	Growth degree
Original → 10% (low)	3→29.8	9.9 times
Original → 15% (low)	3→96	32 times
Original → 20% (medium)	3→238.6	79.5 times
Original → 25% (medium)	3→537.8	179.2 times
Original → 30% (high)	3→941	313.7 times
Original → 40% (extreme high)	3→2002.5	667.5 times

It is clear that the impact on the system reliability is significant when the wind penetration level is high. From *Table 7.7*, the value of LOLE increases 67.2 times (from 29.8 hours/year to 2002.5 hours/year) when the wind penetration goes up by 4 times (from 10% to 40%). When the wind penetration level reaches an extreme high value, the whole generating system becomes insecure and unmanageable, and the reliability level is unacceptable for the system operator. Therefore, the system will be in urgent need of fast response generation to accommodate the intermittency of wind power.

## 7.3.2 The Improvement of Wind-Hydro Cooperation in Reliability

### Case 1: 10% Wind Penetration Level (Low Level)

Applying WHC method to the modified IEEE 118-bus test system at 10% wind penetration level, the simulation results can be represented by the term of Cooperation Scenario (CS), which can be expressed as (CF; DR). CF determines the required amount of PHCES for the cooperation; DR determines the dispatch situation of the required PHCES for generating-pumping (PHES units) and generating-only (hydro units) processes.

For the purpose of reducing the simulation time and simplifying the calculation process, seven CFs and associated DRs, are considered to illustrate the cooperation on reducing the impacts of wind power fluctuations on reliability. In this case, the values of CFs are 0.3, 0.4, 0.5, 0.6, 0.7, 0.8 and 0.9, respectively. However, the value of CF can be very detailed according to the requirement of System Operator (SO). The results presented in Chapter 6 showed that Dispatch Ratio (DR) is playing an important role in the cooperation. In this section, the effects of DR will be analysed in three CFs (CF=0.6, 0.7 and 0.8).

WHC method combines the advantages of the combined reliability assessment method and the flexibility of PHES units to reduce the impacts of wind power fluctuation on system power outputs and maintain the reliability level.

The simulation results of all cooperation scenarios and associated reliability indices in 10% wind penetration are summarized in Appendix VIII. As discussed in the previous chapters, the analysis is mainly focused on LOLE and LOEE. *Figure 7.4* shows the effect of all cooperation scenarios on the value of LOLE at 10% wind penetration level.

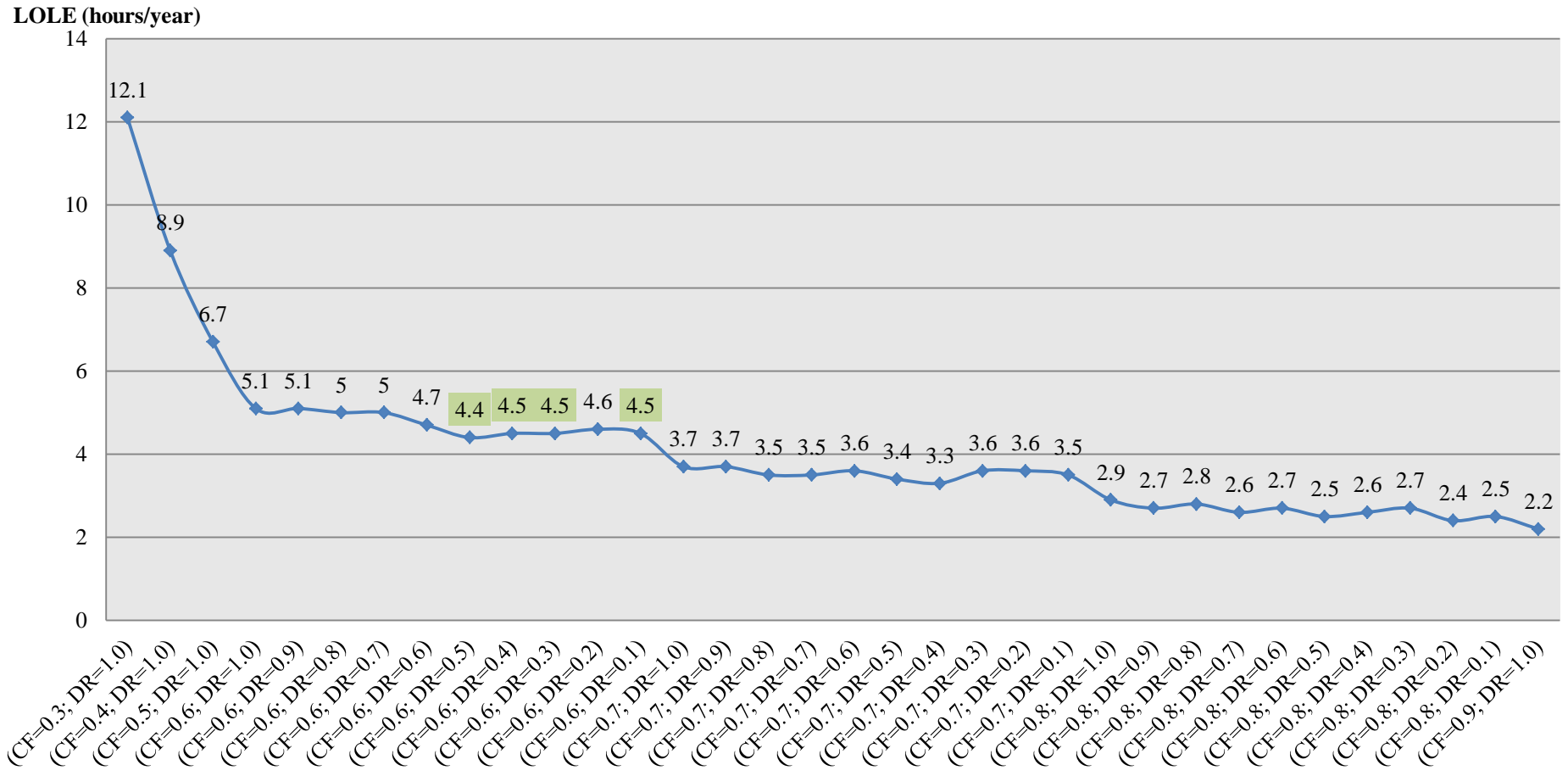


Figure 7.4: Effects of Cooperation Scenarios on Reliability Index LOLE (10% Wind Penetration)

At 10% wind penetration level, the value of LOLE is 29.8 hours/year, which is shown in *Table 7.6*. Then, the value of LOLE drops from 29.8 hour/year to 12.1 hours/year when the installed PHCES capacity is  $(CF=0.3) \times 900$  MW (installed wind capacity) = 270 MW. It means that the decreasing trend is more obviously at the beginning of the cooperation, which has been proved in Chapter 6; in this section, this trend is not included in the above figure for a better illustration of the effects of CS on the value of LOLE at 10% wind penetration level.

*Figure 7.4* shows that WHC can make a great contribution for reducing the impacts of wind power fluctuations and retrieve the reliability level. The values of LOLE decrease significantly while the values of CF increase. When the wind penetration level is low, it is possible to retrieve the system reliability to the original level, even better than the original level, as shown in the above results.

In this case, when  $CF=0.8$  (means that the installed PHCES capacity is 720 MW), the values of LOLE are already less than the original level (3 hours/year), which is shown in *Figure 7.4*. However, the decreasing trend on LOLE becomes almost saturated when there is a large amount of PHCES in the system and the amount of PHCES is still increasing. It means that there is an acceptable limit for WHC in the system. The reliability can remain at the original level before it reaches the limit in this case.

Now, the effects of DR will be investigated by analysing LOLE & LOEE in three cooperation factors ( $CF=0.6, 0.7$  and  $0.8$ ) as follows:

(i). The effects of DR on **LOLE** in these cooperation factors are shown in *Figure 7.5*. The coloured parts in the figure are the minimum values of LOLE in each CF, and the minimum values of LOLE are used to compare with the cases without considering the role of DR ( $DR=1.0$ , all installed capacity is PHES & no hydro capacity). The improvements of DR on the value of LOLE are summarized in *Table 7.8*.

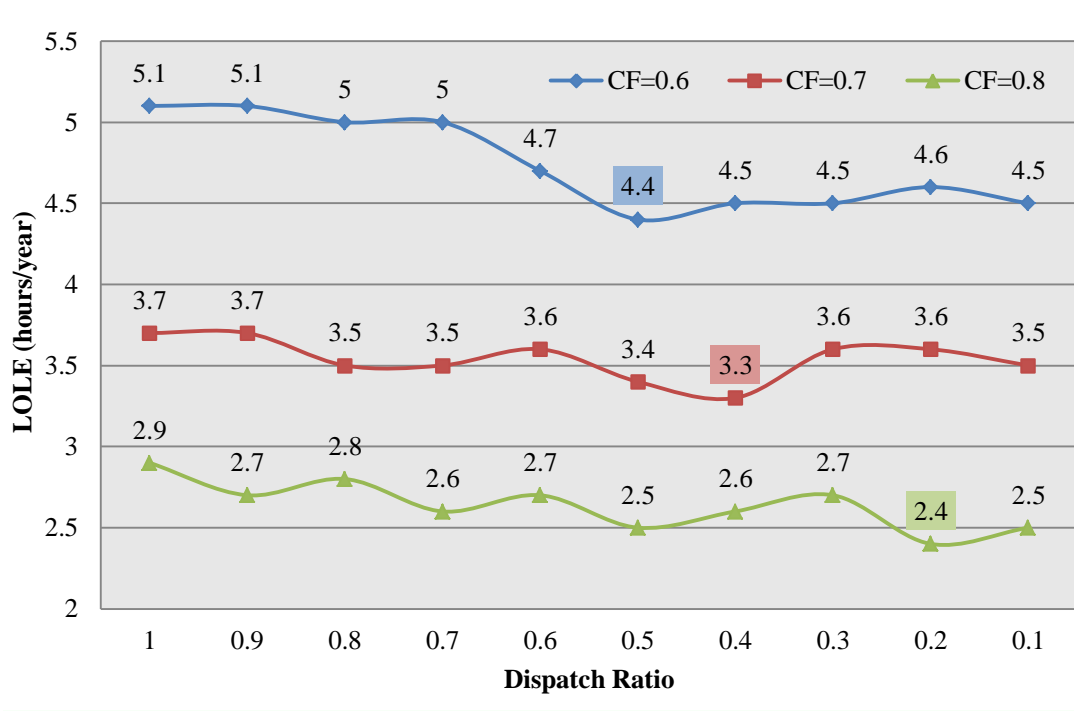


Figure 7.5: Effects of DR on LOLE in CF=0.6, 0.7 & 0.8 (10%)

Table 7.8: Improvements on LOLE by DR in CF=0.6, 0.7&0.8 (10%)

CF	LOLE (hours/year)		Improvement (%)
	DR=1.0 (PHES only)	Minimum (operating values)	
0.6	5.1	4.4	13.7
0.7	3.7	3.3	10.8
0.8	2.9	2.4	17.2

The improvement of the reliability performance can be represented by the reduction on the value of LOLE. For instance, in [Row (2), Column (3)] of Table 7.8, the improvement (%) =  $(5.1 - 4.4) / 5.1 \times 100\% = 13.7\%$ . From Figure 7.5 and Table 7.8, DR could make the cooperation operate more efficient and contribute effectively to the system reliability under the same amount of PHCES. The presented results also prove that the effects of DR on the wind-hydro cooperation are positive, which is

shown in *Figure 7.5* that the values of LOLE (DR=0.9, 0.8..... 0.1) are always less than or equal to the value of LOLE (DR=1.0).

(ii).The effects of DR on *LOEE* in these cooperation factors are shown in *Figure 7.6*. The coloured parts in the figure are the minimum values of LOEE in each CF. The improvements of DR on the value of LOEE are summarized in *Table 7.9*.

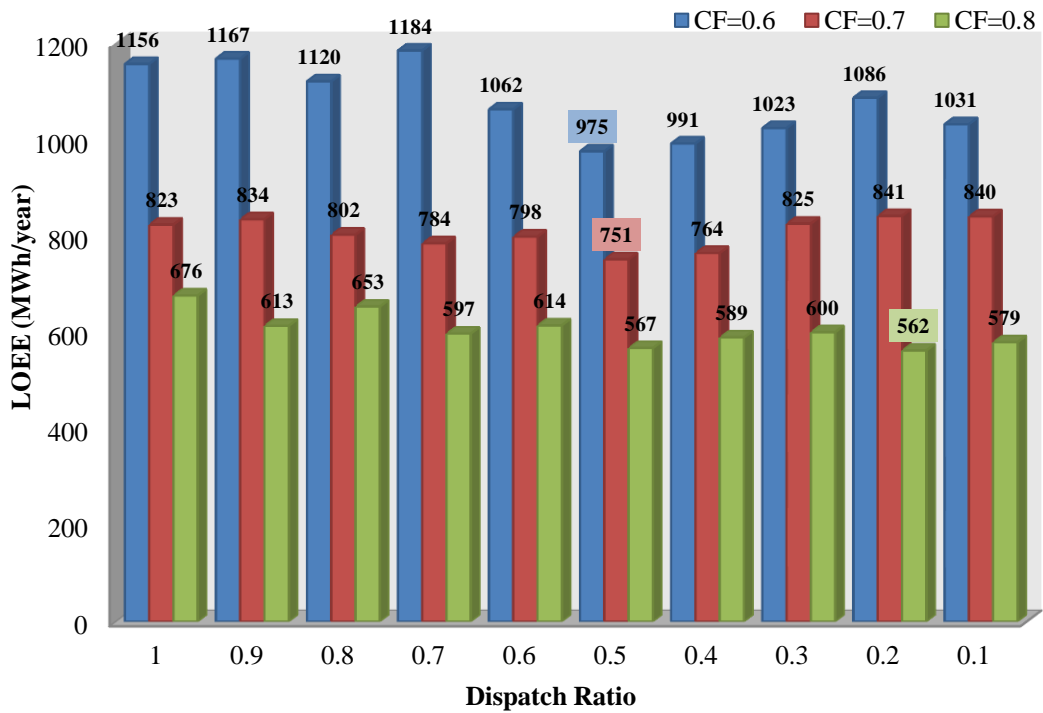


*Figure 7.6: Effects of DR on LOEE in CF=0.6, 0.7 & 0.8 (10%)*

*Table 7.9: Improvements on LOEE by DR in CF=0.6, 0.7&0.8 (10%)*

CF	LOEE (MWh/year)		Improvement (%)	Reduced Amount
	DR=1.0 (PHES only)	Minimum (operating values)		
0.6	1156	975	15.7	181 MWh/year
0.7	823	751	8.7	72 MWh/year
0.8	676	562	16.9	114 MWh/year

The improvement of the reliability performance can also be represented by the reduction on the value of LOEE. For instance, in [Row (2), Column (3)] of Table 7.9, the improvement (%) =  $(1156 - 975) / 1156 \times 100\% = 15.7\%$ . From Figure 7.6 and Table 7.9, DR could effectively reduce the electric energy transmission/distribution losses of the cooperation under the same amount of PHCES. Even a slight improvement on LOEE may represent a great economic benefit on reducing the customer interruption cost (CIC) of the expected energy loss. For instance, at CS (0.7; 0.5), the value of LOEE drops from 823 MWh/year to 751 MWh/year and the reduction of LOEE is 72 MWh/year. According to CIC of residential users in Table 7.4, this improvement can make an economic benefit of saving the cost around  $3.047 \text{ £/kWh} \times 72 \text{ MWh/year} = \text{£ } 219,384$ .

In addition, there is another aspect of cooperation scenarios need to be analysed. From Figures 7.5 and 7.6, the cooperation scenarios (CF=0.6; DR=0.5), **(CF=0.7; DR=0.4)** and (CF=0.8; DR=0.2) have the minimum operating values of LOLE in each CF; on the other hand, CS (0.6; 0.5), **CS (0.7; 0.5)** and CS (0.8; 0.2) have the minimum operating values of LOEE in each CF. So, the minimum operating values of LOLE and LOEE may not appear in the same cooperation scenario (CS). And LOLE has been used as the reliability standard as presented in the previous chapters. The value of LOEE will be used to investigate the economic benefit of CS in future studies.

### **Case 2: 15% Wind Penetration Level (Low Level)**

Applying WHC method to the modified IEEE 118-bus test system at 15% wind penetration level, the simulation results can be represented by the term of Cooperation Scenario (CS), which can be expressed as (CF; DR). For the purpose of simplifying the analysis processes, the simulation procedures and the CSs of this case are the same as that in Case 1 (10% wind penetration).

The simulation results of all cooperation scenarios and associated reliability indices in 15% wind penetration are also summarized in Appendix VIII. As discussed in Case 1, the analysis is mainly focused on LOLE and LOEE. *Figure 7.7* shows the effect of all cooperation scenarios on the value of LOLE at 15% wind penetration level. The original value of LOLE (without wind connection) and the value of LOLE in 15% wind penetration (with wind connection only) have also been added to the figure, which are used to illustrate the effect of CS on the value of LOLE more clearly compared with Case 1.

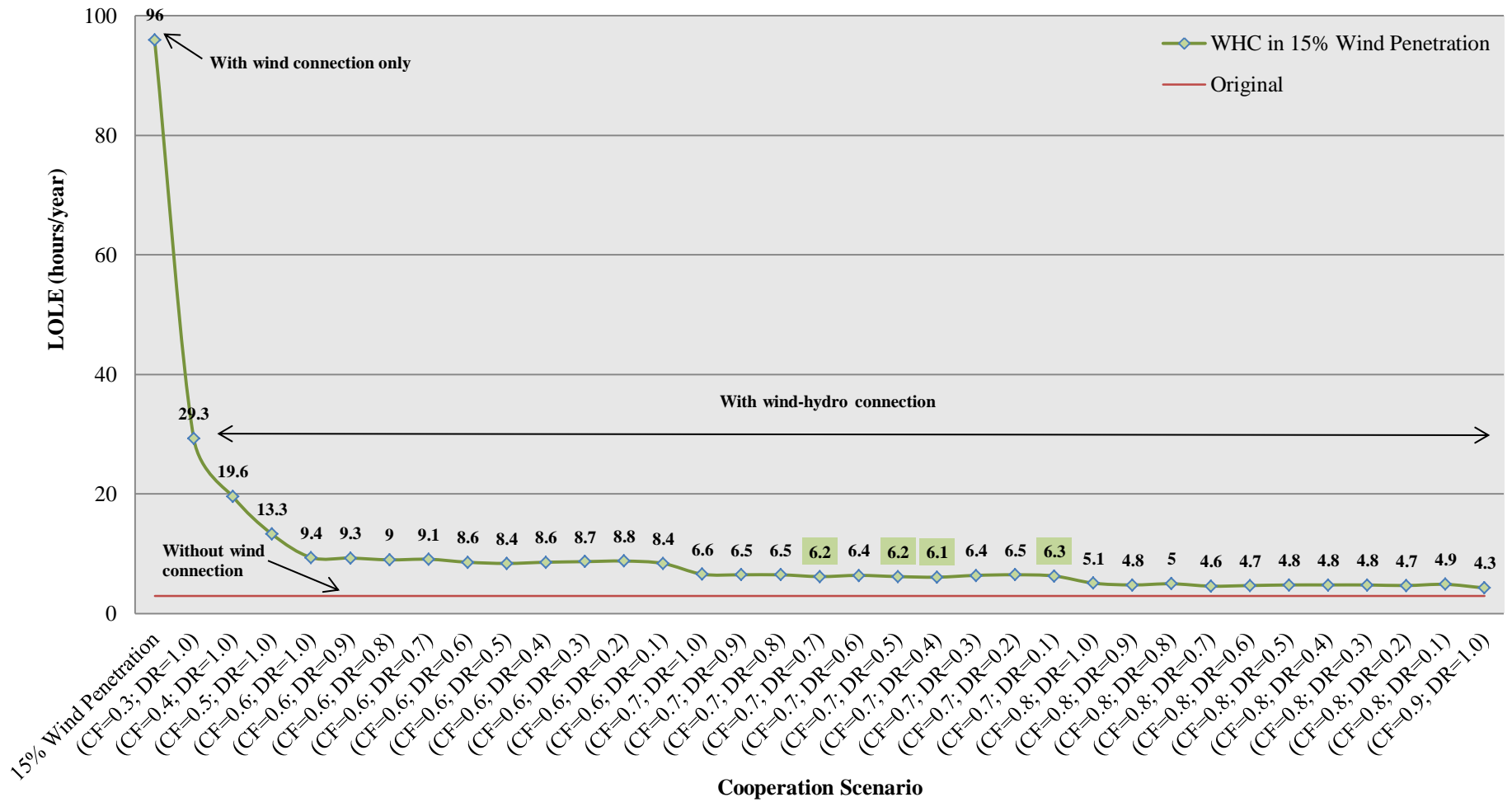


Figure 7.7: Effects of Cooperation Scenarios on Reliability (15% Wind Penetration)

From *Figure 7.7*, the value of LOLE decreases by 69.5%, from 96 hours/year (with wind connection only) to 29.3 hours/year at CS (0.3; 1.0). The improvement of the reliability can be represented by the reduction on the value of LOLE, which means that the system reliability can improve by 69.5% compared with the value in 15% wind penetration. It is clear that even a small amount of PHCES can make a huge contribution for improving the reliability after integrating wind power generation into the power system.

Furthermore, the results show that the decreasing rate on LOLE reduction is getting smaller while the installed capacity of PHCES is continuing to increase. The decreasing trend is not obvious when there is a large amount of PHCES in the system, and the installed capacity of PHCES is still increasing. It is not necessary to install more PHCES to achieve such “a little” reliability improvements due to the capital costs of PHCES stations are significantly expensive and the construction period of a PHCES station is relatively long as discussed in Chapter 6. At CS (0.9; 1.0), the system reliability is improved by 95.5% from 96 hours/year (with wind connection only) to 4.3 hours/year. Although the reliability level is slightly higher than the original, it is still acceptable and reasonable for the power system with 15% wind penetration.

Therefore, for the purpose of better economic benefits and less computation time, the maximum value of CF is set to 0.9 for future studies. In addition, the value of CF can be more than 0.9 in the realistic applications; because of some areas may have huge potential hydro resources.

Now, the effects of DR on LOLE & LOEE in three cooperation factors (CF=0.6, 0.7 and 0.8) are summarized in *Table 7.10*. The values of LOLE and LOEE are shown in *Figure 7.7* and Appendix VIII.

**Table 7.10: Improvements on LOLE & LOEE by DR in CF=0.6, 0.7&0.8 (15%)**

LOLE (hours/year)				LOEE (MWh/year)			
CF	0.6	0.7	0.8	CF	0.6	0.7	0.8
<i>DR=1.0</i> <i>(PHES only)</i>	9.4	6.6	5.1	<i>DR=1.0</i> <i>(PHES only)</i>	2349	1677	1391
<i>Minimum</i> <i>(operating</i> <i>value)</i>	8.4	6.1	4.6	<i>Minimum</i> <i>(operating</i> <i>value)</i>	2062	1590	1254
<i>Improvement</i> <i>(%)</i>	10.6	7.6	9.8	<i>Improvement</i> <i>(%)</i>	12.2	5.2	9.8
<i>Reduction</i> <i>(hours/year)</i>	1.0	0.5	0.5	<i>Reduction</i> <i>(MWh/year)</i>	287	87	137

The improvement of the reliability performance can also be represented by the reductions on the values of LOLF and LOEE. For instance, in [Row (5), Column (2)] of Table 7.10, the improvement (%) =  $(9.4 - 8.4) / 9.4 \times 100\% = 10.6\%$ . From the results in Table 7.10, DR could also make the cooperation operate more efficient and contribute effectively to the system reliability under the same amount of PHCES. Compared with Case 1, the effect of DR on reliability decreases slightly in this case. The improvements on reliability in this case (CF=0.6, 0.7 and 0.8) are 10.6%, 7.6% and 9.8%, respectively. On the other hand, the improvements in 10% wind penetration are 14%, 10.8% and 17.2%, respectively. This difference may be caused by the increasing wind penetration. From Tables 7.9 and 7.10, the improvement (%) on LOEE in this case is also less than that in Case 1; however, the improved reduction amount caused by DR is increasing.

Therefore, DR has better performance on reducing the electric energy transmission/distribution losses of the cooperation at 15% wind penetration level. This effect will be investigated in higher wind penetration levels.

### **Case 3: 20% Wind Penetration Level (Medium Level)**

Applying WHC method to the modified IEEE 118-bus test system at 20% wind penetration level, the simulation results can be represented by the term of Cooperation Scenario (CS). For the purpose of simplifying the analysis processes, the simulation procedures and the CSs of this case are the same as that in Case 1 (10% wind penetration).

The simulation results of all cooperation scenarios and associated reliability indices in 20% wind penetration are also summarized in Appendix VIII. *Figure 7.8* shows the effect of all cooperation scenarios on the value of LOLE at 20% wind penetration level.

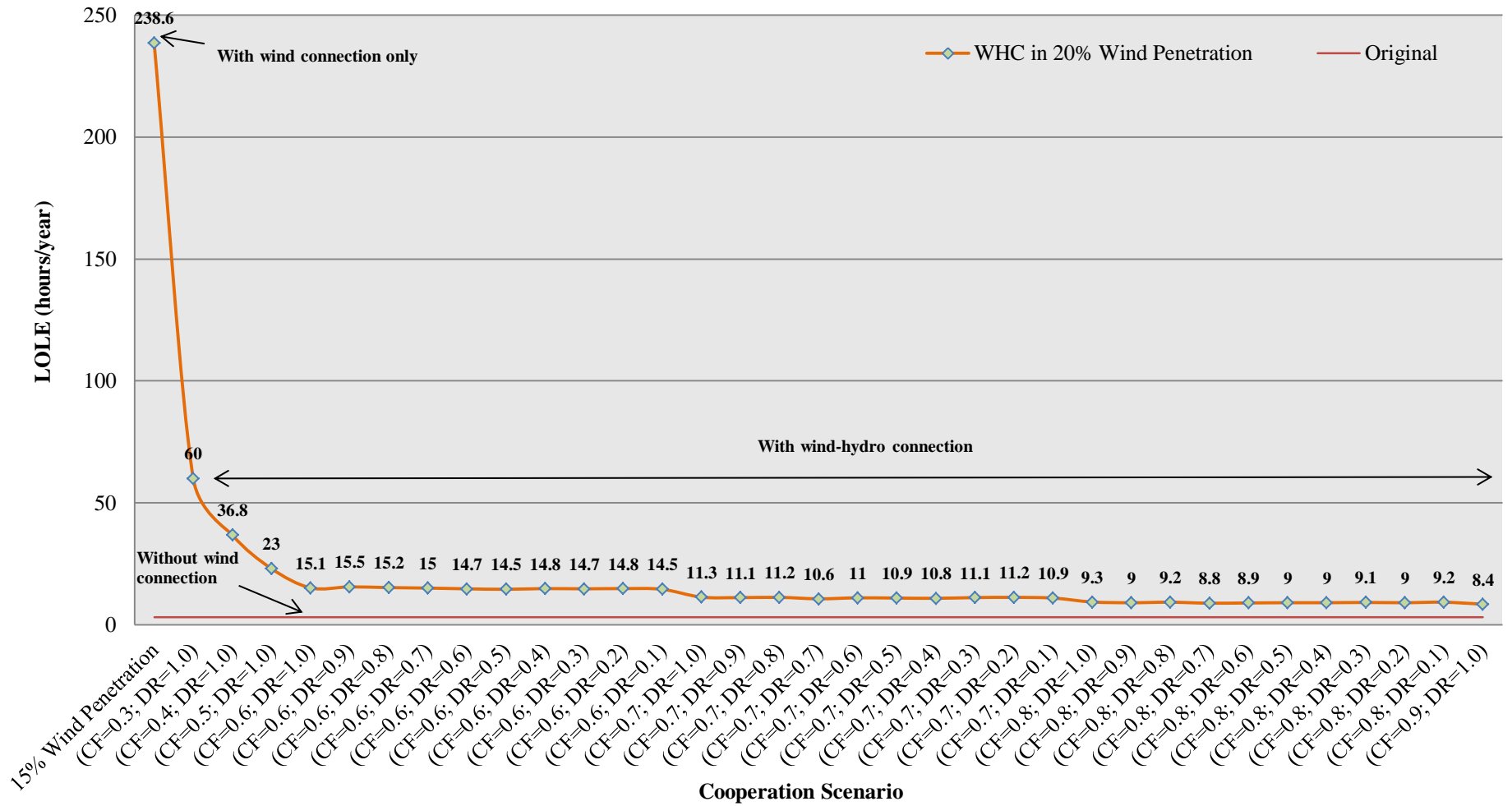


Figure 7.8: Effects of Cooperation Scenarios on Reliability (20% Wind Penetration)

It can be seen that a small amount of PHCES can also make a great contribution for improving the reliability at 20% wind penetration level. From *Figure 7.8*, the value of LOLE at 20% wind penetration level (without WHC) decreases by 74.9%, from 238.6 hours/year (with wind connection only) to 60 hours/year at CS (0.3; 1.0). Then, the values of LOLE are decreasing while the installed PHCES capacity is increasing. At CS (0.9; 1.0), the reliability is improved by 96.5% from 238.6 hours/year (with wind connection only) to 8.4 hours/year.

In the previous cases, the results show that there is an acceptable limit for WHC in the system. *Figure 7.8* shows that the decreasing trend on the value of LOLE becomes almost saturated when there is a large amount of PHCES in the system, and the capacity of PHCES is still increasing. Comparing with CS (0.8; 0.7) & CS (0.9; 1.0), the value of LOLE drops from 8.8 hours/year to 8.4 hours/year; however, the increased PHCES capacity is  $1800 \text{ MW} \times (0.9 - 0.8) = 180 \text{ MW}$ , which is obviously very expensive for the improvement (reduced 0.4 hours/year) on reliability.

Although the reliability is not “coming back” to the original value, CS (0.9; 1.0) = 8.4 hours/year is acceptable and reasonable for the power system at 20% wind penetration level. Therefore, WHC method could effectively reduce the impacts of wind power fluctuations on reliability at medium penetration level. As presented in previous studies, only few countries can reach this target (defined in *section 2.3.3*).

Now, the effects of DR on LOLE & LOEE at 20% wind penetration level are summarized in *Table 7.11*. The values of LOLE and LOEE are shown in *Figure 7.8* and Appendix VIII.

**Table 7.11: Improvements on LOLE & LOEE by DR in CF=0.6, 0.7&0.8 (20%)**

LOLE (hours/year)				LOEE (MWh/year)			
CF	0.6	0.7	0.8	CF	0.6	0.7	0.8
<i>DR=1.0</i> <i>(PHES only)</i>	15.1	11.3	9.3	<i>DR=1.0</i> <i>(PHES only)</i>	4401	3416	3038
<i>Minimum</i> <i>(operating</i> <i>value)</i>	14.5	10.6	8.8	<i>Minimum</i> <i>(operating</i> <i>value)</i>	4113	3295	2848
<i>Improvement</i> <i>(%)</i>	4	6.2	5.4	<i>Improvement</i> <i>(%)</i>	6.5	3.5	6.3
<i>Reduction</i> <i>(hours/year)</i>	0.6	0.7	0.5	<i>Reduction</i> <i>(MWh/year)</i>	288	121	190

From *Table 7.11*, the effects of DR on LOLE are unobvious in 20% wind penetration. The reductions on the values of LOLE are slight compared with their values. On the other hand, DR has slight effects on the reduction of LOEE; however, due to the large amount of LOEE at 20% wind penetration level, even a small improvement can still represent a great economic benefit on reducing the customer interruption cost (CIC) of the expected electric energy losses. For instance, the reduction on LOEE is 121 MWh/year when CF = 0.7, the interruption cost is around  $9.728 \text{ £/kWh} \times 121 \text{ MWh/year} = \text{£ } 1.18 \text{ million}$ . Therefore, DR can make a great contribution for better economic benefits at 20% wind penetration level.

#### **Case 4: 25% Wind Penetration Level (Medium Level)**

WHC method will be applied in the reliability evaluation of the modified IEEE 118-bus test system at 25% wind penetration level. For the purpose of simplifying the analysis processes, the simulation procedures and the CSs of this case are the same as that in Case 1 (10% wind penetration).

The simulation results of all cooperation scenarios and associated reliability indices in 25% wind penetration are also summarized in Appendix VIII. *Figure 7.9* shows the effect of all cooperation scenarios on the value of LOLE at 25% wind penetration level.

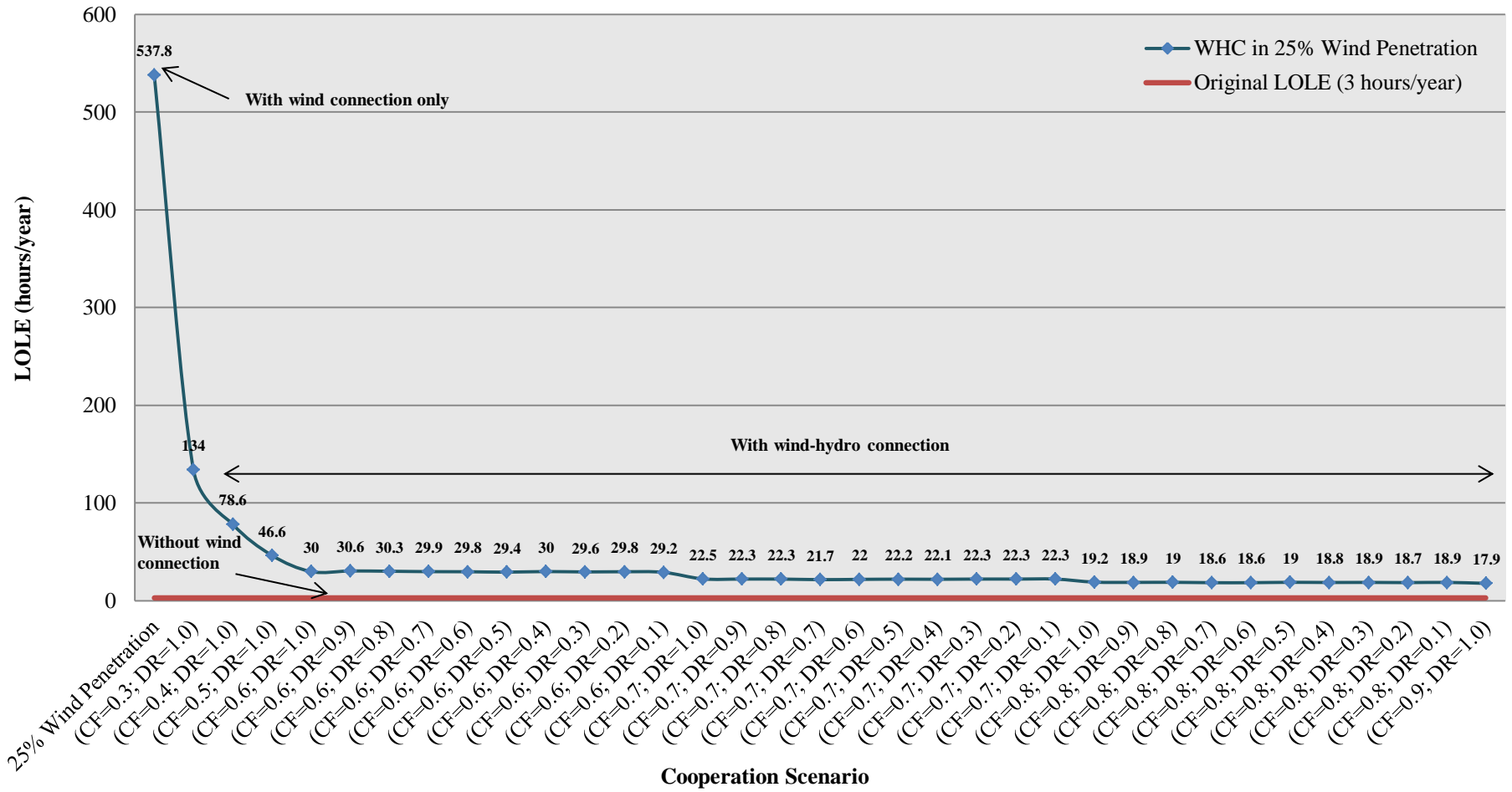


Figure 7.9: Effects of Cooperation Scenarios on Reliability (25% Wind Penetration)

From *Figure 7.9*, the decreasing trend is very similar with the trend in 20% wind penetration (*Figure 7.8*). A small amount of PHCES can also make a great contribution to improve the reliability at 25% wind penetration level. It shows that the value of LOLE at 25% wind penetration level (without WHC) decreases by 75%, from 537.8 hours/year (with wind connection only) to 134 hours/year at CS (0.3; 1.0). Then, the values of LOLE are decreasing while the installed PHCES capacity is increasing. At CS (0.9; 1.0), the reliability is improved by 96.7% from 537.8 hours/year (with wind connection only) to 17.9 hours/year.

The decreasing trend becomes almost saturated in this case. Comparing with CS (0.8; 0.7) & CS (0.9; 1.0), the value of LOLE drops from 18.6 hours/year to 17.9 hours/year; however, the increased PHCES capacity is  $2250 \text{ MW} \times (0.9 - 0.8) = 225 \text{ MW}$ , which is too expensive to accomplish the improvement (reduced 0.7 hours/year) on reliability.

Chapter 2 presented several leading countries in high wind penetration level, which are Denmark -26%, Portugal-19%, Spain-19%, Ireland-18% and Germany-11%. In this case, 25% wind penetration is very difficult for the realistic power systems to accomplish and this target was only achieved by Denmark. At CS (0.9; 1.0), LOLE=17.9 hours/year is still acceptable and reasonable for the power system with 25% wind penetration. Therefore, WHC method could effectively reduce the impacts of wind power fluctuations on reliability at 25% penetration level. As presented in previous studies, only Denmark has reached this target (introduced in *section 2.3.3*).

Now, the effects of DR on LOLE & LOEE at 25% wind penetration level are summarized in *Table 7.12*. The values of LOLE and LOEE are shown in *Figure 7.9* and Appendix VIII.

**Table 7.12: Improvements on LOLE & LOEE by DR in CF=0.6, 0.7&0.8 (25%)**

LOLE (hours/year)				LOEE (MWh/year)			
CF	0.6	0.7	0.8	CF	0.6	0.7	0.8
<i>DR=1.0</i> (PHEs only)	30	22.5	19.2	<i>DR=1.0</i> (PHEs only)	10591	8591	7971
<i>Minimum</i> (operating value)	29.2	21.7	18.6	<i>Minimum</i> (operating value)	10172	8346	7636
<i>Improvement</i> (%)	2.7	3.6	3.1	<i>Improvement</i> (%)	4	2.9	4.2
<i>Reduction</i> (hours/year)	0.8	0.8	0.6	<i>Reduction</i> (MWh/year)	419	245	335

The improvements on LOLE & LOEE by percentages keep decreasing compared with that in 20% wind penetration level, which are shown in *Tables 7.11* and *7.12*. In this case, the amount of LOEE is significantly increasing compared with that in the previous cases. A small improvement can still represent a great economic benefit on reducing the customer interruption cost (CIC) of the expected electric energy losses.

For instance, the reduction on LOEE is 245 MWh/year when CF = 0.7, the interruption cost is around  $9.728 \text{ £/kWh} \times 245 \text{ MWh/year} = \text{£}2.38 \text{ million}$ . Therefore, DR has an excellent performance on saving interruption costs and improving economic benefits at 25% wind penetration level.

### **Case 5: 30% Wind Penetration Level (High Level)**

WHC method will be applied in the reliability evaluation of the modified IEEE 118-bus test system at 30% wind penetration level. Previous cases proved that DR only has slight effect on improving the system reliability (LOLE) when the wind penetration level is very high and the installed PHCES capacity is significantly large.

For the purpose of reducing the simulation time and simplifying the calculation process, seven CFs without associated DRs, are considered to illustrate the cooperation on reducing the impacts of wind power fluctuations on reliability at high wind penetration level.

The simulation results of all cooperation scenarios and associated reliability indices in 30% wind penetration are also summarized in Appendix VIII. *Figure 7.10* shows the effect of all cooperation factors on the value of LOLE at 30% wind penetration level.

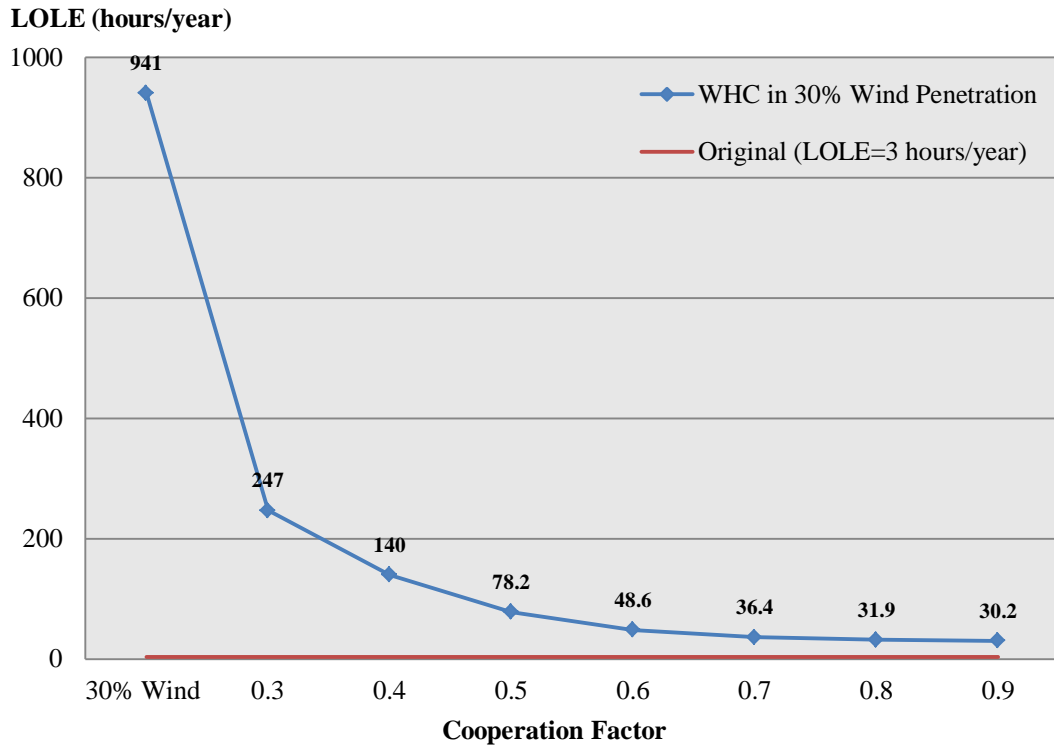


**Figure 7.10: Effect of Cooperation Factor (CF) on Reliability Indices (30% Wind Penetration)**

It is clear that the decreasing trend is very similar with the trends in 20% and 25% wind penetration levels. It shows that the value of LOLE decreases by 74%, from 941 hours/year to 247 hours/year at CS (0.3; 1.0). Then, the values of LOLE are

decreasing while the installed PHCES capacity is increasing. At CS (0.9; 1.0), the reliability is improved by 96.8% from 941 hours/year to 30.2hours/year.

*Figure 7.10* also shows that the decreasing trend on LOLE becomes saturated when the wind penetration level is significantly high. As discussed in the previous case, the present highest wind penetration level is 26% in Denmark, and the wind penetration levels of most countries are less than 10%. And the maximum limit of LOLE is 48 hours/year (determined in Chapter 3), CS (0.9; 1.0) = 30.2 hours/year is still less than the maximum value. So, this improved reliability is still acceptable for the power system with 30% wind penetration. However, the effect of WHC method on reducing the impacts of wind power fluctuations on system reliability is decreasing, and the improved reliability level is close to the maximum limit.

In this case, the results prove that WHC method is still effective for maintaining the power system reliability with high wind penetration, and the latter case is to investigate the effect of the wind-hydro cooperation on extreme high wind penetration level.

#### **Case 6: 40% Wind Penetration Level (Extreme High Level)**

WHC method will be applied in the reliability evaluation of the modified IEEE 118-bus test system at 40% wind penetration level. For the purpose of reducing the simulation time and simplifying the calculation process, five CFs without associated DRs, are considered to illustrate the cooperation on reducing the impacts of wind power fluctuations on reliability at extreme high wind penetration level.

The simulation results of all cooperation scenarios and associated reliability indices in 40% wind penetration are also summarized in Appendix VIII. *Figure 7.11* shows the effect of five cooperation factors on the value of LOLE at 40% wind penetration level.

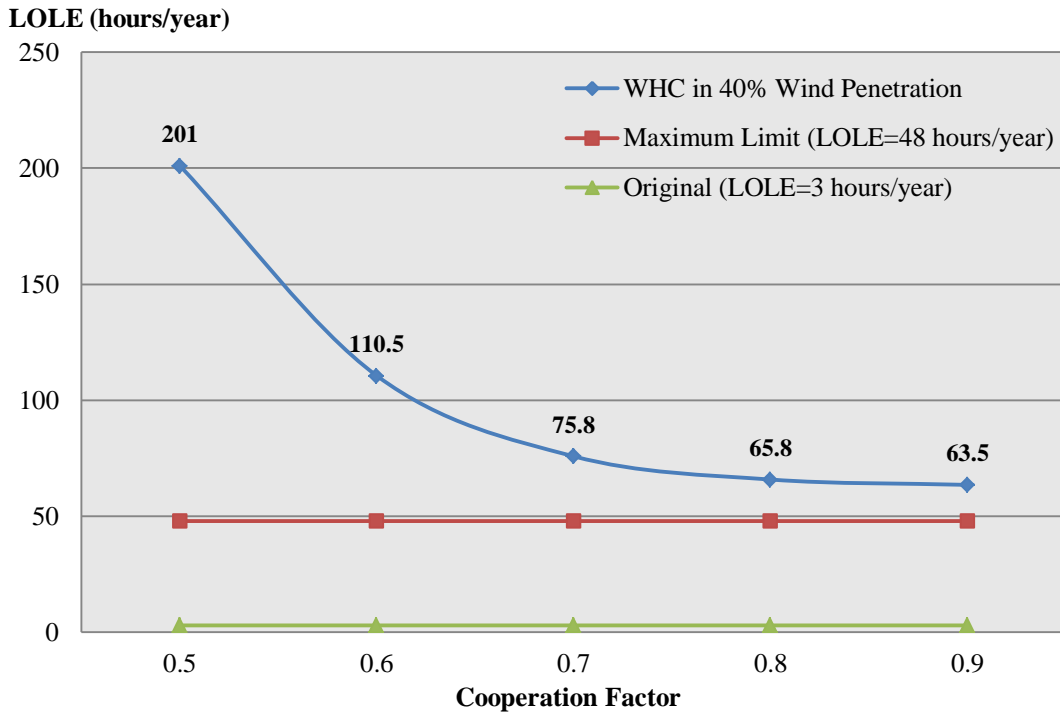


**Figure 7.11: Effect of Cooperation Factor (CF) on Reliability Indices (40% Wind Penetration)**

Figure 7.11 shows that the decreasing trend on LOLE becomes saturated, and the minimum value of LOLE at CS (0.9; 1.0) is 63.5 hours/year, which is larger than the maximum limit of LOLE. Also, the reduced value of LOLE is over 20 times more than the original case. So, all cooperation scenarios of WHC method at 40% wind penetration level are not acceptable for the power system. It is indicated that WHC method is not feasible for the power system with extreme high wind penetration; because of the wind power output fluctuations are so high that the wind-hydro cooperation cannot overcome the intermittent issue.

These six cases represent four types of wind penetration: low level, medium level, high level and extreme high level. The results show that the WHC method can effectively and efficiently reduce the impacts of wind power output fluctuations on power outputs, and retrieve the reliability to an acceptable level even at high wind penetration level. Furthermore, the dispatch ratio (DR) has been proved that can

make a great contribution for better economic benefits by saving huge amount of interruption costs, especially in medium wind penetration cases.

When the wind penetration is extremely high, the WHC method can still effectively mitigate the impact of wind power's intermittency on power systems reliability. However, the results indicate that the improved reliability is not acceptable for the power system considering the given conditions in this thesis.

For absorbing extreme high wind penetration, it may require a large power system with many flexible generation resources. And this assumption will confirm with the wind energy development in Denmark, as discussed in Chapter 2. Danish government is the first government to announce a target of weaning off fossil fuels by 2050. At that time, the Danish energy system will consist purely of renewable energy, with wind power being the main contributor. It is because neighbouring countries such as Germany, Norway and Sweden have much larger electric networks and abundant hydro resources to cooperate with the wind power generation in Danish power system.

### **7.3.3 Determine the Optimal Cooperation Scenario**

In the previous *section 7.3.2*, the improvements of WHC method in reliability have been discussed in details. Presented results proved that the WHC method could effectively reduce the impacts of wind power fluctuations on reliability at different wind penetration levels. Each Cooperation Scenario (CS) represents an improved reliability for the system. The results also showed that the wind-hydro cooperation can operate more efficient with the consideration of the Dispatch Ratio (DR), when the wind penetration level is moderate.

Therefore, this section is focused on determining the optimal cooperation scenario. Each cooperation scenario is defined in terms of a cooperation factor (CF) and a

dispatch ratio (DR), so it is represented by the form of (CF; DR). The optimal cooperation scenario is that the scenario meets the requirement of required acceptable reliability level and also has the best economic benefits among the suitable cooperation scenarios.

Cost-Benefit Analysis (CBA) method is also used in this section and the assumptions remain in the same conditions as mentioned in Chapter 6. Because the high wind penetration is not practical to achieve, the results will be discussed in low and medium wind penetration levels: 10%, 15%, 20% and 25%. And the determined optimal CS will also be used in future sections.

For the purpose of demonstrating the WHC method and simplifying the computation process, the reduced values of LOLE are assumed to be higher than the original case (without wind connection) due to the increasing wind power penetration. This assumption is determined by the multiple of the original value, which is summarized in *Table 7.13*. For higher wind penetration level, the required value of LOLE (reliability standard) is bigger than the lower wind penetration level.

**Table 7.13: Required Acceptable Reliability with WHC**

Wind penetration	Original value of LOLE	Multiple of original	Required value of LOLE
10%	3 hours/year	1.5	4.4~4.5 hours/year
15%	3 hours/year	2	6.0~6.3 hours/year
20%	3 hours/year	3	8.8~9.0 hours/year
25%	3 hours/year	6	18.5~18.7 hours/year

Although the value of LOLE is higher than the original value of LOLE, the electricity customers can be assumed to accept the reliability as the electricity price may be cheaper than the normal condition due to government investments. In addition, the electricity supply may be more flexible and cutting the power off during

off-peak periods of the non-primary consumers by predicting the general variation of wind speed profile. Furthermore, the required acceptable reliability can be either more specifically or more widely, which depends on the system operator (SO).

As presented in Chapter 6, the details of Cost-Benefit Analysis (CBA) method are briefly described as follows:

CBA approach uses the total costs as a basis for ranking cooperation scenarios. Therefore, at the same required reliability level, the optimal cooperation scenario can be determined by using *Equation 6.14* to minimize the value of total costs ( $C$ ). Total costs  $C$  is defined as:  $C = CC + UEC$ ;  $CC$  and  $UEC$  denote the capital costs and unserved energy costs, respectively. In addition,  $UEC = LOEE \times CIC$ ;  $LOEE$  is the Loss of Energy Expectation, which is the simulation result of the power system reliability evaluation in MWh. The customer interruption cost ( $CIC$ ) was presented in *Table 7.4*. The calculation procedure is the same as that in Chapter 6.

### **Case 1: 10% Wind Penetration Level (Low Level)**

The required acceptable reliability level is 4.4~4.5 hours/year. All of the cooperation scenarios were summarized in *Figure 7.4*. From the figure, there are 4 cooperation scenarios meet the requirement, which are CS (0.6; 0.5), CS (0.6; 0.4), CS (0.6; 0.3) and CS (0.6; 0.1). It is clear that all suitable CSs have the same value of CF, which means that they have the same installed capacity of PHCES for the cooperation. So, the capital costs ( $CC$ ) of all suitable scenarios are the same.

Therefore, the objective of CBA is to find the minimum value of  $UEC$  in this case. The results of  $LOEE$  at 10% wind penetration level are summarized in Appendix VIII. The calculation process is shown and illustrated as follows.

$$UEC = LOEE \text{ (MWh/year)} \times CIC \text{ (£/kWh)}$$

$$(1) \text{ CS (0.6; 0.5): } UEC_1 = 975 \text{ MWh/year} \times 0.299 \text{ £/kWh} = \text{£}291,525$$

$$(2) \text{ CS (0.6; 0.4): } UEC_2 = 991 \text{ MWh/year} \times 0.299 \text{ £/kWh} = \text{£}296,309$$

$$(3) \text{ CS (0.6; 0.3): } UEC_3 = 1023 \text{ MWh/year} \times 0.299 \text{ £/kWh} = \text{£}305,877$$

$$(4) \text{ CS (0.6; 0.1): } UEC_4 = 1031 \text{ MWh/year} \times 0.299 \text{ £/kWh} = \text{£}308,269$$

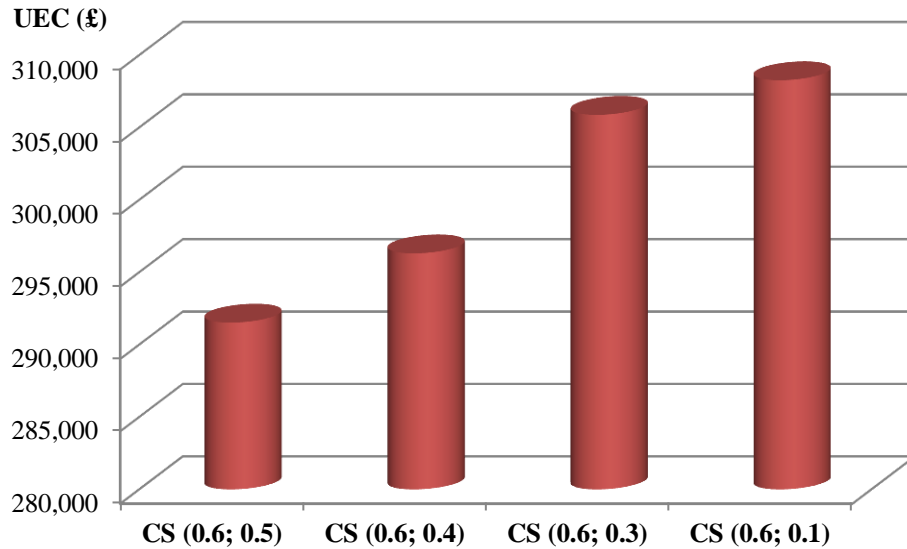


**Figure 7.12: Unserved Energy Costs of Suitable Cooperation Scenarios (10%)**

From *Figure 7.12*, CS (0.6; 0.5) has the minimum value of unserved energy costs (UEC). Therefore, the optimal cooperation scenario for the required acceptable reliability level in 10% wind penetration is CS (0.6; 0.5). From a System Operator (SO) point of view, the optimal cooperation scenario represents:

At 10% wind penetration level, the required reliability level is approximately 4.4~4.5 hours/year. The test system requires PHCES with a total capacity of  $0.6 \times 900 \text{ MW}$  (10% wind penetration) = 540 MW (PHES Capacity: 270 MW for generating-pumping; Hydro Capacity: 270 MW for generating-only) to reduce the impacts of wind power fluctuations on power outputs and retrieve the reliability to the required level with the minimum costs.

### Case 2: 15% Wind Penetration Level (Low Level)

The required acceptable reliability level is 6.0~6.3 hours/year. All of the cooperation scenarios were summarized in *Figure 7.7*. From the figure, there are 4 cooperation scenarios meet the requirement, which are CS (0.7; 0.7), CS (0.7; 0.5), CS (0.7; 0.4) and CS (0.7; 0.1). It is clearly that all suitable CSs also have the same value of CF in this case.

So, the objective of CBA is to find the minimum value of *UEC* in this case. The results of LOEE at 15% wind penetration level are also summarized in Appendix VIII. The calculated results of *UEC* are illustrated in *Figure 7.13*.

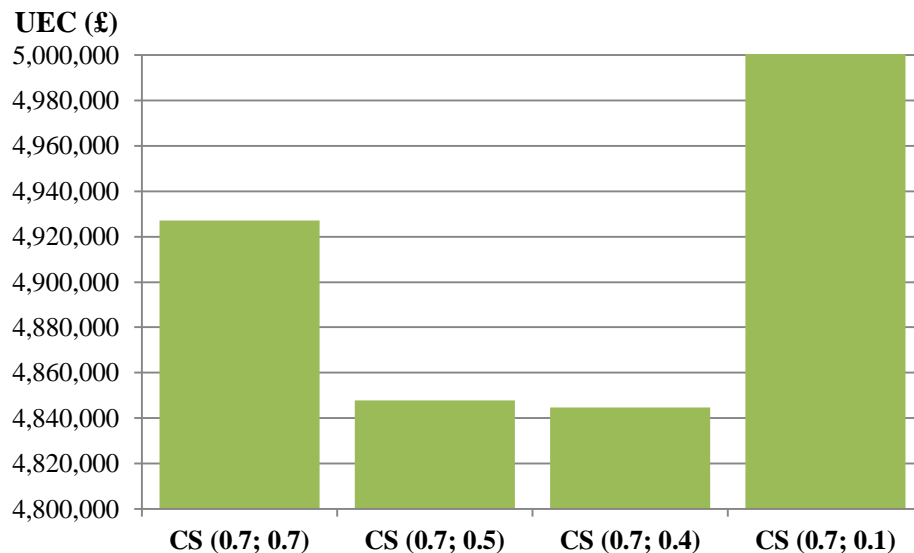


**Figure 7.13: Unserved Energy Costs of Suitable Cooperation Scenarios (15%)**

From *Figure 7.13*, CS (0.7; 0.4) has the minimum value of unserved energy costs. Therefore, the optimal cooperation scenario for the required acceptable reliability level in 15% wind penetration is CS (0.7; 0.4). From a System Operator (SO) point of view, the optimal cooperation scenario represents:

At 15% wind penetration level, the required reliability level is approximately 6.0~6.3 hours/year. The test system requires PHCES with a total capacity of 945 MW (PHES Capacity: 378 MW for generating-pumping; Hydro Capacity: 567 MW for generating-only) to reduce the impacts of wind power fluctuations on power outputs and retrieve the reliability to the required level with the minimum costs.

### Case 3: 20% Wind Penetration Level (Medium Level)

The required acceptable reliability level is 8.8~9.0 hours/year. All of the cooperation scenarios were summarized in *Figure 7.8*. From the figure, there are 6 cooperation scenarios meet the requirement, which are CS (0.8; 0.9), CS (0.8; 0.7), CS (0.8; 0.6), CS (0.8; 0.5), CS (0.8; 0.4) and CS (0.8; 0.2). It is clearly that all suitable CSs also have the same value of CF in this case.

So, the objective of CBA is to find the minimum value of *UEC* in this case. The results of LOEE at 20% wind penetration level are also summarized in Appendix VIII. The calculated results of *UEC* are illustrated in *Figure 7.14*.

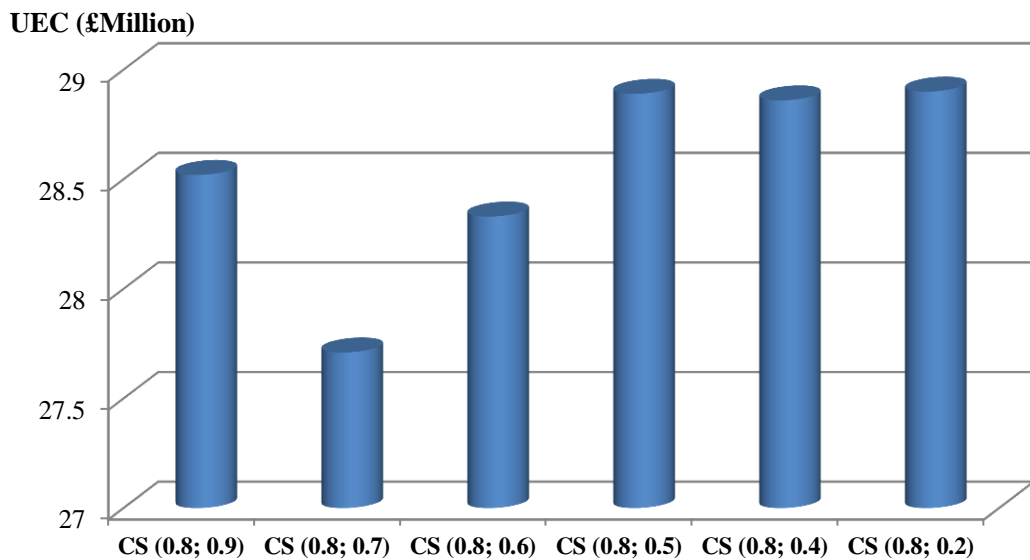


*Figure 7.14: Unserved Energy Costs of Suitable Cooperation Scenarios (20%)*

From *Figure 7.14*, CS (0.8; 0.7) has the minimum value of unserved energy costs. Therefore, the optimal cooperation scenario for the required acceptable reliability level in 20% wind penetration is CS (0.8; 0.7). From a System Operator (SO) point of view, the optimal cooperation scenario represents:

At 20% wind penetration level, the required reliability level is approximately 8.8~9.0 hours/year. The test system requires PHCES with a total capacity of 1440 MW (PHES Capacity: 1008 MW for generating-pumping; Hydro Capacity: 432 MW for generating-only) to reduce the impacts of wind power fluctuations on power outputs and retrieve the reliability to the required level with the minimum costs.

#### **Case 4: 25% Wind Penetration Level (Medium Level)**

The required acceptable reliability level is 18.0~19.0 hours/year. All of the cooperation scenarios were summarized in *Figure 7.9*. From the figure, there are 9 cooperation scenarios meet the requirement, which are CS (0.8; 0.9), CS (0.8; 0.8)..... CS (0.8; 0.2), CS (0.8; 0.1). It is clear that all suitable CSs also have the same value of CF in this case.

So, the objective of CBA is to find the minimum value of *UEC* in this case. The results of LOEE at 25% wind penetration level are also summarized in Appendix VIII. The calculated results of *UEC* are illustrated in *Figure 7.15*.

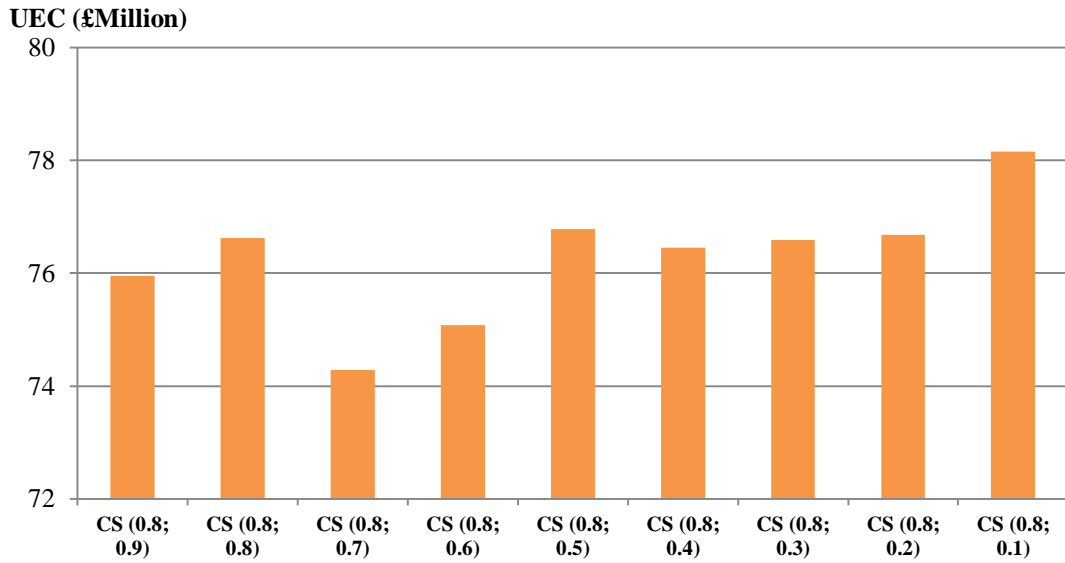


**Figure 7.15: Unserved Energy Costs of Suitable Cooperation Scenarios (25%)**

From *Figure 7.15*, CS (0.8; 0.7) has the minimum value of unserved energy costs. Therefore, the optimal cooperation scenario for the required acceptable reliability level in 25% wind penetration is CS (0.8; 0.7). From a System Operator (SO) point of view, the optimal cooperation scenario represents:

At 25% wind penetration level, the required reliability level is approximately 18.0~19.0 hours/year. The test system requires PHCES with a total capacity of 1800 MW (PHES Capacity: 1260 MW for generating-pumping; Hydro Capacity: 540 MW for generating-only) to reduce the impacts of wind power fluctuations on power outputs and retrieve the reliability to the required level with the minimum costs.

From **Case 1** to **Case 4**, the results show that the effects of WHC method on reliability are decreasing while the wind penetration is going up. It leads to the number of suitable CS for the required reliability level is increasing significantly, which are summarized as follows: **Case 1**: 4, **Case 2**: 4, **Case 3**: 6 and **Case 4**: 9. However, the results also show that even a slight improvement made by the cooperation on the value of LOEE can still represent a great economic benefit on reducing the interruption cost (CIC) of the unserved electric energy. For instance, the

difference on *UEC* between CS (0.8; 0.9) and CS (0.8; 0.7) is approximately £ 2 Million in **Case 4**, which is shown in *Figure 7.15*. The economic benefit on saving the unserved energy costs is significant, although the improvements on the reliability (reduced value of LOLE) are very similar.

Therefore, WHC method has been proved that it can effectively reduce the impacts of wind power fluctuations on power outputs, maintain a reasonable reliability level and make a great contribution for economic benefits at system long-term planning by analysing the simulation results presented in *section 7.3.2* and *7.3.3*.

## **7.4 Evaluation of Modified IEEE 118-Bus Test System: Short-term Operational Planning**

The previous section focused on investigating the effects of the proposed method on reliability in long-term planning of the modified IEEE 118-bus test system. And the results proved that it can effectively reduce the impacts of wind power fluctuations on power outputs and retrieve the reliability to an acceptable level. The dispatch ratio (DR) has also been proved that could make an excellent contribution for economic benefits by saving the unserved electric energy costs.

In power systems, the electric energy transmission/distribution losses are caused by the power-flow on the electric network. For short-term operational planning, it is necessary to investigate the effect of WHC method on reducing electric energy transmission/distribution losses (same as *electric network losses*) in the network. *Figure 7.16* is a clear version of the one-line diagram of IEEE 118-Bus system, which will be used to analyse the power-flow in short-term operating condition.

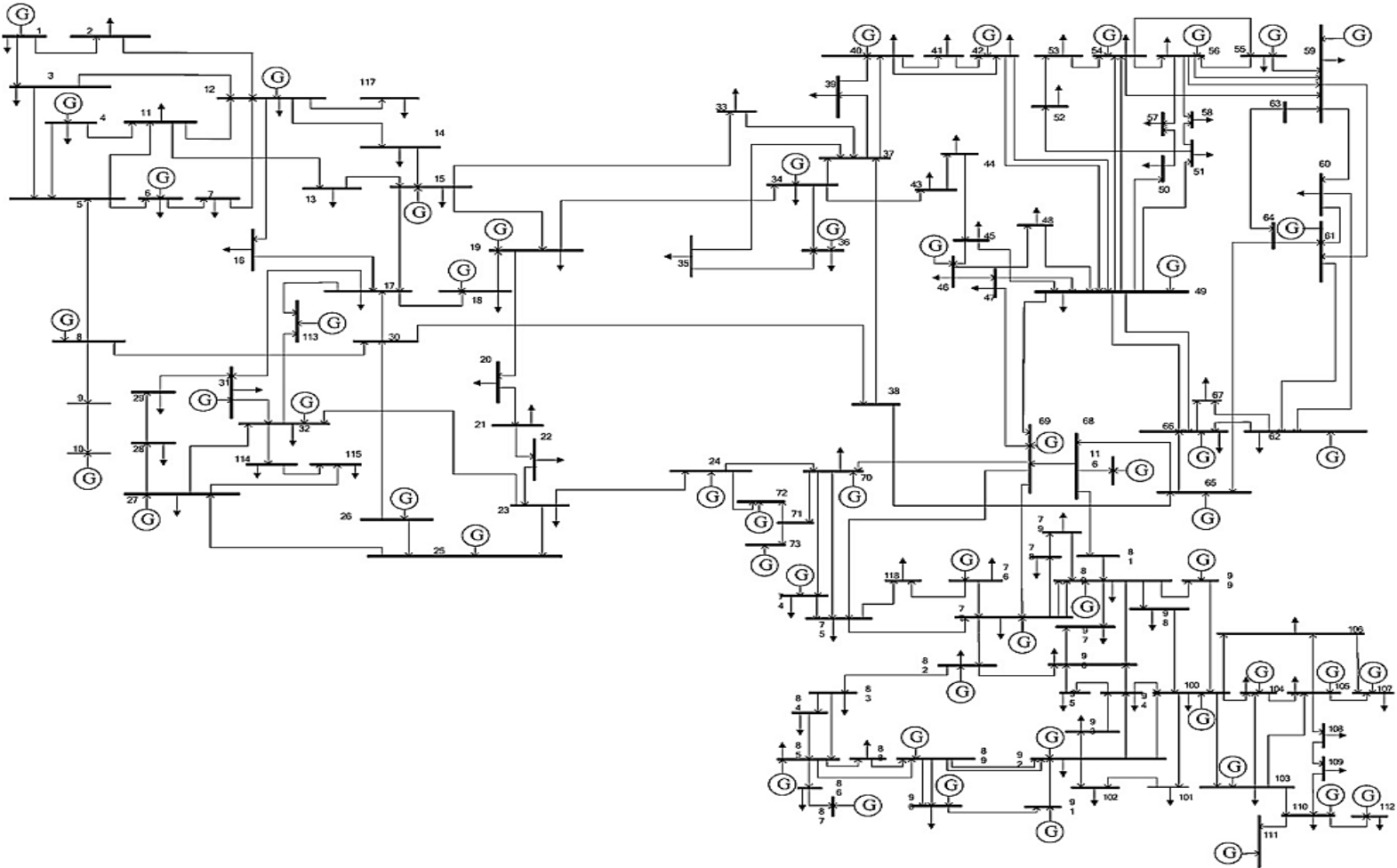
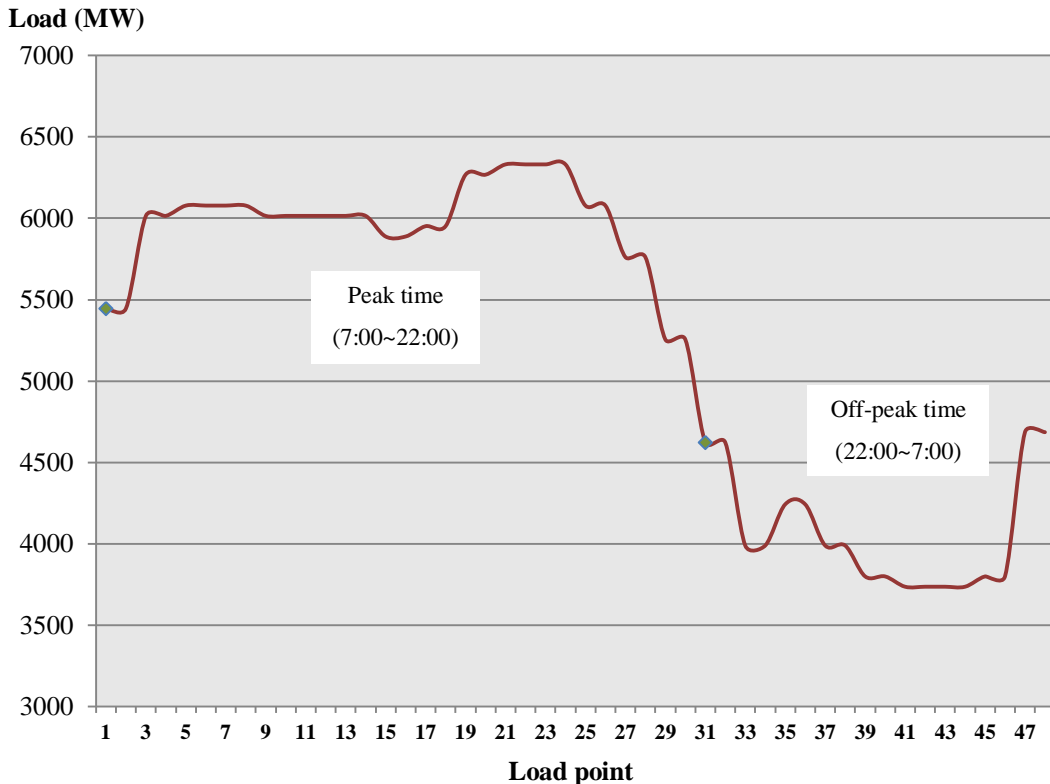


Figure 7.16: Diagram of Modified IEEE 118-Bus Test System for Short-term Operating [133]

In this section, the proposed WHC method will be applied in **MATPOWER** with an actual 24-hour daily load variation to evaluate the effect of the wind-hydro cooperation on the electric network.

*MATPOWER* is a package of Matlab M-files for solving power-flow and optimal power-flow problems. The IEEE 118-bus test case in this software includes bus data, generators' data and branch data, which means that it has sufficient information to run the power-flow simulation. The actual daily load curve is modified based on the hourly load model (introduced in Chapter 4) and the power-flow results of the modified IEEE 118-bus test case. The daily load curve is shown in *Figure 7.17*, and the data of this variation are summarized in *Table 7.14*. For the purpose of analysing the wind power output fluctuation, the time interval of this load model is set to 30 minutes. As discussed in *section 4.3*, the peak time is 7:00~22:00 and the off-peak time is 22:00~7:00 during a daily load profile.



*Figure 7.17: Daily Load Curve (24 hours, 48 load points)*

**Table 7.14: 24-Hour Load Data with 30 Minutes Time Interval**

Load No.	Time interval	Load (MW)
1	7:00~7:30	5445
2	7:30~8:00	5445
3	8:00~8:30	6014.8
4	8:30~9:00	6014.8
5	9:00~9:30	6078.1
6	9:30~10:00	6078.1
7	10:00~10:30	6078.1
8	10:30~11:00	6078.1
9	11:00~11:30	6014.8
10	11:30~12:00	6014.8
11	12:00~12:30	6014.8
12	12:30~13:00	6014.8
13	13:00~13:30	6014.8
14	13:30~14:00	6014.8
15	14:00~14:30	5888.1
16	14:30~15:00	5888.1
17	15:00~15:30	5951.5
18	15:30~16:00	5951.5
19	16:00~16:30	6268
20	16:30~17:00	6268
21	17:00~17:30	6331.3
22	17:30~18:00	6331.3
23	18:00~18:30	6331.3
24	18:30~19:00	6331.3
25	19:00~19:30	6078.1
26	19:30~20:00	6078.1
27	20:00~20:30	5761.5
28	20:30~21:00	5761.5
29	21:00~21:30	5255
30	21:30~22:00	5255
31	22:00~22:30	4621.9
32	22:30~23:00	4621.9
33	23:00~23:30	3988.7
34	23:30~0:00	3988.7
35	0:00~0:30	4242
36	0:30~1:00	4242
37	1:00~1:30	3988.7
38	1:30~2:00	3988.7
39	2:00~2:30	3798.8
40	2:30~3:00	3798.8
41	3:00~3:30	3735.5
42	3:30~4:00	3735.5
43	4:00~4:30	3735.5
44	4:30~5:00	3735.5
45	5:00~5:30	3798.8
46	5:30~6:00	3798.8
47	6:00~6:30	4685.2
48	6:30~7:00	4685.2

From *Figure 7.17* and *Table 7.14*, the periods of peak load happen between 17:00~19:00. The impact of the load variation on the electric network losses will also be investigated in this study.

Four wind penetration levels (10%, 15%, 20% and 25%) and associated optimal cooperation scenarios (CS) are applied in *MATPOWER* for analysing the effect of WHC method on the electric network, which are summarized in *Table 7.15*. In this section, the simulations are not optimal power-flows on the electric network. The

displacements on conventional generation and the wind power injection points are randomly selected in the modified IEEE 118-bus test case.

**Table 7.15: Optimal Cooperation Scenarios in Different Wind Penetrations**

Wind Penetration	Cooperation Scenario
10%	CS (0.6; 0.5)
15%	CS (0.7; 0.4)
20%	CS (0.8; 0.7)
25%	CS (0.8; 0.7)

## 7.5 Short-term Operational Planning: Effects on Electric Network Losses

The simulation of the power-flow on the modified IEEE 118-bus electric network is using the *MATPOWER* to obtain the results of electric network losses. The simulation results are discussed in three main aspects:

- Analysing the impacts of load variations and wind power fluctuations on network losses and discussing the effects of WHC on reducing the network losses. In this section, 10% wind penetration level will be used for instance.
- Analysing the impacts of different wind penetration levels on network losses and discussing the effects of the wind-hydro cooperation on reducing the network losses at these penetration levels.

- The wind power outputs are all from a single wind farm case in the previous sections. It is necessary to discuss the effects of the multiple wind farms scenario on reducing the network losses at these penetration levels.

### **7.5.1 Impacts of Load Variation and Wind Power Fluctuation on Network Losses & Effects of WHC on Reducing Network Losses**

In this section, the wind penetration is 10% and the wind power output is from a single wind farm. The data of the 24-hour (30 minutes interval) wind power output are modified based on the simulation results, which were obtained by using the Weibull distribution function and Monte Carlo Simulation method in Chapter 5. For the purpose of illustrating the impacts of wind power output fluctuation on the electric network losses, the data of the wind power output (10% wind penetration) are summarized as percentages (%) of the rated output in Appendix IX.

The power-flows on the modified IEEE 118-bus test system are simulated by *MATPOWER* in each time interval of the 24-hour period (48 intervals). The simulation results of the electric network losses in 10%, 15%, 20% and 25% wind penetrations are summarized in Appendix X for future cases. And the impacts of load variations and wind power output fluctuations on the electric network losses at 10% wind penetration level are shown in *Figure 7.18* and *Figure 7.19*, respectively.

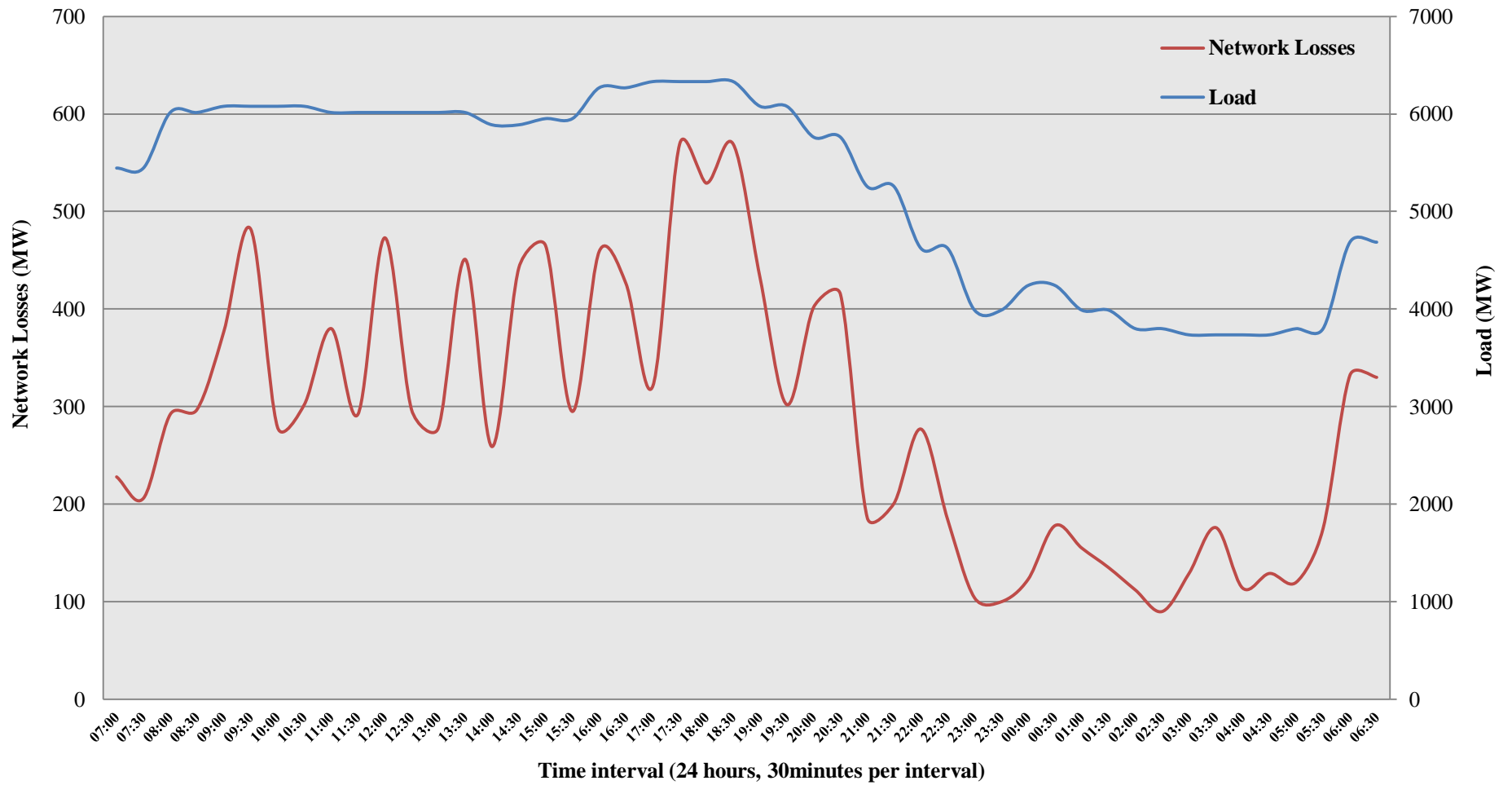
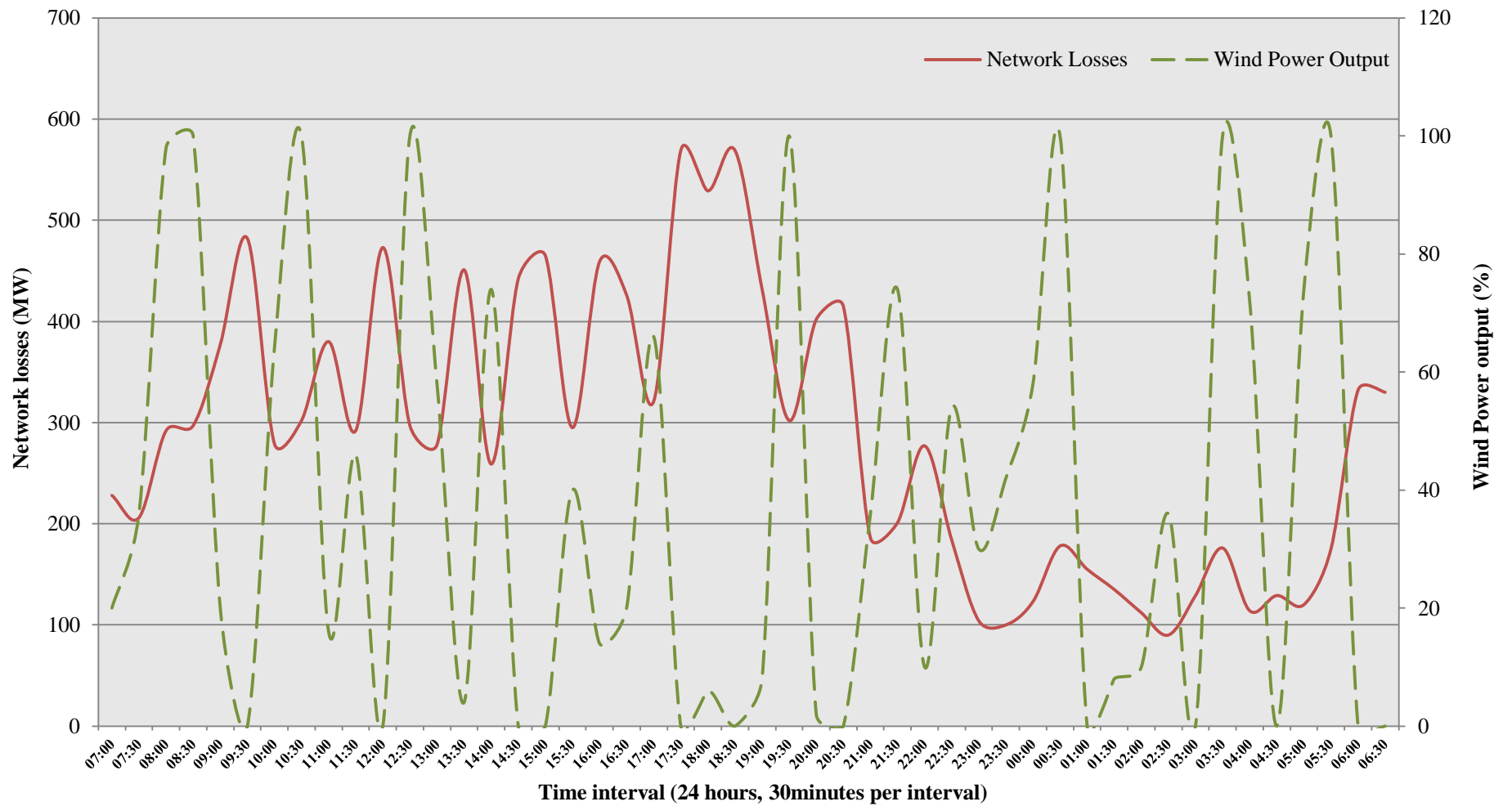


Figure 7.18: Impacts of Load Variations on Network Losses



**Figure 7.19: Impacts of Wind Power Output Fluctuations on Network Losses**

*Figure 7.18* shows that the variation trend of the network-loss curve is similar with the trend of the daily load curve. The electric network losses are increasing while the load demands are going up during the peak periods, and the losses are decreasing while the load demands are going down during the off-peak periods. Furthermore, in pace with the rising of load demands, the network losses will be significantly increased, which are shown in peak load periods 17:00~19:00.

Although the general trends of the network-loss curve and the daily load curve are similar, the network-loss curve keeps fluctuating in this case. So, *Figure 7.18* proves that the network-loss fluctuations are irrelevant with the load demand variations.

From *Figure 7.19*, it is clear that the fluctuations on the network losses are caused by the wind power output fluctuations. Also, the variation trend of the network-loss curve is contrary with the output curve of wind power. When the wind power output is high, it corresponds to a low level of network losses. And at a high level of network losses, it relates to a low wind power output scenario. From these two figures, the simulation results show that the network losses will be extremely large during periods of high load demands and low wind power outputs. In this case, the period is 17:30~19:00, which are peak load periods and the worst wind power output scenarios.

Now, it is necessary to investigate the effect of the WHC method on reducing the electric network losses. The optimal cooperation scenario CS (0.6; 0.5) is employed to analyse the effects on the electric network. As discussed in previous studies, the PHES units can change from generating units to loads. However, it may change the overall load profile of the reliability evaluation for long-term system planning. In this section, the pumping process will also be considered due to its influence on the electric network at short-term system operating. The effects of WHC method on reducing network losses at different wind penetrations are summarized in Appendix XI. The impacts of wind power on network losses and the effects of WHC method on reducing network losses in 10% wind penetration are shown in *Figures 7.20* and *7.21*.

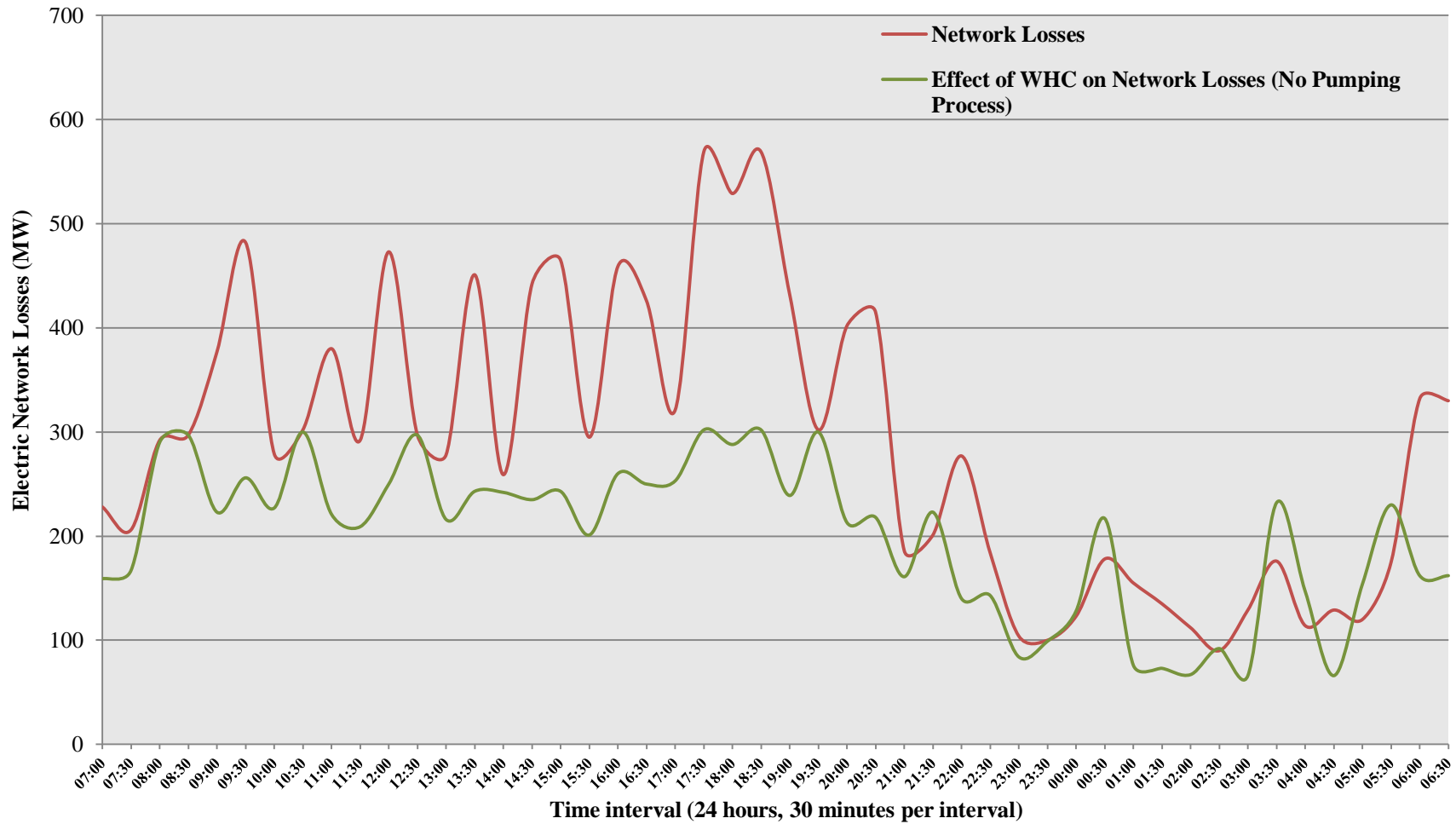


Figure 7.20: Effects of WHC on Reducing Electric Network Losses in 10% Wind Penetration (No Pumping Process)

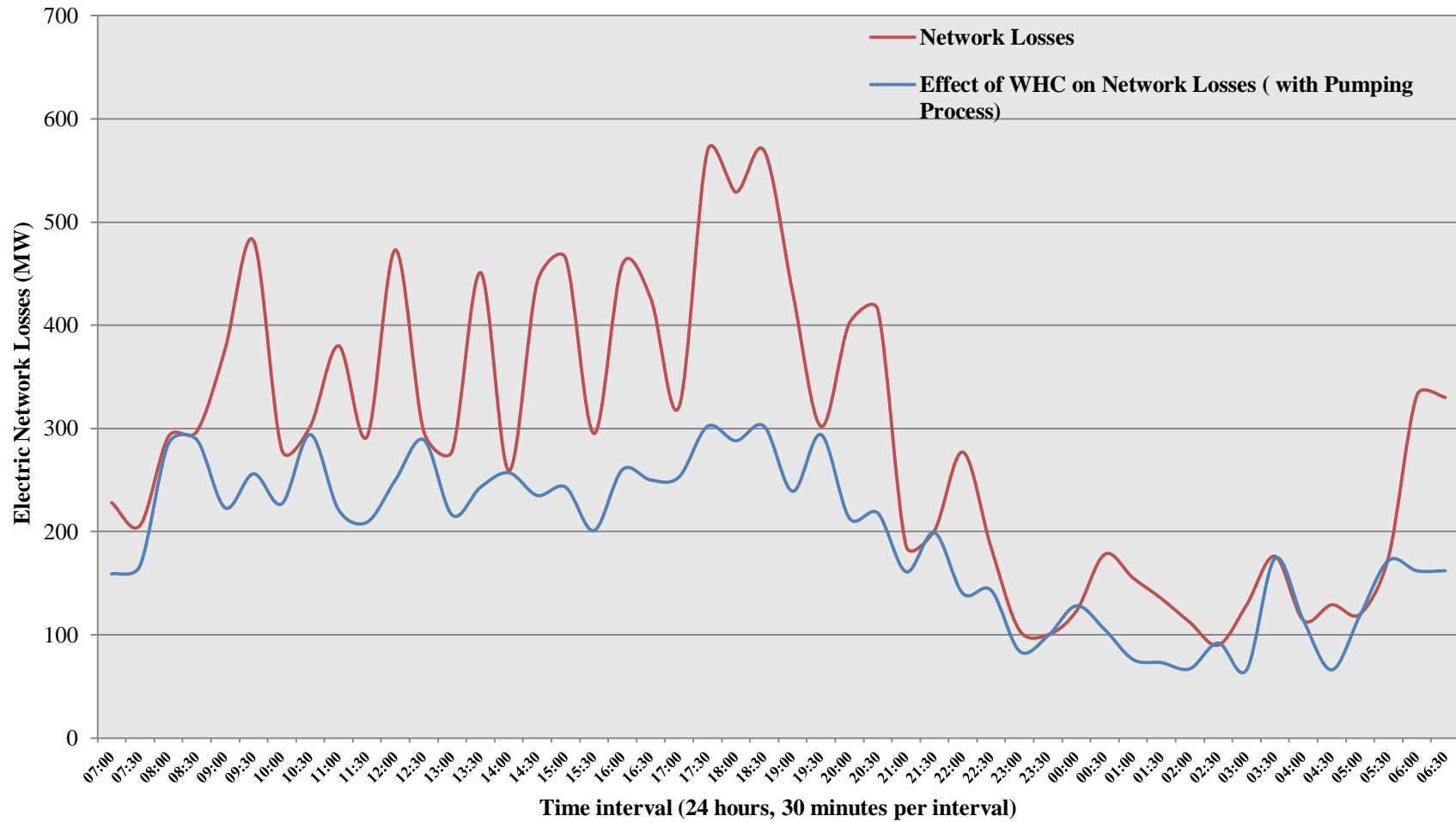


Figure 7.21: Effects of WHC on Reducing Electric Network Losses in 10% Wind Penetration (with Pumping Process)

*Figure 7.20* shows a significant improvement on reducing the electric network losses by using WHC method, the curve of the electric network losses is decreasing rapidly during the peak load periods. Comparing the results of network losses between these two scenarios, the maximum reduction on the electric network losses is 51.2% (18:00~18:30), which can be calculated by using the simulation results in Appendix XI.

However, there are several periods that the application of WHC may cause a slight increase in network losses, such as 0:00~1:00, 3:30~4:30 and 5:00~6:00; most of these situations are off-peak periods. The surplus electric energy on the electric network may cause this issue, which is generated by high wind power output during low load-demand periods. As discussed in previous sections, the pumping processes of the installed PHES units are not considered in this scenario. Theoretically, the slight increase on the electric network losses may be solved by considering the pumping process of WHC method on short-term operating phase.

For a better economic benefit, the pumping processes use the surplus electricity to pump water back to the upper reservoir. It could reduce the surplus electric energy generated by wind power. *Figure 7.21* proves that the pumping process of WHC method could reduce the network losses caused by surplus wind energy during the off-peak periods. In the latter cases, pumping processes will be considered for analysing the effect of WHC method on reducing the electric network losses.

Therefore, the simulation results in this section prove that the electric network losses can be reduced effectively and maintained at a lower and more stable level by using WHC method at 10% wind penetration level.

## 7.5.2 Impacts of Different Wind Power Penetration Levels on Network Losses & Effects of WHC on Reducing Network Losses

In the previous section, the impacts of wind power on network losses and the effects of WHC method on reducing network losses in 10% wind penetration have been discussed. The results showed that WHC method could reduce the electric network losses in 10% wind penetration. Now, the network losses on the electric network power-flows at 15%, 20% & 25% wind penetration levels are simulated in the same procedures, which have been used in *section 7.5.1*.

For the purpose of investigating the effects of WHC method on reducing the electric network losses, the optimal cooperation scenarios in these wind penetrations are applied in *MATPOWER*. As presented in *section 7.4*, the optimal cooperation scenarios are: CS (0.7; 0.4) in 15% wind penetration, CS (0.8; 0.7) in 20% wind penetration and CS (0.8; 0.7) in 25% wind penetration.

*Section 7.5.1* presented that the simulation results of the electric network losses in 10%, 15%, 20% and 25% wind penetrations were summarized in Appendix X, and the effects of WHC method on reducing network losses in these wind penetrations were presented in Appendix XI.

Therefore, *MAPOWER* is able to analyse the impacts of wind penetrations and the effects of WHC method by comparing these simulation results. The impacts of different wind penetrations on the electric network losses are shown in *Figure 7.22*. The effects of WHC method on reducing the network losses could be illustrated by *Figure 7.23*. In addition, the maximum value of the network losses at each wind penetration level will also be shown in *Figure 7.23* for analysing the effect of WHC method on the electric network power-flow.

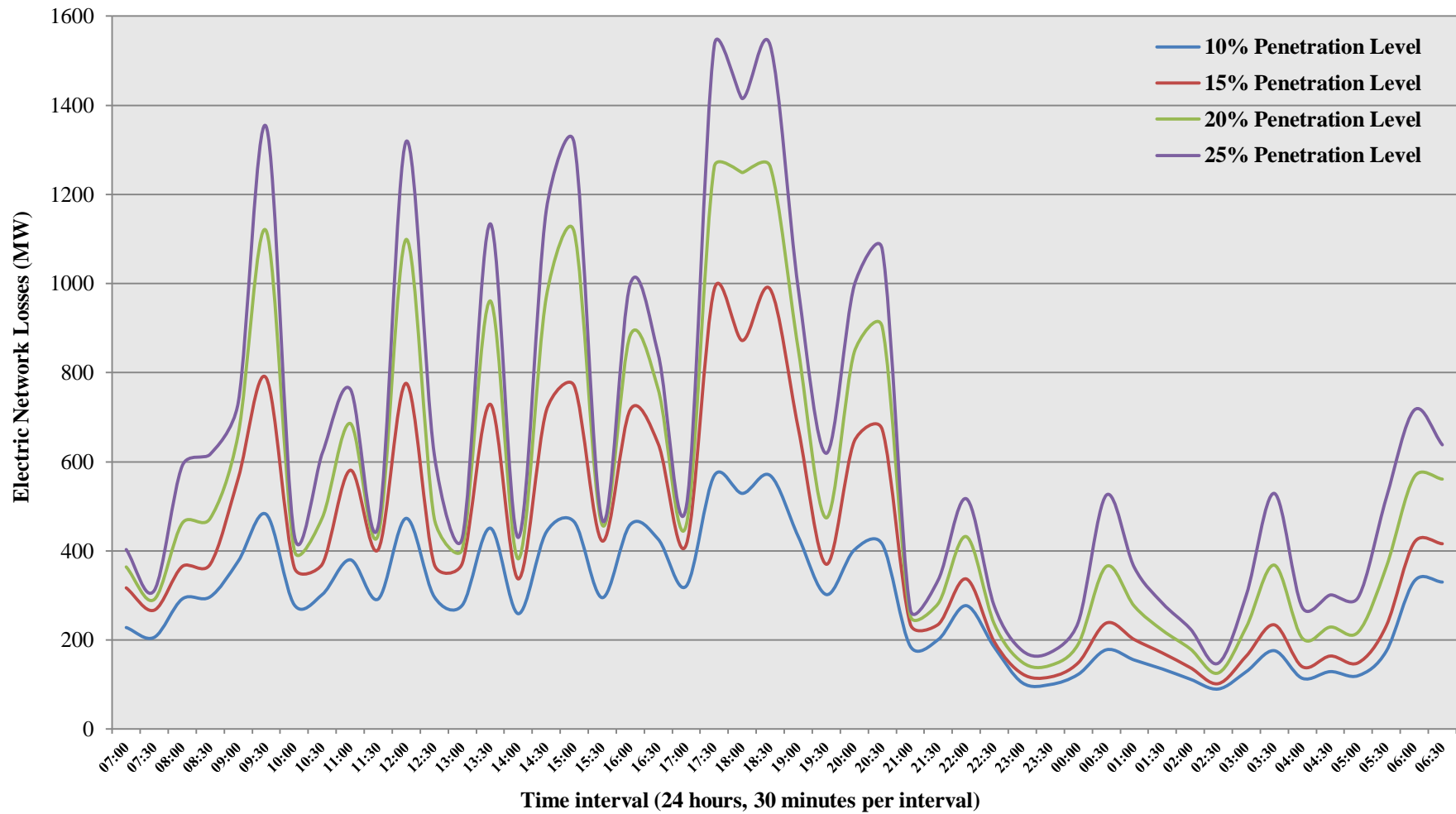


*Figure 7.22: Electric Network Losses at 4 Different Wind Penetration Levels*

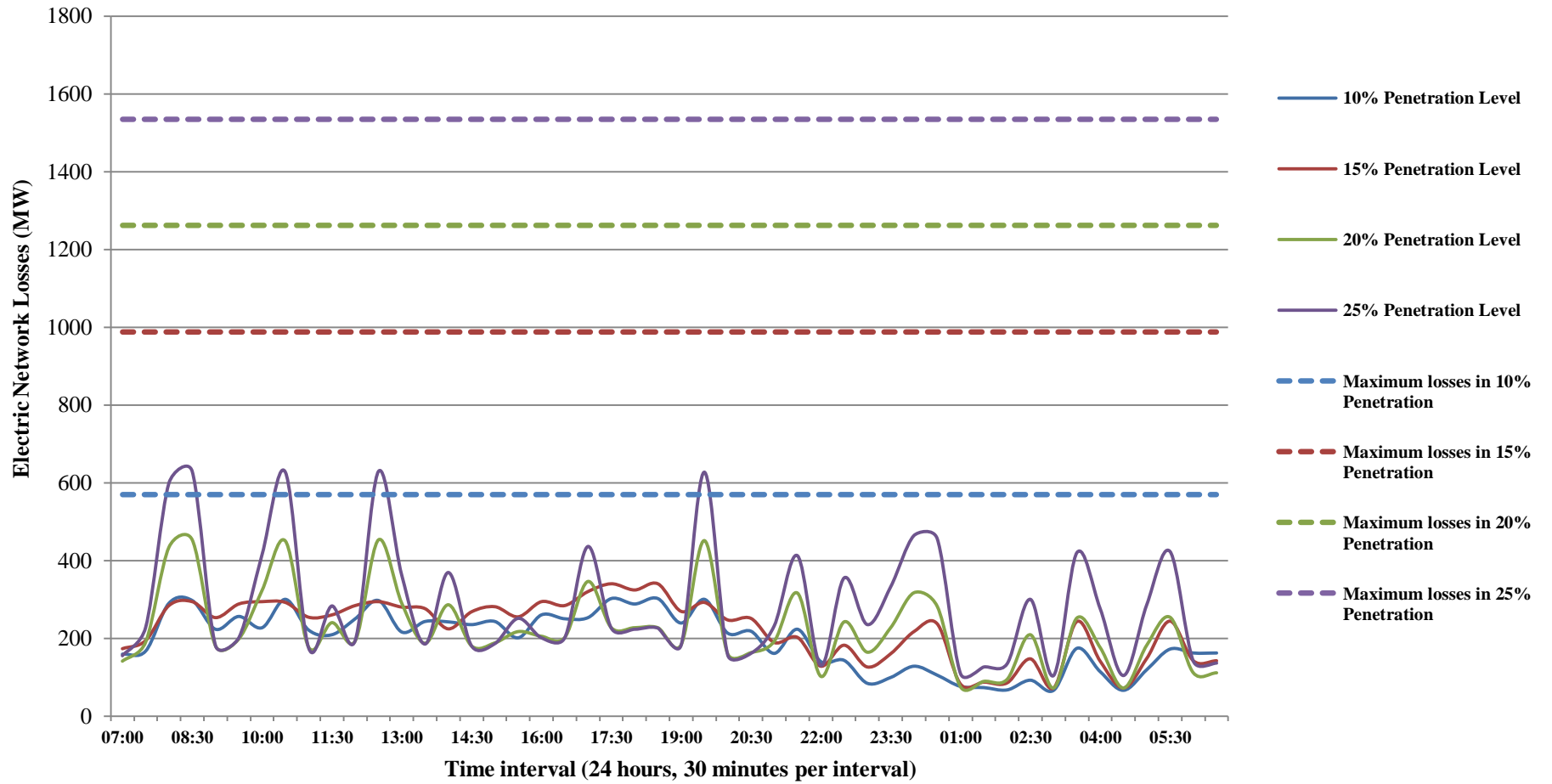


Figure 7.23: Effects of WHC on Reducing Electric Network Losses at 10%, 15%, 20%&25% Wind Penetration Levels

From *Figure 7.22*, the electric network losses on power-flows are increasing while the wind penetrations are increasing. The variation trends of the network losses are similar for these wind penetrations; however, the amount of the electric network losses will increase significantly when the wind penetration is high. Moreover, the amount of fluctuation on network losses during off-peak periods is also rapidly going up due to the increasing wind power outputs and low load demands.

At each wind penetration level, the comparisons between the curves of network losses with WHC and the maximum values of network losses without WHC prove that the proposed method could make a contribution on reducing the electric network losses at different wind penetration levels, which is shown in *Figure 7.23*. From the figure, it is clear that the effect of WHC method during the peak periods is more obvious than that during off-peak periods.

Furthermore, *Figure 7.23* shows that the curves of network losses with WHC in low wind penetrations (10% and 15%) are more stable than the curves with WHC in medium wind penetrations (20% and 25%). It indicates that the increasing wind penetration has significant impacts on the electric network losses due to the wind power intermittency.

As presented in *section 7.5.1*, the power-flows on the modified IEEE 118-bus test system are simulated by *MATPOWER* in each time interval of the 24-hour period (48 intervals). In this section, the improved performance of the wind-hydro cooperation on reducing electric network losses could be represented by the network-loss reduction, which is shown in *Table 7.16* by comparing the simulation results in each time interval from Appendix X and Appendix XI.

**Table 7.16: Performances of WHC on Network-Loss Reductions**

Wind penetration level	Improved performance on reduction	Maximum reduction (%)
10%	<b>43</b> time intervals reduced; <b>24</b> time intervals reduce over 40%	51%
15%	<b>41</b> time intervals reduced; <b>23</b> time intervals reduce over 40%	66%
20%	<b>42</b> time intervals reduced; <b>26</b> time intervals reduce over 40%	83%
25%	<b>36</b> time intervals reduced; <b>25</b> time intervals reduce over 40%	86%

From *Table 7.16*, the results show that the improved performance on the reduction of network losses is remarkable at each wind penetration level. WHC could significantly reduce the electric network losses even at high wind penetration levels during the peak periods. The reduction (%) is the ratio of reduced values of network losses with WHC method to the values of network losses without WHC in all time intervals. It can be seen that the degree of decreasing trend is going up while the wind penetration is increasing. However, the slight increases on electric network losses caused by high wind power outputs during off-peak periods still exist, and the trends are more obvious at higher wind penetration level.

Considering the current conditions in the Modified IEEE 118-Bus Test System and the assumptions of WHC method, Wind-Hydro Cooperation is an effective tool to reduce the electric energy transmission losses for power systems at short-term operating phase. However, the effects of WHC method on reducing the network losses depend on the locations of integrated wind farms and PHCES stations. The proposed method may not be effective to reduce the transmission network energy losses in different power systems with different generation-load distribution.

### 7.5.3 Impacts of Multiple Wind Farm Outputs on Electric Network Losses

In the previous reliability evaluations and power-flows on the electric network, the wind power generation was assumed to be generated by a single wind farm. It is used to highlight the effect of WHC method on the electric network under the poor circumstance, because the simulation results in *section 5.6* have proved that multiple wind farm outputs are more stable than the single wind farm output.

In this section, 5-wind farm case will be used to analyse the impacts of multiple wind farm outputs on the electric network losses at different wind penetration levels (10%, 15%, 20% and 25%). The power-flows on the modified IEEE 118-bus test system are simulated by *MATPOWER* in each time interval of the 24-hour period (48 intervals).

For the purpose of illustrating the impacts of 5-wind farm power output on the electric network losses, the data of the wind power output are shown as percentages (%) of the rated output and associated electric network losses are summarized in Appendix XII. *Figure 7.24* shows a comparison between the single wind farm case and 5-wind farm case at different wind penetration levels.

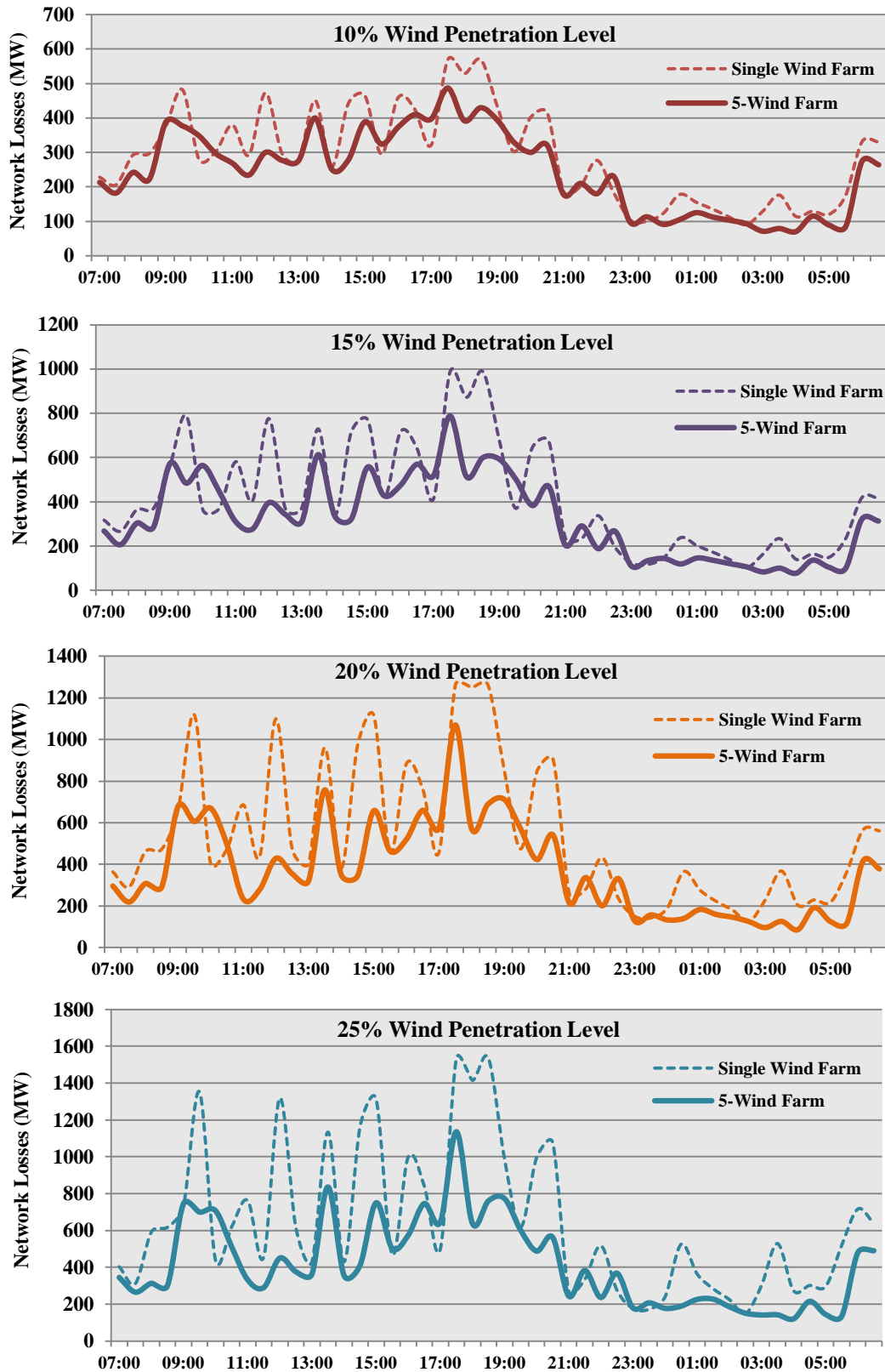


**Figure 7.24: Impacts of Single-Wind Farm Output and 5-Wind Farm Output on Electric Network Losses (10%, 15%, 20%&25% Wind Penetrations)**

Figure 7.24 shows that the network-loss curve of 5-wind farm case is smoother than that in single wind farm case, and the values of network losses are decreasing compared with those in single wind farm case. In this section, the improved performance of the wind-hydro cooperation on reducing electric network losses could also be represented by the network-loss reduction, which is shown in Table 7.17 by comparing the simulation results in each time interval from Appendix XII.

**Table 7.17: Performance of Multiple Wind Farm Output on Electric Network Losses Reductions**

Wind penetration level	Improved performance on reduction	Maximum reduction level
10%	<b>39</b> time intervals reduced; <b>4</b> time intervals reduce over 40%	55%
15%	<b>38</b> time intervals reduced; <b>12</b> time intervals reduce over 40%	58%
20%	<b>39</b> time intervals reduced; <b>17</b> time intervals reduce over 40%	66%
25%	<b>39</b> time intervals reduced; <b>20</b> time intervals reduce over 40%	74%

The reduction (%) is the ratio of reduced values of network losses with multiple wind farm case to the values of network losses with single wind farm case in all time intervals. For instance, the maximum reduction case in 25% wind penetration (05:30~06:00), the network losses decrease from 519 MW (single-wind farm case) to 134 MW (5-wind farm case), so the maximum reduction level =  $(519-134)/519 \times 100\% = 74\%$ . From the improved performances shown in Table 7.17, the effect of 5-wind farm case is more obvious at higher wind penetration levels.

Therefore, multiple wind farm outputs could effectively reduce the electric network losses and have better improved performances compared with the single wind farm output. Theoretically, WHC method with multiple wind farm outputs may amplify the effect on reducing the network losses. This hypothesis could be tested in future works, which relates to the research areas.

## 7.6 Summary

This chapter presented the modified IEEE 118-bus test system as a case study for testing the validity of WHC method in large power system. The modified test system has been extensively used over the electrical industry, which represented a portion of the Midwestern US Electric Power System. Also, six different wind penetrations (low, medium, high and extreme high levels) were employed to analyse the effect of WHC method on long-term planning and short-term operating of the modified IEEE 118-bus test system. Through application to a large set of case studies, the proposed WHC method was used to:

- Evaluate the impacts of wind power generation on the system reliability assessment at different wind penetration levels.
- Cooperate with wind power in each wind penetration case; analyse the effect of the wind-hydro cooperation on reducing the impacts of wind power output fluctuations and quantify the required Pump-Hydro Combined Energy Storage (PHCES) capacity.
- Evaluate the impacts of load variations and wind power output fluctuations on the electric network losses.
- Analyse the effects of the optimal cooperation scenarios (CS) on reducing the electric network losses at each wind penetration level.

This case study includes long-term system planning and short-term operation planning taking into accounts the different penetration levels of wind power. Firstly, the impact of wind power integration on reliability is significant with the increasing wind penetration. The generating system will become insecure and unmanageable when the wind penetration reaches an extreme high wind penetration.

The proposed WHC method was employed to reduce the impacts of wind power output fluctuations on the system power outputs and retrieve the reliability to an acceptable and reasonable level. The simulation results of the reliability evaluation of the modified IEEE 118-bus test system were represented by the cooperation scenario (CS). CS includes the information of the installed capacity of PHCES and the operational mode of PHCES in the reliability evaluation of the modified IEEE 118-bus test system, which was expressed as CS (CF; DR). The results also showed that DR could contribute to the economic benefits of the test system by reducing the unserved energy costs. Finally, the optimal CS for the required reliability level was decided by using the CBA approach to minimize the total costs.

The studies have also highlighted the effects of WHC method on reducing the electric network losses at different wind penetration levels. In the short-term operational planning, the results proved that the optimal CSs could significantly reduce the electric network losses with the increasing wind penetration, especially during the peak periods. The pumping process has also been considered to cooperate with the low load demands during the off-peak periods to absorb the surplus electrical energy. Furthermore, the results also showed that the multiple wind farm case could have better performances on reducing the electric network losses compared with the single wind farm case.

Therefore, this chapter has proved that the proposed method could effectively mitigate the impacts of wind power output fluctuations on reliability and efficiently reduce the electric energy transmission/distribution losses caused by the wind power integration.

The modified IEEE 118-bus test system is a large power system for educational purposes, although the data of the entire system is relatively complete. Hence, it is necessary to apply the proposed method to practical power systems. This issue is addressed in the next chapter.

# Chapter 8. Reliability Evaluation of Eastern Gansu Power Grid

## 8.1 Introduction

Chapter 6 presented the modified Roy Billinton Test System as a simple illustrative example to analyse the Wind-Hydro Cooperation at two different wind penetration levels. Chapter 7 explained the Wind-Hydro Cooperation (WHC) method by using the modified IEEE 118-bus test system as a larger power system. The results in these case studies proved that the WHC method could effectively mitigate the impacts of wind power output fluctuations on power systems reliability and reduce the effects of wind power integration on the electric network power flows. Consequently, it is necessary to apply the WHC method to a practical power system in this chapter.

As discussed in Chapter 3, the reliability standard in this thesis was assumed, based on the standard of a Chinese power system. Therefore, this chapter presents the eastern Gansu power grid (in the northwest of China) as a case study to investigate the effect of WHC method on the practical power system reliability.

Gansu is one of the provinces with abundant wind resources in China. In the province, wind energy resources increase from southeast to northwest. So, the province could divide into two regions in this case study: eastern and western Gansu. Areas with high potential are mainly throughout the western Gansu. However, most of the large scale wind farms in this area are not connected to the grid due to the weak economic environment and the limited transmission capacity. On the other hand, eastern Gansu is the load centre of the province, and the hydro resources in the area are also abundant. Recently, several high voltage transmission lines are under

construction, which are encouraged by the fast-growing local economy and the large-scale government financial investment.

Hence, the eastern Gansu power grid (EGPG) is appropriate for the application of WHC method. It is the load centre with huge potential of hydro power resources, and the wind penetration level is going up due to the increasing transmission capacity. The aim of this chapter is to analyse the impacts of wind power on EGPG and use the WHC method to reduce the effects of wind power output fluctuations and retrieve the reliability to the original level of EGPG.

This chapter is arranged as follows: *section 8.2* introduces the details of eastern Gansu power grid (EGPG) with an emphasis on the developments of wind energy and Pump-Hydro Energy Storage (PHES) system. The generating system, load model and the composition of the electricity market in EGPG are presented in *section 8.3*. The target for future wind penetration in EGPG is described in *section 8.4*. *Section 8.5* discusses the effects of the Wind-Hydro Cooperation (WHC) method on EGPG reliability with the increased wind penetration.

## **8.2 Description of Eastern Gansu Power Grid (EGPG)**

The northwest district of China is relatively less developed compared with other regions, whereas it is rich in wind energy resources. The location of Gansu province is shown in *Figure 8.1* for a better understanding of the electric network distribution [134]. Gansu is one of the provinces with abundant wind resources in China. According to a related report by the Gansu Meteorological Bureau, it has a theoretically overall wind reserve of 237,000 MW, which accounts for 7.3% of the nation's total [135]. In addition, there is a technically exploitable of 40,000 MW, which ranks 6<sup>th</sup> in China. As presented in the previous section, the province will be

divided into: eastern and western regions in this chapter. *Figure 8.2* shows the map of city distribution in Gansu province, and the black curve is shown as the border for the eastern and western regions [136].



*Figure 8.1: Location of Gansu Province in China [134]*



*Figure 8.2: City Distribution in Gansu Province [136]*

### **Eastern Gansu Power Grid (EGPG):**

From *Figure 8.2*, it is clear that most of the cities are distributed in the eastern Gansu, including the capital city of Gansu province (Lanzhou). Also, the eastern region is the main site for both population and industry. So, the load demands in Gansu power system are mainly distributed in this area.

Furthermore, the water resource in Gansu province is unevenly distributed. It has a theoretical overall hydro power reserve of 18,130 MW, and a technically exploitable 12,000 MW of hydropower [137]. Most of the exploitable hydro power resources are distributed in the eastern region, including the Yellow River, Inland River and Taohe River. In China's 12<sup>th</sup> Five-Year Plan (2011-2015), over 60 major hydro power stations will commence in China, which will include some constructions in Gansu province [138]. Now, there are 35 medium and large-scale hydro power stations (the installed capacity is more than 25 MW) in Gansu, who shoulder the responsibility for peak shaving, frequency adjustment and emergency standby [139].

The first pure pump-hydro energy storage (PPHES) station in Gansu has been approved for construction with a total installed capacity of 1200 MW in November 2013 [140]. The location this PPHES station is in Zhangye, which is the city near the border between eastern and western regions. The construction period of this station is 4.5 years, which means that the station will start to work in May 2017. The developments of hydro power and pump-hydro storage system are falling behind the wind energy development in the eastern Gansu province.

It is an urge to reduce the effects of wind power output fluctuations on power outputs and Eastern Gansu Power Grid (EGPG) reliability. In this chapter, it is possible to apply the WHC method to reduce the effects by upgrading the hydro power plant to Pump-Hydro Combined Energy Storage (PHCES) station.

As presented in *section 6.2.1*, there was a significant potential in increasing PHES capacity simply by upgrading and renovating many existing conventional hydro power stations. In eastern Gansu, Liujiaxia hydroelectric station is on the upper Yellow River in Linxia, which is close to Lanzhou (shown in *Figure 8.2*). This station has been operated for 40 years with a total installed capacity of 1225 MW [141], which is suitable for upgrading to a large PHCES station. And the increasing wind penetration from the western region will be described in the following section.

### **Wind Power Generation in Western Gansu:**

In the western region, Jiuquan district serves as the most high-value centre of wind resources and its exploitable quantity accounts for more than 85% of Gansu province [139]. In 2009, NEA (National Energy Administration) issued “New Energy Resource Industrial Revitalization Plan” to build eight huge wind power bases of 10 GW scale [46]. Jiuquan wind power base is one of them.

According to China’s 11<sup>th</sup> Five- Year (2005- 2010) Plan, the installed wind power capacity in Jiuquan has been to 5160 MW (completed in Oct. 2010). In the 12<sup>th</sup> Five-Year Plan (2011- 2015), 7550 MW new added wind power capacity will be completed [46]. This ambitious development of wind power in Jiuquan left potential problems for the integration and operation of wind farms and power grid. As local power demands and transmission capacity in Jiuquan are limited, a large percentage of wind power output from Jiuquan wind power base have to be abandoned [142]. In Oct. 2010, the Xinjiang-to-Northwest 750 kV transmission network was put into operation. This line eased the issue of limited transmission capacity; however, it can only transmit 30% of Jiuquan’s wind power [46]. The transmission system of western Gansu region is shown in *Figure 8.3*.



**Figure 8.3: Transmission Network of Western Gansu in 2010 [143]**

From *Figure 8.3*, Jiuquan wind power base is far away from the load centre and connects to main Gansu grid through 566 km Jiuquan- Jinchang- Yongdeng double circuit 750 kV transmission lines. Furthermore, several high voltage transmission lines will be operated soon, which will be responsible for the delivery of wind power to Eastern Gansu Power Grid (EGPG). And the wind penetration in EGPG will increase significantly due to the increasing wind power integration from Jiuquan wind power base.

The objective of this chapter is to use WHC method reduce the effects of wind power fluctuations on power outputs and retrieve the reliability to the original level with increased wind penetration. It is assumed that the Pump-Hydro Combined Energy Storage (PHCES) station in this chapter is upgraded from Liujiaxia hydroelectric station, so the maximum limit of the installed PHCES capacity is 1225 MW (Installed Capacity of Liujiaxia hydroelectric station).

Without reliable and up-to-date information of EGPG, the data of generation capacity, wind power capacity, wind penetration and load demand are modified

based on the “China Renewable Energy Electricity Production Analysis Report” issued by State Grid Energy Research Institute in 2012 [121]. For the purpose of analysing the development of wind energy in EGPG, the period of May 2009 to May 2013 will be investigated. The wind penetration was increasing significantly during this 4-year period due to increasing wind power integration and transmission capacity. According to the report in [121], the wind penetration was increased from 8% to 20%. The details of EGPG reliability evaluation will be presented in the following sections.

## **8.3 Eastern Gansu Power Grid (EGPG) Reliability Evaluation: 8% Wind Penetration**

As presented in previous chapters, the reliability of the power system was evaluated by using the combined method of Frequency & Duration (F&D) method and Monte Carlo Simulation (MCS) method. For the purpose of evaluating wind power generation, Weibull distribution and MCS method were employed to simulate the power output from a wind farm. The load demands were modified based on the same load model with different values of annual peak load. In this section, the reliability evaluation of EGPG follows the same simulation procedure to analyse the impacts of wind power fluctuation on the reliability in 8% wind penetration. The simulation results of the reliability evaluation are also represented by three reliability indices: LOLE (loss of load expectation, in hours/year), LOEE (loss of energy expectation, in MWh/year) and LOLF (loss of load frequency, in occurrence /year).

According to the report in [121], the data of EGPG is summarized in *Table 8.1*. For the purpose of reducing the simulation time and simplifying the calculation process, only three types of generation are considered in EGPG: thermal, hydro and wind

power generation. And the generation capacity-dispatch of the grid is shown in *Figure 8.4*.

**Table 8.1: Basic System Data of EGPG in May 2009 [121]**

Thermal generation capacity	3750 MW
Hydro generation capacity	850 MW
Wind power capacity	400 MW
Total capacity	5000 MW
Peak load	3450 MW
Wind penetration level	8%

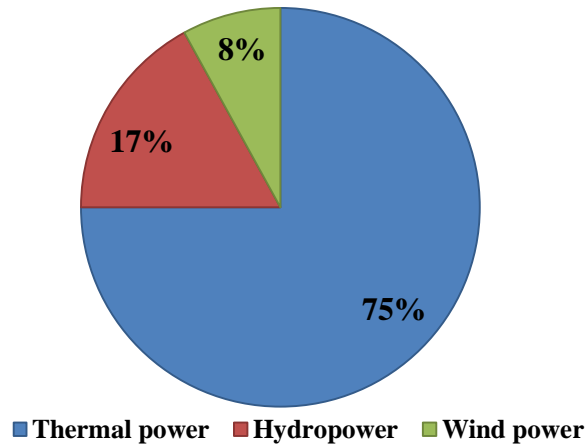


**Figure 8.4: Grid-dispatching Installed Capacity Ratio of Different Energy Sources in May 2009**

*Figure 8.4* shows that the thermal power generation dominates the generating system of EGPG. Without access to the reliable data from the industry, the generating system data and load demand model are modified based on the data in IEEE Reliability Test System [104]. The conventional generating units' output and additional reliability data are shown in *Table 8.2*. For the purpose of illustrating the impacts of wind power fluctuation on reliability, the conventional units are represented by two-state model: “up” or “down”, as described in Chapter 2.

**Table 8.2: Conventional Generating Unit Reliability Data**

Unit size (MW)	Type	No. of units	FOR	MTTF (hours)	MTTR (hours)	Failure rate per year
50	Thermal	3	0.01	1980	20	4.4
125	Hydro	2	0.04	1200	50	7.3
300	Thermal	2	0.02	2190	45	4.0
300	Hydro	2	0.01	4380	45	2.0
500	Thermal	2	0.05	950	50	9.2
1000	Thermal	1	0.12	1100	150	7.9
1000	Thermal	1	0.08	1150	100	7.6

As presented in Chapter 4, the output of a conventional generator can be simulated by combining its failure rate ( $\lambda$ ) and Mean Time to Repair (MTTR) into Monte Carlo Simulation (MCS). Then, the total conventional generation output can be calculated by combining the outputs of all the generators in EGPG. And the load demand is simulated by using the value of annual peak load and the load variation model (presented in *section 4.3*). Wind turbine output is simulated by using Weibull distribution and MCS, and the wind farm output is calculated by combining all wind turbine outputs in the farm. The parameters of Weibull distribution and wind turbine are the same as presented in Chapters 6 and 7.

For the purpose of illustrating the conventional generation output and simplifying the simulation procedure, *Figure 8.5* presents the superimposition of chronological total conventional generation capacity (without wind power generation) and system load of EGPG.

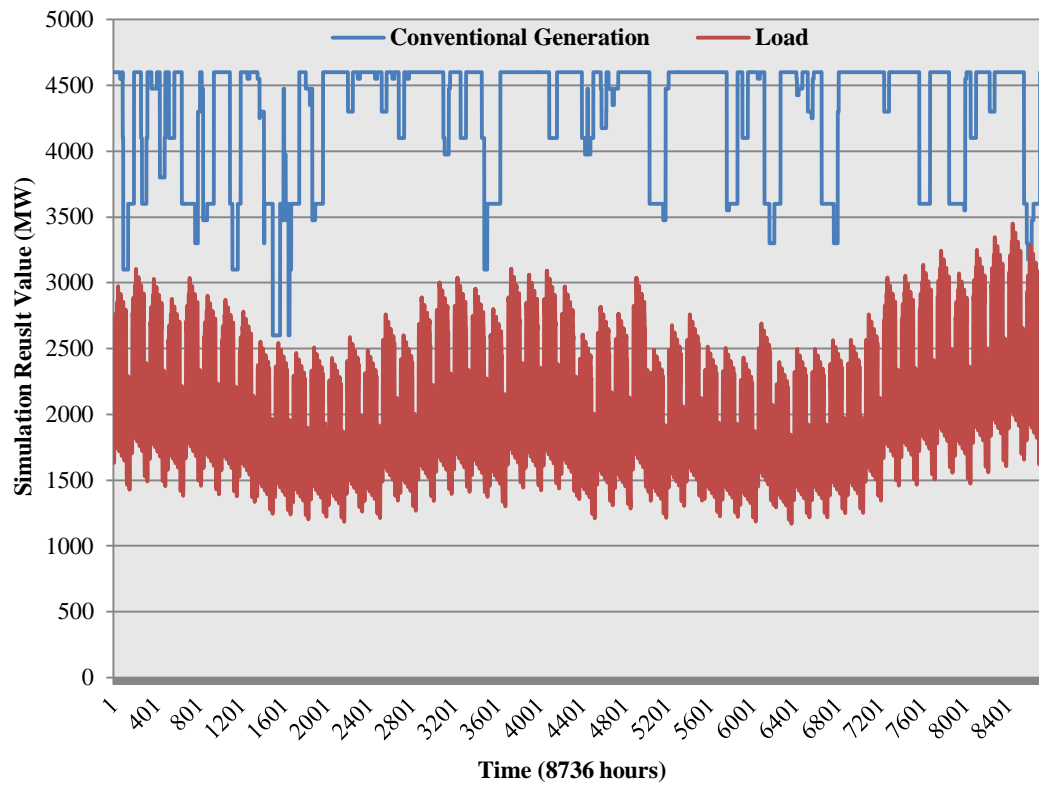


**Figure 8.5: Superimposition of Conventional Generation & Load in EGPG**

The conventional generation output curve is smooth without output fluctuations, which is shown in *Figure 8.5*. Then, it is expected that the total generation output curve has the output fluctuations due to wind power integration. *Figure 8.6* presents the superimposition of chronological total generation capacity (with wind power generation) and system load of EGPG.

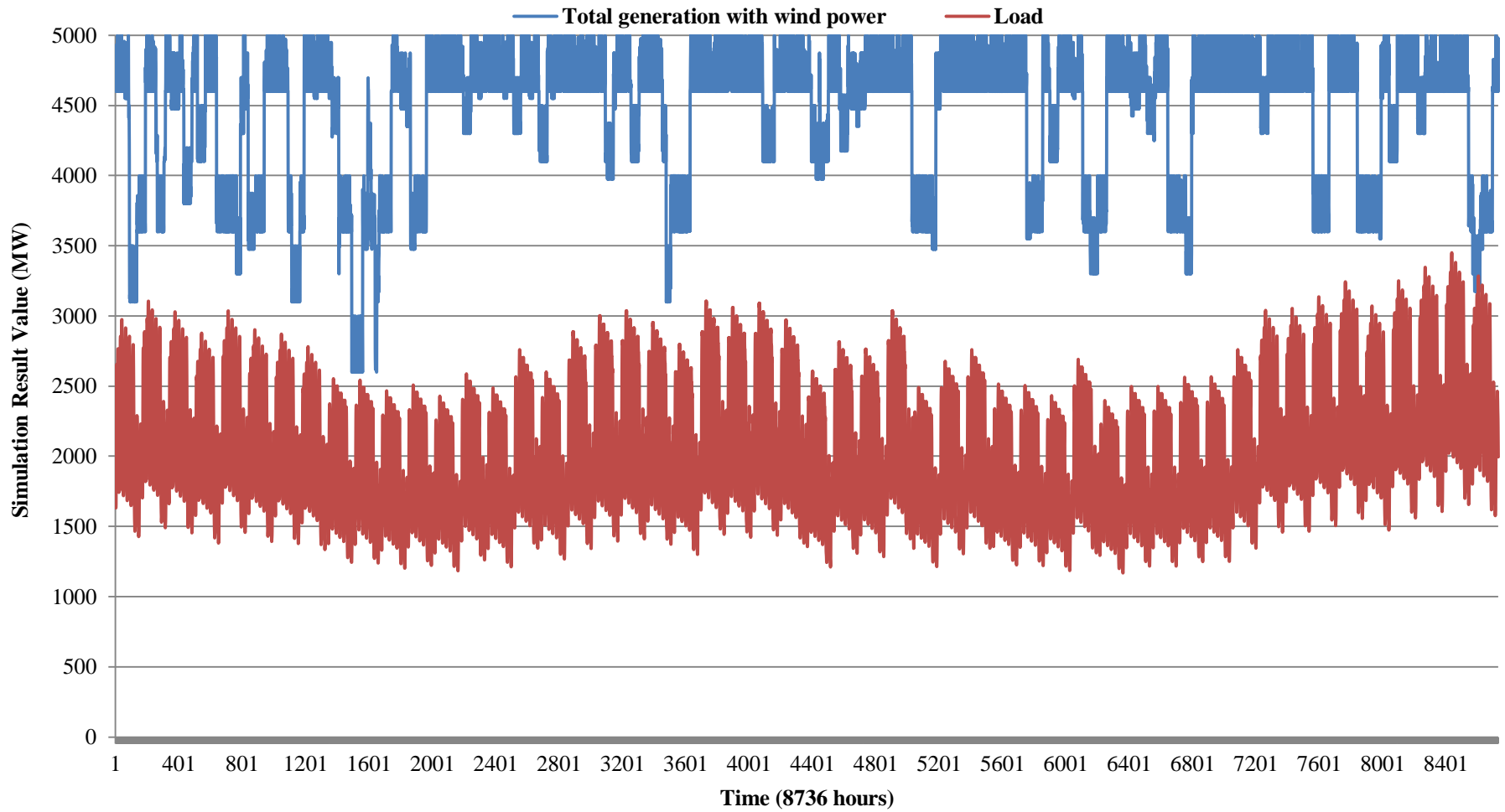


*Figure 8.6: Superimposition of Total Generation & Load in EPG (8% Wind Penetration)*

From *Figure 8.6*, it can be seen that the total generation output curve is fluctuating due to the intermittency of wind power output. An outage will occur when the load demand exceeds the total available generation output. As presented in previous chapters, the reliability evaluations were simulated by using Matlab and the simulation results were represented by LOLE, LOEE and LOLF. These reliability indices demonstrate different aspects of the outage. In this section, the simulation results are calculated by using the combined reliability analysis method of F&D and MCS in Matlab, and the calculation process has been simulated for a sufficiently long period (details were discussed in *section 3.3.1*). The results are presented as follows:

- The loss of load expectation (LOLE) is 21.3 hours/year, which means that the **total period** of load exceeds the generation output. It is the reliability standard in this thesis, which has been discussed in the previous chapters.
- The loss of energy expectation (LOEE) is 5474 MWh/year, which represents the unserved electric energy during the **total period**.
- The loss of load frequency (LOLF) is 6.0 occ. /year, which represents the frequency of the loss of load scenario in the simulation.

Therefore, the reliability evaluation of EGPG is simulated by using the combined reliability analysis method and Monte Carlo Simulation method. The reliability indices are summarized in *Table 8.3*.

**Table 8.3: Reliability Indices of EGPG in 8% Wind Penetration (May 2009)**

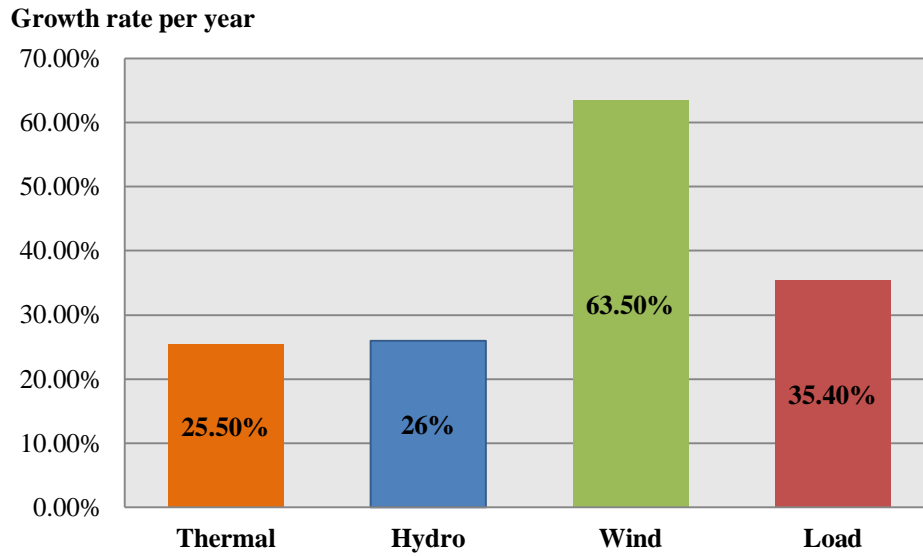
Wind Penetration	LOLE (hours/year)	LOEE (MWh/year)	LOLF (occ./year)
8%	21.3	5474	6.0

From *Table 8.3*, the value of LOLE was 21.3 hours/year in eastern Gansu power grid at the end of May 2009. As presented in *section 3.5*, the reliability standard of China is 1~2 days (LOLE is 24~48 hours). The previous chapters proved that the increasing wind penetration could harm the system reliability and make the value of LOLE goes up significantly. The value of LOLE in this section is lower than the maximum limit of LOLE. So, it is acceptable for EGPG in 8% wind penetration.

In this chapter, the value of LOLE at 8% wind penetration level will be used as the original reliability level for future Wind-Hydro Cooperation planning in the latter case. It means that the target of the WHC method is to “pull back” the value of LOLE at the increased wind penetration scenario (20%) to the predetermined value of LOLE in this section.

## **8.4 Eastern Gansu Power Grid (EGPG) Reliability Evaluation: 20% Wind Penetration**

As presented in *section 8.2*, the wind penetration has been increased to 20% (May 2013) in eastern Gansu power grid (EGPG). It was encouraged by the fast-growing economy and the large-scale government financial investment. Without access to the up-to-date information for the power company, the developments of load demand and generating system are modified based on the “Internal Energy and Electricity Price Analysis Report” by State Grid Energy Research Institute [121, 144]. In this section, the growth rates per year for generating system and load demand are assumed to be the same during the 4-Year period (May 2009 to May 2013). The growth rates of generating system and load demand are summarized in *Figure 8.7*.



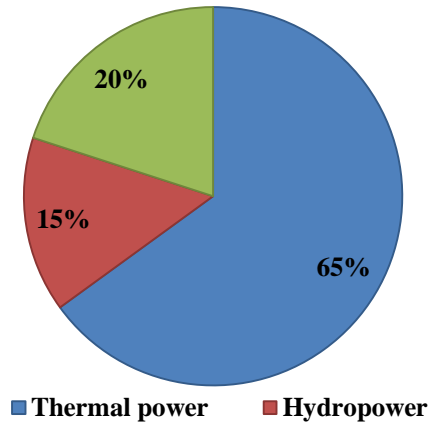
**Figure 8.7: Growth Rates per year of Generating System & Load (May 2009 to May 2013)**

Figure 8.7 shows that the growth rates of wind power generation and load demand are higher than the others. It proves that the “New Energy Resource Industrial Revitalization Plan” (introduced in section 8.2) encouraged the developments of wind energy in Western Gansu and the local economy in eastern Gansu. The increments on generating system capacity and load demand will be calculated based on the data shown in Figure 8.7. The estimated data of generating system capacity and load demand in EGPG are summarized in Table 8.4. The estimated data in Table 8.4 is used as the basis for the reliability analysis in this section.

**Table 8.4: Increments on Generation Capacity & Load**

Type	Capacity (MW) May 2009	Increment (MW)	Capacity (MW) May 2013
Thermal	3750	5550	9300
Hydro	850	1290	2140
Wind	400	2460	2860
Load	3450	8150	11600

At the end of May 2013, the total installed generation capacity is 14,300 MW and the peak load is 11,600 MW. *Figure 8.8* presents that the wind penetration of EGPG is 20% in May 2013.



***Figure 8.8: Grid-dispatching Installed Capacity Ratio of Different Energy Sources in May 2013***

Without access to the reliable data from the industry, the generating system data and load demand model are modified based on the data in *section 8.3* accordingly. The output of a conventional generator can be simulated by combining its failure rate ( $\lambda$ ) and Mean Time to Repair (MTTR) into Monte Carlo Simulation (MCS). Then, the total conventional generation output can be calculated by combining the outputs of all the generators in EGPG. And the load demand is simulated by using the value of annual peak load (May 2013) and the load variation model (presented in *section 4.3*). Wind turbine output is simulated by using Weibull distribution and MCS, and the wind farm output is calculated by combining all wind turbine outputs in the farm. The parameters of Weibull distribution and wind turbine are the same as presented in Chapters 6 and 7.

For the purpose of illustrating the total generation output and load demand, *Figure 8.9* presents the superimposition of chronological total generation output (with wind power generation) and system load of EGPG in 20% wind penetration.

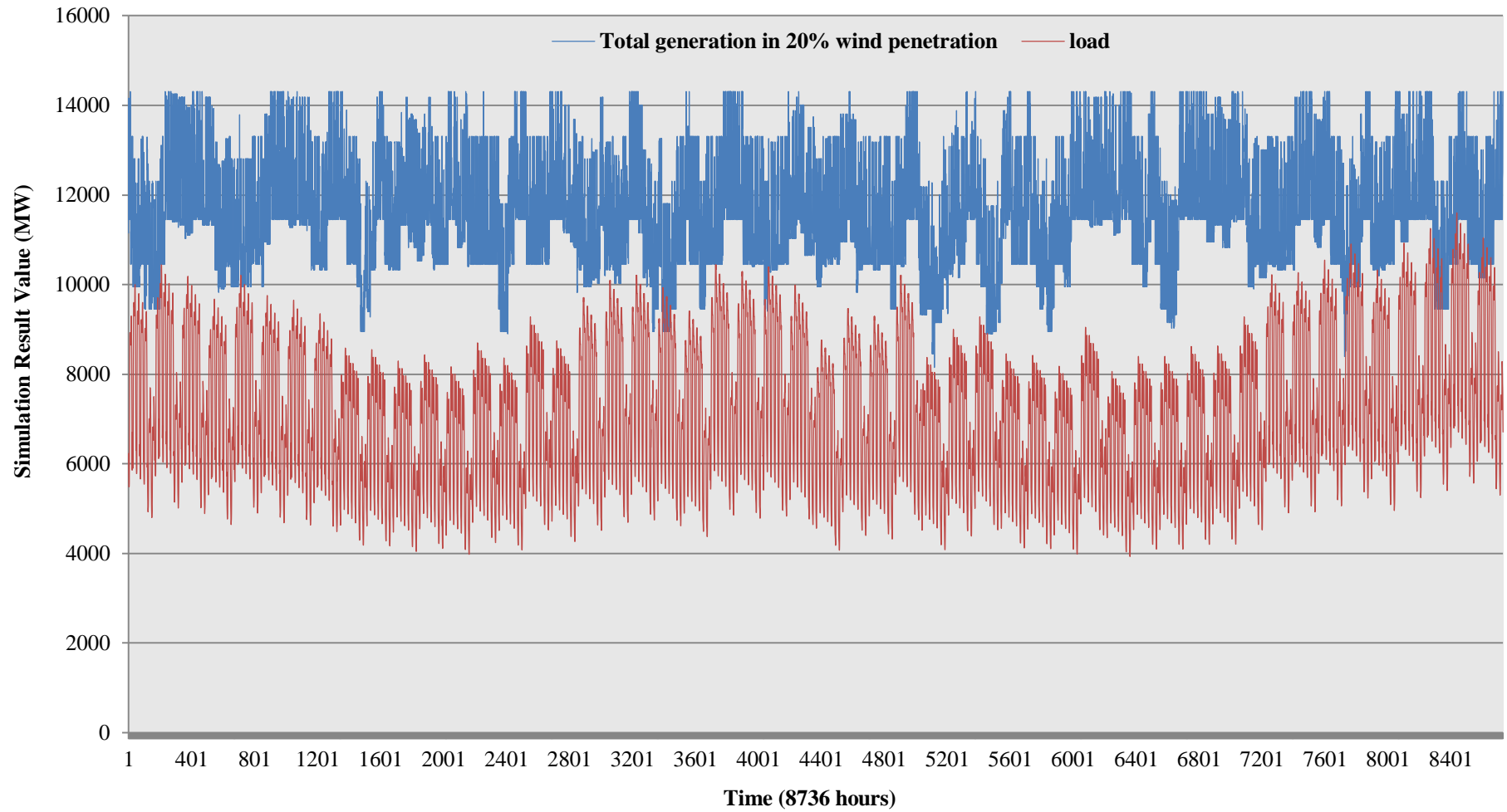


*Figure 8.9: Superimposition of Total Generation & Load in EGPG (20% Wind Penetration)*

From *Figure 8.9*, it is clear that the total generation output curve has a higher fluctuation in 20% wind penetration than that in 8% wind power penetration. The increasing wind penetration harms the EGPG reliability, which is illustrated by the increasing occurrences of load exceeds the total generation output compared with that in 8% wind penetration case.

An outage will occur when the load demand exceeds the total available generation output. As presented in previous chapters, the reliability evaluations were simulated by using Matlab and the simulation results were represented by LOLE, LOEE and LOLF. In this section, the simulation results are calculated by using the combined reliability analysis method of F&D and MCS in Matlab, and the calculation process has been simulated for a sufficiently long period (details were discussed in *section 3.3.1*). The results are presented as follows:

- The loss of load expectation (LOLE) is 124.6 hours/year, which means that the **total period** of load exceeds the generation output.
- The loss of energy expectation (LOEE) is 74390 MWh/year, which represents the unserved electric energy during the **total period**.
- The loss of load frequency (LOLF) is 61.8 occ. /year, which represents the frequency of the loss of load scenario in the simulation.

Therefore, the simulation results of EGPG reliability evaluation in 20% wind penetration are summarized in *Table 8.5*. And the comparison of the value of LOLE between 8% and 20% wind penetration is shown in *Figure 8.10*.

**Table 8.5: Reliability Indices of EGPG in 20% Wind Penetration (May 2013)**

Wind Penetration	LOLE (hours/year)	LOEE (MWh/year)	LOLF (occ./year)
20%	124.6	74390	61.8

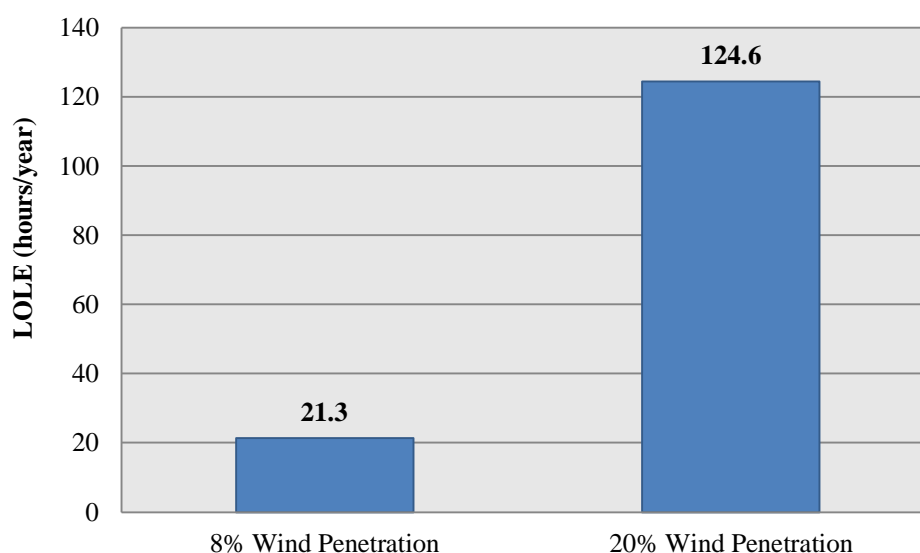
**Figure 8.10: Comparison of LOLE between 8 % and 20% Wind Penetration**

Figure 8.10 shows that the value of LOLE increases significantly when the wind penetration increases from 8% to 20% in EGPG. The value of LOLE increases from 21.3 hours/year (8% wind penetration) to 124.6 hours/year (20% wind penetration). According to the reliability standard of China (the acceptable standard is 24~48 hours/year), the value of LOLE in this case is more than 2 times of the maximum limit of LOLE. So, it is unacceptable for EGPG in 20% wind penetration. Moreover, the simulation results on LOEE indicate that the amount of unserved electric energy is going up rapidly due to the increasing scale of the electric network in EGPG.

In this section, the results prove that the increasing wind penetration harms the EGPG reliability. In the previous section, the value of LOLE at 8% wind penetration level has been used as the original reliability level for future Wind-Hydro Cooperation planning. So, the target for the application of WHC method is to reduce

the value of LOLE from 124.6 hours/year to 21.3 hours/year. This application of WHC method is addressed in the next section.

## **8.5 Effect of Wind-Hydro Cooperation on EGPG Reliability in 20% Wind Penetration**

As presented in Chapter 6, the simulation results of reliability evaluations with WHC method were represented by the term of Cooperation Scenario CS (CF; DR); CF represents the required capacity of Pump-Hydro Combined Energy Storage (PHCES), and DR determines the operation mode of the installed PHCES. In the wind-hydro cooperation, the assigned PHES units in PHCES system will generate electricity to cooperate with wind power when the integrated wind generation output is less than 70% of its rated power output; contrarily, PHES units will not provide generation support.

In the previous section, the aim of the wind-hydro cooperation in Eastern Gansu Power Grid (EGPG) has been decided. Therefore, the objective of WHC method is to find the optimal cooperation scenario CS (CF; DR) to reduce the increased value of LOLE (*124.6 hours/year, May 2013*) to the original value of LOLE (*21.3 hours/year, May 2009*).

For the purpose of analysing the effect of WHC method on EGPG reliability and simplifying the calculation process, the stated reliability level (value of LOLE as presented in Chapter 6) is assumed to 21.1~21.5 hours/year. Then, the Wind-Hydro Cooperation (WHC) method is applied to the eastern Gansu power grid (EGPG) at 20% wind penetration level, the simulation results are summarized in *Table 8.6* and

Figure 8.11, respectively. In addition, the simulated cooperation scenarios in this section are focus on the results that are close to the stated reliability level.

**Table 8.6: Effect of Wind-Hydro Cooperation on EGPG Reliability Indices**

<b>Status</b>	<b>LOLE (hours/year)</b>	<b>LOEE (MWh/year)</b>	<b>LOLF (occ./year)</b>
20% Wind Penetration	124.6	74390	61.8
CS (0.4; 1.0)	22.4	11459	11.4
CS (0.4; 0.9)	21.7	10859	11.3
CS (0.4; 0.8)	21.4	10694	11.2
CS (0.4; 0.7)	22.0	11147	11.6
CS (0.4; 0.6)	21.9	11044	11.5
CS (0.4; 0.5)	21.5	10674	11.6
CS (0.4; 0.4)	21.2	10638	11.4
CS (0.4; 0.3)	21.5	10771	11.6
CS (0.4; 0.2)	21.6	10838	11.7
CS (0.4; 0.1)	22.0	11303	11.8

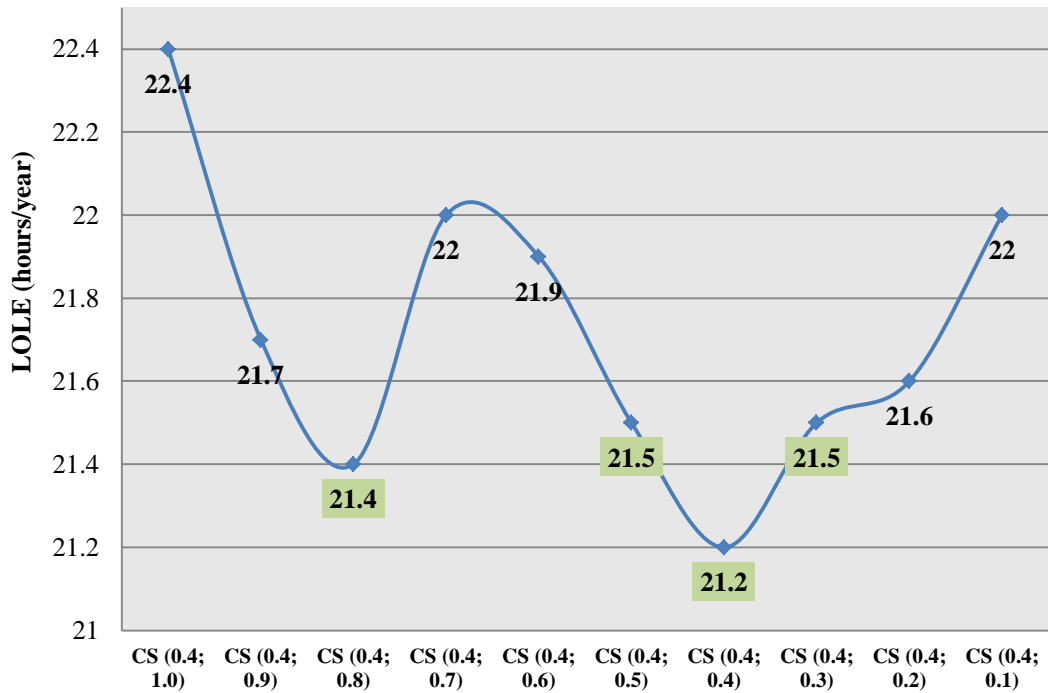


**Figure 8.11: Effect of Wind-Hydro Cooperation on LOLE in EGPG (20% Wind Penetration Level)**

It is clear that four cooperation scenarios (CS) are within the stated reliability scope as coloured in *Table 8.6* and *Figure 8.8*, respectively. As introduced in Chapter 6, the Cost-Benefit Analysis (CBA) method will be used to determine the optimal cooperation scenario. In this section, the stated reliability level is the same for all cooperation scenarios. So, the objective of the CBA method is to find the minimum value of the total costs ( $C$ ) in suitable CSs. The details of the total costs are briefly summarized as (details presented in Chapter 6):

$$C = CC + UEC;$$

$CC$ : Capital cost;

$UEC$ : Unserved energy costs,  $UEC = LOEE \times CIC$ ;  $CIC$  is customer interruption cost.

It is clear that all suitable CSs have the same value of CF, which means that they have the same installed capacity of PHCES for the cooperation. So, the capital costs

( $CC$ ) of these four CSs are the same. Therefore, the objective is to find the minimum value of  $UEC$ . The simulation results of LOEE in these CSs were summarized in *Table 8.6*. The data of the customer interruption cost ( $CIC$ ) is summarized in *Table 8.7*, which is constructed based on *Table 2.10* in *section 2.7.5*.

**Table 8.7: CIC for Seven Components in Eastern Gansu Electricity Market**

Type	CIC (£/kWh)
Industrial	55.8
Residential	15.7
Large user	8.2
Commercial	83.0
Government	26.0
Agriculture	4.1
Office	119.2

According to the Standard Industrial Classification (SIC) presented in Chapter 2, there are 7 main types of customers: industrial, residential, large user, commercial, government, agriculture and office. *Figure 8.12* shows the proportions of the components in eastern Gansu electricity market, which is modified based on [144].

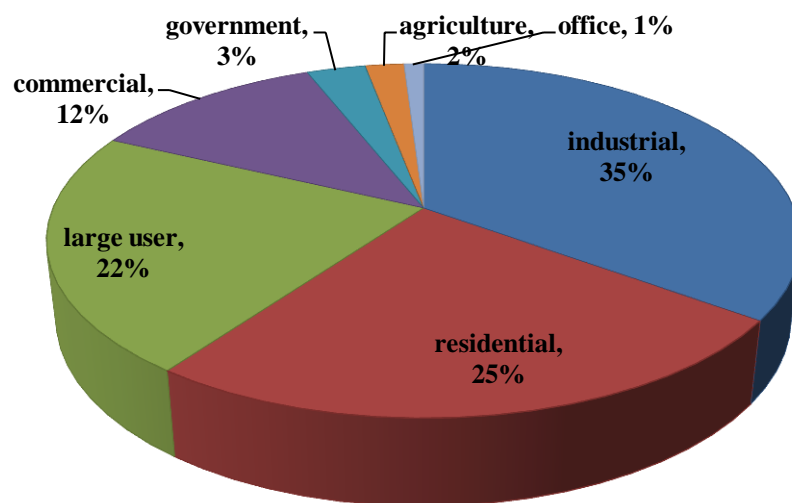


**Figure 8.12: Seven Components in Eastern Gansu Electricity Market [144]**

The calculation procedures of  $UEC$  are illustrated in *Figure 8.13*. The details of CS (0.4; 0.8) calculation will be presented for illustrating the procedure.

$$(1) \text{ CS (0.4; 0.8): } UEC_1 = 35\% \times LOEE_1 \times CIC_{\text{industrial}} + 25\% \times LOEE_1 \times CIC_{\text{residential}} + 22\% \times LOEE_1 \times CIC_{\text{Large user}} + 12\% \times LOEE_1 \times CIC_{\text{commercial}} + 3\% \times LOEE_1 \times CIC_{\text{government}} + 2\% \times LOEE_1 \times CIC_{\text{agriculture}} + 1\% \times LOEE_1 \times CIC_{\text{office}} = \text{£ } 387.9 \text{ Million}$$

$$(2) \text{ CS (0.4; 0.5): } UEC_2 = \text{£ } 387.2 \text{ Million}$$

$$(3) \text{ CS (0.4; 0.4): } UEC_3 = \text{£ } 385.9 \text{ Million}$$

$$(4) \text{ CS (0.4; 0.3): } UEC_4 = \text{£ } 390.7 \text{ Million}$$

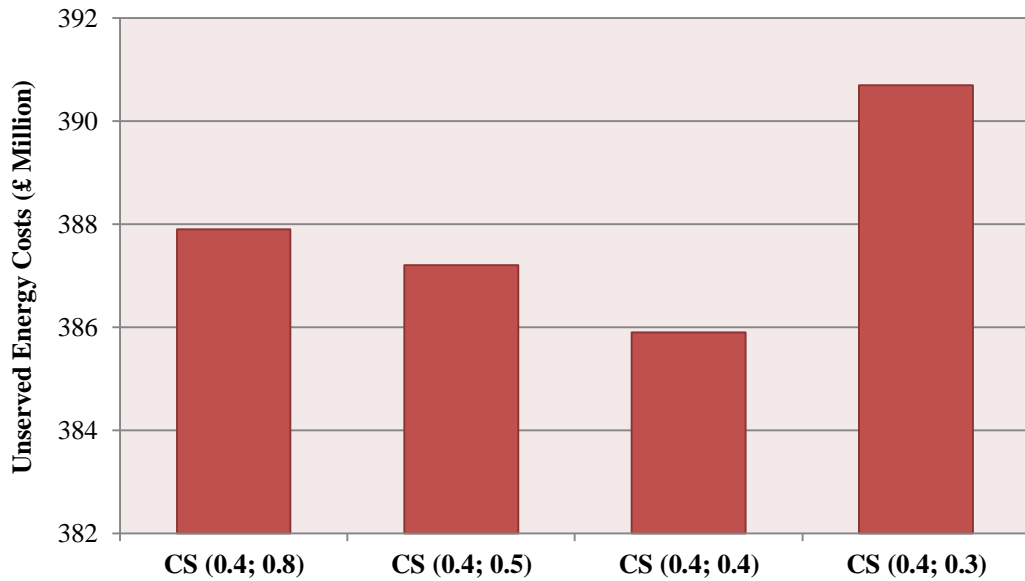


**Figure 8.13: Unserved Energy Costs of Suitable Cooperation Scenarios**

From *Figure 8.13*, CS (0.4; 0.4) has the minimum value of unserved energy costs. Therefore, the optimal cooperation scenario for the stated reliability level in 20% wind penetration is CS (0.4; 0.4).

From a System Operator (SO) point of view, the optimal cooperation scenario represents:

From May 2009 to May 2013, the wind penetration increased from 8% to 20%. In the meantime, the value of LOLE rose from 21.3 to 124.6 hours/year. For the purpose of reducing the impacts of wind power fluctuations on the reliability and retrieving the reliability to the original level, eastern Gansu power grid (EGPG) requires PHCES with the total capacity of **1144 MW** (PHES capacity: **458 MW**, Hydro capacity: 686 MW) to reduce the impacts of wind power fluctuations on power outputs and retrieve the reliability with the minimum costs. As presented in *section 8.2*, it was assumed that the PHCES station is upgraded from Liujiaxia hydroelectric station with the maximum installed capacity of **1225 MW**. Therefore, the optimal CS fulfils the requirement, and the amount of the hydro-to-PHES upgrade is 458 MW. The effect of CS (0.4; 0.4) on EGPG reliability in 20% wind penetration is illustrated in *Figure 8.14*.

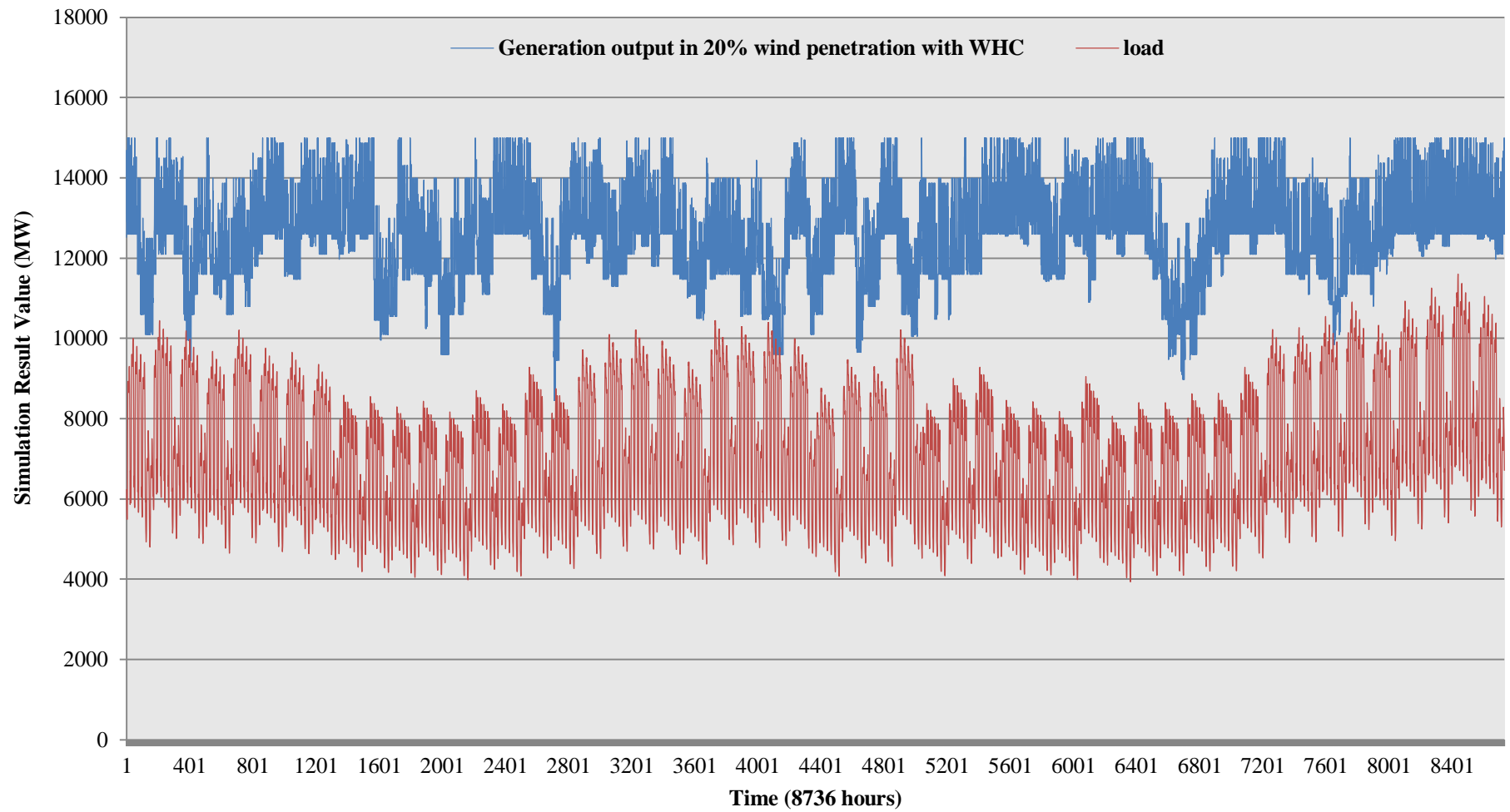


*Figure 8.14: Superimposition of Total Generation & Load in EGPG with WHC (20% Wind Penetration)*

From *Figure 8.14*, it is clear that the effects of wind power fluctuations have been reduced, which are illustrated by the decreasing occurrences of load exceeds the total generation output compared with that in *Figure 8.9* (20% penetration). However, the fluctuation degree of the power outputs increased compared with that in *Figure 8.6* (8% penetration). Therefore, the simulation results prove that the WHC method can effectively and efficiently reduce the impacts of wind power output fluctuations on EPGG reliability, and retrieve the reliability to the stated level with the increasing wind penetration.

## 8.6 Summary

The proposed WHC method in Chapter 6 was applied to a practical power system. This chapter presented the eastern Gansu power grid (EGPG) as a case study to investigate the effect of WHC method on the practical power system reliability. EGPG is the load centre in the Gansu province with huge potential of hydro power resources. Wind power is the fastest growing energy market in the Gansu province, which is driven by the fast-growing local economy and the large-scale government financial investment.

The EGPG reliability evaluation was simulated based on the development of EGPG from May 2009 to May 2013. The wind penetration has been increased significantly during this 4-year period due to increasing wind power integration and transmission system capacity. The wind penetration was increased from 8% to 20% in EGPG. The increasing wind penetration could harm the EGPG reliability due to the effects of wind power output fluctuations on the total power output. The reliability level of EGPG was represented by the value of LOLE.

The objective of WHC method was to reduce the effects of wind power output fluctuations and retrieve the increased value of LOLE (May 2013) to the stated value of LOLE (May 2009). The simulation results proved that the WHC method could effectively fulfil the requirement within the predetermined conditions in this practical power system. Furthermore, the required amount of Pump-Hydro Combined Energy Storage (PHCES) capacity was assumed to be upgraded from an existing hydro power plant. It may attract the attention of the system operator (SO) to upgrade the appropriate existing hydro power plants to PHCES stations due to the construction period of PHCES station is long and associated capital costs are significantly expensive.

# Chapter 9. Conclusions

## 9.1 Introduction

Electric networks are targeting the future sustainable power systems; it will need to integrate a large proportion of renewable energy generation, with different operating characteristics, connected in new locations throughout the network. Among these renewable energy generation sources, wind power is the fastest developing renewable energy source in electric networks. Operating this sustainable power system will be a challenge. Due to its variable and intermittent nature, large penetration of wind power generation will increase the fluctuations and uncertainty on the system generation output. At the same time, the remaining generation may become less flexible. It will affect the generation and demand balance and system adequacy. The main implication of this is the likely decrease of system reliability.

The scope of this research includes the development of approaches and methodologies to assess power systems reliability with increasing wind penetration. For the purpose of analysing the reliability evaluations, power system reliability assessment methods, and the wind power output model need to be clearly understood. It is known that different reliability analysis approaches were described and discussed in details. Most of the methods are effective to analyse the conventional generation system, but there is a lack of capabilities to accommodate the intermittent nature of wind generation. Then, Monte Carlo Simulation (MCS) method was presented to simulate the operation of each component in the system without consideration of the component output nature by applying the random number and different kinds of distribution function. The elements of the methodologies are developed based on detailed simulation of system operation, considering different system conditions.

Following the discussions, the combined reliability analysis method of Frequency & Duration (F&D) method and MCS method is developed to assess the power systems reliability with increasing wind power penetration.

Also, it is important to model the wind speed variation to obtain the wind power output and analyse the effects of wind power fluctuations on the system reliability. Following this, Weibull distribution function is used to represent the wind speed variations by modifying Weibull scale and shape parameters. Then, the simulated results of wind power outputs show that the output curve is fluctuating. It will cause the total generation output to become unstable and decrease the reliability. Moreover, several operating reserve assessment methodologies are discussed to reduce the effects on the reliability caused by the wind power fluctuations. However, the conventional operating reserve methods cannot fulfil the requirement. The reliability analysis indicated that the effects of wind power fluctuations could be reduced with a fast response, quick start-up energy source to generate the required operating reserve.

Consequently, for the purpose of reducing the effects of wind power fluctuations, the cooperation between wind power and other renewable energy sources has been investigated. Then, the wind-hydro cooperation (WHC) was developed to reduce the effects in different wind penetrations. In many case studies, the results illustrated that WHC is an effective tool to reduce the effects of wind power fluctuations on system power outputs and maintain the reliability.

Lastly, it should be highlighted that the operational mode of Pump-Hydro Combined Energy Storage (PHCES) technology used in WHC method is not yet determined due to the lack of operating information. Accordingly, a part of this thesis addressed an assumption to perform the operation of PHCES station.

## 9.2 Contributions and Findings of this Research

This thesis performs fundamental research aiming at reducing the effects of wind power fluctuations on power outputs and maintaining the system reliability. Detailed modelling of the generating system output (thermal, hydro and wind) has been analysed and presented. The well-proven software tools *MATLAB* and *MATPOWER* support the study. The following section presents the key findings of this work in response to the detailed research question outlined in Chapter 1. This is then followed by the suggestions for future works.

***Main contribution 1: develop the combined reliability assessment method of Frequency & Duration (F&D) method and Monte Carlo Simulation (MCS) method to analyse the power system reliability with different wind penetrations***

Many reliability analysis methodologies have been presented in past works. A critical outcome of this work is the development of a complicated reliability assessment approach for analysing the power system reliability considering the impacts of wind power penetration. This approach is applied in case studies, which are used to investigate the impacts of wind power output fluctuations on power systems reliability. The fundamental advantages of the proposed approach are summarized as follows:

- a. This approach is capable of combining the advantages of both F&D method and MCS method. The reliability evaluation of the power system has been analysed by considering the system is continuously operating, repairing and maintaining in F&D method. On the other hand, MCS method could apply random number and different kinds of distribution function to simulate the operation of each component in the system without considering the component's output nature. The results showed that the proposed approach is

an effective tool to accommodate the intermittent nature of wind power and analyse the associated impacts of wind power fluctuations on the reliability.

- b. The operation of conventional generating unit was constructed by using MATLAB with the associated reliability data: Mean Time to Repair (MTTR), failure rate per year and the rated power output. Also, wind power output has been evaluated by using Weibull distribution function to represent the wind speed variations. These reliability evaluations were simulated based on MCS method in a sufficiently long period. So, the simulation results of reliability indices have been proved applicable for future practical applications.

***Main contribution 2: propose Wind-Hydro Cooperation (WHC) method to reduce the effect of wind power fluctuation on power output and maintain the power system reliability***

The wind speed variation and wind power output have been investigated. The intermittent nature of wind energy caused the high fluctuation on the system power output. The conventional operating reserve assessment methods cannot accommodate the wind power output fluctuations. The simulated results indicate that the effects of wind power fluctuations can be reduced with a fast response, quick start-up energy source to generate the required operating reserve and cooperate with wind power.

The contribution of this work is the development of an original methodology for the wind-hydro cooperation (WHC). The basic theory of this methodology is to use Pump-Hydro Combined Energy Storage (PHCES) technology to cooperate with wind power generation. The main advantages of the proposed WHC method are:

- It combines the advantages of the combined reliability analysis method of F&D method and MCS method with the flexibility of Pump-Hydro Combined Energy Storage (PHCES) system to reduce the impacts of wind

power fluctuation on power system reliability for both long-term and short-term operational planning.

- It can easily be applied in different power systems for reliability evaluations. This will only require the system data to modify the generating system output model and load demand model.
- The simulation results of the proposed method were represented by the term of Cooperation Scenario (CS), which includes the information of the cooperation and leads to improved reliability levels. So, it is convenient and straightforward for the system operator (SO) to plan the developments of wind power and PHCES in different power systems at the stated reliability level.

The proposed WHC method was applied to an extensive set of case studies aimed at identifying the validity of the wind-hydro cooperation in different sizes of power systems. There were three test power systems in this thesis to illustrate the wind-hydro cooperation: **1)** a small test system for validation purposes; **2)** a larger power system for analysing the effects of the proposed WHC method on long-term system planning and short-term operational planning; **3)** a practical power system for the proposed WHC method to solve the reliability issues caused by the increasing wind penetration. The findings of the studies are briefly summarized as follows:

- a) WHC method was employed to the modified Roy Billinton Test System (MRBTS) to validate the feasibility and analyse the impact of wind power penetration on MRBTS reliability. The simulation results proved that the WHC method could effectively reduce the effects of wind power output fluctuations on MRBTS reliability at 10% and 15% wind penetration levels.
- b) The details of the modified IEEE 118-bus test system have been presented. In this case, WHC method will be tested in a large electric network for both

long-term system planning and short-term operational planning. In the long-term system planning, six wind penetrations including low, medium, high and extreme high levels were analysed and the results proved that the WHC method could make a great contribution to reduce the effects of wind power fluctuations and maintain the system reliability even at high wind penetration level. However, presented results also showed that WHC method may not fulfil the requirement of system reliability considering the given conditions at extreme high wind penetration level.

- c) In the short-term operational planning of the modified IEEE 118-bus test system, four wind penetrations and associated optimal cooperation scenarios were applied to the system with a daily load variation model to study the effects of WHC method on the electric network at these wind penetration levels. The simulation results proved that there is a significant improvement on reducing electric energy transmission/distribution losses by using the wind-hydro cooperation, especially during the peak load periods.
- d) Finally, WHC method was applied to a practical power system in the eastern Gansu region to investigate the effect of the proposed cooperation on the reliability within the existing system conditions. The presented results proved that the wind-hydro cooperation is feasible for the eastern Gansu power grid by upgrading the existing hydro plant to a PHCES station.

Therefore, the improvements of the proposed WHC method on the power system reliability evaluation compared with other power system reliability assessment methods can be summarized in *Table 9.1*.

**Table 9.1: Improvements of Wind-Hydro Cooperation Method**

<i>Aspects of the improvement</i>	<i>Details</i>
Considering the wind power output fluctuations	<i>It is effective to assess power systems reliability in different wind penetrations by utilising the advantages of the combined reliability analysis method and PHCES technology.</i>
Considering the economic benefits	<i>It concerns the economic operation profits of power systems by using the Cost-Benefit Analysis (CBA) method to calculate the customer interruption costs (CIC).</i>
Applicable for different power systems	<i>It has been applied in three different power systems for reliability evaluations. It requires minor system data to assess the system reliability.</i>

***Main contribution 3: propose a new operational mode of Pump-Hydro Combined Energy Storage (PHCES) system to cooperate with the fluctuating wind power output***

Past works stated that a PHCES system uses both pumped water and natural stream flow water to generate electricity, so it consists of hydro power generation and PHES power generation. Hydro units use natural stream flow water to generate electricity. PHES units generate electricity to reduce the effects of wind power fluctuation on power outputs when the integrated wind power output is low, and pump water back to the reservoir when the power output from wind generation is at a high level. The operational mode of Pump-Hydro Combined Energy Storage (PHCES) technology has not been investigated clearly in the electric networks. Therefore, another key contribution of this work is to propose an operational mode of PHCES system for the wind-hydro cooperation. The main features of the proposed operational mode can be summarized as follows:

- i. It consists of both pumped water and natural flow water to generate electricity. In the proposed operational mode, PHES units are assigned to cooperate with wind power to offset the power imbalance caused by wind fluctuation. If the power output from the wind farm is less than a specified value termed as the cooperation criterion, the PHES units assigned to cooperate with wind power are responsible for providing the required support. The rest of hydro units operate as normal generating units to contribute to the system adequacy and security.
  
- ii. The proposed operational mode has been represented by a weekly operation cycle with consideration of the short-term operational periods. The generating-pumping process has also been explained in details. It contains two independent pumping procedures: (1) PHES units will use the surplus of electricity generation to pump water back to the upper reservoir due to high wind power output ( $\geq 70\%$  rated power output). (2) PHES units will pump water to the upper reservoir during daily off-peak periods.

The operational mode was applied to the modified Roy Billinton Test System (MRBTS) for verification and validation. The results proved that it could guarantee the availability of the upper reservoir for the wind-hydro cooperation. Furthermore, the effect of generating-pumping process on the electric network has been investigated in the modified IEEE 118-bus test system. The simulated results by *MATPOWER* indicated that it could make a significant contribution to reduce the electric energy transmission/distribution losses, especially during the peak periods. The advantages of the proposed operational mode can be briefly summarized in *Table 9.2*.

**Table 9.2: Advantages of the Proposed Operational Mode**

<i>Advantage</i>	<i>Descriptions</i>
Efficient for the cooperation between wind power and PHCES system	<i>It contains PHES units (for the generating-pumping process) and hydro units (for generating-only), and it uses both pumped water and natural flow water to generate electricity.</i>
Reduce the effect of wind output fluctuations on power outputs	<i>If the wind power output is less than a specified value, the PHES units are responsible for providing the required support.</i>
Reduce the effect of the surplus electricity generation on electric networks	<i>PHES units use the surplus of electricity generation to pump water back to the upper reservoir due to high wind power output. And PHES units also pump water to the upper reservoir during daily off-peak periods.</i>

## 9.3 Future Work

This thesis contributes to the power system reliability evaluation with increasing wind power penetration, and proposes the Wind-Hydro Cooperation (WHC) method to reduce the effects of wind power output fluctuations on power outputs and maintain the system reliability. However, the proposed method and associated case studies have been investigated in details, due to the time constraint, there are some possible expansion and improvements that can be considered for the methodologies and concepts proposed in this thesis.

In this section, some possible directions for future research are presented.

- Presented works mainly focused on the power systems, which are dominated by the thermal power generation. Due to the increasing variable renewable energy sources, it is necessary to investigate the effect of the wind-hydro cooperation in a small nuclear-hydro-wind power system; the thermal generation will be assumed to be replaced completely. The requirement of peak shaving capability is very strict for regulating the nuclear power stations (which are not load-following). So, it is critical to find the optimal cooperation scenario (CS) to reduce the effects of wind power fluctuations on the reliability and regulate the non-load following nuclear power generation.
- The proposed operational mode of the pump-hydro combined energy storage (PHCES) technology is not the optimum for the generating-pumping process. It is possible to investigate the optimum operational mode of the generating-pumping process by using more detailed operating data and PHCES parameters.
- The efficiencies of the generating and pumping processes are not considered in the PHCES operation. So, it is necessary to investigate the practical

generating-pumping process in PHCES systems with the actual industrial data of the efficiencies.

- Due to a lack of real practical data and without access to the up-to-date information, it is impossible to test these reliability evaluation methods in real practical systems. Although reliability simulations are based on the random numbers generated by the powerful software and tested repeatedly for a significant long period, and the accuracy and validity of these simulation results have been proved; it is better to test the proposed methodologies with real operational data in practical power systems.
  
- Besides the proposed wind-hydro cooperation discussed in this thesis, there are a few more renewable energy cooperation can be considered for large-scale application in power systems. For instance, wind-solar-PHES joint operation has been developed recently. However, there is a lack of evaluation methods for this, and it is difficult to estimate the economic benefits without applicable power systems.

## Reference

1. *UK Renewable Energy Roadmap Update 2012* by UK Department of Energy & Climate Change. December 2012; Available from: [https://www.gov.uk/government/uploads/system/uploads/attachment\\_data/file/80246/11-02-13\\_UK\\_Renewable\\_Energy\\_Roadmap\\_Update\\_FINAL\\_DRAFT.pdf](https://www.gov.uk/government/uploads/system/uploads/attachment_data/file/80246/11-02-13_UK_Renewable_Energy_Roadmap_Update_FINAL_DRAFT.pdf).
2. Silva, V.L.F.d.P.d., *Value of flexibility in systems with large wind penetration*, in *Imperial College London* 2010, University of London.
3. *Building a low carbon economy- the UK's contribution to trackling climate change*, 2008: Committee on Climate Change London.
4. Chowdhury, A.A., et al., *System reliability worth assessment at a midwest utility—survey results for residential customers*. *International Journal of Electrical Power & Energy Systems*, 2005. **27**(9–10): p. 669-673.
5. Roy Billinton, R.N.A., *Reliability Evaluation of Power Systems*. 2nd Edition ed. 1996, New York and London: Plenum Press.
6. Kottick, D., M. Blau, and Y. Frank, *Reliability of supply to consumers as a function of the installed generation reserve margin*. *Electric Power Systems Research*, 1995. **33**(1): p. 63-67.
7. Doherty, R. and M. O'Malley, *A new approach to quantify reserve demand in systems with significant installed wind capacity*. *Power Systems, IEEE Transactions on*, 2005. **20**(2): p. 587-595.
8. Matos, M.A. and R.J. Bessa, *Setting the Operating Reserve Using Probabilistic Wind Power Forecasts*. *Power Systems, IEEE Transactions on*, 2011. **26**(2): p. 594-603.
9. Ela, E., et al. *Evolution of operating reserve determination in wind power integration studies*. in *Power and Energy Society General Meeting, 2010 IEEE*. 2010.

10. Montero, F.P. and J.J. Perez, *Wind-Hydro Integration: Pumped Storage to Support Wind*. Hydro Review, June 2009.
11. Krau, S., G. LAFRANCE, and L. Lafond, *Large scale wind farm integration: a comparison with a traditional hydro option*, in *EWEA Global Wind Power Conference* April 2-5, 2002: Paris.
12. Vogstad, K.O., *Utilizing the complementary characteristics of wind power and hydropower through coordinated hydro production scheduling using EMPS model*, in *Nordic Wind Energy Conference* March 13-14, 2000: Trondheim.
13. Vogstad, K.O., et al., *System benefits of coordinating wind power and hydropower in a deregulated market*, in *Proceedings of Wind Power for the 21st Century* 2000: Kassel.
14. M. Korpås, J.O.G.T., K. Uhlen, E.S. Hause, T. Gjengedal, *Planning and operation of large wind farms in areas with limited power transfer capacity*, in *Proceedings of 2006 EWEC* February 27–March 2, 2006: Athens.
15. J. Matevosyan, M. Olsson, and L. Soder, *Hydropower planning coordinated with wind power in areas with congestion problems for trading on the spot and the regulating market*. Electric Power Systems Research, 2009. **vol. 79**: p. pp. 39-48.
16. Korpaas, M., A.T. Holen, and R. Hildrum, *Operation and sizing of energy storage for wind power plants in a market system*. International Journal of Electrical Power & Energy Systems, 2003. **25**(8): p. 599-606.
17. Castronuovo, E.D. and J.A. Peas Lopes, *On the optimization of the daily operation of a wind-hydro power plant*. Power Systems, IEEE Transactions on, 2004. **19**(3): p. 1599-1606.
18. J.M. Angarita, J.G.U., *Combining hydro-generation and wind energy. Bidding and operation on electricity spot markets*, in *Electr. Power Syst. Res.*, **77**, pp. 393–400 April 2007.
19. J. Matevosyan, L.S., *Optimal daily planning for hydro power system coordinated with wind power in areas with limited export capability*, in *Proceedings of 2006 PMAFS* June 11-15, 2006: Stockholm.

20. Kaldellis, J.K. and K.A. Kavadias, *Optimal wind-hydro solution for Aegean Sea islands' electricity-demand fulfilment*. Applied Energy, 2001. **vol 70**: p. pp 333-354.
21. JK, K., *The solution of the energy demand problems for the islands of Aegean sea, using renewable energy sources*, in *5th national conference on the soft energy resources*1996: Athens. p. p. 464-473.
22. Kaldellis, J.K., K. Kavadias, and E. Christinakis, *Evaluation of the wind-hydro energy solution for remote islands*. Energy Conversion and Management, 2001. **42**(9): p. 1105-1120.
23. Vlachou D, C.E., Kavadias K, Kaldellis J, *Optimum wind-hydro energy station operation, using an advanced fluid flow analysis code*, in *3rd national congress on computational mechanics*1999: Greece. p. p. 811-20.
24. Tuohy, A. and M. O'Malley. *Impact of pumped storage on power systems with increasing wind penetration*. in *Power & Energy Society General Meeting, 2009. PES '09. IEEE*. 2009.
25. Ummels, B.C., E. Pelgrum, and W.L. Kling, *Integration of large-scale wind power and use of energy storage in the netherlands' electricity supply*. Renewable Power Generation, IET, 2008. **2**(1): p. 34-46.
26. Ancona, D.F., et al., *Operational constraints and economic benefits of wind-hydro hybrid systems analysis of systems in the U.S./Canada and Russia*, in *Wind Energy Conference* June 2003: Madrid, Spain.
27. Chi-Keung, W., et al., *The Impact of Wind Generation on Wholesale Electricity Prices in the Hydro-Rich Pacific Northwest*. Power Systems, IEEE Transactions on, 2013. **28**(4): p. 4245-4253.
28. Zafirakis, D., et al., *Modeling of financial incentives for investments in energy storage systems that promote the large-scale integration of wind energy*. Applied Energy, 2013. **105**(0): p. 138-154.
29. Karki, R., H. Po, and R. Billinton, *Reliability Evaluation Considering Wind and Hydro Power Coordination*. Power Systems, IEEE Transactions on, 2010. **25**(2): p. 685-693.

30. Saidur, R., et al., *A review on global wind energy policy*. Renewable and Sustainable Energy Reviews, 2010. **14**(7): p. 1744-1762.
31. Shuo, Z., L. Gengyin, and Z. Ming. *Calculation and analysis of capacity credit of wind farms based on Monte-Carlo simulation*. in *Power and Energy Society General Meeting, 2010 IEEE*. 2010.
32. Ensslin, C., et al. *Current methods to calculate capacity credit of wind power, IEA collaboration*. in *Power and Energy Society General Meeting - Conversion and Delivery of Electrical Energy in the 21st Century, 2008 IEEE*. 2008.
33. van Wijk, A.J.M., N. Halberg, and W.C. Turkenburg, *Capacity credit of wind power in the Netherlands*. Electric Power Systems Research, 1992. **23**(3): p. 189-200.
34. Voorspools, K.R. and W.D. D'Haeseleer, *An analytical formula for the capacity credit of wind power*. Renewable Energy, 2006. **31**(1): p. 45-54.
35. *GWEC Global wind statistics 2012*. Access Date: March 2013; Available from: [http://www.gwec.net/wp-content/uploads/2013/02/GWEC-PRstats-2012\\_english.pdf](http://www.gwec.net/wp-content/uploads/2013/02/GWEC-PRstats-2012_english.pdf).
36. *World Wind Energy Report 2010*. Access Date: June 2011; Available from: [http://www.wwindea.org/home/images/stories/pdfs/worldwindenergyreport2010\\_s.pdf](http://www.wwindea.org/home/images/stories/pdfs/worldwindenergyreport2010_s.pdf).
37. Sawin, J.L. *Wind Power Increase in 2008 Exceeds 10-year Average*. Access Date: October 2010; Available from: <http://vitalsigns.worldwatch.org/vs-trend/wind-power-increase-2008-exceeds-10-year-average>.
38. Shuai, S. and K.L. Lo. *Reliability assessment of power system considering the impact of wind energy*. in *Universities Power Engineering Conference (UPEC), 2012 47th International*. 2012.
39. *Continuing boom in wind energy – 20 GW of new capacity in 2007*. Access Date: October 2010; Available from: [http://www.ewea.org/news/detail/?tx\\_ttnews%5Btt\\_news%5D=574&cHash=f07703f56c86d0ef5642e37067104922](http://www.ewea.org/news/detail/?tx_ttnews%5Btt_news%5D=574&cHash=f07703f56c86d0ef5642e37067104922).

40. *Wind Power is the fastest growing source of electricity in the world.* Access Date: October 2010; Available from: [http://www.ibm.com/smarterplanet/us/en/smart\\_grid/article/wind\\_power.html](http://www.ibm.com/smarterplanet/us/en/smart_grid/article/wind_power.html).
41. *Wind Powering America Fact Sheet Series: Wind Energy Benefits.* Access Date: October 2010; Available from: [http://wind.jmu.edu/vwec/Fact%20Sheets%20&%20Presentations/Fact%20Sheets/wpa\\_factsheet\\_series.pdf](http://wind.jmu.edu/vwec/Fact%20Sheets%20&%20Presentations/Fact%20Sheets/wpa_factsheet_series.pdf).
42. *Wind and Water Power Program: Wind Energy Benefits.* Access Date: July 2011; Available from: <http://www1.eere.energy.gov/wind/pdfs/49053.pdf>.
43. Greenspace, U. *Clean Energy: Wind Power.* Access Date: December 2012; Available from: <http://www.greenpeace.org.uk/climate/wind-power>.
44. Torbellino, S.A. *Renewable Energy.* Access Date: January 2013; Available from: <http://www.torbellinosa.com/renewable-energy/>.
45. *Global Wind Report Annual Market Update 2011* Access Date: December 2012; Available from: [http://gwec.net/wp-content/uploads/2012/06/Annual\\_report\\_2011\\_lowres.pdf](http://gwec.net/wp-content/uploads/2012/06/Annual_report_2011_lowres.pdf).
46. Ming, Z., Z. Kun, and D. Jun, *Overall review of China's wind power industry: Status quo, existing problems and perspective for future development.* *Renewable and Sustainable Energy Reviews*, 2013. **24**(0): p. 379-386.
47. Leung, D.Y.C. and Y. Yang, *Wind energy development and its environmental impact: A review.* *Renewable and Sustainable Energy Reviews*, 2012. **16**(1): p. 1031-1039.
48. Xu, J., D. He, and X. Zhao, *Status and prospects of Chinese wind energy.* *Energy*, 2010. **35**(11): p. 4439-4444.
49. Observ'ER. *Worldwide electricity production from renewable energy sources: stats and figures series: Forteenth Inventory- Edition 2012.* Access Date: January 2012; Available from: <http://www.energies-renouvelables.org/observ-er/html/inventaire/pdf/14e-inventaire-Chap02.pdf>.
50. Ryan Wiser, M.B. *2011 Wind technologies market report by U.S. Department of Energy.* Access Date: January 2012; Available from:

- [http://www1.eere.energy.gov/wind/pdfs/2011\\_wind\\_technologies\\_market\\_report.pdf](http://www1.eere.energy.gov/wind/pdfs/2011_wind_technologies_market_report.pdf).
51. Danish Wind Industry Association 'Wind Energy'. Access Date: March 2013; Available from: <http://denmark.dk/en/green-living/wind-energy/>.
  52. Global wind energy outlook 2012. Access Date: March 2013; Available from: [http://www.gwec.net/wp-content/uploads/2012/11/GWEO\\_2012\\_lowRes.pdf](http://www.gwec.net/wp-content/uploads/2012/11/GWEO_2012_lowRes.pdf).
  53. Ackermann, T., *Wind Power in Power Systems*. 2012, CPI Group Ltd, Croydon, CR0 4YY, UK: Wiley. pp41.
  54. Benoit Robyns, A.D., Bruno Francois, Antoine Henneton and Jonathan Sprooten, *Electricity Production from Renewable Energies*. 2012, London, UK: John Wiley & Sons. pp83.
  55. Ackermann, T., *Wind Power in Power Systems*. 2012, CPI Group Ltd, Croydon, CR0 4YY, UK: Wiley. pp42.
  56. Ackermann, T., *Wind Power in Power Systems*. 2012, CPI Group Ltd, Croydon, CR0 4YY, UK: Wiley. pp73-74.
  57. GWEC. *Global Wind Energy Council: Wind Figures: Wind in Numbers*. Access Date: June 2013; Available from: <http://www.gwec.net/global-figures/wind-in-numbers/>.
  58. *Renewable Energy Focus: Belgium inaugurates wind farm with largest wind turbines*. Access Date: October 2010; Available from: <http://www.renewableenergyfocus.com/view/5588/belgium-inaugurates-wind-farm-with-largest-wind-turbines/>.
  59. Billinton, R. and G. Bai, *Generating capacity adequacy associated with wind energy*. Energy Conversion, IEEE Transactions on, 2004. **19**(3): p. 641-646.
  60. Castro Sayas, F. and R.N. Allan, *Generation availability assessment of wind farms*. Generation, Transmission and Distribution, IEE Proceedings-, 1996. **143**(5): p. 507-518.
  61. Billinton, R. and Y. Li, *Incorporating multi-state unit models in composite system adequacy assessment*. European Transactions on Electrical Power, 2007. **17**(4): p. 375-386.

62. Zhou, Y., *PhD Thesis: Some Issues of Integrating Wind Power Generation into Electric Networks*, in *Department of Electronic and Electrical Engineering* 2009, University of Strathclyde: United Kingdom.
63. Billinton, R. and H. Dange, *Incorporating Wind Power in Generating Capacity Reliability Evaluation Using Different Models*. *Power Systems*, IEEE Transactions on, 2011. **26**(4): p. 2509-2517.
64. Billinton, R., et al., *Adequacy Assessment Considerations in Wind Integrated Power Systems*. *Power Systems*, IEEE Transactions on, 2012. **27**(4): p. 2297-2305.
65. Valenzuela, O., et al., *Hybridization of intelligent techniques and ARIMA models for time series prediction*. *Fuzzy Sets and Systems*, 2008. **159**(7): p. 821-845.
66. Jia, J.-s., et al., *Ecological footprint simulation and prediction by ARIMA model—A case study in Henan Province of China*. *Ecological Indicators*, 2010. **10**(2): p. 538-544.
67. Karki, R., H. Po, and R. Billinton, *A simplified wind power generation model for reliability evaluation*. *Energy Conversion*, IEEE Transactions on, 2006. **21**(2): p. 533-540.
68. Karki, R., P. Hu, and R. Billinton. *Reliability Evaluation of a Wind Power Delivery System Using an Approximate Wind Model*. in *Universities Power Engineering Conference, 2006. UPEC '06. Proceedings of the 41st International*. 2006.
69. *The WindPower and UK Wind Speed Database programs: Wind Turbine Characteristics*. Access Date: December 2012; Available from: [http://www.wind-power-program.com/turbine\\_characteristics.htm](http://www.wind-power-program.com/turbine_characteristics.htm).
70. Mohanpurkar, M. and R.G. Ramakumar. *Probability density functions for power output of Wind Electric Conversion Systems*. in *Power and Energy Society General Meeting, 2010 IEEE*. 2010.
71. GWEC. *Global Wind Energy Council: 30 Years of Policies for Wind Energy: Lessons from 12 Wind Energy Markets*. Access Date: June 2013; Available

- from: <http://www.gwec.net/30-years-policies-wind-energy-lessons-12-wind-energy-markets/>.
72. Lewis, J.I. and R.H. Wiser, *Fostering a renewable energy technology industry: An international comparison of wind industry policy support mechanisms*. *Energy Policy*, 2007. **35**(3): p. 1844-1857.
  73. Gramlich, R. *AWEA's Wind Energy for a New Era Report*. *American Wind Energy Association*. Access Date: October 2010; Available from: [http://www.newwindagenda.org/pdf/Report\\_ClimateSection.pdf](http://www.newwindagenda.org/pdf/Report_ClimateSection.pdf).
  74. Changliang, X. and S. Zhanfeng, *Wind energy in China: Current scenario and future perspectives*. *Renewable and Sustainable Energy Reviews*, 2009. **13**(8): p. 1966-1974.
  75. Arthouros Zervos, S.S. *Global Wind 2007 Report from Global Wind Energy Council*. Access Date: October 2010; 2nd Edition:[Available from: [http://gwec.net/wp-content/uploads/2012/06/gwec-08-update\\_FINAL.pdf](http://gwec.net/wp-content/uploads/2012/06/gwec-08-update_FINAL.pdf)].
  76. Roy Billinton, R.N.A., *Introduction*, in *Reliability Evaluation of Power Systems*. 1996, Plenum Press: New York and London.
  77. Allan, R., *Power system reliability assessment—A conceptual and historical review*. *Reliability Engineering & System Safety*, 1994. **46**(1): p. 3-13.
  78. Garba, A., *Chapter 4. Generating Capacity Adequacy Evaluation*, in *PhD Thesis: Operating Reserve Assessment with Renewable Generation*. October 2008, University of Strathclyde: United Kingdom.
  79. Roy Billinton, R.N.A., *Chapter 2: Generating Capacity - basic probability methods*, in *Reliability Evaluation of Power Systems*. 1996, Plenum Press: New York and London.
  80. Roy Billinton, W.L., *Reliability Assessment of Electrical Power Systems Using Monte Carlo Methods*. 1994, New York: Plenum Press.
  81. Billinton, R., et al., *A reliability test system for educational purposes-basic data*. *Power Systems, IEEE Transactions on*, 1989. **4**(3): p. 1238-1244.
  82. Debnath, K. and L. Goel, *Power system planning — a reliability perspective*. *Electric Power Systems Research*, 1995. **34**(3): p. 179-185.

83. Dzobo, O., C.T. Gaunt, and R. Herman, *Investigating the use of probability distribution functions in reliability-worth analysis of electric power systems*. International Journal of Electrical Power & Energy Systems, 2012. **37**(1): p. 110-116.
84. Freund, J.E., *Chapter 8 Sampling Distributions*, in *Mathematical Statistics with Applications*. 2004, Irwin Miller and Marylees Miller.
85. Paish, O., *Small hydro power: technology and current status*. Renewable and Sustainable Energy Reviews, 2002. **6**(6): p. 537-556.
86. Deane, J.P., B.P. Ó Gallachóir, and E.J. McKeogh, *Techno-economic review of existing and new pumped hydro energy storage plant*. Renewable and Sustainable Energy Reviews, 2010. **14**(4): p. 1293-1302.
87. Ming, Z., Z. Kun, and L. Daoxin, *Overall review of pumped-hydro energy storage in China: Status quo, operation mechanism and policy barriers*. Renewable and Sustainable Energy Reviews, 2013. **17**(0): p. 35-43.
88. Dursun, B. and B. Alboyaci, *The contribution of wind-hydro pumped storage systems in meeting Turkey's electric energy demand*. Renewable and Sustainable Energy Reviews, 2010. **14**(7): p. 1979-1988.
89. Cepin, M., *Assessment of Power System Reliability: Methods and Applications*. 2011, London: Springer Verlag
90. Roy Billinton, R.N.A., *Reliability Evaluation of Engineering Systems: Concepts and Techniques*. 1992, Second Edition Plenum Press, New York and London.
91. Hall, J.D., R.J. Ringlee, and A.J. Wood, *Frequency and Duration Methods for Power System Reliability Calculations: I - Generation System Model*. Power Apparatus and Systems, IEEE Transactions on, 1968. **PAS-87**(9): p. 1787-1796.
92. Deshmukh, R.G. and R. Ramakumar, *Reliability analysis of combined wind-electric and conventional generation systems*. Solar Energy, 1982. **28**(4): p. 345-352.

93. Dobakhshari, A.S. and M. Fotuhi-Firuzabad, *A Reliability Model of Large Wind Farms for Power System Adequacy Studies*. Energy Conversion, IEEE Transactions on, 2009. **24**(3): p. 792-801.
94. Li, W., *Risk Assessment of Power Systems: Models, Methods and Applications*, ed. M.E. EI-Hawary. 2005, IEEE Press John Wiley & Sons INC.
95. Garba, A., *PhD Thesis: Operating Reserve Assessment with Renewable Generation*, in *Department of Electronic and Electrical Engineering* 2008, University of Strathclyde: UK.
96. Billinton, R., C.L. Wee, and G. Hamoud, *Digital Computer Algorithms for the Calculation of Generating Capacity Reliability Indices*. Power Apparatus and Systems, IEEE Transactions on, 1982. **PAS-101**(1): p. 203-211.
97. Billinton, R. and L. Gan, *Use of Monte Carlo simulation in teaching generating capacity adequacy assessment*. Power Systems, IEEE Transactions on, 1991. **6**(4): p. 1571-1577.
98. Sankarakrishnan, A. and R. Billinton, *Sequential Monte Carlo simulation for composite power system reliability analysis with time varying loads*. Power Systems, IEEE Transactions on, 1995. **10**(3): p. 1540-1545.
99. Goel, L., X. Liang, and Y. Ou, *Monte Carlo simulation-based customer service reliability assessment*. Electric Power Systems Research, 1999. **49**(3): p. 185-194.
100. Billinton, R., H. Chen, and R. Ghajar, *A sequential simulation technique for adequacy evaluation of generating systems including wind energy*. Energy Conversion, IEEE Transactions on, 1996. **11**(4): p. 728-734.
101. *Department of Energy & Climate Change Annex C: Reliability Standard Methodology*. Access Date: October 2013; Available from: [https://www.gov.uk/government/uploads/system/uploads/attachment\\_data/file/223653/emr\\_consultation\\_annex\\_c.pdf](https://www.gov.uk/government/uploads/system/uploads/attachment_data/file/223653/emr_consultation_annex_c.pdf).
102. *Electric Networks Planning Reliability Study Report by China Electric Power Planning & Engineering Institute*. Access Date: March 2012; Available from: <http://wenku.baidu.com/view/9fe926126c175f0e7cd13762.html>.

103. Venu, V.V. and A.K. Verma, *A probabilistic transmission pricing methodology considering transmission reliability margins*. International Journal of Systems Assurance Engineering and Management, 2010. **1**((2)): p. 113-119.
104. Subcommittee, P.M., *IEEE Reliability Test System*. Power Apparatus and Systems, IEEE Transactions on, 1979. **PAS-98**(6): p. 2047-2054.
105. Grigg, C., et al., *The IEEE Reliability Test System-1996. A report prepared by the Reliability Test System Task Force of the Application of Probability Methods Subcommittee*. Power Systems, IEEE Transactions on, 1999. **14**(3): p. 1010-1020.
106. Roy Billinton, R.N.A., *Reliability Evaluation of Power Systems: Appendix 2 Analysis of the IEEE Reliability Test System*. 2nd Edition ed. 1996, New York and London: Plenum Press.
107. Tony Burton, J.N., David Sharpe, Erin Bossanyi, *Wind Energy Handbook*. 2011, UK: John Wiley & Sons.
108. Ahmad Shamshad, W.M.W.H., M.A Bawadi, Mohd. Sannusi S.A, *Analysis of Wind Speed Variations and Estimation of Weibull Parameters for Wind Power Generation in Malaysia*, 2009, Working Paper by Open Access Repository of USM Research & Publication: Malaysia.
109. Tai-Her, Y. and W. Li, *A Study on Generator Capacity for Wind Turbines Under Various Tower Heights and Rated Wind Speeds Using Weibull Distribution*. Energy Conversion, IEEE Transactions on, 2008. **23**(2): p. 592-602.
110. Kumaraswamy, B.G., B.K. Keshavan, and Y.T. Ravikiran. *Analysis of seasonal wind speed and wind power density distribution in Aimangala wind form at Chitradurga Karnataka using two parameter weibull distribution function*. in *Power and Energy Society General Meeting, 2011 IEEE*. 2011.
111. Johnson, G.L., *Economic Design of Wind Electric Systems*. Power Apparatus and Systems, IEEE Transactions on, 1978. **PAS-97**(2): p. 554-562.

112. Devroye, L., *On the computer generation of random variables with a given characteristic function*. Computers & Mathematics with Applications, 1981. **7**(6): p. 547-552.
113. Devroye, L., *Non-Uniform Random Variate Generation*. 1986, Spring-Verlag, New York Inc.: R.R.Donnelley & Sons, Harrisonburg, Virginia.
114. Technologystudent. *Pump Storage Systems by A Design and Technology Site*. Access Date: Sep 2011; Available from: <http://www.technologystudent.com/energy1/pstr1.htm>.
115. Corps, A., *Engineering and Design: Hydropower (Engineer Manual No. 1110-2-1701)*. 1985, Washington, DC: Army Corps of Engineers, Department of the Army.
116. Yang, C.-J. and R.B. Jackson, *Opportunities and barriers to pumped-hydro energy storage in the United States*. Renewable and Sustainable Energy Reviews, 2011. **15**(1): p. 839-844.
117. *Seawater Pumped-Storage Power Plant* Access Date: Sep 2011; Available from: <http://www.kankeiren.or.jp/kankyoen/pdf/en108.pdf>.
118. Loisel, R., et al., *Valuation framework for large scale electricity storage in a case with wind curtailment*. Energy Policy, 2010. **38**(11): p. 7323-7337.
119. Connolly, D., et al., *Modelling the existing Irish energy-system to identify future energy costs and the maximum wind penetration feasible*. Energy, 2010. **35**(5): p. 2164-2173.
120. Deane, J.P., E.J. McKeogh, and B.P.O. Gallachoir, *Derivation of Intertemporal Targets for Large Pumped Hydro Energy Storage With Stochastic Optimization*. Power Systems, IEEE Transactions on, 2013. **28**(3): p. 2147-2155.
121. *International Energy and Electricity Price Analysis Report by State Grid Energy Research Institute*. 2012, Beijing: China Electric Power Press.
122. Shuming, F. and H. Wakabayashi. *The cost-benefit analysis on traffic network reliability after disaster*. in *Transportation, Mechanical, and Electrical Engineering (TMEE), 2011 International Conference on*. 2011.

123. Neudorf, E.G., et al., *Cost-benefit analysis of power system reliability: two utility case studies*. Power Systems, IEEE Transactions on, 1995. **10**(3): p. 1667-1675.
124. Tinnium, K.N., P. Rastgoufard, and P.F. Duvoisin. *Cost-benefit analysis of electric power system reliability*. in *System Theory, 1994., Proceedings of the 26th Southeastern Symposium on*. 1994.
125. *Siah Bishe Pumped Storage Project- Iran*. Access Date: June 2013; Available from: [http://www.muetszenberg.ch/iran/Siah\\_Bishe.pdf](http://www.muetszenberg.ch/iran/Siah_Bishe.pdf).
126. Anagnostopoulos, J.S. and D.E. Papantonis, *Pumping station design for a pumped-storage wind-hydro power plant*. Energy Conversion and Management, 2007. **48**(11): p. 3009-3017.
127. Aihara, R., et al. *Optimal operation scheduling of pumped storage hydro power plant using efficient optimization algorithm*. in *Power System Technology (POWERCON), 2012 IEEE International Conference on*. 2012.
128. Corporate, D. *Bath County Pumped Storage Station*. 2014; Available from: <https://www.dom.com/about/stations/hydro/bath-county-pumped-storage-station.jsp>.
129. *Bath County Pump-hydro storage station*. Access Date: May 2014; Available from: <http://baike.baidu.com/view/325882.htm>.
130. *New version for the Pump Hydro Storage station development*. Access Date: May 2014; Available from: [http://chinaneast.xinhuanet.com/zhuanti/2009-08/28/content\\_17533599.htm](http://chinaneast.xinhuanet.com/zhuanti/2009-08/28/content_17533599.htm).
131. Boyle, G., *Renewable Energy- Power for a Sustainable Future (Third edition)*. 2012, Oxford: Oxford University Press. 566.
132. *Power System Test Case Archive: 118 Bus Power Flow Test Case by University of Washington*. Access Date: January 2012; Available from: [http://www.ee.washington.edu/research/pstca/pf118/pg\\_tca118bus.htm](http://www.ee.washington.edu/research/pstca/pf118/pg_tca118bus.htm).
133. Kamalinia, S., M. Shahidehpour, and A. Khodaei, *Security-constrained expansion planning of fast-response units for wind integration*. Electric Power Systems Research, 2011. **81**(1): p. 107-116.

134. *Location of Gansu Province in China* by Wikipedia. 15 Sep 2011; Available from:  
[http://en.wikipedia.org/wiki/File:Gansu\\_in\\_China\\_\(%2Ball\\_claims\\_hatched\).svg](http://en.wikipedia.org/wiki/File:Gansu_in_China_(%2Ball_claims_hatched).svg).
135. He, S., et al. *Integration of wind farm into Gansu power grid and its operation*. in *Sustainable Power Generation and Supply, 2009. SUPERGEN '09. International Conference on*. 2009.
136. *Western Region: Gansu in Gansu Economic and Social Development Report 2012*. Access Date: Nov 2013; Available from:  
<http://www.chinaknowledge.com/Business/Provincedetails.aspx?subchap=8&content=55>.
137. Qiao, A., *The Current Status and Sustainable Development of Hydropower in Gansu*. *Journal of Investigation and Research*, 2007. **9**: p. 86-7.
138. *The Medium and Long-term Program of Renewable Energy Development 2007*, China National Development and Reform Commission: Beijing.
139. Yunna, W. and X. Ruhang, *Current status, future potentials and challenges of renewable energy development in Gansu province (Northwest China)*. *Renewable and Sustainable Energy Reviews*, 2013. **18**(0): p. 73-86.
140. *The first pumped hydro energy storage station is constructing in Gansu with the investment of £850 million*. 2013 Access Date: Nov. 2013]; Available from: <http://www.sinohydro.com/664-998-685515.aspx>.
141. Sun, L. and J. Lin. *Impact of climate change on precipitation in the upstream of Liujiaxia reservoir*. in *Geoscience and Remote Sensing Symposium, 2009 IEEE International, IGARSS 2009*. 2009.
142. Haiyan, L., et al. *Wind energy resources exploitation and large-scale, non-grid-connection wind-powered industrial bases, construction in China Northwest Territories*. in *World Non-Grid-Connected Wind Power and Energy Conference, 2009. WNWEC 2009*. 2009.
143. Hong, S., et al. *Study on integration and transmission of large scale wind power in JiuQuan area Gansu Province China*. in *Integration of Wide-Scale*

- Renewable Resources Into the Power Delivery System, 2009 CIGRE/IEEE PES Joint Symposium. 2009.*
144. Xizheng, Z., Z. Xiaoqian, and J. Shaojun, *Electric Power Load Characteristics Analysis & Prediction. 2002, Beijing: China Electric Power Press.*

# Appendix

## Appendix I Comparison of Individual Probability (IP), Cumulative Probability (CP) & Complementary Cumulative Probability (CCP)

In Probability Theory and Statistics, probability is a measure of the likelihood of occurrence of an event. It has been used widely in such areas of study as mathematics, statistics, finance and science, and so on. In this thesis, probability is used to illustrate the generating unit capacity outage model. The definitions of these probabilities are briefly summarized in *Table I.1*.

*Table I.1: Definitions of IP, CP and CCP*

Index	Definition
IP	The probability of each individual capacity outage
CP	The probability of finding a quantity of capacity <b>less than (<math>\leq</math>)</b> or equal to the indicated amount
CCP	The probability of finding a quantity of capacity <b>more than (<math>\geq</math>)</b> or equal to the indicated amount (1- CP)

The *test system 2* in *section 2.8.1* will be used to illustrate these definitions in details. *Table II.2* summarized the calculation results of individual probabilities (IP), cumulative probabilities (CP) and complementary cumulative probabilities (CCP).

**Table II.2: Calculation Results of IP, CP and CCP in the Test System**

Capacity Outage (MW)	IP	CP	CCP
0	0.784718	<b>0.784718</b>	<b>1</b>
40	0.192176	<b>0.976894</b>	<b>0.215214</b>
80	0.021571	<b>0.998465</b>	<b>0.023038</b>
120	0.001467	<b>1</b>	<b>0.001467</b>

From *Table II.2*, it is clear that CP and CCP represent different operating statuses of the power system. For instance, when Capacity Outage= 40 MW, the associated **CP** and **CCP** are 0.976894 and 0.215214, respectively.

***Explanations:***

**CP** represents the probability of the capacity outage is less than or equal to 40 MW in the test system is 0.976894.

**CCP** represents the probability of the capacity outage is more than or equal to 40 MW in the test system is 0.215214.

## Appendix II MATLAB Codes of System Load Model

```

peak_load=185; % this is the value of the annual peak load
i_load=1;
j_load=1;
m_load=1;
n_load=1;
x_load=1;
y_load=1;
k_load=1;

out_load=zeros(52,1);
out_load1=zeros(52,1); % weekly peak load
out_load2=zeros(7,1); % daily peak load
out_load3=zeros(24,1);
out_load4=zeros(24,1); % weekdays hourly peak load (Week 1-8 & 44-52)
out_load5=zeros(8736,1); % annual load profile
out_load6=zeros(24,1); % weekends hourly peak load (Week 1-8 & 44-52)

out_load1(:,1)=[0.862;0.9;0.878;0.834;0.88;0.841;0.832;...
0.806;0.74;0.737;0.715;0.727;0.704;0.75;...
0.721;0.8;0.754;0.837;0.87;0.88;0.856;...
0.811;0.9;0.887;0.896;0.861;0.755;0.816;...
0.801;0.88;0.722;0.776;0.8;0.729;0.726;...
0.705;0.78;0.695;0.724;0.724;0.743;0.744;...
0.8;0.881;0.885;0.909;0.94;0.89;0.942;0.97;1;0.952];

out_load2(:,1)=[0.93;1;0.98;0.96;0.94;0.77;0.75];

out_load4(:,1)=[0.67;0.63;0.60;0.59;0.59;0.60;0.74;0.86;0.95;0.96;0.
96;0.95;0.95;0.95;0.93;0.94;0.99;1;1;0.96;0.91;0.83;0.73;0.63];

out_load6(:,1)=[0.78;0.72;0.68;0.66;0.64;0.65;0.66;0.70;0.80;0.88;0.
90;0.91;0.90;0.88;0.87;0.87;0.91;1;0.99;0.97;0.94;0.92;0.87;0.81];

out_load7(:,1)=[0.63;0.62;0.6;0.58;0.59;0.65;0.72;0.85;0.95;0.99;1;0
.99;0.93;0.92;0.9;0.88;0.9;0.92;0.96;0.98;0.96;0.9;0.8;0.7];
% weekdays hourly peak load (Week 9-17 & 31-43)

out_load8(:,1)=[0.75;0.73;0.69;0.66;0.65;0.65;0.68;0.74;0.83;0.89;0.
92;0.94;0.91;0.9;0.9;0.86;0.85;0.88;0.92;1;0.97;0.95;0.9;0.85];
% weekends hourly peak load (Week 9-17 & 31-43)

out_load9(:,1)=[0.64;0.6;0.58;0.56;0.56;0.58;0.64;0.76;0.87;0.95;0.9
9;1;0.99;1;1;0.97;0.96;0.96;0.93;0.92;0.92;0.93;0.87;0.72];
% weekdays hourly peak load (Week 18-30)

out_load10(:,1)=[0.74;0.7;0.66;0.65;0.64;0.62;0.62;0.66;0.81;0.86;0.
91;0.93;0.93;0.92;0.91;0.91;0.92;0.94;0.95;0.95;1;0.93;0.88;0.8];
% weekends hourly peak load (Week 18-30)

while i_load<53

```

```
% Week 1-8
while i_load<9
out_load(i_load,1)=out_load1(i_load,1)*peak_load;
    j_load=1;
    for j_load=drange(1:1:5)
        out_load3(m_load,1)=out_load2(j_load,1)*out_load(i_load,1);
        for k_load=drange(1:1:24)

out_load5(x_load,1)=out_load4(k_load,1)*out_load3(m_load,1);
        x_load=x_load+1;
        end
        m_load=m_load+1;
    end
    for j_load=drange(6:1:7)
        out_load3(n_load,1)=out_load2(j_load,1)*out_load(i_load,1);
        for k_load=drange(1:1:24)

out_load5(x_load,1)=out_load6(k_load,1)*out_load3(n_load,1);
        x_load=x_load+1;
        end
        n_load=n_load+1;
    end
    i_load=i_load+1;
end

% Week 9-17
while i_load>8 && i_load<18
    out_load(i_load,1)=out_load1(i_load,1)*peak_load;
    j_load=1;
    for j_load=drange(1:1:5)
        out_load3(m_load,1)=out_load2(j_load,1)*out_load(i_load,1);
        for k_load=drange(1:1:24)

out_load5(x_load,1)=out_load7(k_load,1)*out_load3(m_load,1);
        x_load=x_load+1;
        end
        m_load=m_load+1;
    end
    for j_load=drange(6:1:7)
        out_load3(n_load,1)=out_load2(j_load,1)*out_load(i_load,1);
        for k_load=drange(1:1:24)

out_load5(x_load,1)=out_load8(k_load,1)*out_load3(n_load,1);
        x_load=x_load+1;
        end
        n_load=n_load+1;
    end
    i_load=i_load+1;
end

% Week 18-30
while i_load>17 && i_load<31
    out_load(i_load,1)=out_load1(i_load,1)*peak_load;
    j_load=1;
    for j_load=drange(1:1:5)
```

```

        out_load3(m_load,1)=out_load2(j_load,1)*out_load(i_load,1);
        for k_load=drange(1:1:24)

out_load5(x_load,1)=out_load9(k_load,1)*out_load3(m_load,1);
    x_load=x_load+1;
    end
    m_load=m_load+1;
end
for j_load=drange(6:1:7)
    out_load3(n_load,1)=out_load2(j_load,1)*out_load(i_load,1);
    for k_load=drange(1:1:24)

out_load5(x_load,1)=out_load10(k_load,1)*out_load3(n_load,1);
    x_load=x_load+1;
    end
    n_load=n_load+1;
end
    i_load=i_load+1;
end

% Week 31-43
while i_load>30 && i_load<44
    out_load(i_load,1)=out_load1(i_load,1)*peak_load;
    j_load=1;
    for j_load=drange(1:1:5)
        out_load3(m_load,1)=out_load2(j_load,1)*out_load(i_load,1);
        for k_load=drange(1:1:24)

out_load5(x_load,1)=out_load7(k_load,1)*out_load3(m_load,1);
    x_load=x_load+1;
    end
    m_load=m_load+1;
end
for j_load=drange(6:1:7)
    out_load3(n_load,1)=out_load2(j_load,1)*out_load(i_load,1);
    for k_load=drange(1:1:24)

out_load5(x_load,1)=out_load8(k_load,1)*out_load3(n_load,1);
    x_load=x_load+1;
    end
    n_load=n_load+1;
end
    i_load=i_load+1;
end

% Week 44-52
while i_load>43 && i_load<53
    out_load(i_load,1)=out_load1(i_load,1)*peak_load;
    j_load=1;
    for j_load=drange(1:1:5)
        out_load3(m_load,1)=out_load2(j_load,1)*out_load(i_load,1);
        for k_load=drange(1:1:24)

out_load5(x_load,1)=out_load4(k_load,1)*out_load3(m_load,1);
    x_load=x_load+1;

```

```
        end
        m_load=m_load+1;
    end
    for j_load=drange(6:1:7)
        out_load3(n_load,1)=out_load2(j_load,1)*out_load(i_load,1);
        for k_load=drange(1:1:24)

out_load5(x_load,1)=out_load6(k_load,1)*out_load3(n_load,1);
        x_load=x_load+1;
        end
        n_load=n_load+1;
    end
    i_load=i_load+1;
end
end
out_load5(:,1); % this is the simulation result of the annual load
demand
```

## Appendix III MATLAB Codes of Conventional Generator & Wind Turbine Power Output Model

### *Conventional generator power output:*

```

a=1;
a1=1;
a2=1;
a3=1;

out1=zeros(8736,1);
out2=zeros(8736,1);

while a1<8737      % generator up state
    out1(a1,1)=1;
    a1=a1+1;
end

for a2=1:2      % generator down state; a2: failure rate per year
    t1=fix(8691*rand(1));
    a3=t1+1:t1+46;    % MTTR period
    out1(a3,1)=0;
end

while a<8737
    out2(a,1)=5*out1(a,1); % generator power output
    a=a+1;
end

```

### *Wind turbine power output:*

```

hour=1;
outwind=zeros(8736,2);
windoutput=zeros(8736,1);
i_wind=1;

Pwr=3; % rated power output of wind turbine
Vci=4; % cut-in speed
Vr=10; % rated speed
Vco=25; % cut-out speed

A=(Vci*(Vci+Vr)-4*Vci*Vr*((Vci+Vr)/(2*Vr))^3)/(Vci-Vr)^2;
B=(4*(Vci+Vr)*((Vci+Vr)/(2*Vr))^3-(3*Vci+Vr))/(Vci-Vr)^2;
C=(2-4*((Vci+Vr)/(2*Vr))^3)/(Vci-Vr)^2;

while hour<8737
    outwind(i_wind,1)=i;
    n1= wblrnd(7,2); % Weibull distribution
    outwind(i_wind,2)=n1;

    if (outwind(i_wind,2)<Vci)
        Pw=0;
    end
end

```

```
elseif ((Vci<outwind(i_wind,2)) && (outwind(i_wind,2)<Vr))
    Pw=(A+B*outwind(i_wind,2)+C*outwind(i_wind,2)^2)*Pwr;

elseif ((Vr<outwind(i_wind,2)) && (outwind(i_wind,2)<Vco))
    Pw=Pwr;

    else
        Pw=0;

    end;
windoutput(i_wind,1)=Pw; % wind turbine power output

i_wind=i_wind+1;
hour=hour+1;

end
```

## Appendix IV Reliability Indices of All Cooperation Scenarios in MRBTS

### At 10% Wind Penetration Level

Cooperation Scenario	LOLE (hour/year)	LOEE (MWh/year)	LOLF (occ./year)
CS (0.3; 1.0)	3.63	38	1.27
CS (0.3; 0.8)	3.91	41.45	1.37
CS (0.3; 0.6)	3.61	37.6	1.34
CS (0.3; 0.4)	3.76	38.39	1.43
CS (0.3; 0.2)	3.81	40.27	1.46
CS (0.5; 1.0)	2.64	25.88	0.89
CS (0.5; 0.8)	2.66	25.21	0.93
CS (0.5; 0.6)	2.64	25.88	0.97
CS (0.5; 0.4)	2.88	26.82	1.09
CS (0.5; 0.2)	2.55	25.12	0.99
CS (0.6; 1.0)	2.24	21	0.75
CS (0.6; 0.9)	2.26	21.35	0.77
CS (0.6; 0.8)	2.14	20.33	0.74
CS (0.6; 0.7)	2.21	21.29	0.8
CS (0.6; 0.6)	2.13	20.82	0.78
CS (0.6; 0.5)	2	19.73	0.75
CS (0.6; 0.4)	2.11	20.7	0.81
CS (0.6; 0.3)	1.89	19.3	0.73
CS (0.6; 0.2)	2.04	19.21	0.85
CS (0.6; 0.1)	2.03	19.1	0.86
CS (0.7; 1.0)	1.88	17	0.63
CS (0.7; 0.9)	1.93	18	0.68
CS (0.7; 0.8)	1.75	15.74	0.61
CS (0.7; 0.7)	1.76	16.3	0.64
CS (0.7; 0.6)	1.75	17.4	0.63
CS (0.7; 0.5)	1.69	15.85	0.69
CS (0.7; 0.4)	1.74	15.38	0.71
CS (0.7; 0.3)	1.78	16.56	0.73
CS (0.7; 0.2)	1.63	14.55	0.67
CS (0.7; 0.1)	1.63	15.06	0.7
CS (0.8; 1.0)	1.55	14.95	0.49
CS (0.8; 0.9)	1.52	14.16	0.54
CS (0.8; 0.8)	1.46	13.45	0.51
CS (0.8; 0.7)	1.41	15.4	0.49
CS (0.8; 0.6)	1.4	13	0.56
CS (0.8; 0.5)	1.38	12.82	0.56
CS (0.8; 0.4)	1.36	12.47	0.56
CS (0.8; 0.3)	1.33	14.55	0.51
CS (0.8; 0.2)	1.4	11.9	0.6
CS (0.8; 0.1)	1.34	11.72	0.59
CS (0.9; 1.0)	1.35	11.52	0.5

## Appendix V Reliability Indices of All Cooperation Scenarios in MRBTS

### At 15% Wind Penetration Level

Cooperation Scenario	LOLE (hour/year)	LOEE (MWh/year)	LOLF (occ./year)
CS (0.3; 1.0)	5.44	59.46	2.36
CS (0.3; 0.8)	5.64	63.16	2.43
CS (0.3; 0.6)	5.33	58.42	2.45
CS (0.3; 0.4)	5.66	62	2.57
CS (0.3; 0.2)	5.59	62.54	2.52
CS (0.5; 1.0)	3.3	33.95	1.39
CS (0.5; 0.8)	3.4	34.73	1.44
CS (0.5; 0.6)	3.4	34.91	1.49
CS (0.5; 0.4)	3.57	36.49	1.59
CS (0.5; 0.2)	3.3	33.86	1.51
CS (0.6; 1.0)	2.65	26.15	1.07
CS (0.6; 0.9)	2.62	25.94	1.08
CS (0.6; 0.8)	2.49	24.64	1.05
CS (0.6; 0.7)	2.65	26.81	1.13
CS (0.6; 0.6)	2.52	25.13	1.12
CS (0.6; 0.5)	2.42	25	1.09
CS (0.6; 0.4)	2.52	26.16	1.17
CS (0.6; 0.3)	2.35	24.63	1.09
CS (0.6; 0.2)	2.38	23.75	1.17
CS (0.6; 0.1)	2.38	23.67	1.17
CS (0.7; 1.0)	2.14	19.9	0.88
CS (0.7; 0.9)	2.2	21.45	0.9
CS (0.7; 0.8)	1.94	16.98	0.86
CS (0.7; 0.7)	2	18.98	0.89
CS (0.7; 0.6)	1.94	19.5	0.87
CS (0.7; 0.5)	1.89	18.2	0.9
CS (0.7; 0.4)	2.06	18.51	1
CS (0.7; 0.3)	2.04	19.97	0.96
CS (0.7; 0.2)	1.83	16	0.91
CS (0.7; 0.1)	1.88	18.2	0.92
CS (0.8; 1.0)	1.7	16.83	0.68
CS (0.8; 0.9)	1.61	15.2	0.69
CS (0.8; 0.8)	1.56	14.6	0.69
CS (0.8; 0.7)	1.52	16.9	0.64
CS (0.8; 0.6)	1.49	14.08	0.72
CS (0.8; 0.5)	1.47	13.87	0.72
CS (0.8; 0.4)	1.45	13.75	0.72
CS (0.8; 0.3)	1.45	16.1	0.66
CS (0.8; 0.2)	1.58	13.68	0.8
CS (0.8; 0.1)	1.44	13.1	0.73
CS (0.9; 1.0)	1.41	12.33	0.61

### Appendix VI Wind Power Output Data for 1 Week (168 hours) in MRBTS

Hour	Output (%)						
1	34.9	43	0	85	4.7	127	0.2
2	34.8	44	2.2	86	16.9	128	37.4
3	25	45	0	87	1.8	129	27.2
4	37.1	46	0	88	5.9	130	0
5	50.6	47	0	89	17	131	0
6	0	48	24.5	90	52.8	132	0
7	0	49	3.4	91	36.6	133	1.6
8	0	50	29.2	92	24	134	0
9	0	51	85.2	93	67.4	135	1.2
10	79.2	52	54.9	94	20.2	136	41.2
11	50	53	22.8	95	17.9	137	55.1
12	100	54	5.7	96	27.3	138	41.4
13	23.1	55	46.5	97	0	139	71.6
14	40.7	56	5.5	98	0	140	2.7
15	7	57	1.4	99	0	141	1
16	100	58	6.1	100	30.3	142	23.4
17	51.5	59	0	101	87.3	143	45.4
18	3.4	60	80.5	102	21.6	144	0
19	4.5	61	100	103	0	145	64.5
20	6.3	62	1.6	104	100	146	0
21	0	63	48.1	105	54.3	147	40.3
22	2.5	64	9.3	106	27.2	148	0
23	3.6	65	4.1	107	58.8	149	1.3
24	100	66	24	108	100	150	37
25	36.8	67	19.3	109	0	151	53.3
26	19.3	68	0	110	0	152	0
27	0	69	64.8	111	13.6	153	72
28	6.9	70	0	112	52.4	154	5.3
29	0.2	71	0	113	0	155	7
30	8.7	72	62.6	114	0.5	156	37.9
31	0	73	53	115	0.8	157	1.3
32	40.3	74	0	116	15.8	158	11.5
33	0	75	46.7	117	0	159	9
34	1.6	76	6.7	118	0	160	10.5
35	33.8	77	11	119	54.7	161	0
36	28.4	78	0	120	12.8	162	18.9
37	73.7	79	0	121	14.9	163	0.1
38	1	80	5.3	122	0	164	51.5
39	0	81	0	123	16	165	8.6
40	4.7	82	37.6	124	0	166	42.3
41	0	83	0	125	100	167	45.2
42	2.2	84	55.2	126	7.3	168	1

**Appendix VII Thermal Generators' Rated Outputs of  
Modified IEEE 118-Bus Test System**

Thermal Generator	Rated Output (MW)	Thermal Generator	Rated Output (MW)
Generator 1	400	Generator 28	100
Generator 2	400	Generator 29	100
Generator 3	400	Generator 30	100
Generator 4	400	Generator 31	100
Generator 5	400	Generator 32	100
Generator 6	400	Generator 33	100
Generator 7	350	Generator 34	100
Generator 8	350	Generator 35	50
Generator 9	350	Generator 36	50
Generator 10	350	Generator 37	50
Generator 11	350	Generator 38	50
Generator 12	350	Generator 39	50
Generator 13	350	Generator 40	50
Generator 14	350	Generator 41	50
Generator 15	200	Generator 42	50
Generator 16	200	Generator 43	50
Generator 17	200	Generator 44	50
Generator 18	200	Generator 45	50
Generator 19	200	Generator 46	50
Generator 20	200	Generator 47	50
Generator 21	200	Generator 48	50
Generator 22	200	Generator 49	50
Generator 23	100	Generator 50	50
Generator 24	100	Generator 51	50
Generator 25	100	Generator 52	50
Generator 26	100	Generator 53	50
Generator 27	100	Generator 54	50

**Appendix VIII Reliability Indices of All Cooperation Scenarios in Modified  
IEEE 118-Bus Test System at  
10%, 15%, 20%, 25%, 30% & 40% Wind Penetration Levels**

	<b>Cooperation Scenario</b>	<b>LOLE (hour/year)</b>	<b>LOEE (MWh/year)</b>	<b>LOLF (occ./year)</b>
	<b>10% Wind Penetration Level</b>	CS (0.3; 1.0)	12.1	2940
CS (0.4; 1.0)		8.9	2064	4.3
CS (0.5; 1.0)		6.7	1594	3.2
CS (0.6; 1.0)		5.1	1156	2.4
CS (0.6; 0.9)		5.1	1167	2.4
CS (0.6; 0.8)		5	1120	2.4
CS (0.6; 0.7)		5	1184	2.4
CS (0.6; 0.6)		4.7	1062	2.4
CS (0.6; 0.5)		4.4	975	2.3
CS (0.6; 0.4)		4.5	991	2.4
CS (0.6; 0.3)		4.5	1023	2.4
CS (0.6; 0.2)		4.6	1086	2.4
CS (0.6; 0.1)		4.5	1031	2.4
CS (0.7; 1.0)		3.7	823	1.7
CS (0.7; 0.9)		3.7	834	1.8
CS (0.7; 0.8)		3.5	802	1.8
CS (0.7; 0.7)		3.5	784	1.7
CS (0.7; 0.6)		3.6	798	1.8
CS (0.7; 0.5)		3.4	751	1.8
CS (0.7; 0.4)		3.3	764	1.8
CS (0.7; 0.3)		3.6	825	1.8
CS (0.7; 0.2)		3.6	841	1.9
CS (0.7; 0.1)		3.5	840	1.9
CS (0.8; 1.0)		2.9	676	1.4
CS (0.8; 0.9)		2.7	613	1.3
CS (0.8; 0.8)		2.8	653	1.4
CS (0.8; 0.7)		2.6	597	1.3
CS (0.8; 0.6)		2.7	614	1.3
CS (0.8; 0.5)		2.9	566	1.3
CS (0.8; 0.4)		2.6	589	1.4
CS (0.8; 0.3)		2.7	600	1.4
CS (0.8; 0.2)		2.4	562	1.3
CS (0.8; 0.1)	2.5	579	1.4	
CS (0.9; 1.0)	2.2	511	1.1	

<b>15% Wind Penetration Level</b>	<b>Cooperation Scenario</b>	<b>LOLE (hour/year)</b>	<b>LOEE (MWh/year)</b>	<b>LOLF (occ./year)</b>
	CS (0.3; 1.0)	29.3	7875	15.7
	CS (0.4; 1.0)	19.6	5003	10.5
	CS (0.5; 1.0)	13.3	3433	7
	CS (0.6; 1.0)	9.4	2349	4.9
	CS (0.6; 0.9)	9.3	2360	5
	CS (0.6; 0.8)	9	2312	4.8
	CS (0.6; 0.7)	9.1	2344	4.9
	CS (0.6; 0.6)	8.6	2179	4.8
	CS (0.6; 0.5)	8.4	2062	4.7
	CS (0.6; 0.4)	8.6	2161	4.9
	CS (0.6; 0.3)	8.7	2169	4.9
	CS (0.6; 0.2)	8.8	2251	4.9
	CS (0.6; 0.1)	8.4	2193	4.8
	CS (0.7; 1.0)	6.6	1677	3.4
	CS (0.7; 0.9)	6.5	1684	3.4
	CS (0.7; 0.8)	6.5	1678	3.5
	CS (0.7; 0.7)	6.2	1617	3.4
	CS (0.7; 0.6)	6.4	1678	3.6
	CS (0.7; 0.5)	6.2	1589	3.5
	CS (0.7; 0.4)	6.1	1590	3.4
	CS (0.7; 0.3)	6.4	1716	3.6
	CS (0.7; 0.2)	6.5	1708	3.6
	CS (0.7; 0.1)	6.3	1668	3.5
	CS (0.8; 1.0)	5.1	1391	2.6
	CS (0.8; 0.9)	4.8	1300	2.6
	CS (0.8; 0.8)	5	1335	2.6
	CS (0.8; 0.7)	4.6	1254	2.5
	CS (0.8; 0.6)	4.7	1280	2.5
	CS (0.8; 0.5)	4.8	1262	2.6
	CS (0.8; 0.4)	4.8	1300	2.6
CS (0.8; 0.3)	4.8	1313	2.6	
CS (0.8; 0.2)	4.7	1284	2.6	
CS (0.8; 0.1)	4.9	1337	2.7	
CS (0.9; 1.0)	4.3	1145	2.3	

<b>20% Wind Penetration Level</b>	<b>Cooperation Scenario</b>	<b>LOLE (hour/year)</b>	<b>LOEE (MWh/year)</b>	<b>LOLF (occ./year)</b>
	CS (0.3; 1.0)	60	17241	33.7
	CS (0.4; 1.0)	36.8	10136	21
	CS (0.5; 1.0)	23	6530	13
	CS (0.6; 1.0)	15.1	4401	8.4
	CS (0.6; 0.9)	15.5	4492	8.7
	CS (0.6; 0.8)	15.2	4377	8.6
	CS (0.6; 0.7)	15	4371	8.6
	CS (0.6; 0.6)	14.7	4230	8.6
	CS (0.6; 0.5)	14.5	4113	8.4
	CS (0.6; 0.4)	14.8	4311	8.5
	CS (0.6; 0.3)	14.7	4254	8.6
	CS (0.6; 0.2)	14.8	4322	8.5
	CS (0.6; 0.1)	14.5	4270	8.4
	CS (0.7; 1.0)	11.3	3416	6.2
	CS (0.7; 0.9)	11.1	3407	6.1
	CS (0.7; 0.8)	11.2	3434	6.3
	CS (0.7; 0.7)	10.6	3294	6
	CS (0.7; 0.6)	11	3450	6.2
	CS (0.7; 0.5)	10.9	3345	6.2
	CS (0.7; 0.4)	10.8	3329	6.1
	CS (0.7; 0.3)	11.1	3490	6.2
	CS (0.7; 0.2)	11.2	3454	6.3
	CS (0.7; 0.1)	10.9	3375	6.2
	CS (0.8; 1.0)	9.3	3038	5
	CS (0.8; 0.9)	9	2932	4.9
	CS (0.8; 0.8)	9.2	2983	5
	CS (0.8; 0.7)	8.8	2848	4.9
	CS (0.8; 0.6)	8.9	2912	4.9
	CS (0.8; 0.5)	9	2970	5
	CS (0.8; 0.4)	9	2967	5
CS (0.8; 0.3)	9.1	2991	5	
CS (0.8; 0.2)	9	2971	5	
CS (0.8; 0.1)	9.2	3084	5	
CS (0.9; 1.0)	8.4	2780	4.5	

<b>25% Wind Penetration Level</b>	<b>Cooperation Scenario</b>	<b>LOLE (hour/year)</b>	<b>LOEE (MWh/year)</b>	<b>LOLF (occ./year)</b>
	CS (0.3; 1.0)	134	44260	75.6
	CS (0.4; 1.0)	78.6	25024	45
	CS (0.5; 1.0)	46.6	15376	26.5
	CS (0.6; 1.0)	30	10591	16.8
	CS (0.6; 0.9)	30.6	10844	17.1
	CS (0.6; 0.8)	30.3	10621	17.2
	CS (0.6; 0.7)	29.9	10493	17
	CS (0.6; 0.6)	29.8	10382	17
	CS (0.6; 0.5)	29.4	10172	16.9
	CS (0.6; 0.4)	30	10568	17
	CS (0.6; 0.3)	29.6	10384	16.8
	CS (0.6; 0.2)	29.8	10466	17
	CS (0.6; 0.1)	29.2	10363	16.7
	CS (0.7; 1.0)	22.5	8591	12.1
	CS (0.7; 0.9)	22.3	8629	12
	CS (0.7; 0.8)	22.3	8708	12.2
	CS (0.7; 0.7)	21.7	8347	12
	CS (0.7; 0.6)	22	8602	12
	CS (0.7; 0.5)	22.2	8583	12.2
	CS (0.7; 0.4)	22.1	8554	12.1
	CS (0.7; 0.3)	22.3	8732	12.2
	CS (0.7; 0.2)	22.3	8714	12.2
	CS (0.7; 0.1)	22.3	8625	12.3
	CS (0.8; 1.0)	19.2	7971	10.1
	CS (0.8; 0.9)	18.9	7807	10
	CS (0.8; 0.8)	19	7876	10
	CS (0.8; 0.7)	18.6	7636	10
	CS (0.8; 0.6)	18.6	7719	9.9
	CS (0.8; 0.5)	19	7893	10
	CS (0.8; 0.4)	18.8	7859	10
CS (0.8; 0.3)	18.9	7873	10	
CS (0.8; 0.2)	18.7	7882	9.9	
CS (0.8; 0.1)	18.9	8035	10	
CS (0.9; 1.0)	17.9	7603	9.4	

	<b>Cooperation Scenario</b>	<b>LOLE (hour/year)</b>	<b>LOEE (MWh/year)</b>	<b>LOLF (occ./year)</b>
	<b>30% Wind Penetration Level</b>	CS (0.3; 1.0)	247	92507
CS (0.4; 1.0)		140	50050	80.8
CS (0.5; 1.0)		78.2	29642	44.8
CS (0.6; 1.0)		48.6	20692	26.9
CS (0.6; 0.9)		49.3	21142	27.3
CS (0.6; 0.8)		49.1	20906	27.4
CS (0.6; 0.7)		48.4	20516	27.2
CS (0.6; 0.6)		48.7	20676	27.3
CS (0.6; 0.5)		48.2	20320	27.1
CS (0.6; 0.4)		48.8	20880	27.2
CS (0.6; 0.3)		48.3	20511	27
CS (0.6; 0.2)		48.6	20582	27.2
CS (0.6; 0.1)		47.8	20467	26.8
CS (0.7; 1.0)		36.4	17254	19.1
CS (0.7; 0.9)		36.3	17620	19.1
CS (0.7; 0.8)		36.3	17741	19.2
CS (0.7; 0.7)		35.8	17190	19.2
CS (0.7; 0.6)		35.8	17453	19
CS (0.7; 0.5)		36	17572	19
CS (0.7; 0.4)		36	17536	19.1
CS (0.7; 0.3)		36.4	17757	19.2
CS (0.7; 0.2)		36.3	17730	19.2
CS (0.7; 0.1)		36.2	17653	19.3
CS (0.8; 1.0)		31.9	16583	16.3
CS (0.8; 0.9)		31.5	16483	16
CS (0.8; 0.8)		31.6	16550	16.2
CS (0.8; 0.7)		31.3	16308	16.1
CS (0.8; 0.6)		31.3	16324	16
CS (0.8; 0.5)		31.6	16651	16.1
CS (0.8; 0.4)		31.5	16562	16
CS (0.8; 0.3)	31.4	16557	16	
CS (0.8; 0.2)	31.4	16647	16	
CS (0.8; 0.1)	31.6	16787	16.2	
CS (0.9; 1.0)	30.2	16258	15.3	

<b>40% Wind Penetration Level</b>	<b>Cooperation Scenario</b>	<b>LOLE (hour/year)</b>	<b>LOEE (MWh/year)</b>	<b>LOLF (occ./year)</b>
	CS (0.3; 1.0)	669	337301	369
	CS (0.4; 1.0)	383	174660	220
	CS (0.5; 1.0)	201	95364	116
	CS (0.6; 1.0)	110.5	63992	60.5
	CS (0.6; 0.9)	110.9	64929	60.8
	CS (0.6; 0.8)	110.6	64649	60.8
	CS (0.6; 0.7)	110.1	63780	60.9
	CS (0.6; 0.6)	109.9	64405	60.4
	CS (0.6; 0.5)	109.9	63740	60.6
	CS (0.6; 0.4)	110.3	64546	60.8
	CS (0.6; 0.3)	109.1	63427	60.2
	CS (0.6; 0.2)	110.4	63959	60.8
	CS (0.6; 0.1)	109.5	63561	60.4
	CS (0.7; 1.0)	75.8	54373	38
	CS (0.7; 0.9)	75.7	54728	38.1
	CS (0.7; 0.8)	75.5	54821	38.1
	CS (0.7; 0.7)	75.5	54140	38.1
	CS (0.7; 0.6)	75	54182	38
	CS (0.7; 0.5)	75	54384	37.8
	CS (0.7; 0.4)	75.2	54557	38
	CS (0.7; 0.3)	75.5	54826	38
	CS (0.7; 0.2)	76	54990	38.3
	CS (0.7; 0.1)	75.2	54559	37.9
	CS (0.8; 1.0)	65.8	52315	31.3
	CS (0.8; 0.9)	65.1	52053	31
	CS (0.8; 0.8)	65.6	52353	31.1
	CS (0.8; 0.7)	65.3	52092	31.1
	CS (0.8; 0.6)	64.9	51836	30.9
	CS (0.8; 0.5)	65.4	52436	31.1
	CS (0.8; 0.4)	65.2	52205	31
CS (0.8; 0.3)	65.3	52282	31.1	
CS (0.8; 0.2)	65	52281	30.9	
CS (0.8; 0.1)	65.4	52596	31.1	
CS (0.9; 1.0)	63.5	51662	30.1	

**Appendix IX Wind Power Output in Percentages of Rated Output in 10% Wind Penetration (24 hours)**

<b>No.</b>	<b>Time interval</b>	<b>Output (%)</b>
<b>1</b>	7:00~7:30	20
<b>2</b>	7:30~8:00	36
<b>3</b>	8:00~8:30	98
<b>4</b>	8:30~9:00	100
<b>5</b>	9:00~9:30	20
<b>6</b>	9:30~10:00	0
<b>7</b>	10:00~10:30	64
<b>8</b>	10:30~11:00	100
<b>9</b>	11:00~11:30	16
<b>10</b>	11:30~12:00	46
<b>11</b>	12:00~12:30	0
<b>12</b>	12:30~13:00	100
<b>13</b>	13:00~13:30	58
<b>14</b>	13:30~14:00	4
<b>15</b>	14:00~14:30	74
<b>16</b>	14:30~15:00	0
<b>17</b>	15:00~15:30	0
<b>18</b>	15:30~16:00	40
<b>19</b>	16:00~16:30	14
<b>20</b>	16:30~17:00	20
<b>21</b>	17:00~17:30	66
<b>22</b>	17:30~18:00	0
<b>23</b>	18:00~18:30	6
<b>24</b>	18:30~19:00	0

<b>No.</b>	<b>Time interval</b>	<b>Output (%)</b>
<b>25</b>	19:00~19:30	8
<b>26</b>	19:30~20:00	100
<b>27</b>	20:00~20:30	2
<b>28</b>	20:30~21:00	0
<b>29</b>	21:00~21:30	36
<b>30</b>	21:30~22:00	74
<b>31</b>	22:00~22:30	10
<b>32</b>	22:30~23:00	54
<b>33</b>	23:00~23:30	30
<b>34</b>	23:30~0:00	42
<b>35</b>	0:00~0:30	58
<b>36</b>	0:30~1:00	100
<b>37</b>	1:00~1:30	0
<b>38</b>	1:30~2:00	8
<b>39</b>	2:00~2:30	10
<b>40</b>	2:30~3:00	36
<b>41</b>	3:00~3:30	0
<b>42</b>	3:30~4:00	100
<b>43</b>	4:00~4:30	72
<b>44</b>	4:30~5:00	0
<b>45</b>	5:00~5:30	74
<b>46</b>	5:30~6:00	100
<b>47</b>	6:00~6:30	0
<b>48</b>	6:30~7:00	0

**Appendix X Electric Network Losses in 10%, 15%, 20% & 25% Penetrations**

Time Interval	Electric Network Losses (MW)			
	10% Penetration	15% Penetration	20% Penetration	25% Penetration
07:00	228	317	364	403
07:30	206	267	291	311
08:00	292	365	462	591
08:30	297	370	473	617
09:00	377	563	662	733
09:30	482	788	1118	1352
10:00	279	363	402	436
10:30	302	370	474	619
11:00	380	581	686	763
11:30	292	403	436	456
12:00	473	776	1099	1319
12:30	297	370	473	617
13:00	278	372	404	429
13:30	451	729	961	1134
14:00	259	337	382	430
14:30	442	714	969	1164
15:00	465	770	1115	1314
15:30	295	422	458	469
16:00	459	717	884	999
16:30	426	640	762	841
17:00	321	414	458	499
17:30	569	987	1262	1534
18:00	529	872	1249	1415
18:30	569	987	1262	1534
19:00	432	675	852	988
19:30	302	370	474	619
20:00	402	646	846	996
20:30	415	672	902	1076
21:00	186	236	255	269
21:30	201	235	282	335
22:00	277	337	432	517
22:30	184	196	236	276
23:00	104	124	150	176
23:30	100	117	143	172
00:00	123	149	191	240
00:30	178	238	365	525
01:00	155	201	276	363
01:30	135	171	222	283
02:00	112	138	180	225
02:30	90	102	126	148
03:00	129	164	229	301
03:30	176	234	368	529
04:00	114	140	204	273
04:30	129	164	229	301
05:00	120	149	218	296
05:30	175	232	364	519
06:00	332	419	566	716
06:30	330	416	561	638

### Appendix XI Electric Network Losses with WHC Method

Time Interval	Electric Network Losses (MW)			
	10% Penetration	15% Penetration	20% Penetration	25% Penetration
07:00	159	173	141	155
07:30	167	194	190	228
08:00	290	284	434	599
08:30	297	294	453	629
09:00	223	253	180	181
09:30	256	288	198	201
10:00	227	294	323	415
10:30	300	292	450	627
11:00	221	254	177	175
11:30	209	260	240	283
12:00	250	284	193	194
12:30	297	294	453	629
13:00	216	280	290	362
13:30	243	276	187	185
14:00	242	224	286	369
14:30	235	268	180	180
15:00	243	281	188	186
15:30	201	255	217	251
16:00	260	294	205	201
16:30	250	284	202	201
17:00	253	320	346	436
17:30	302	340	227	226
18:00	288	324	227	223
18:30	302	340	227	226
19:00	239	269	183	182
19:30	300	292	451	627
20:00	213	247	160	157
20:30	218	251	163	161
21:00	161	189	192	232
21:30	223	202	316	412
22:00	140	128	102	130
22:30	143	182	242	355
23:00	84	126	164	235
23:30	99	160	227	332
00:00	128	217	317	464
00:30	105	237	282	456
01:00	76	82	75	109
01:30	73	87	89	126
02:00	67	85	94	134
02:30	92	147	209	300
03:00	66	72	72	104
03:30	174	243	252	420
04:00	114	141	176	276
04:30	66	72	72	104
05:00	119	148	182	286
05:30	172	244	254	423
06:00	162	142	111	141
06:30	162	142	111	136

### Appendix XII Electric Network Losses in Five-Wind Farm Case

Time Interval	Electric Network Losses (MW)			
	10% Penetration	15% Penetration	20% Penetration	25% Penetration
07:00	213	268	296	345
07:30	182	206	219	265
08:00	242	304	308	313
08:30	222	285	291	299
09:00	389	573	679	745
09:30	377	484	606	700
10:00	348	564	670	707
10:30	297	445	494	512
11:00	269	309	233	332
11:30	234	276	278	290
12:00	300	396	429	450
12:30	277	343	355	376
13:00	276	310	320	362
13:30	400	613	758	836
14:00	251	336	350	356
14:30	278	321	343	411
15:00	389	557	658	750
15:30	324	427	464	503
16:00	373	475	520	574
16:30	410	570	660	746
17:00	397	518	575	645
17:30	487	788	1070	1136
18:00	392	513	571	638
18:30	430	600	689	761
19:00	393	592	712	773
19:30	329	501	571	602
20:00	300	383	423	488
20:30	321	469	540	562
21:00	177	204	213	243
21:30	210	291	337	383
22:00	180	188	201	236
22:30	231	268	332	368
23:00	97	110	128	179
23:30	113	134	157	207
00:00	91	144	133	177
00:30	105	119	140	189
01:00	125	146	183	226
01:30	112	135	159	227
02:00	103	120	146	186
02:30	93	106	125	151
03:00	71	83	96	141
03:30	79	100	126	142
04:00	70	77	86	120
04:30	115	136	192	215
05:00	89	104	125	144
05:30	84	98	117	134
06:00	275	322	417	479
06:30	264	313	378	490